Discrete Dynamics in Nature and Society

Stability and Bifurcations Analysis of Discrete Dynamical Systems

Lead Guest Editor: Abdul Qadeer Khan
Guest Editor: Tarek Ibrahim

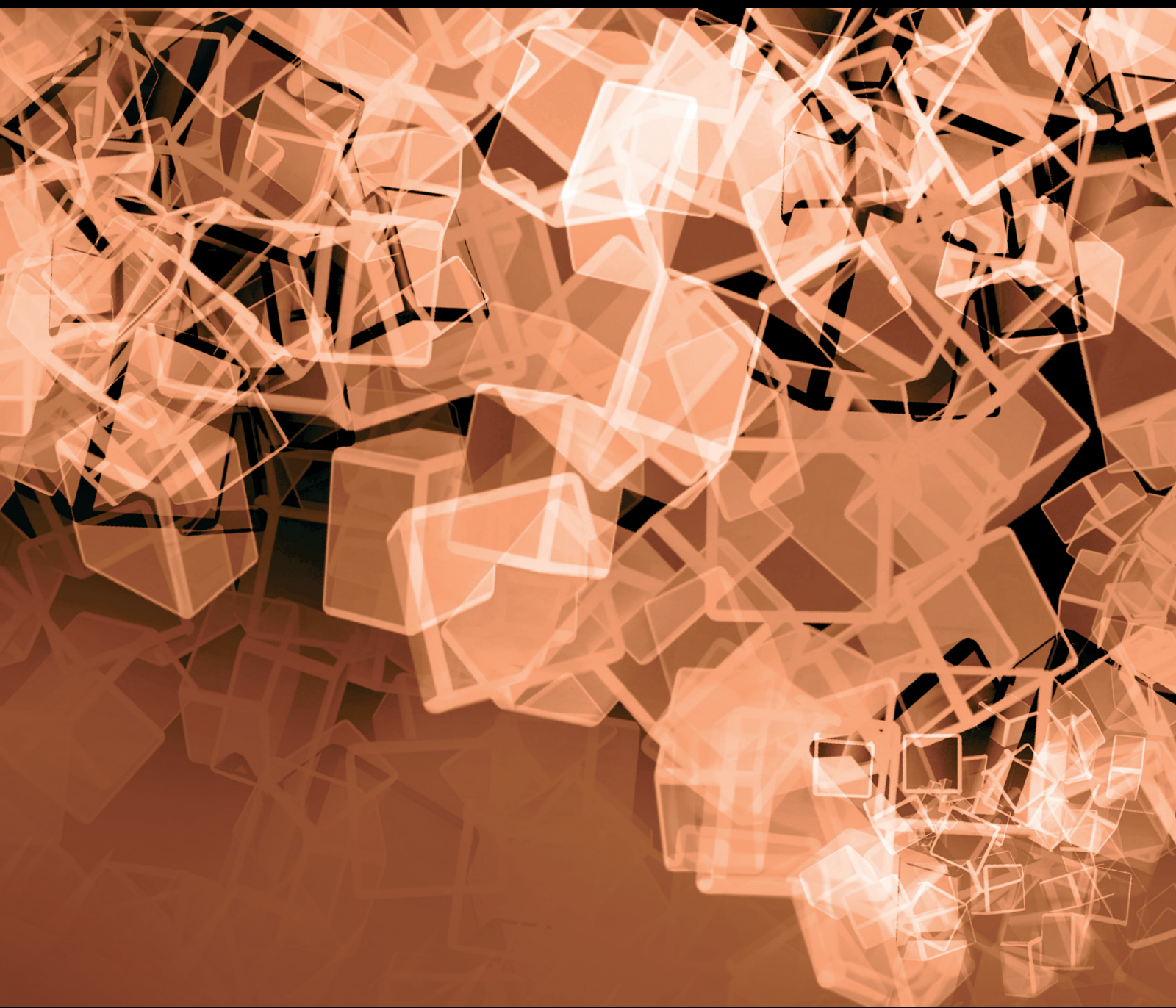

Stability and Bifurcations Analysis of Discrete Dynamical Systems

Discrete Dynamics in Nature and Society

Stability and Bifurcations Analysis of Discrete Dynamical Systems

Lead Guest Editor: Abdul Qadeer Khan
Guest Editors: Tarek Ibrahim

Editorial Board

Contents

Hindawi
Discrete Dynamics in Nature and Society
Volume 2019, Article ID 8474706, 2 pages
https://doi.org/10.1155/2019/8474706

Editorial

Stability and Bifurcations Analysis of Discrete Dynamical Systems

A. Q. Khan [1] **and Tarek F. Ibrahim** [2,3]

[1] *Department of Mathematics, University of Azad Jammu & Kashmir, Muzaffarabad 13100, Pakistan*
[2] *Department of Mathematics, Faculty of Sciences and arts, King Khalid University, Abha, Saudi Arabia*
[3] *Department of Mathematics, Faculty of Science, Mansoura University, Mansoura 35516, Egypt*

Correspondence should be addressed to A. Q. Khan; abdulqadeerkhan1@gmail.com

Received 23 December 2018; Accepted 24 December 2018; Published 7 February 2019

The importance of difference equations cannot be overemphasized. These equations model discrete physical phenomena on one hand and are integral part of numerical schemes used to solve differential equations, on the other hand. This widens the applicability of such equations to many branches of scientific knowledge. Discrete dynamical systems are described by difference equations and potentially have applications in probability theory, economics, biology, computer science, control engineering, genetics, signal processing, population dynamics, health sciences, ecology, physiology, physics, etc.

This special issue provides a platform to disseminate original research in the fields of difference equations, discrete dynamical systems, and bifurcation theory. This was an excellent opportunity for researchers to share their findings with the scientific community.

All manuscripts submitted to this special issue have been reviewed through peer-reviewing process. Based on the reviewers' reports, 11 out of 26 original research articles have been accepted for publication in this well-reputed Journal. A brief summary of each published article in this special issue by providing a short editorial note has also been presented as follows.

In the paper "Dynamics and Stability Analysis of a Brucellosis Model with Two Discrete Delays," P. O. Lolika and S. Mushayabasa have investigated the dynamics and stability analysis of a Brucellosis Model with two discrete delays in which first delay represents the incubation period while the second accounts for the time needed to detect and cull infectious animals. Feasibility and stability of the model steady states have been investigated both analytically and numerically. Furthermore, the occurrence of Neimark-Sacker bifurcation has also been investigated.

In the research article "Dynamics Analysis and Control of a Five-Term Fractional-Order System," L. Yang and X. Liu have proposed a new fractional-order chaotic system with five terms. They have studied the stability about equilibria of the model. Moreover, rich dynamics with interesting characteristics have been demonstrated by phase portraits and bifurcation diagrams numerically.

In the research article "An Improved Computationally Efficient Method for Finding the Drazin Inverse," H. B. Jebreen and Y. Chalco-Cano have proposed a computationally effective iterative scheme for finding the Drazin inverse. The convergence has been investigated analytically by applying a suitable initial matrix.

In the research article "Stability Analysis and Control Optimization of a Prey-Predator Model with Linear Feedback Control," Y. Li et al. have provided an appropriate balance between the chemical and biological control and therefore a Smith predator-prey system has also been established for integrated pest management. They have studied the existence and uniqueness of the order-one periodic solution by means of the subsequent function method to confirm the feasibility of the biological and chemical control strategy of pest management. Furthermore, the stability of the system has also been proved by the limit method of the successor points' sequences and the analogue of the Poincare criterion.

In the original research article "Global Asymptotic Stability and Naimark-Sacker Bifurcation of Certain Mix Monotone Difference Equation," M. R. S. Kulenovic et al. have investigated the local and global dynamics about equilibrium point of second-order rational difference equations with positive parameters and initial conditions. Finally it has also been investigated that the difference equation has undergone a Neimark-Sacker bifurcation resulting in the existence of the locally stable periodic solution of unknown period.

In the article "Stochastic P-Bifurcation of a Bistable Viscoelastic Beam with Fractional Constitutive Relation under Gaussian White Noise," Y. Li et al. have studied the stochastic P-bifurcation problem for axially moving of a bistable viscoelastic beam with fractional derivatives of high order nonlinear terms under Gaussian white noise excitation. They have shown that the fractional derivative term is equivalent to a linear combination of the damping force and restoring force so that the original system can be simplified to an equivalent system by principle for minimum mean square error. They have also obtained the stationary Probability Density Function (PDF) of the system's amplitude by stochastic averaging and critical parametric condition for stochastic P-bifurcation of amplitude by singularity theory. Finally, Y. Li et al. have analyzed the types of the stationary PDF curves of the system qualitatively by choosing parameters corresponding to each region within the transition set curve.

In the paper titled "Exponential Stability and Robust H_∞ Control for Discrete-Time Time-Delay Infinite Markov Jump Systems," Y. Liu and T. Hou have investigated the exponential stability and robust H_∞ control problem for a class of discrete-time time-delay stochastic systems with infinite Markov jump and multiplicative noises where the jumping parameters are modeled as an infinite-state Markov chain. They have also derived the new sufficient condition in terms of matrix inequalities to guarantee the mean square exponential stability of the equilibrium point by using a novel Lyapunov-Krasovskii functional, and then some sufficient conditions for the existence of feedback control have also been presented to guarantee that the resulting closed-loop system has mean square exponential stability for the zero exogenous disturbance and satisfies a prescribed H_∞ performance level. Numerical simulations have also been presented to verify theoretical results.

In the article "New Qualitative Results for Solutions of Functional Differential Equations of Second Order," C. Tunç and S. Erdur have studied the existence of periodic solutions, stability of zero solution, asymptotic stability of zero solution, square integrability of the first derivative of solutions, and boundedness of solutions of nonlinear functional differential equations of second-order by the second method of Lyapunov. They have also obtained the sufficient conditions guaranteeing the existence of periodic solutions, stability of zero solution, asymptotic stability of zero solution, square integrability of the first derivative of solutions, and boundedness of solutions of the equations thus considered.

In the article "Bifurcations of a New Fractional-Order System with a One-Scroll Chaotic Attractor," X. Liu et al. have presented a new fractional-order system which has shown a chaotic attractor of the one-scroll structure. They have also investigated the stability analysis about equilibrium points and determined the generation conditions of the one-scroll structure for the attractor based on the stability analysis. Furthermore, in a commensurate-order case, bifurcations with the variation of a system parameter have also been investigated as derivative orders decrease from 0.99. In an incommensurate-order case, bifurcations with the variation of a derivative order have also been analyzed as other orders are decreased from 1.

In the article "The Impact of User Behavior on Information Diffusion in D2D Communications: A Discrete Dynamical Model," C. Gan et al. have explored the impact of user behavior on information diffusion in D2D (Device-to-Device) communications. A discrete dynamical model, which combined network metrics and user behaviors, including social relationship, user influence, and interest, has been proposed and analyzed. Specifically, combined with social tie and user interest, the success rate of data dissemination between D2D users has been described, and the interaction factor, user influence, and stability factor have also been defined. Furthermore, the state transition process of user has been depicted by a discrete-time Markov chain, and global stability analysis of the proposed model has also been performed.

Finally, in "Double Delayed Feedback Control of a Non-Linear Finance System," Z. Jiang et al. have investigated a class of chaotic finance system with double delayed feedback control. Specifically, they have studied the stability analysis about equilibrium, existence of periodic solutions, and properties of the branching periodic solutions by using center manifold theory.

Conflicts of Interest

The editors declare that they have no conflicts of interest regarding the publication of this Special Issue.

Acknowledgments

We are greatly acknowledging the contribution of **Professor Dr. Muhammad Naeem Qureshi (Late)** who improved the quality of the initial proposal for this Special Issue. We would like to pay a great homage to all of the authors for their valuable contributions rendered in this respect and also to the reviewers for their valuable suggestions made in the evaluation of the papers during the reviewing process.

A. Q. Khan
Tarek F. Ibrahim

Hindawi
Discrete Dynamics in Nature and Society
Volume 2019, Article ID 7254121, 17 pages
https://doi.org/10.1155/2019/7254121

Research Article

Double Delayed Feedback Control of a Nonlinear Finance System

Zhichao Jiang,[1] **Yanfen Guo**,[2] **and Tongqian Zhang**[3,4]

[1]*Fundamental Science Department, North China Institute of Aerospace Engineering, Langfang 065000, China*
[2]*Fundamental Education Department, Beijing Polytechnic College, Beijing 100042, China*
[3]*College of Mathematics and Systems Science, Shandong University of Science and Technology, Qingdao 266590, China*
[4]*State Key Laboratory of Mining Disaster Prevention and Control Co-Founded by Shandong Province and the Ministry of Science and Technology, Shandong University of Science and Technology, Qingdao 266590, China*

Correspondence should be addressed to Tongqian Zhang; zhangtongqian@sdust.edu.cn

Received 16 September 2018; Revised 16 November 2018; Accepted 26 November 2018; Published 5 February 2019

Academic Editor: Douglas R. Anderson

In this paper, a class of chaotic finance system with double delayed feedback control is investigated. Firstly, the stability of equilibrium and the existence of periodic solutions are discussed when delays change and cross some threshold value. Then the properties of the branching periodic solutions are given by using center manifold theory. Further, we give an example and numerical simulation, which implies that chaotic behavior can be transformed into a stable equilibrium or a stable periodic solution. Also, we give the local sensitivity analysis of parameters on equilibrium.

1. Introduction

Chaos applied to various disciplines of natural science and social science is a complex dynamic phenomenon. Chaotic systems with nonlinearity have been extensively investigated by many communities [1–5], and so on. In 1985, chaos was first discovered in the economic field, which had great impact imposed on the prominent economies. In economic field, chaos means that the economic operation has its intrinsic uncertainty.

Nonlinear methods are an important research method that has been widely used to explain complex economic phenomena [6–10]. In economic field, financial risks mean the possibilities of suffering losses caused by uncertainly endogenous factors in financial or investment activities, which displays irregularly fluctuations. The source of risks derives from the strange attractor, while the key of risk management is to control the chaotic attractor. In fact, one of the features of chaos in the economic system is financial crisis. In the passed few decades, a lot of ways to control or synchronize chaos have been proposed, such as OGY method [11], PC method [12], fuzzy control [13], impulsive control [14–18], linear feedback control [19–23], delayed feedback method [24–29], multiple delayed feedback control [30–35], and so on. Nowadays, the delayed dynamic systems occupy a central position in many fields, such as biology, transport control, and chemistry [36–39]. Since many economic processes have time-delay characteristics [40–44], they are unsuitable using ordinary differential equations (ODEs) to describe. Some authors concluded that the chaotic behavior of a microeconomic system could be stabilized to periodic orbits by using delayed feedback control, which seemed more applicable to experimental systems and avoided heavy data processing. In [6, 7], the authors proposed a financial system including four parts (production, money, stock, and labor force). Furthermore, they proposed a simplified model which is described using three variables: X represents the interest rate, Y represents the investment demand, and Z represents the price index. The three-dimensional model is given as follows:

$$\begin{aligned} \dot{X}(t) &= Z(t) + (Y(t) - a)X(t), \\ \dot{Y}(t) &= 1 - bY(t) - X^2(t), \\ \dot{Z}(t) &= -X(t) - cZ(t), \end{aligned} \tag{1}$$

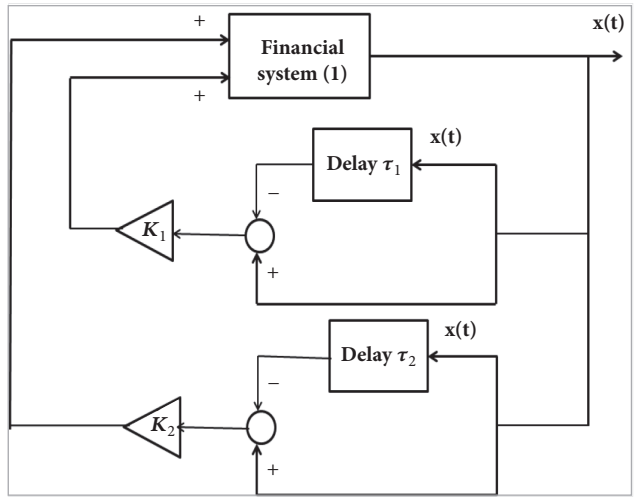

Figure 1: The delayed feedback control graph.

where $a > 0$ is the saving amount, $b > 0$ is the cost per investment, and $c > 0$ is the elasticity of demand of commercial markets. For system (1), the feedback control with one delay had been studied by many authors [45–47]. In 2008, Chen [48] firstly prevented the feedback control with three delays in system (1) as follows:

$$\begin{aligned}\dot{X}(t) &= Z(t) + (Y(t) - a)X(t) \\ &\quad + k_1\left[X(t) - X\left(t-\tau_1\right)\right], \\ \dot{Y}(t) &= 1 - bY(t) - X^2(t) + k_2\left[Y(t) - Y\left(t-\tau_2\right)\right], \\ \dot{Z}(t) &= -X(t) - cZ(t) + k_3\left[Z(t) - Z\left(t-\tau_3\right)\right],\end{aligned} \tag{2}$$

where k_i represent the feedback strengths and τ_i represent delays, $i = 1, 2, 3$. In [47], by the numerical simulations, Chen firstly gave the dynamic behavior of system (2) with only one $k_i \neq 0$ and then gave the dynamic behavior when all $k_i \neq 0$ $(i = 1, 2, 3)$ and $\tau_1 = \tau_2 = \tau_3 = \tau$. After that, Woo-Sik Son et al. [49] gave the theory analysis for the above results. We find that system (2) with one delay has obtained complete results and the delayed feedback control method is valid. But system (2) with multiple different delays has not completely been investigated. Therefore, our objective is to study system (2) with two different delays. Next, we assume that $k_3 = 0$ and $k_1, k_2 \neq 0$, the other cases are similar to analyze, then system (2) becomes

$$\begin{aligned}\dot{X}(t) &= Z(t) + (Y(t) - a)X(t) \\ &\quad + k_1\left[X(t) - X\left(t-\tau_1\right)\right], \\ \dot{Y}(t) &= 1 - bY(t) - X^2(t) + k_2\left[Y(t) - Y\left(t-\tau_2\right)\right], \\ \dot{Z}(t) &= -X(t) - cZ(t),\end{aligned} \tag{3}$$

and the delayed feedback control graph is shown in Figure 1, where $\mathbf{x}(\mathbf{t})$ is the state vector of the system.

We consider system (3) with the parameters $a = 0.9, b = 0.2$, and $c = 1.2$ [50]. When $\tau_1 = \tau_2 = 0$, system (3) has a chaotic attractor (see Figure 2).

We choose the initial conditions for system (3) as

$$\begin{aligned}X(\theta) &= \varphi_1(\theta), \\ Y(\theta) &= \varphi_2(\theta), \\ Z(\theta) &= \varphi_3(\theta),\end{aligned} \tag{4}$$

where $\varphi(\theta) = (\varphi_1(\theta), \varphi_2(\theta), \varphi_3(\theta))^T \in C, \theta \in [-\tau, 0], \tau = \max\{\tau_1, \tau_2\}$ and C denotes the Banach space $C([-\tau, 0], \mathbb{R}^3)$.

This paper is arranged as follows. In Section 2, the stability of equilibrium and existence of Hopf bifurcations are obtained by investigating the distribution of roots of characteristic equation. In Section 3, an algorithm is derived for deciding the properties of the branching periodic solutions by computing center manifold. In Section 4, some numerical simulations are given for verifying the theoretical analyses. In Section 5, the local sensitivity analyses of parameters on equilibrium are given. At last, we give a brief conclusion and discussion.

2. Stability of Equilibrium and Local Hopf Bifurcation

The existence and uniqueness of solutions and stability of equilibrium have always been an important issue for differential and difference systems [51–54]. Let the right sides of system (3) be zero; it can obtain the equilibrium as follows.

Lemma 1. *(i) If the condition $c - b - abc \leq 0$ holds, then system (3) has a unique boundary equilibrium $E_0(0, 1/b, 0)$.*

(ii) If the condition $c - b - abc > 0$ holds, then system (3) has three equilibria: E_0 and

$$\mathbf{E}^*_{\pm}\left(\pm\sqrt{\frac{c-b-abc}{c}}, \frac{1+ac}{c}, \mp c^{-3/2}\sqrt{c-b-abc}\right). \tag{5}$$

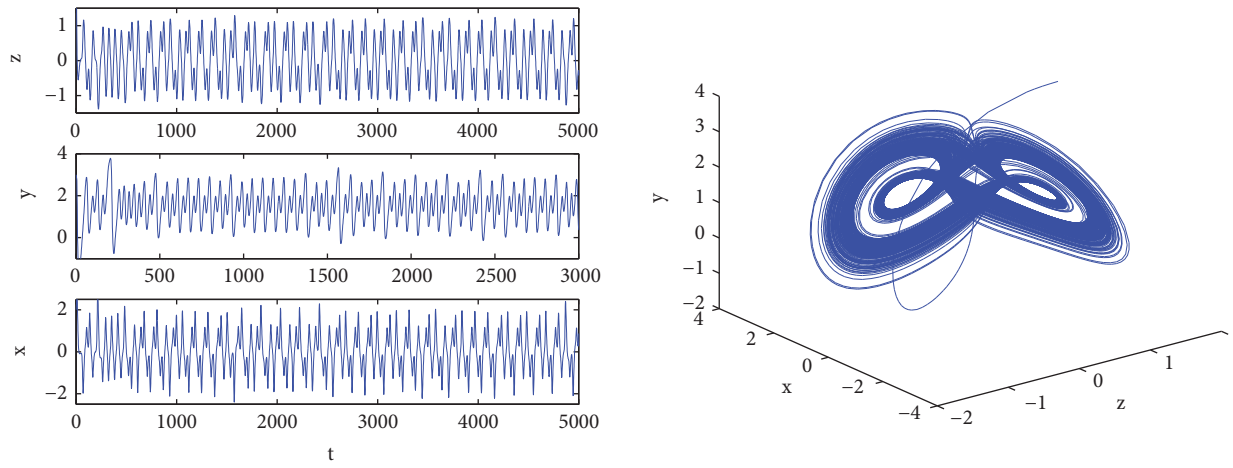

Figure 2: Chaos phenomenon exists for system (3) when $\tau_1 = \tau_2 = 0$.

Remark 2. If the cost per investment is smaller than some value $(c/(1+ac))$, then $\mathbf{E}_{\pm}^{*}$ is feasible.

In this paper, it always assumes that $c - b - abc > 0$ holds and only considers the stability of $\mathbf{E}_{+}^{*}$ and the other one can be analyzed in the same way.

Let $\mathbf{u}_1(t) = X(t) - x^*$, $\mathbf{u}_2(t) = Y(t) - y^*$, $\mathbf{u}_3(t) = Z(t) - z^*$, where $x^* = \sqrt{(c-b-abc)/c}$, $y^* = (1+ac)/c$, and $z^* = -c^{-3/2}\sqrt{(c-b-abc)/c}$, then system (3) becomes

$$\begin{aligned}
\dot{\mathbf{u}}_1(t) &= \left(k_1 + \frac{1}{c}\right)\mathbf{u}_1(t) + x^*\mathbf{u}_2(t) + \mathbf{u}_3(t) \\
&\quad - k_1\mathbf{u}_1(t-\tau_1) + \mathbf{u}_1(t)\mathbf{u}_2(t), \\
\dot{\mathbf{u}}_2(t) &= -2x^*\mathbf{u}_1(t) + (k_2 - b)\mathbf{u}_2(t) - k_2\mathbf{u}_2(t-\tau_2) \\
&\quad - \mathbf{u}_1^2(t), \\
\dot{\mathbf{u}}_3(t) &= -\mathbf{u}_1(t) - c\mathbf{u}_3(t),
\end{aligned} \tag{6}$$

whose characteristic equation is

$$\begin{aligned}
&\lambda^3 + a_2\lambda^2 + a_1\lambda + a_0 + k_1 e^{-\lambda\tau_1}\left[\lambda^2 + b_1\lambda + b_0\right] \\
&\quad + k_2 e^{-\lambda\tau_2}\left[\lambda^2 + c_1\lambda + c_0\right] + k_1 k_2 e^{-\lambda(\tau_1+\tau_2)}(\lambda + c) \\
&\quad = 0,
\end{aligned} \tag{7}$$

where

$$\begin{aligned}
a_0 &= ck_1(k_2 - b) + 2cx^{*2}, \\
a_1 &= (k_2 - b)\left(k_1 + \frac{1}{c} - c\right) - ck_1 + 2x^{*2}, \\
a_2 &= c - k_1 - \frac{1}{c} - (k_2 - b), \\
b_0 &= c(b - k_2), \\
b_1 &= c + b - k_2, \\
c_0 &= -ck_1, \\
c_1 &= c - k_1 - \frac{1}{c}.
\end{aligned} \tag{8}$$

Now we analyze the distribution of roots of (7) by using the method in [55, 56].

When $\tau_1 = \tau_2 = 0$, (7) becomes

$$\begin{aligned}
&\lambda^3 + (a_2 + k_1 + k_2)\lambda^2 + (a_1 + k_1b_1 + k_2c_1 + k_1k_2)\lambda \\
&\quad + a_0 + k_1b_0 + k_2c_0 + ck_1k_2 = 0.
\end{aligned} \tag{9}$$

It has $a_0 + k_1b_0 + k_2c_0 + ck_1k_2 = 2(c - b - abc) > 0$ if $c - b - abc > 0$.

Let

$$\begin{aligned}
&c + b > \frac{1}{c}, \\
&\left(c - \frac{1}{c}\right)\left[c - \frac{1}{c} + b^2\right] + \frac{2}{c}\left(b - \frac{1}{c}\right)(c - b - abc) \\
&\quad > 0.
\end{aligned} \tag{H_1}$$

Then $a_2 + k_1 + k_2 = c - 1/c + b > 0$ and $(a_2 + k_1 + k_2)(a_1 + k_1b_1 + k_2c_1 + k_1k_2) - (a_0 + k_1b_0 + k_2c_0 + ck_1k_2) = (c - 1/c)^2 + b^2(c - 1/c) + (2/c)(b - 1/c)(c - b - abc) > 0$ under (H_1). By using Routh-Hurwitz criterion, all roots of (9) have negatively real parts if (H_1) holds.

Next, let $\tau_2 = 0$ and use τ_1 as parameter, then (7) becomes

$$\begin{aligned}
&\lambda^3 + (a_2 + k_2)\lambda^2 + (a_1 + k_2c_1)\lambda + a_0 + k_2c_0 \\
&\quad + k_1 e^{-\lambda\tau_1}\left[\lambda^2 + (b_1 + k_2)\lambda + b_0 + k_2c\right] = 0.
\end{aligned} \tag{10}$$

Let $\mathbf{i}\omega$ $(\omega > 0)$ be the root of (10), then ω satisfies

$$\begin{aligned} &-\omega^3 + (a_1 + k_2c_1)\,\omega \\ &\quad = k_1\left(b_0 + k_2c - \omega^2\right)\sin\omega\tau_1 \\ &\qquad - k_1\left(b_1 + k_2\right)\omega\cos\omega\tau_1, \\ &\left(a_2 + k_2\right)\omega^2 - a_0 - k_2c_0 \\ &\quad = k_1\left(b_0 + k_2c - \omega^2\right)\cos\omega\tau_1 \\ &\qquad + k_1\left(b_1 + k_2\right)\omega\sin\omega\tau_1. \end{aligned} \tag{11}$$

Squaring and adding in the both sides of (11), it has

$$\omega^6 + \mathfrak{p}\omega^4 + \mathfrak{q}\omega^2 + \mathfrak{r} = 0, \tag{12}$$

where

$$\begin{aligned} \mathfrak{p} &= \left(k_2 + a_2\right)^2 - 2\left(a_1 + k_2c_1\right) - k_1^2, \\ \mathfrak{q} &= \left(a_1 + k_2c_1\right)^2 - 2\left(a_2 + k_2\right)\left(a_0 + k_2c_0\right) \\ &\quad + 2k_1^2\left(b_0 + k_2c\right)^2 - k_1^2\left(b_1 + k_2\right)^2, \\ \mathfrak{r} &= 2\left(c - b - abc\right)\left[\left(c - b - abc\right) - k_1bc\right]. \end{aligned} \tag{13}$$

Let $z = \omega^2$, then (12) becomes

$$\mathfrak{h}(z) := z^3 + \mathfrak{p}z^2 + \mathfrak{q}z + \mathfrak{r} = 0. \tag{14}$$

Hence $\mathfrak{h}'(z) = 3z^2 + 2\mathfrak{p}z + \mathfrak{q}$. Let $\triangle = \mathfrak{p}^2 - 3\mathfrak{q}$ and $z_1 = (-\mathfrak{p} + \sqrt{\triangle})/3$, from Ruan and Wei [55], it knows that (14) has at least one positive root if $\mathfrak{r} < 0$; (14) has no positive roots if $\mathfrak{r} \geq 0$ and $\triangle < 0$; if $\mathfrak{r} \geq 0$, then (14) has positive roots iff $\mathfrak{h}(z_1) \leq 0$. Hence, under the condition $c - b - abc > 0$, it has the following lemma.

Lemma 3. *(i) Equation (14) has at least one positive root if* $c - b - abc < k_1bc$.

(ii) Equation (14) has no positive root if $c - b - abc \geq k_1bc$ *and* $\Delta \leq 0$.

(iii) If $c - b - abc \geq k_1bc$ *and* $\Delta > 0$, *then (14) has one positive roots iff* $z_1^* > 0$ *and* $\mathfrak{h}(z_1^*) \leq 0$, *where* $\Delta = \mathfrak{p}^2 - 3\mathfrak{q}$, $z_1^* = (-\mathfrak{p} + \sqrt{\Delta})/3$.

It assumes that (14) has three positive roots, denoted by z_k $(k = 1, 2, 3)$. Then (12) has three positive roots $\omega_k = \sqrt{z_k}$. Substituting ω_k into (11) yields

$$\begin{aligned} \cos\omega\tau_1 &= \frac{\left(b_0 + k_2c - \omega^2\right)\left[\left(a_2 + k_2\right)\omega^2 - a_0 - k_2c_0\right] + \left(b_1 + k_2\right)\left[\omega^2 - a_1 - k_2c_1\right]\omega^2}{k_1\left(b_0 + k_2c - \omega^2\right)^2 + k_1\left(b_1 + k_2\right)^2\omega^2} := \mathfrak{Q}_1(\omega), \\ \sin\omega\tau_1 &= \frac{\omega\left(b_0 + k_2c - \omega^2\right)\left[-\omega^2 + a_1 + k_2c_1\right] + \omega\left(b_1 + k_2\right)\left[\left(a_2 + k_2\right)\omega^2 - a_0 - k_2c_0\right]}{k_1\left(b_0 + k_2c - \omega^2\right)^2 + k_1\left(b_1 + k_2\right)^2\omega^2} := \mathfrak{Q}_2(\omega), \end{aligned} \tag{15}$$

and furthermore, it has

$$\tau_{1k}^{(j)} = \begin{cases} \dfrac{1}{\omega_k}\left[\arccos\left(\mathfrak{Q}_1(\omega_k)\right) + 2j\pi\right], & \mathfrak{Q}_2(\omega_k) \geq 0, \\ \dfrac{1}{\omega_k}\left[2\pi - \arccos\left(\mathfrak{Q}_1(\omega_k)\right) + 2j\pi\right], & \mathfrak{Q}_2(\omega_k) < 0, \end{cases} \quad k = 1, 2, 3,\ \ j = 0, 1, \cdots, \tag{16}$$

where $\omega_k\tau_{1k}^{(j)} \in (0, 2\pi]$ is determined by the sign of $\sin\omega_k\tau_{1k}^{(j)}$. Define

$$\tau_1^0 = \min_{1\leq k\leq 3, j\geq 0}\left\{\tau_{1k}^{(j)}\right\}. \tag{17}$$

Let $\lambda(\tau_1) = \sigma(\tau_1) + i\omega(\tau_1)$ be the root of (10) satisfying $\sigma(\tau_{1k}^{(j)}) = 0, \omega(\tau_{1k}^{(j)}) = \omega_k$.

Lemma 4. *It assumes that* $\mathfrak{h}'(z_k) \neq 0$. *Then*

$$\operatorname{sign}\left\{\frac{\mathbf{d}\left(\operatorname{Re}\lambda\left(\tau_{1k}^{(j)}\right)\right)}{\mathbf{d}\tau_1}\right\} = \operatorname{sign}\left\{\mathfrak{h}'\left(z_k\right)\right\} \neq 0. \tag{18}$$

Proof. Substituting $\lambda(\tau_1)$ into (10) and taking the derivative of both sides with respect to τ_1, it has

$$\left[\frac{\mathbf{d}\lambda}{\mathbf{d}\tau_1}\right]^{-1} = \frac{\left[3\lambda^2 + 2\left(a_2 + k_2\right)\lambda + a_1 + k_2c_1\right]e^{\lambda\tau_1}}{k_1\lambda\left[\lambda^2 + \left(b_1 + k_2\right)\lambda + b_0 + k_2c\right]}$$

$$+\frac{2\lambda+b_1+k_2}{\lambda\left[\lambda^2+(b_1+k_2)\lambda+b_0+k_2c\right]}-\frac{\tau_1}{\lambda}. \tag{19}$$

Hence, using $z_k=\omega_k^2$ and (10), it has

$$\begin{aligned}\left[\frac{\mathbf{d}\,\mathrm{Re}\,\lambda\left(\tau_{1k}^{(j)}\right)}{\mathbf{d}\tau_1}\right]^{-1}&=\mathrm{Re}\left\{\frac{\left[3\lambda^2+2(a_2+k_2)\lambda+a_1+k_2c_1\right]e^{\lambda\tau_1}+k_1(2\lambda+b_1+k_2)}{k_1\lambda\left[\lambda^2+(b_1+k_2)\lambda+b_0+k_2c\right]}-\frac{\tau_1}{\lambda}\right\}\Bigg|_{\tau_1=\tau_{1k}^{(j)}}\\&=\mathrm{Re}\left\{\frac{-\left[3\lambda^2+2\lambda(a_2+k_2)+a_1+k_2c_1\right]}{\lambda^3+(a_2+b_2)\lambda^2+(a_1+k_2c_1)\lambda+a_0+k_2c_0}+\frac{2\lambda+b_1+k_2}{\lambda^2+(b_1+k_2)\lambda+b_0+k_2c}\right\}\Bigg|_{\tau_1=\tau_{1k}^{(j)}}\\&=\mathrm{Re}\left\{\frac{\left[3\omega_k^2-(a_1+k_2c_1)\right]-2\mathrm{i}\omega_k(a_2+b_2)}{\left[-(a_2+b_2)\omega_k^2+a_0+k_2c_0\right]+\mathrm{i}\left[-\omega_k^3+\omega_k(a_1+k_2c_1)\right]}+\frac{b_1+k_2+2\mathrm{i}\omega_k}{-\omega_k^2+b_0+k_2c+\mathrm{i}\omega_k(b_1+k_2)}\right\}\\&=\frac{1}{\Theta}\left(3\omega_k^6+2\mathfrak{p}\omega_k^4+\mathfrak{q}\omega_k^2\right)=\frac{z_k}{\Theta}\mathfrak{h}'(z_k),\end{aligned} \tag{20}$$

where $\Theta=k_1^2[b_1^2\omega_k^4+(\omega_k^2-b_0)\omega_k^2]$. Since $\Theta>0$ and $z_k>0$, then it has

$$\mathrm{sign}\left\{\frac{\mathbf{d}\left(\mathrm{Re}\,\lambda\left(\tau_{1k}^{(j)}\right)\right)}{\mathbf{d}\tau_1}\right\}=\mathrm{sign}\left\{\mathfrak{h}'(z_k)\right\}. \tag{21}$$

□

By Lemmas 3 and 4 and applying the Hopf bifurcation theorem for FDE [57–61], it has the following theorem.

Theorem 5. *When $\tau_2=0$, suppose that (H_1) is satisfied.*

(i) If $c-b-abc>k_1bc$ and $\Delta\le 0$, then, for any $\tau_1\ge 0$, all roots of (10) has negatively real parts and $\mathbf{E}_+^*$ is locally asymptotically stable.

(ii) If either $c-b-abc<k_1bc$ or $c-b-abc\ge k_1bc$ and $\Delta>0, z_1^*>0, \mathfrak{h}(z_1^*)\le 0$ hold, then $\mathfrak{h}(z)=0$ has at least a positive root z_k, for $\tau_1\in[0,\tau_1^0)$, all roots of (10) have negatively real parts, and $\mathbf{E}_+^*$ is locally asymptotically stable.

(iii) If conditions (ii) and $\mathfrak{h}'(z_k)\ne 0$ hold, then system (3) undergoes Hopf bifurcations at $\mathbf{E}_+^*$ when $\tau_1=\tau_{1k}^{(j)}$, $j=0,1,2,\ldots,k=1,2,3$.

Remark 6. When $\tau_2=0$ and (H_1) hold, Theorem 5 tells us that, through adjusting the cost per investment, the system will tend to $\mathbf{E}_+^*$ or vibrates around $\mathbf{E}_+^*$. Under this situation, the state of system goes from order to order, that is, the macroeconomic operation is definite.

It has known that (H_1) guarantees that all roots of (9) have negatively real parts. Now we assume that (H_1) is violated. For convenience, denote

$$\begin{aligned}A&=a_2+k_1+k_2=c-\frac{1}{c}+b,\\B&=2-\frac{3b}{c}-2ab+bc,\\C&=2c(1-ab)-2b,\end{aligned} \tag{22}$$

then (9) becomes

$$\lambda^3+A\lambda^2+B\lambda+C=0. \tag{23}$$

Let $\lambda=\Lambda-A/3$, then (23) becomes

$$\Lambda^3+p_1\Lambda+q_1=0, \tag{24}$$

where $p_1=B-A^2/3$ and $q_1=2A^3/27-AB/3+C$.

Define

$$\begin{aligned}\Delta_1&=\left(\frac{p_1}{3}\right)^3+\left(\frac{q_1}{2}\right)^2,\\\gamma&=\sqrt[3]{-\frac{q_1}{2}+\sqrt{\Delta_1}},\\\rho&=\sqrt[3]{-\frac{q_1}{2}-\sqrt{\Delta_1}}.\end{aligned} \tag{25}$$

From Cardano's formula, it has the following theorem.

Theorem 7. *If $\Delta_1>0$, then (24) has a real root $\gamma+\rho$ and a pair of complex roots $-(\gamma+\rho)/2\pm\mathbf{i}(\sqrt{3}(\gamma-\rho)/2)$, that is to say, (23) has a real root $\gamma+\rho-A/3$, and a pair of complex roots $-((\gamma+\rho)/2+A/3)\pm\mathbf{i}(\sqrt{3}(\gamma-\rho)/2)$.*

(ii) If $\triangle_1<0$, then (24) has three real roots and (23) has also three real roots.

Furthermore, it assumes that

$$\begin{aligned}\Delta_1&>0,\\\gamma+\rho-\frac{A}{3}&<0,\\\frac{\gamma+\rho}{2}+\frac{A}{3}&<0,\\\gamma-\rho&\ne 0.\end{aligned} \tag{H_2}$$

Theorem 8. *When $\tau_2 = 0$, suppose that the condition (H_2) is satisfied.*

(i) If $c - b - abc > k_1 bc$ and $\Delta \le 0$, then, for any $\tau_1 \ge 0$, (10) has at least one root with positively real parts and $\mathbf{E}_+^*$ is unstable.

(ii) If either $c - b - abc < k_1 bc$ or $c - b - abc \ge k_1 bc$ and $\Delta > 0, z_1^* > 0, \mathfrak{h}(z_1^*) \le 0$ hold, then $\mathfrak{h}(z) = 0$ has at least one positive root z_k, for $\tau_1 \in [0, \tau_1^0)$, (10) has at least one root with positively real parts, and $\mathbf{E}_+^*$ is unstable. In addition, if $\mathbf{d}\,\mathrm{Re}\,\lambda(\tau_1^0)/\mathbf{d}\tau_1 < 0$, then $\mathbf{E}_+^*$ is locally asymptotically stable when $\tau_1 \in (\tau_1^0, \tau_1^1)$, where τ_1^1 is the second bifurcating value.

(iii) If conditions (ii) and $\mathfrak{h}'(z_k) \ne 0$ hold, then system (3) undergoes Hopf bifurcations at $\mathbf{E}_+^*$ when $\tau_1 = \tau_{1k}^{(j)}$, $j = 0, 1, 2, \ldots$, $k = 1, 2, 3$.

Remark 9. When $\tau_2 = 0$ and (H_2) hold, Theorem 8 tells us that it can still adjust the cost per investment b, such that the system tends to $\mathbf{E}_+^*$ or vibrates around $\mathbf{E}_+^*$ under some conditions. Under this situation, the state of system goes from chaos to order; that is, the financial crisis may be eliminated.

From the above discussions, it knows that system (3) possibly makes stability switches as τ_1 varying when $\tau_2 = 0$. Define I is stable interval of τ_1. Let $\tau_1 \in I$ and $\lambda = \mathbf{i}\varpi(\tau_2)$ $(\varpi > 0)$ be the root of (7), then it has

$$\begin{aligned}
&\varpi^6 + \left[a_2^2 - 2a_1 + k_1^2 - k_2^2\right]\varpi^4 + \left[a_1^2 - 2a_2 a_0\right. \\
&\quad \left. + k_1^2\left(b_1^2 - 2b_0\right) - k_2^2\left(c_1^2 + k_1^2 - 2c_0\right)\right]\varpi^2 + a_0^2 \\
&\quad + k_1^2 b_0^2 - k_2^2\left(k_1^2 c^2 + c_0^2\right) + M_1 \cos\varpi\tau_1 + M_2 \sin\varpi\tau_1 \\
&\quad = 0,
\end{aligned} \tag{26}$$

where

$$\begin{aligned}
M_1 &= 2k_1\left(a_2 - b_1\right)\varpi^4 + 2k_1\left[b_1 a_1 - \left(a_0 + b_0 a_2\right)\right. \\
&\quad \left. - k_2^2\left(c_1 - c\right)\right]\varpi^2 + 2k_1\left(a_0 b_0 - c c_0 k_2^2\right), \\
M_2 &= -2k_1\left\{\varpi^5 + \left(a_2 b_1 - a_1 - b_0 - k_2^2\right)\varpi^3\right. \\
&\quad \left. + \left(a_1 b_0 - b_1 a_0 + k_2^2\left(c c_1 + c_0\right)\right)\varpi\right\}.
\end{aligned} \tag{27}$$

We know that (26) has finite positive roots $\varpi_i (i = 1, 2, \ldots, k)$. For every fixed ϖ_i, there exists a sequence $\{\tau_{2i}^j \mid j = 0, 1, 2, 3, \cdots\}$ satisfying (26). Define $\tau_2^0 = \tau_{2i_0}^0 = \min\{\tau_{2i}^j \mid i = 1, 2, \ldots, k; j = 0, 1, 2, \cdots\}$, $\varpi_0 = \varpi_{i_0}$. When $\tau_2 = \tau_2^0$, $\pm\mathbf{i}\varpi_0$ are a pair of roots of (7).

$$\frac{\mathbf{d}\,\mathrm{Re}\,\lambda\left(\tau_2^0\right)}{\mathbf{d}\tau_2} \ne 0. \tag{H_3}$$

Hence, by Hopf bifurcation theorem [57], it has the next result.

Theorem 10. *Suppose that either (H_1) or (H_2) is satisfied and $\tau_1 \in I$.*

(i) If (26) has no positive roots, then for any $\tau_2 \ge 0$, all roots of (7) have negatively real parts and $\mathbf{E}_+^*$ is locally asymptotically stable.

(ii) If (26) has positive roots, then all roots of (7) have negatively real parts when $\tau_2 \in [0, \tau_2^0)$ and $\mathbf{E}_+^*$ is locally asymptotically stable. In addition, if (H_3) holds, then system (3) undergoes Hopf bifurcation at $\mathbf{E}_+^*$ when $\tau_2 = \tau_2^0$.

Remark 11. When $\tau_2 > 0$ and (H_1) or (H_2) hold, Theorem 10 tells us that, through adjusting the parameters (a, b, c, τ_2), the system will tend to $\mathbf{E}_+^*$ or vibrates around $\mathbf{E}_+^*$. Under this situation, the state of system goes from order to order or from chaos to order.

3. Property of Hopf Bifurcation

In the above section, the sufficient conditions that system (3) undergoes a Hopf bifurcation at $\mathbf{E}_+^*$ when $\tau_2 = \tau_2^0$ have already been obtained. In this section, it assumes that Theorem 10 (ii) is satisfied and establishes the explicit formula for determining the properties of Hopf bifurcation at $\tau_2 = \tau_2^0$ by using the method developed in [62].

For convenience, it assumes that $\tau_1 = \tau_1^* > \tau_2^0$ and lets $\bar{\tau}_2 = \tau_2^0 + \mu$ and drops the bar for simplifying. Then $\mu = 0$ is the Hopf bifurcation value. Since $\tau_1^* > \tau_2^0$, the phase space $C = C([-\tau_1^*, 0], \mathbb{R}^3)$, system (3) is transformed into the following FDE in C:

$$\dot{\mathfrak{u}}_t = \mathfrak{L}_\mu\left(\mathfrak{u}_t\right) + \mathfrak{f}\left(\mu, \mathfrak{u}_t\right), \tag{28}$$

where $\mathfrak{u}_t(\theta) = \mathfrak{u}(t + \theta) \in C$ and $\mathfrak{L}_\mu : C \longrightarrow \mathbb{R}^3, \mathfrak{f} : \mathbb{R} \times C \longrightarrow \mathbb{R}^3$ are given, respectively, by

$$\mathfrak{L}_\mu\varphi = A_1\varphi(0) + B_1\varphi\left(-\tau_1^*\right) + B_2\varphi\left(-\tau_2^0\right), \tag{29}$$

where

$$\begin{aligned}
A_1 &= \begin{pmatrix} k_1 + \dfrac{1}{c} & x^* & 1 \\ -2x^* & k_2 - b & 0 \\ -1 & 0 & -c \end{pmatrix}, \\
B_1 &= \begin{pmatrix} -k_1 & 0 & 0 \\ 0 & 0 & 0 \\ 0 & 0 & 0 \end{pmatrix}, \\
B_2 &= \begin{pmatrix} 0 & 0 & 0 \\ 0 & -k_2 & 0 \\ 0 & 0 & 0 \end{pmatrix}, \\
f\left(\mu, \varphi\right) &= \begin{pmatrix} \varphi_1(0)\,\varphi_2(0) \\ -\varphi_1^2(0) \\ 0 \end{pmatrix},
\end{aligned} \tag{30}$$

where $\varphi = (\varphi_1, \varphi_2, \varphi_3)^T$.

By Riesz representation theorem, there exists a bounded variation function $\eta(\nu,\mu)$ for $\nu \in [-\tau_1^*, 0]$, such that

$$\mathfrak{L}_\mu \varphi = \int_{-\tau_1^*}^{0} d\eta(\nu,\mu)\,\varphi(\nu). \tag{31}$$

For $\varphi \in C^1([-\tau_1^*, 0], \mathbb{R}^3)$, define

$$\mathscr{A}(\mu)\varphi = \begin{cases} \dot{\varphi}(\theta), & \theta \in [-\tau_1^*, 0), \\ \int_{-\tau_1^*}^{0} d\eta(\nu,\mu)\,\varphi(\nu), & \theta = 0, \end{cases} \tag{32}$$

and

$$\mathscr{R}(\mu)\varphi = \begin{cases} 0, & \theta \in [-\tau_1^*, 0), \\ \mathfrak{f}(\mu,\varphi), & \theta = 0. \end{cases} \tag{33}$$

For $u_t = u(t+\theta)$, it has $\mathbf{d}u_t/\mathbf{d}\theta = \mathbf{d}u_t/\mathbf{d}t$ and system (28) becomes

$$\dot{\mathfrak{u}}_t = \mathscr{A}(\mu)u_t + \mathscr{R}(\mu)u_t. \tag{34}$$

For $\psi \in C^* := C([0,\tau_1^*], \mathbb{R}^{3*})$ and $\varphi \in C([-\tau_1^*, 0], \mathbb{R}^3)$, define

$$\mathscr{A}^*\psi(s) = \begin{cases} -\dot{\psi}(\nu), & \nu \in (0, \tau_1^*], \\ \int_{-\tau_1^*}^{0} d\eta^T(t,0)\,\psi(-t), & \nu = 0, \end{cases} \tag{35}$$

and the inner product

$$\langle \psi, \varphi \rangle = \overline{\psi}(0)\varphi(0) - \int_{-\tau_1^*}^{0}\int_{\xi=0}^{\theta} \overline{\psi}(\xi-\theta)\,d\eta(\theta)\,\varphi(\xi)\,d\xi, \tag{36}$$

where $\eta(\theta) = \eta(\theta, 0)$. It knows that $\mathscr{A}^*$ and $\mathscr{A} = \mathscr{A}(0)$ are adjoint operators, then $\pm\mathbf{i}\omega_0$ are eigenvalues of $\mathscr{A}(0)$ and $\mathscr{A}^*$ when $\tau_2 = \tau_2^0$.

By computations, it can obtain that $\mathbf{q}(\theta) = (1, \vartheta, \varsigma)^T e^{\mathbf{i}\omega_0\theta}$ is the eigenvector of $\mathscr{A}$ corresponding to the eigenvalue $\mathbf{i}\omega_0$, and $\mathbf{q}^*(s) = \overline{D}(1, \vartheta^*, \varsigma^*)e^{\mathbf{i}\omega_0 s}$ is the eigenvector of $\mathscr{A}^*$ corresponding to the eigenvalue $-\mathbf{i}\omega_0$. Therefore, it has that

$$\begin{aligned} \langle \mathbf{q}^*(s), \mathbf{q}(\theta) \rangle &= 1, \\ \langle \mathbf{q}^*(s), \overline{\mathbf{q}}(\theta) \rangle &= 0, \end{aligned} \tag{37}$$

where

$$\begin{aligned} \vartheta &= -\frac{2x^*}{b + k_2\left(e^{-\mathbf{i}\omega_0\tau_2^0} - 1\right) + \mathbf{i}\omega_0}, \\ \varsigma &= -\frac{1}{c + \mathbf{i}\omega_0}, \\ \varsigma^* &= \frac{1}{c - \mathbf{i}\omega_0}, \\ \vartheta^* &= \frac{x^*}{b + k_2\left(e^{-\mathbf{i}\omega_0\tau_2^0} - 1\right) - \mathbf{i}\omega_0}, \\ D &= \Big[1 + \vartheta^*\overline{\vartheta^*} + \varsigma^*\overline{\varsigma^*} - \tau_1^* k_1 e^{-\mathbf{i}\omega_0\tau_1^*} \\ &\quad - \vartheta\overline{\vartheta^*}\tau_2^0 k_2 e^{-\mathbf{i}\omega_0\tau_2^0}\Big]^{-1}. \end{aligned} \tag{38}$$

Let $\mathfrak{u}_t$ be the solution of system (28) at $\mu = 0$. Define $\mathbf{z}(t) = \langle \mathbf{q}^*, \mathfrak{u}_t \rangle$, then

$$\dot{\mathbf{z}}(t) = \langle \mathbf{q}^*, \dot{\mathfrak{u}}_t \rangle = \mathbf{i}\omega_0\mathbf{z}(t) + \overline{\mathbf{q}}^*(0)\,\widehat{\mathfrak{f}}(\mathbf{z}, \overline{\mathbf{z}}), \tag{39}$$

where

$$\begin{aligned} \widehat{\mathfrak{f}} &= f(0, \mathscr{W}(\mathbf{z}, \overline{\mathbf{z}}) + 2\,\mathrm{Re}\{\mathbf{z}\mathbf{q}\}), \\ \mathscr{W}(\mathbf{z}, \overline{\mathbf{z}}) &= \mathfrak{u}_t - 2\,\mathrm{Re}\{\mathbf{z}\mathbf{q}\}, \\ \mathscr{W}(\mathbf{z}, \overline{\mathbf{z}}) &= \mathscr{W}_{20}\frac{\mathbf{z}^2}{2} + \mathscr{W}_{11}\mathbf{z}\overline{\mathbf{z}} + \mathscr{W}_{02}\frac{\overline{\mathbf{z}}^2}{2} + \cdots. \end{aligned} \tag{40}$$

Rewrite (39) as

$$\dot{\mathfrak{u}}_t = \mathbf{i}\omega_0\mathbf{z}(t) + \mathbf{g}(\mathbf{z}, \overline{\mathbf{z}}), \tag{41}$$

where

$$\mathbf{g}(\mathbf{z}, \overline{\mathbf{z}}) = \mathbf{g}_{20}\frac{\mathbf{z}^2}{2} + \mathbf{g}_{11}\mathbf{z}\overline{\mathbf{z}} + \mathbf{g}_{02}\frac{\overline{\mathbf{z}}^2}{2} + \mathbf{g}_{21}\frac{\mathbf{z}^2\overline{\mathbf{z}}}{2}\cdots. \tag{42}$$

Substituting (3) and (39) into $\dot{\mathscr{W}} = \dot{\mathfrak{u}}_t - \dot{\mathbf{z}}\mathbf{q} - \dot{\overline{\mathbf{z}}}\,\overline{\mathbf{q}}$, it has

$$\begin{aligned} \dot{\mathscr{W}} &= \begin{cases} \mathscr{A}\mathscr{W} - 2\,\mathrm{Re}\left\{\overline{\mathbf{q}}^*(0)\,\widehat{\mathfrak{f}}\mathbf{q}(\theta)\right\}, & \theta \in [-\tau_1^*, 0) \\ \mathscr{A}\mathscr{W} - 2\,\mathrm{Re}\left\{\overline{\mathbf{q}}^*(0)\,\widehat{\mathfrak{f}}\mathbf{q}(\theta)\right\} + \widehat{\mathfrak{f}}, & \theta = 0 \end{cases} \\ &\overset{\mathrm{def}}{=} \mathscr{A}\mathscr{W} + \mathscr{H}(\mathbf{z}, \overline{\mathbf{z}}, \theta), \end{aligned} \tag{43}$$

where

$$\mathscr{H}(\mathbf{z}, \overline{\mathbf{z}}, \theta) = \mathscr{H}_{20}(\theta)\frac{\mathbf{z}^2}{2} + \mathscr{H}_{11}(\theta)\mathbf{z}\overline{\mathbf{z}} + \mathscr{H}_{02}(\theta)\frac{\overline{\mathbf{z}}^2}{2} + \cdots. \tag{44}$$

By comparing the coefficients, it can obtain

$$\begin{aligned}
\mathbf{g}_{20} &= 2D\left(\vartheta - \overline{\vartheta^*}\right),\\
\mathbf{g}_{11} &= D\left(\vartheta + \overline{\vartheta} - 2\overline{\vartheta^*}\right),\\
\mathbf{g}_{02} &= 2D\left(\overline{\vartheta} - \overline{\vartheta^*}\right),\\
\mathbf{g}_{21} &= 2D\left[\mathscr{W}_{11}^{(2)}(0) + \frac{1}{2}\mathscr{W}_{20}^{(2)}(0)\right.\\
&\quad \left. + \mathscr{W}_{20}^{(1)}(0)\left(\frac{1}{2}\overline{\vartheta} - \overline{\vartheta^*}\right) + \mathscr{W}_{11}^{(1)}(0)\left(\vartheta - 2\overline{\vartheta^*}\right)\right],
\end{aligned} \tag{45}$$

where

$$\begin{aligned}
\mathscr{W}_{20}(\theta) &= \frac{\mathbf{i}\mathbf{g}_{20}}{\omega_0}\mathbf{q}(0)e^{\mathbf{i}\omega_0\theta} + \frac{\mathbf{i}\overline{\mathbf{g}}_{02}}{3\omega_0}\overline{\mathbf{q}}(0)e^{-\mathbf{i}\omega_0\theta} + E_1 e^{2\mathbf{i}\omega_0\theta},\\
\mathscr{W}_{11}(\theta) &= -\frac{\mathbf{i}\mathbf{g}_{11}}{\omega_0}\mathbf{q}(0)e^{\mathbf{i}\omega_0\theta} + \frac{\mathbf{i}\overline{\mathbf{g}}_{11}}{\omega_0}\overline{\mathbf{q}}(0)e^{-\mathbf{i}\omega_0\theta} + E_2,\\
E_1 &= \begin{pmatrix} 2\mathbf{i}\omega_0 - \left(k_1 + \frac{1}{c}\right) + k_1 e^{-2\mathbf{i}\omega_0\tau_1^*} & -x^* & -1\\ 2x^* & 2\mathbf{i}\omega_0 + b + k_2\left(e^{-2\mathbf{i}\omega_0\tau_2^0} - 1\right) & 0\\ 1 & 0 & 2\mathbf{i}\omega_0 + c \end{pmatrix}^{-1} \times \begin{pmatrix} \vartheta\\ -1\\ 0 \end{pmatrix},\\
E_2 &= \begin{pmatrix} \frac{1}{c} & x^* & 1\\ -2x^* & -b & 0\\ -1 & 0 & -c \end{pmatrix}^{-1} \times \begin{pmatrix} -\left(\vartheta + \overline{\vartheta}\right)\\ 2\\ 0 \end{pmatrix}.
\end{aligned} \tag{46}$$

Substituting E_1 and E_2 into $\mathscr{W}_{20}(\theta)$ and $\mathscr{W}_{11}(\theta)$, then g_{21} can be expressed. Thus we may compute the following important quantities:

$$\begin{aligned}
\mathsf{C}_1(0) &= \frac{i}{2\omega_0}\left(\mathbf{g}_{20}\mathbf{g}_{11} - 2\left|\mathbf{g}_{11}\right|^2 - \frac{1}{3}\left|\mathbf{g}_{02}\right|^2\right) + \frac{\mathbf{g}_{21}}{2},\\
\kappa_2 &= -\frac{\operatorname{Re}\{\mathsf{C}_1(0)\}}{\operatorname{Re}\lambda'(0)},\\
\iota_2 &= 2\operatorname{Re}\{\mathsf{C}_1(0)\},\\
\mathsf{T}_2 &= -\frac{\operatorname{Im}\{\mathsf{C}_1(0)\} + \kappa_2 \operatorname{Im}\lambda'(0)}{\omega_0}.
\end{aligned} \tag{47}$$

Theorem 12. *If $\kappa_2 > 0$ (< 0), Hopf bifurcation is supercritical (subcritical). If $\iota_2 < 0$ (> 0), periodic solution is stable (unstable). If $\mathsf{T}_2 > 0$ (< 0), the period of periodic solution is increase (decrease).*

4. Numerical Simulations

In this section, we give an example:

$$\begin{aligned}
\dot{X}(t) &= Z + (Y - 0.9)X - \left[X(t) - X\left(t - \tau_1\right)\right],\\
\dot{Y}(t) &= 1 - 0.2Y - X^2 - 2\left[Y(t) - Y\left(t - \tau_2\right)\right],\\
\dot{Z}(t) &= -X - 1.2Z.
\end{aligned} \tag{48}$$

With these parameters, it can obtain $\mathbf{E}_+^*(0.8083, 1.7333, -0.6736)$ and (H_2) is satisfied. When $\tau_2 = 0$, by computation, it can obtain that (12) has two positive roots $\omega_1 \doteq 1.9997$, $\omega_2 \doteq 0.9752$. Substituting them into (16) gives, respectively,

$$\begin{aligned}
\tau_{11}^j &= 2.5811 + 3.1421j,\\
\tau_{12}^{(j)} &= 0.3795 + 6.4430j,\\
&\qquad (j = 0, 1, 2, \cdots).
\end{aligned} \tag{49}$$

Furthermore, $\operatorname{Re}\lambda(\tau_{11}^{(j)})/\mathbf{d}\tau_1 > 0$, $\mathbf{d}\operatorname{Re}\lambda(\tau_{12}^{(j)})/\mathbf{d}\tau_1 < 0$. By Theorem 8, $\mathbf{E}_+^*$ is asymptotically stable when $\tau_1 \in (0.3795, 2.5911)$ and unstable for $\tau_1 \in [0, 0.3795)$, which means that the stability switches occur. These results are illustrated in Figures 3–5.

Let $\tau_1^* = 0.5 \in (0.3795, 2.5911)$; we obtain $\tau_2^0 \doteq 5.7469$. By Theorem 10, it knows that $\mathbf{E}_+^*$ is asymptotically stable for $\tau_1^* = 0.5$ and $\tau_2 \in [0, 5.7469)$. Furthermore, it has $\mathsf{C}_1(0) = -0.8562 - 1.4758\mathbf{i}$, $\beta_2 < 0$ and $\mu_2 > 0$. Therefore, at $\tau_2^0 \doteq 5.7469$, the periodic solution is orbitally asymptotically stable, and the Hopf bifurcation is forward (see Figures 6 and 7).

Next, we investigate the effect of two different delays. Firstly, we choose $\tau_1 = \tau_2 = 0.1$ and find system (3) has chaos phenomenon (see Figure 8). When choosing $\tau_1 = 0.1$ and $\tau_2 = 1.8$, we find that chaos phenomenon disappears and the solutions of system (48) approach stable equilibrium (see Figure 9). When choosing $\tau_1 = 0.1$ and $\tau_2 = 3.9$, chaos phenomenon disappears and appears stable periodic solutions (see Figure 10). The above results show that double delayed feedback control is superior to delayed feedback control. Hence, we improve the results in [48].

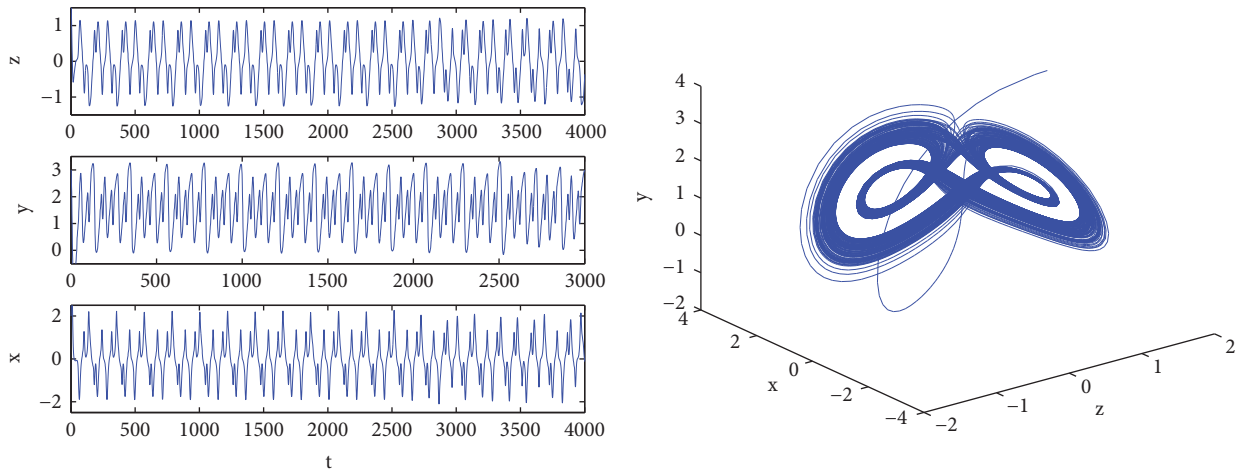

Figure 3: $\mathbf{E}_+^*$ is unstable and chaos still exists with $\tau_1 = 0.1 \in [0, 0.3795)$ and $\tau_2 = 0$.

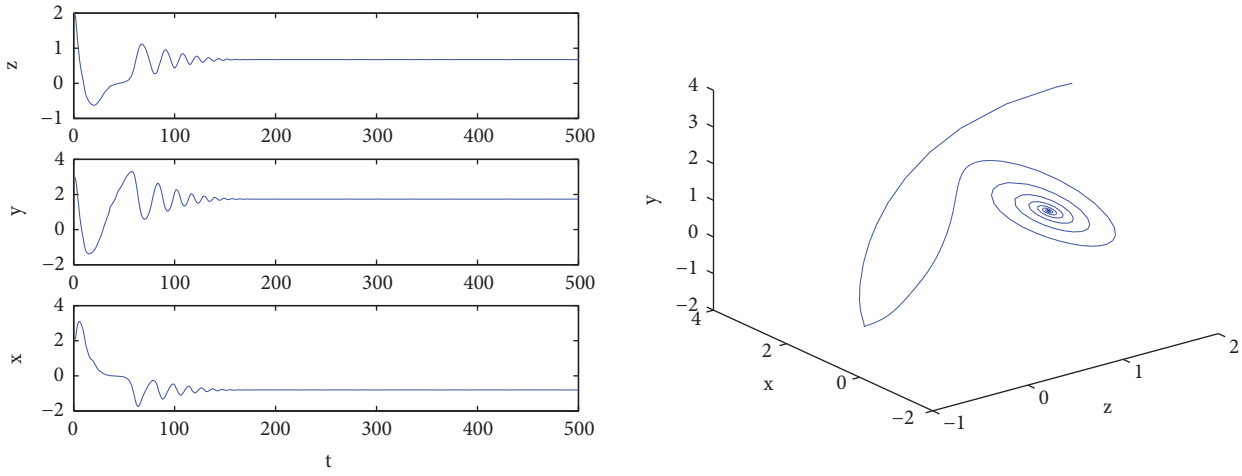

Figure 4: $\mathbf{E}_+^*$ becomes stable and chaos disappears with $\tau_1 = 0.8 \in (2.2945, 4.3572)$ and $\tau_2 = 0$.

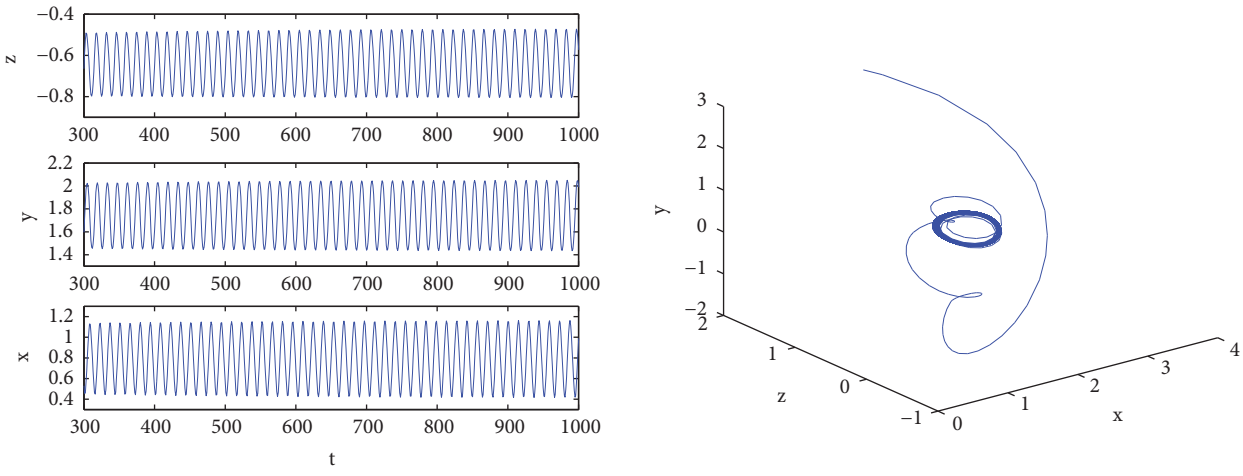

Figure 5: $\mathbf{E}_+^*$ is unstable, and a stable periodic solution appears with $\tau_1 = 2.77$ and $\tau_2 = 0$.

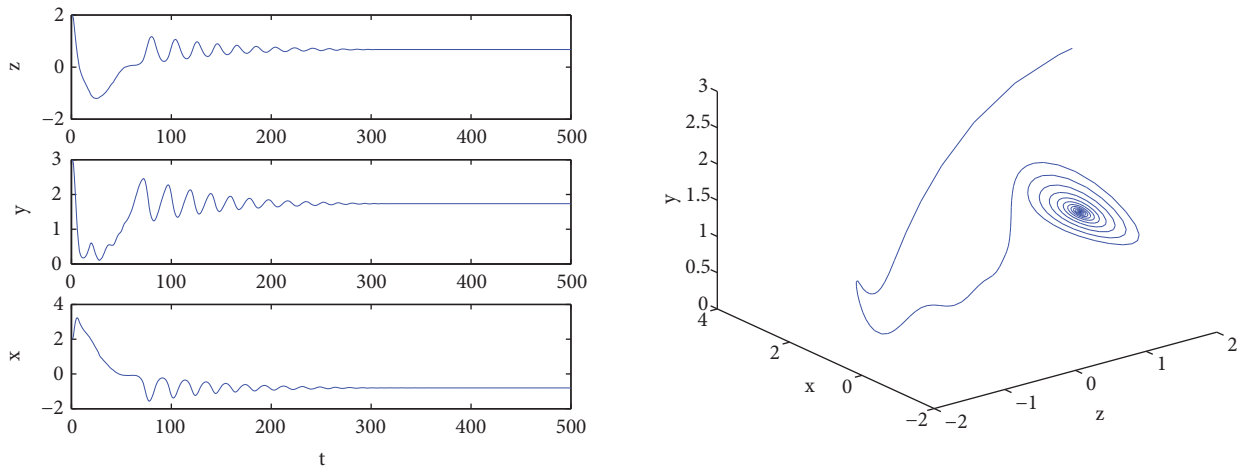

Figure 6: $\mathbf{E}_+^*$ is asymptotically stable with $\tau_1 = 0.5$ and $\tau_2 = 1$.

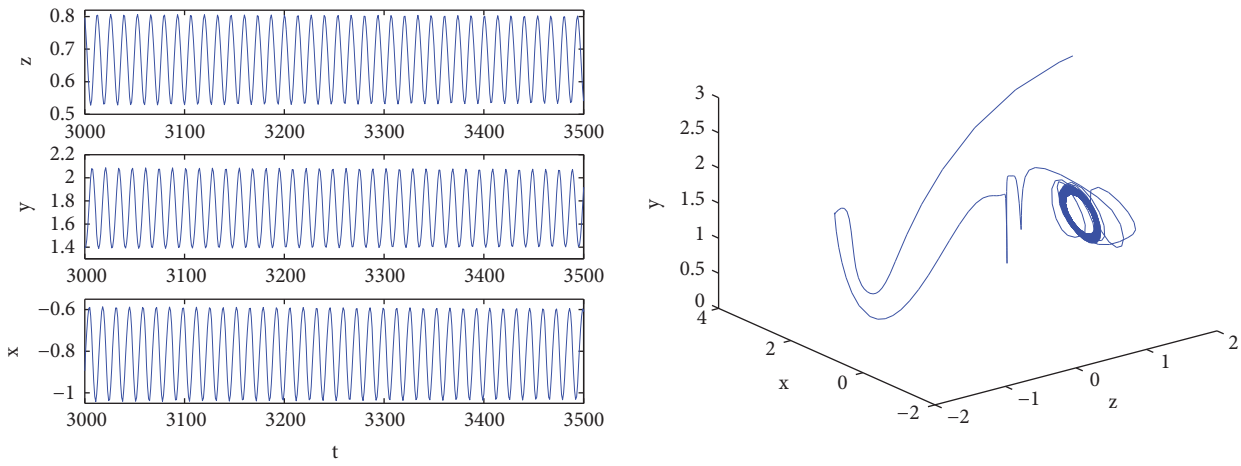

Figure 7: $\mathbf{E}_+^*$ is unstable, and a periodic solution appears with $\tau_1 = 0.5$ and $\tau_2 = 5.8$.

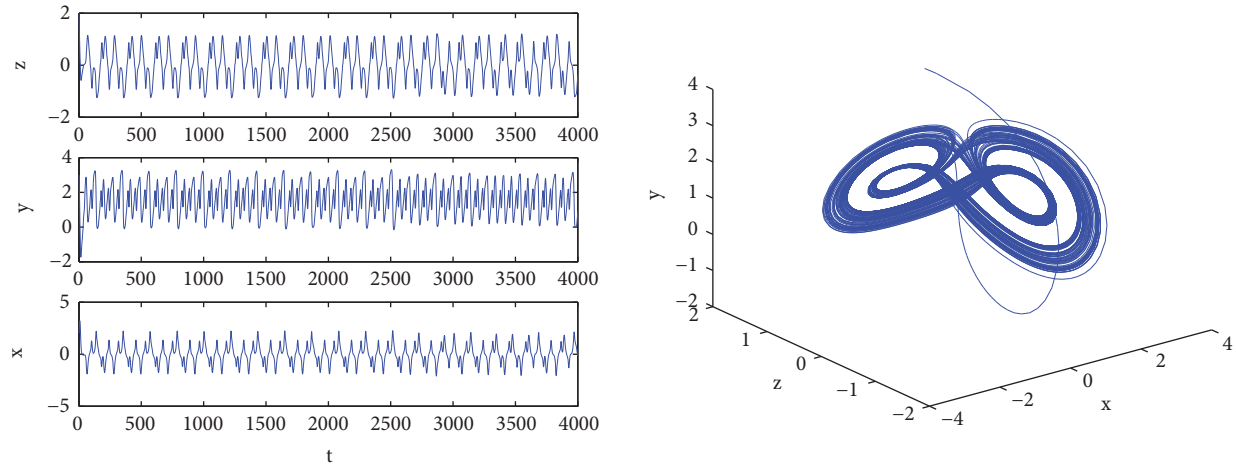

Figure 8: $\mathbf{E}_+^*$ is unstable and chaos exists with $\tau_1 = 0.1$ and $\tau_2 = 0.1$.

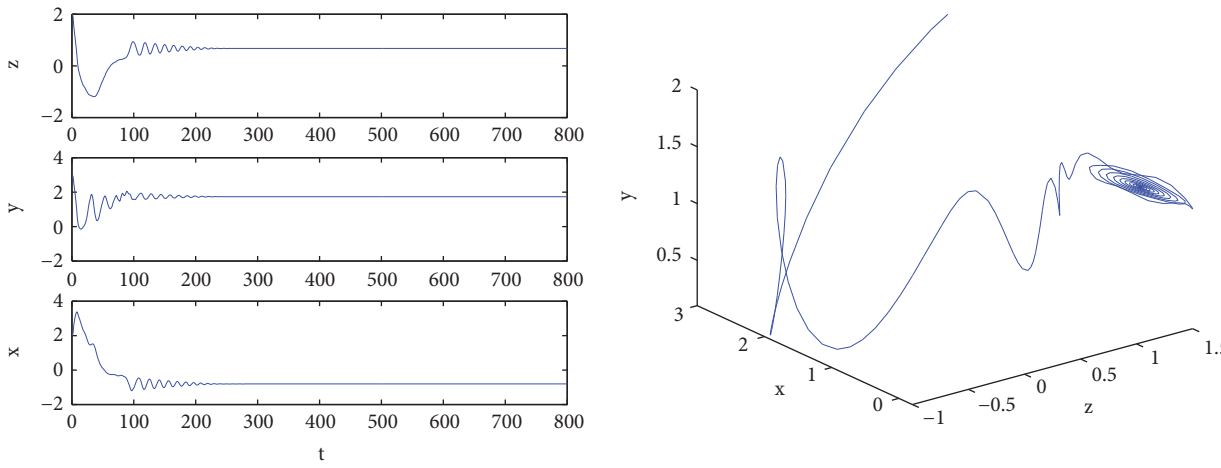

Figure 9: $\mathbf{E}_+^*$ becomes stable and chaos disappears with $\tau_1 = 0.1$ and $\tau_2 = 1.8$.

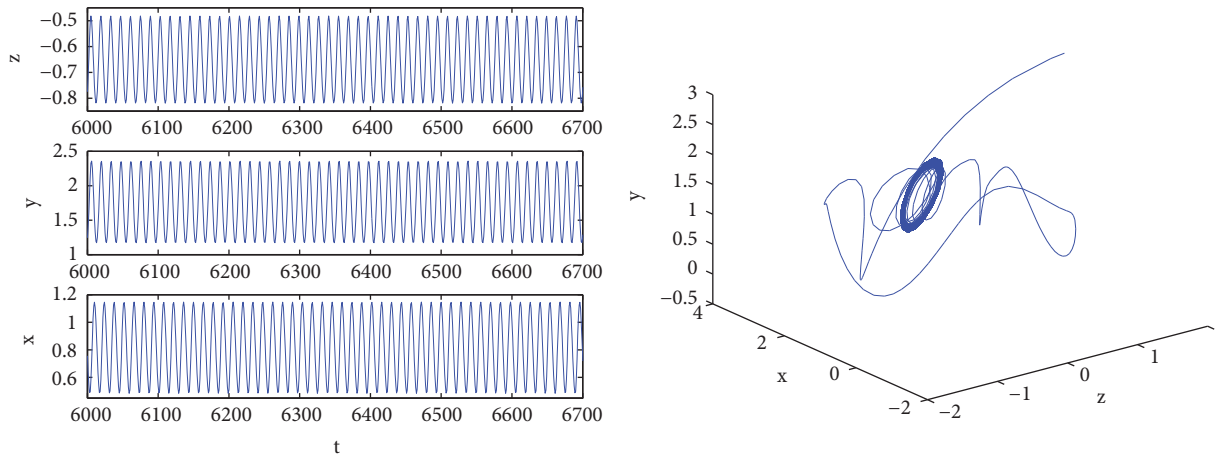

Figure 10: $\mathbf{E}_+^*$ is unstable, and a periodic solution appears with $\tau_1 = 0.1$ and $\tau_2 = 3.9$.

Using the same methods, it can also obtain the similar results in the following systems by choosing suitable k_1, k_2:

$$\begin{aligned}\dot{X}(t) &= Z + (Y - a)X + k_1\left[X(t) - X\left(t - \tau_1\right)\right],\\ \dot{Y}(t) &= 1 - bY - X^2,\\ \dot{Z}(t) &= -X - cZ + k_2\left[Z(t) - Z\left(t - \tau_2\right)\right],\end{aligned} \tag{50}$$

and

$$\begin{aligned}\dot{X}(t) &= Z + (Y - 0.9)X,\\ \dot{Y}(t) &= 1 - 0.2Y - X^2 + k_1\left[Y(t) - Y\left(t - \tau_2\right)\right],\\ \dot{Z}(t) &= -X - 1.2Z + k_2\left[Z(t) - Z\left(t - \tau_1\right)\right].\end{aligned} \tag{51}$$

In [48], Chen investigated the dynamics of system (2) with three delays by numerical simulations with $k_1 = k_2 = k_3 = 0.1$ and $\tau_1 = \tau_2 = \tau_3$, and Chen found that the dynamics of this case have become more complex (the inverse period doubling, period doubling routes, and chaos). Next, we further consider system (2) with three delays by numerical simulations with $a = 0.9, b = 0.2, c = 1.2$, $k_1 = -1, k_2 = -2$, and $k_3 = -0.5$. System (2) becomes

$$\begin{aligned}\dot{X}(t) &= Z + (Y - 0.9)X - \left[X(t) - X\left(t - \tau_1\right)\right],\\ \dot{Y}(t) &= 1 - 0.2Y - X^2 - 2\left[Y(t) - Y\left(t - \tau_2\right)\right],\\ \dot{Z}(t) &= -X - 1.2Z - 0.5\left[Z(t) - Z\left(t - \tau_3\right)\right].\end{aligned} \tag{52}$$

We find that when $\tau_1 = \tau_2 = \tau_3 = 0.1$, system (52) has chaos phenomenon (see Figure 11), while when $\tau_1 = 0.1, \tau_2 = 2, \tau_3 = 0.2$, chaos phenomenon disappears and the solutions of system (52) trend to stable equilibrium (see Figure 12). Using the same methods, we can also give the theory analysis of the above result for system (2) and the similar conclusions can be obtained.

Finally, it will investigate the effect of b for system (1) for chaos to generate. Firstly, we fix $a = 0.9$ and $c > 2.852$; it can obtain the Hopf bifurcation curve in (c, b) plane (see Figure 13). When $c > 2.852$ is chosen, it can obtain b value where Hopf bifurcation will occur. The conditions here are

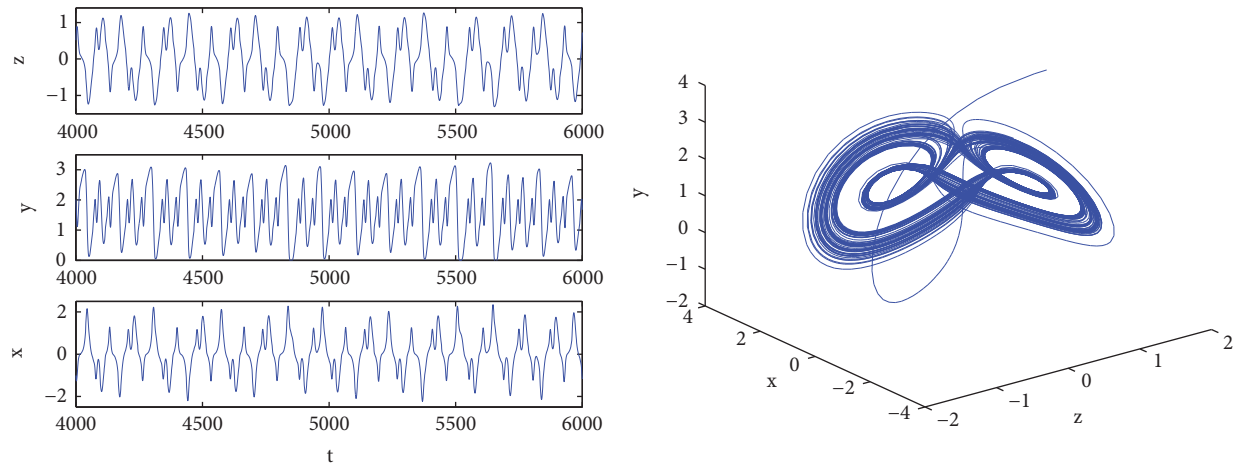

Figure 11: The equilibrium is unstable and chaos exists for system (52) with $\tau_1 = \tau_2 = \tau_3 = 0.1$.

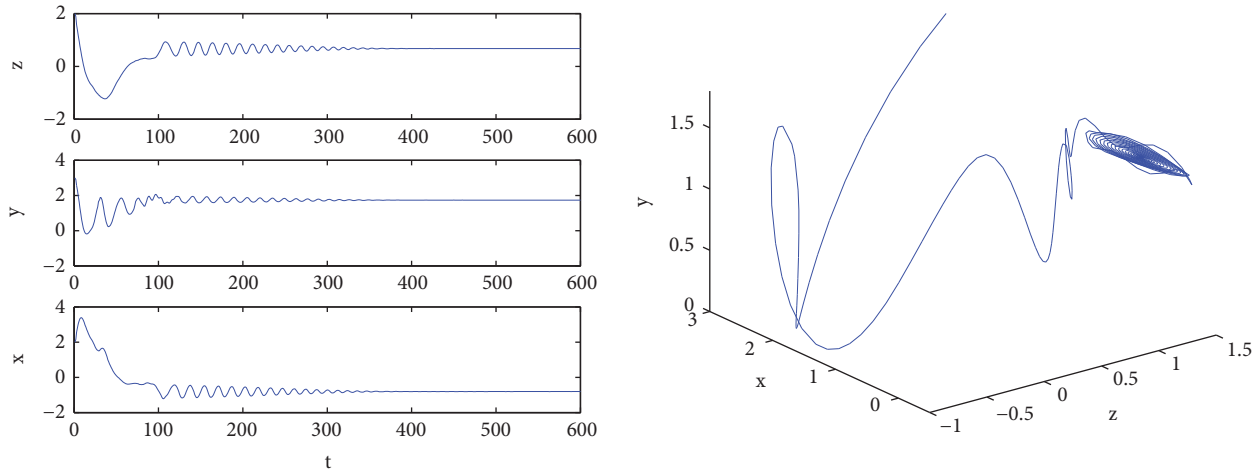

Figure 12: The equilibrium becomes stable and chaos disappears for system (52) with $\tau_1 = 0.1$, $\tau_2 = 2$, and $\tau_3 = 0.2$.

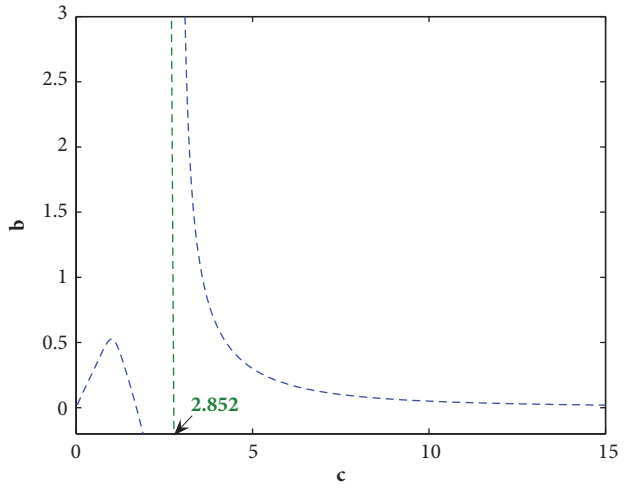

Figure 13: The bifurcation curve in (c,b) plane for system (1) with $a = 0.9$.

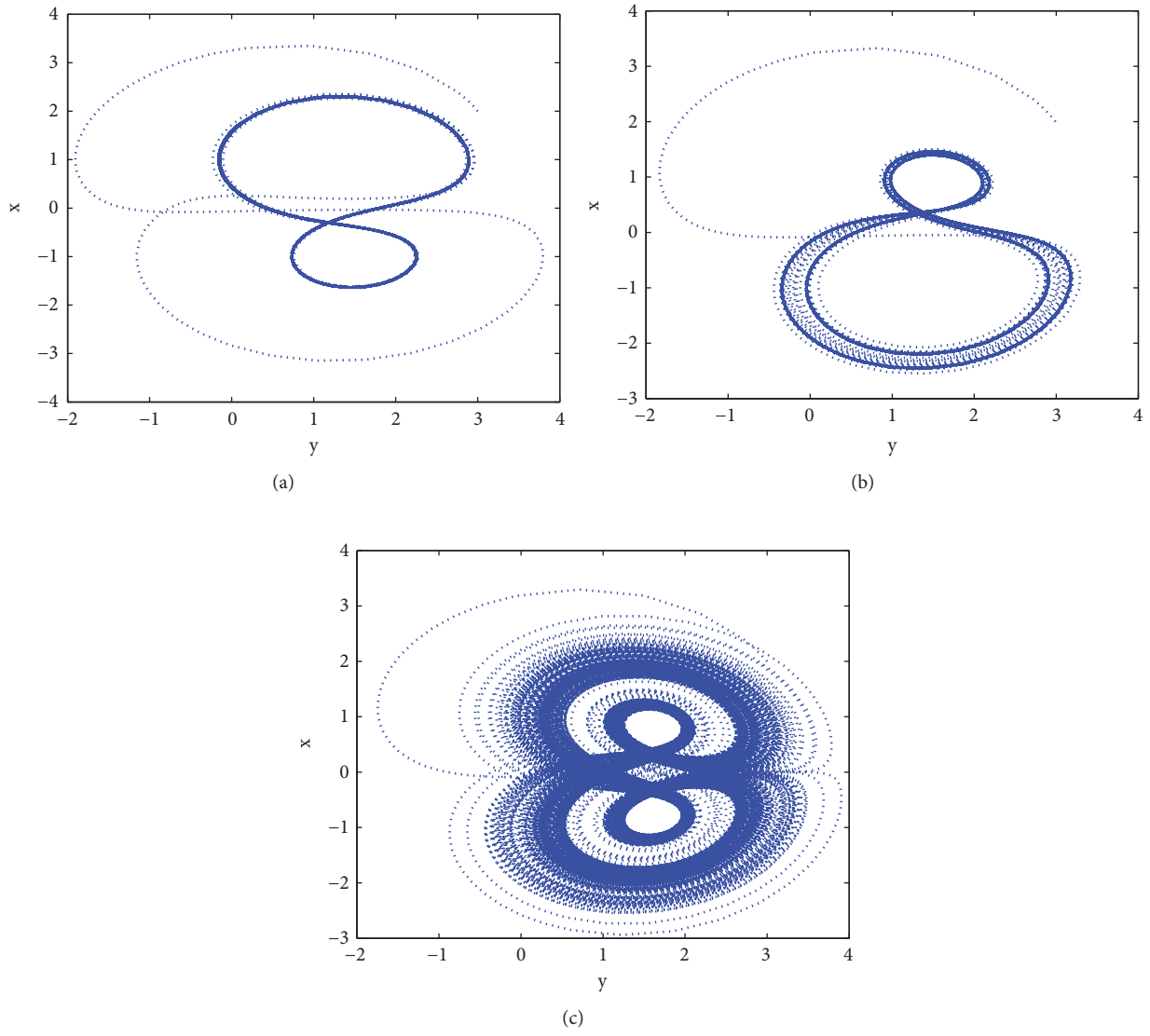

Figure 14: For (a), $b = 0.01$. For (b), $b = 0.1$. For (c), $b = 0.2$.

just sufficient for the existence of Hopf bifurcation about b parameter.

Next, we fix $a = 0.9$, $c = 1.2$, choosing $b = 0.01, 0.1, 0.2$, respectively. When $b = 0.01$, system has a periodic solution. Increasing b, system will produce period doubling bifurcation and ultimately lead to chaos (see Figures 14 and 15). These show that the cost per investment b makes system change from order to chaos, which means the importance of the cost per investment to control chaos.

5. Local Sensitivity Analysis

Local sensitivity analysis index allows us to measure the relative change of a state variable as parameter changing. Next, we use the following definition of normalized forward sensitivity index to perform local sensitivity analysis and compute normalized sensitivity indices.

Definition 13 (see [63]). The normalized forward sensitivity index of a variable, $\mathbf{u}$, that depends differentiably on a parameter, q, is defined as

$$\Upsilon_q^{\mathbf{u}} = \frac{\partial \mathbf{u}}{\partial q} \times \frac{q}{\mathbf{u}}. \tag{53}$$

To perform local sensitivity analysis, we set $a = 0.9, b = 0.2, c = 1.2$.

Tables 1–3 show the effect of parameters a, b, c on equilibrium $\mathbf{E}_+^*(x^*, y^*, z^*)$.

Table 1 shows that decreasing (respectively, increasing) the savings amount a by 1% will increase (respectively, decrease) the interest rate x^* by 0.1378%. Decreasing (respectively, increasing) the cost per investment b by 1% will increase (respectively, decrease) the interest rate x^* by 0.2653%. Increasing (respectively, decreasing) the elasticity

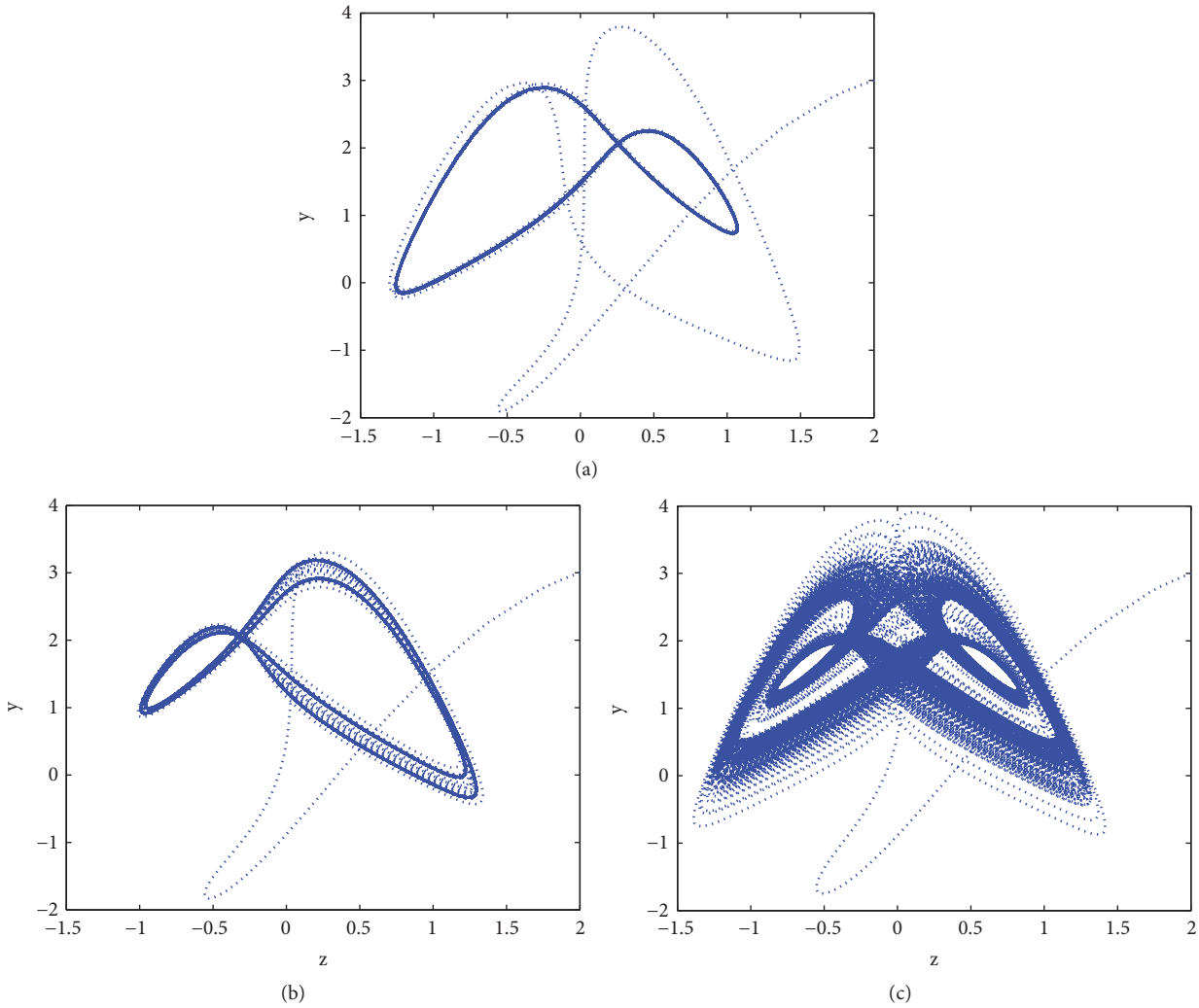

Figure 15: For (a), $b = 0.01$. For (b), $b = 0.1$. For (c), $b = 0.2$.

Table 1: Normalized sensitivity indexes and order of importance of x^* to the three parameters evaluated at the values $a = 0.9$, $b = 0.2$, and $c = 1.2$.

Parameter	Local sensitivity index	Order of importance
a	-0.1378	2
b	-0.2653	1
c	+0.1276	3

Table 2: Normalized sensitivity indexes and order of importance of y^* to the three parameters evaluated at the values $a = 0.9$, $b = 0.2$, and $c = 1.2$.

Parameter	Local sensitivity index	Order of importance
a	+0.5192	1
b	0	3
c	-0.4808	2

of demand of commercial markets c by 1% will increase (respectively, decrease) the interest rate x^* by 0.1276%. The conclusion is that the cost per investment is the most important factor to the interest rate.

Table 2 shows that increasing (decreasing) the savings amount a by 1% will increase (decrease) the investment demand y^* by 0.5192%. Decreasing (respectively, increasing) the cost per investment c by 1% will increase (decrease) the investment demand y^* by 0.4808%. The conclusion is that the savings amount is the most important factor to the investment demand.

Table 3 shows that decreasing (increasing) the savings amount a by 1% will increase (decrease) the price index z^* by 0.1378%. Decreasing (increasing) the cost per investment b by 1% will increase (decrease) the price index z^* by 0.2653%. Decreasing (increasing) the elasticity of demand of commercial markets c by 1% will increase (decrease) the price index z^* by 0.8724%. The conclusion is that the elasticity of

Table 3: Normalized sensitivity indexes and order of importance of z^* to the three parameters evaluated at the values $a = 0.9$, $b = 0.2$, and $c = 1.2$.

Parameter	Local sensitivity index	Order of importance
a	-0.1378	3
b	-0.2653	2
c	-0.8724	1

demand of commercial markets is the most important factor to the price index.

6. Conclusions and Discussions

Bifurcation in nonlinear finance system with one delay has been studied by many researchers. However, there are few papers to focus on nonlinear finance system with multiple delay feedback control. In this paper, we analyze a chaotic finance system using double delayed feedback control and find that the stability switches can occur when τ_1 varies in the case of $\tau_2 = 0$. The conclusion shows that if the saving amount, cost per investment, and the elasticity of demand are fixed, the feedback control used on the interest rate term can cause periodic fluctuations of the system when the feedback strength is fixed and chaotic phenomenon vanish. That is, it is effective in eliminating financial crisis using delayed feedback control in the interest rate term.

Then fix τ_1 in a stability interval, regarding τ_2 as parameter; it can show that there exists the first critical value of τ_2 at which the equilibrium loses its stability and the Hopf bifurcation occurs. These conclusions show that if the feedback control used on the interest rate term under some delay is invalid to remove chaos, then it may add the feedback control to the investment demand term at the same time, which can make chaos disappear and the system produces regular vibrations. The results tell us that the double delayed feedback control can be considered better method than single delayed feedback control for the control of chaotic attractor.

Our results show that, for a class of chaotic finance system, the chaos oscillation can be controlled by delays. In addition, by choosing different delays and numerical simulations, we improve the results in [48] and show that the multiple delayed feedback control is more effective than one delayed feedback control.

In addition, we also obtain that system can produce chaos by period doubling bifurcation when increasing the cost per investment b, which means the importance of the cost per investment to control chaos. At last, local sensitivity analyses of parameters a, b, c on equilibrium are given. The conclusions are that the cost per investment is the most important factor to the interest rate; the savings amount is the most important factor to the investment demand; the elasticity of demand of commercial markets is the most important factor to the price index.

Data Availability

All the data in this study is hypothetical to verify the correctness of the theoretical results.

Conflicts of Interest

The authors declare that there are no conflicts of interest regarding the publication of this paper.

Acknowledgments

Z. Jiang was supported by National Natural Science Foundation of China (nos. 11801014 and 11875001), Natural Science Foundation of Hebei Province (no. A2018409004), and Doctoral Research Fund Project of North China Institute of Aerospace Engineering from China (no. BKY-2016-01); Y. Guo was supported by Scientific Research Project of Beijing Polytechnic College from China (no. bgzyky201744z); T. Zhang was supported by SDUST Research Funds (no. 2014TDJH102) and Scientific Research Foundation of Shandong University of Science and Technology for Recruited Talents.

References

[1] Z. Zhang, H. Shao, Z. Wang, and H. Shen, "Reduced-order observer design for the synchronization of the generalized Lorenz chaotic systems," *Applied Mathematics and Computation*, vol. 218, no. 14, pp. 7614–7621, 2012.

[2] Y. Li, X. Huang, Y. Song, and J. Lin, "A new fourth-order memristive chaotic system and its generation," *International Journal of Bifurcation and Chaos*, vol. 25, no. 11, Article ID 1550151, 2015.

[3] S. A. David, J. A. Machado, D. D. Quintino, and J. M. Balthazar, "Partial chaos suppression in a fractional order macroeconomic model," *Mathematics and Computers in Simulation*, vol. 122, pp. 55–68, 2016.

[4] M. Guo, Y. Xue, Z. Gao, Y. Zhang, G. Dou, and Y. Li, "Dynamic analysis of a physical sbt memristor-based chaotic circuit," *International Journal of Bifurcation and Chaos*, vol. 27, no. 13, Article ID 1730047, 2017.

[5] F. X. An and F. Q. Chen, "Multipulse orbits and chaotic dynamics of an aero-elastic fgp plate under parametric and primary excitations," *International Journal of Bifurcation and Chaos*, vol. 27, no. 04, Article ID 1750050, 2017.

[6] J. Ma and Y. Chen, "Study for the bifurcation topological structure and the global complicated character of a kind of nonlinear finance system (i)," *Applied Mathematics and Mechanics*, vol. 22, no. 11, pp. 1240–1251, 2001.

[7] J. H. Ma and Y. S. Chen, "Study for the bifurcation topological structure and the global complicated character of a kind of nonlinear finance system (ii)," *Applied Mathematics and Mechanics*, vol. 22, pp. 1375–1382, 2001.

[8] Z. Wang, X. Huang, and G. D. Shi, "Analysis of nonlinear dynamics and chaos in a fractional order financial system with time delay," *Computers & Mathematics with Applications*, vol. 62, no. 3, pp. 1531–1539, 2011.

[9] Baogui Xin and Yuting Li, "0-1 Test for Chaos in a Fractional Order Financial System with Investment Incentive," *Abstract and Applied Analysis*, vol. 2013, Article ID 876298, 10 pages, 2013.

[10] M. Yang, B. Cai, and G. Cai, "Projective synchronization of a modified three-dimensional chaotic finance system," *International Journal of Nonlinear Science*, vol. 10, no. 1, pp. 32–38, 2010.

[11] E. Ott, C. Grebogi, and J. A. Yorke, "Controlling chaos," *Physical Review Letters*, vol. 64, no. 11, pp. 1196–1199, 1990.

[12] L. M. Pecora and T. L. Carroll, "Synchronization in chaotic systems," *Physical Review Letters*, vol. 64, no. 8, pp. 821–824, 1990.

[13] K. Tanaka, T. Ikeda, and H. O. Wang, "A unified approach to controlling chaos via an lmi-based fuzzy control system design," *IEEE Transactions on Circuits and Systems I: Fundamental Theory and Applications*, vol. 45, no. 10, pp. 1021–1040, 1998.

[14] T. Zhang, X. Meng, Y. Song, and T. Zhang, "A stage-structured predator-prey SI model with disease in the prey and impulsive effects," *Mathematical Modelling and Analysis*, vol. 18, no. 4, pp. 505–528, 2013.

[15] F. Bian, W. Zhao, Y. Song, and R. Yue, "Dynamical analysis of a class of prey-predator model with beddington-deangelis functional response, stochastic perturbation, and impulsive toxicant input," *Complexity*, vol. 2017, Article ID 3742197, 18 pages, 2017.

[16] T. Zhang, W. Ma, X. Meng, and T. Zhang, "Periodic solution of a prey-predator model with nonlinear state feedback control," *Applied Mathematics and Computation*, vol. 266, pp. 95–107, 2015.

[17] H. Liu and H. Cheng, "Dynamic analysis of a prey–predator model with state-dependent control strategy and square root response function," *Advances in Difference Equations*, vol. 2018, no. 63, 2018.

[18] J. Wang, H. Cheng, H. Liu, and Y. Wang, "Periodic solution and control optimization of a prey-predator model with two types of harvesting," *Advances in Difference Equations*, vol. 2018, no. 1, 2018.

[19] M. Rafikov and J. M. Balthazar, "On control and synchronization in chaotic and hyperchaotic systems via linear feedback control," *Communications in Nonlinear Science and Numerical Simulation*, vol. 13, no. 7, pp. 1246–1255, 2008.

[20] N. J. Peruzzi, F. R. Chavarette, J. M. Balthazar, A. M. Tusset, A. L. Perticarrari, and R. M. Brasil, "The dynamic behavior of a parametrically excited time-periodic mems taking into account parametric errors," *Journal of Vibration and Control*, vol. 22, no. 20, pp. 4101–4110, 2016.

[21] Y. Li, H. Cheng, J. Wang, and Y. Wang, "Dynamic analysis of unilateral diffusion Gompertz model with impulsive control strategy," *Advances in Difference Equations*, vol. 2018, no. 32, 2018.

[22] J. Wang, H. Cheng, X. Meng, and B. G. Pradeep, "Geometrical analysis and control optimization of a predator-prey model with multi state-dependent impulse," *Advances in Difference Equations*, vol. 2017, no. 252, 2017.

[23] J. Wang, H. Cheng, Y. Li, and X. Zhang, "The geometrical analysis of a predator-prey model with multi-state dependent impulses," *Journal of Applied Analysis and Computation*, vol. 8, no. 2, pp. 427–442, 2018.

[24] X. Meng, F. Li, and S. Gao, "Global analysis and numerical simulations of a novel stochastic eco-epidemiological model with time delay," *Applied Mathematics and Computation*, vol. 339, pp. 701–726, 2018.

[25] V. Pyragas and K. Pyragas, "Delayed feedback control of the lorenz system: An analytical treatment at a subcritical hopf bifurcation," *Physical Review E: Statistical, Nonlinear, and Soft Matter Physics*, vol. 73, Article ID 036215, 2006.

[26] H. Chang, Z. Wang, Y. Li, and G. Chen, "Dynamic analysis of a bistable bi-local active memristor and its associated oscillator system," *International Journal of Bifurcation and Chaos*, vol. 28, no. 08, Article ID 1850105, 2018.

[27] X. Guan, G. Feng, and C. Chen, "A stabilization method of chaotic systems based on full delayed feedback controller design," *Physics Letters A*, vol. 348, no. 3, pp. 210–221, 2006.

[28] J. Zhang, X. Wu, L. Xing, C. Zhang, H. Iu, and T. Fernando, "Bifurcation analysis of five-level cascaded H-bridge inverter using proportional-resonant plus time-delayed feedback," *International Journal of Bifurcation and Chaos*, vol. 26, no. 11, Article ID 1630031, 2016.

[29] Y. Song, A. Miao, T. Zhang, X. Wang, and J. Liu, "Extinction and persistence of a stochastic SIRS epidemic model with saturated incidence rate and transfer from infectious to susceptible," *Advances in Difference Equations*, vol. 2018, no. 293, 2018.

[30] A. Ahlborn and U. Parlitz, "Stabilizing unstable steady states using multiple delay feedback control," *Physical Review Letters*, vol. 93, Article ID 264101, 2004.

[31] A. Ahlborn and U. Parlitz, "Controlling dynamical systems using multiple delay feedback control," *Physical Review E: Statistical, Nonlinear, and Soft Matter Physics*, vol. 72, Article ID 016206, 2005.

[32] Z. Yan, G. Zhang, J. Wang, and W. Zhang, "State and output feedback finite-time guaranteed cost control of linear itô stochastic systems," *Journal of Systems Science & Complexity*, vol. 28, no. 4, pp. 813–829, 2015.

[33] J. Wang, K. Liang, X. Huang, Z. Wang, and H. Shen, "Dissipative fault-tolerant control for nonlinear singular perturbed systems with Markov jumping parameters based on slow state feedback," *Applied Mathematics and Computation*, vol. 328, no. 1, pp. 247–262, 2018.

[34] J. Chen, T. Zhang, Z. Zhang, C. Lin, and B. Chen, "Stability and output feedback control for singular Markovian jump delayed systems," *Mathematical Control and Related Fields*, vol. 8, no. 2, pp. 475–490, 2018.

[35] T. Zhang, X. Liu, X. Meng, and T. Zhang, "Spatio-temporal dynamics near the steady state of a planktonic system," *Computers & Mathematics with Applications*, vol. 75, no. 12, pp. 4490–4504, 2018.

[36] W. Wang and T. Zhang, "Caspase-1-mediated pyroptosis of the predominance for driving CD4 + T cells death: A nonlocal spatial mathematical model," *Bulletin of Mathematical Biology*, vol. 80, no. 3, pp. 540–582, 2018.

[37] T. Zhang, W. Ma, and X. Meng, "Global dynamics of a delayed chemostat model with harvest by impulsive flocculant input," *Advances in Difference Equations*, vol. 2017, no. 115, 2017.

[38] T. Zhang, X. Meng, and T. Zhang, "Global analysis for a delayed SIV model with direct and environmental transmissions," *Journal of Applied Analysis and Computation*, vol. 6, no. 2, pp. 479–491, 2016.

[39] T. Zhang, X. Meng, and T. Zhang, "Global dynamics of a virus dynamical model with cell-to-cell transmission and cure rate," *Computational and Mathematical Methods in Medicine*, vol. 2015, Article ID 758362, 8 pages, 2015.

[40] L. D. Cesare and M. Sportelli, "A dynamic IS-LM model with delayed taxation revenues," *Chaos, Solitons & Fractals*, vol. 25, no. 1, pp. 233–244, 2005.

[41] L. Fanti and P. Manfredi, "Chaotic business cycles and fiscal policy: an IS-LM model with distributed tax collection lags," *Chaos, Solitons & Fractals*, vol. 32, no. 2, pp. 736–744, 2007.

[42] M. Neamtu, D. Opris, and C. Chilarescu, "Hopf bifurcation in a dynamic IS-LM model with time delay," *Chaos, Solitons & Fractals*, vol. 34, no. 2, pp. 519–530, 2007.

[43] I. SenGupta, "Generalized BN–S stochastic volatility model for option pricing," *International Journal of Theoretical and Applied Financee*, vol. 19, no. 02, Article ID 1650014, 2016.

[44] A. Issaka and I. SenGupta, "Analysis of variance based instruments for Ornstein-Uhlenbeck type models: swap and price index," *Annals of Finance*, vol. 13, no. 4, pp. 401–434, 2017.

[45] Y. Ding, W. Jiang, and H. Wang, "Hopf-pitchfork bifurcation and periodic phenomena in nonlinear financial system with delay," *Chaos, Solitons & Fractals*, vol. 45, no. 8, pp. 1048–1057, 2012.

[46] R. Zhang, "Bifurcation analysis for a kind of nonlinear finance system with delayed feedback and its application to control of chaos," *Journal of Applied Mathematics*, vol. 2012, Article ID 316390, 18 pages, 2012.

[47] Q. Gao and J. Ma, "Chaos and Hopf bifurcation of a finance system," *Nonlinear Dynamics*, vol. 58, no. 209, 2009.

[48] W.-C. Chen, "Dynamics and control of a financial system with time-delayed feedbacks," *Chaos, Solitons & Fractals*, vol. 37, no. 4, pp. 1198–1207, 2008.

[49] W.-S. Son and Y.-J. Park, "Delayed feedback on the dynamical model of a financial system," *Chaos, Solitons & Fractals*, vol. 44, no. 4, pp. 208–217, 2011.

[50] M. Yang and G. Cai, "Chaos control of a non-linear finance system," *Journal of Uncertain Systems*, vol. 5, no. 4, pp. 263–270, 2011.

[51] X. Fan, Y. Song, and W. Zhao, "Modeling Cell-to-Cell Spread of HIV-1 with Nonlocal Infections," *Complexity*, vol. 2018, Article ID 2139290, 10 pages, 2018.

[52] A. Q. Khan and A. Sharif, "Some 3×6 systems of exponential difference equations," *Discrete Dynamics in Nature and Society*, vol. 2018, Article ID 8362837, 35 pages, 2018.

[53] T. Zhang, T. Zhang, and X. Meng, "Stability analysis of a chemostat model with maintenance energy," *Applied Mathematics Letters*, vol. 68, pp. 1–7, 2017.

[54] Z. Chang, X. Meng, and T. Zhang, "A new way of investigating the asymptotic behaviour of a stochastic SIS system with multiplicative noise," *Applied Mathematics Letters*, vol. 87, pp. 80–86, 2019.

[55] S. Ruan and J. Wei, "On the zeros of a third degree exponential polynomial with applications to a delayed model for the control of testosterone secretion," *IMA Journal of Maths with Applications in Medicine & Biology*, vol. 18, pp. 41–52, 2001.

[56] S. Ruan and J. Wei, "On the zeros of transcendental functions with applications to stability of delay differential equations with two delays," *Dynamics of Continuous, Discrete and Impulsive Systems Series A: Mathematical Analysis*, vol. 10, no. 6, pp. 863–874, 2003.

[57] J. H. Hale, *Theory of Functional Differential Equations*, Springer, New York, NY, USA, 1977.

[58] L. Li, Z. Wang, Y. Li, H. Shen, and J. Lu, "Hopf bifurcation analysis of a complex-valued neural network model with discrete and distributed delays," *Applied Mathematics and Computation*, vol. 330, pp. 152–169, 2018.

[59] Z. Jiang and L. Wang, "Global Hopf bifurcation for a predator-prey system with three delays," *International Journal of Bifurcation and Chaos*, vol. 27, no. 07, Article ID 1750108, 2017.

[60] Z. Wang, X. Wang, Y. Li, and X. Huang, "Stability and hopf bifurcation of fractional-order complex-valued single neuron model with time delay," *International Journal of Bifurcation and Chaos*, vol. 27, no. 13, Article ID 1750209, 2017.

[61] A. Miao, T. Zhang, J. Zhang, and C. Wang, "Dynamics of a stochastic SIR model with both horizontal and vertical transmission," *Journal of Applied Analysis and Computation*, vol. 8, no. 4, pp. 1108–1121, 2018.

[62] B. D. Hassard, N. D. Kazarinoff, and Y.-H. Wan, *Theory and Application of Hopf Bifurcation*, Cambridge University Press, Cambridge, UK, 1981.

[63] N. Chitnis, J. M. Hyman, and J. M. Cushing, "Determining important parameters in the spread of malaria through the sensitivity analysis of a mathematical model," *Bulletin of Mathematical Biology*, vol. 70, no. 5, pp. 1272–1296, 2008.

Hindawi
Discrete Dynamics in Nature and Society
Volume 2019, Article ID 8341514, 15 pages
https://doi.org/10.1155/2019/8341514

Research Article

Bifurcations of a New Fractional-Order System with a One-Scroll Chaotic Attractor

Xiaojun Liu[1,2] **Ling Hong**[3] **Lixin Yang**[4] **and Dafeng Tang**[3]

[1]*School of Mathematics and Statistics, Tianshui Normal University, Tianshui 741001, China*
[2]*School of Sciences, Xi'an University of Architecture and Technology, Xi'an 710055, China*
[3]*State Key Laboratory for Strength and Vibration of Mechanical Structures, Xi'an Jiaotong University, Xi'an 710049, China*
[4]*School of Arts and Sciences, Shaanxi University of Science and Technology, Xi'an 710021, China*

Correspondence should be addressed to Xiaojun Liu; flybett3952@126.com

Received 29 August 2018; Revised 27 October 2018; Accepted 12 November 2018; Published 1 January 2019

Guest Editor: Tarek F. Ibrahim

In this paper, a new fractional-order system which has a chaotic attractor of the one-scroll structure is presented. Firstly, the stability of the equilibrium points of the system is investigated. And based on the stability analysis, the generation conditions of the one-scroll structure for the attractor are determined. In a commensurate-order case, bifurcations with the variation of a system parameter are investigated as derivative orders decrease from 0.99. In an incommensurate-order case, bifurcations with the variation of a derivative order are analyzed as other orders decrease from 1.

1. Introduction

Fractional calculus is a field of applied mathematics that deals with derivatives and integrals of arbitrary orders. Although the seeds of fractional derivatives were planted over 300 years ago, the development of fractional calculus is very slow at an early stage for the absence of geometrical interpretation and applications. In the recent several decades, it has been applied to almost every field of science, engineering, economics, secures communication, and so on [1–5].

It is well known that fractional calculus is very suitable for the description of properties of various real materials. Meanwhile, fractional calculus provides an excellent instrument for the description of memory and hereditary properties of various materials and processes. This is the main advantage of fractional derivatives in comparison with classical integer-order models, in which such effects are in fact neglected. The advantages of fractional derivatives become apparent in modeling mechanical and electrical properties of real materials [6].

Many new fractional-order systems were presented in recent years. Meanwhile, rich and complex dynamics, such as periodic solutions, chaos windows, all kinds of bifurcations, boundary, and interior crises were observed in these systems. For example, Chua system with a derivative order 2.7 makes chaos motion [7]. Chaotic dynamics of a damped van der Pol equation with fractional order is investigated in [8]. Chen studied the nonlinear dynamics and chaos in a fractional-order financial system [9]. A periodically forced complex Duffing's oscillator was proposed, and chaos for the system was studied in detail [10]. Bifurcation, chaos control, and synchronization were investigated for a fractional-order Lorenz system with the complex variables [11]. In [12], boundary and interior crises were determined in a fractional-order Duffing system by a global numerical computation method. A proposed standard for the publication of new chaotic systems was studied in [13]. The authors investigated a simple chaotic flow with a plane of equilibria in [14].

It is well known that bifurcation theory concerns the changes in qualitative or topological structures of limiting motions such as equilibriums, periodic solutions, homoclinic orbits, heteroclinic orbits, and invariant tori for nonlinear evolution equations as some relevant parameters in the equations vary. Generally, the subject can be traced back to the very earlier work of Poincare around 1892 [15]. Nowadays, it is a fundamental tool to analyze nonlinear problems which enables us to understand how and when a system organizes new states and patterns near the original "trivial"

one when a control parameter crosses a critical value. For fractional-order systems, a bifurcation implies a qualitative or topological change in dynamics with a variation of a system parameter or derivative order, and bifurcation analysis becomes harder due to the nonlocal property of the operator of fractional calculus. Many references have studied the bifurcations of fractional-order systems [16–20]. However, these investigations mainly focus on the bifurcation of a fractional-order system as a system parameter or a derivative order varies. To our knowledge, few works concerns bifurcations with the variation of both a system parameter and a derivative order or with the variation of both a derivative order and other orders.

Compared with integer-order chaotic systems, fractional-order chaotic systems with more complex dynamic characteristics and more system parameters can provide higher security for secure communication [21, 22]. In [23], the authors investigated the synchronization of a three-dimensional integer-order system. The differential equations of the system with simple structure were similar to those of the Lorenz system. It is well known that the Lorenz system has a chaotic attractor with double-scroll structure. The system in [23] has a chaotic attractor with only one-scroll and very abundant dynamic behaviors. Motivated by the above, in this paper, a corresponding fractional-order system is proposed and studied. Firstly, the stability of equilibrium points of the system is investigated. In a commensurate-order case, bifurcations with the variation of a system parameter are investigated as derivative orders decrease from 0.99. In an incommensurate-order case, bifurcations with the variation of a derivative order are analyzed as the other orders decrease from 1. Period-doubling and saddle-node bifurcations can be observed from the bifurcation diagrams by numerical simulations.

The remainder of the paper is organized as follows. In Section 2, the definitions of the fractional calculus and related preliminaries are given. A new fractional-order system with one-scroll attractor is presented in Section 3. In Section 4, bifurcations in the two cases of commensurate-order and incommensurate-order are analyzed, respectively. Conclusions of the paper are drawn in Section 5.

2. Fractional Derivatives and Preliminaries

2.1. Definitions. Fractional calculus can be considered as a generalization of integration and differentiation. The operator ${}_aD_t^q$ of fractional calculus can be defined by

$$ {}_aD_t^q = \begin{cases} \dfrac{d^q}{dt^q} & R(q) > 0 \\ 1 & R(q) = 0 \\ \displaystyle\int_a^t (d\tau)^q & R(q) < 0, \end{cases} \tag{1} $$

where q denotes the derivative order and $R(q)$ corresponds to the real part of q. The numbers a and t represent the limits of the operator.

In general, three definitions of fractional derivative are used frequently, namely, the Grunwald-Letnikov definition, the Riemann-Liouville, and the Caputo definitions [6, 24].

The Grunwald-Letnikov definition (GL) derivative with fractional order q can be described by

$$ {}_a^{GL}D_t^q = \lim_{h\to 0} \frac{1}{h^q} \sum_{j=0}^{[(t-a)/h]} (-1)^q \binom{q}{j} f(t-jh), \tag{2} $$

where the symbol $[\cdot]$ represents the integer part.

The Riemann-Liouville (RL) definition is

$$ {}_a^{RL}D_t^q f(t) = \frac{d^n}{dt^n} \frac{1}{\Gamma(n-q)} \int_a^t \frac{f(\tau)}{(t-\tau)^{q-n+1}} d\tau, \quad n-1 < q < n, \tag{3} $$

where $\Gamma(\cdot)$ denotes the gamma function.

The Caputo (C) fractional derivative is defined as follows:

$$ {}_a^{C}D_t^q f(t) = \frac{1}{\Gamma(n-q)} \int_a^t (t-\tau)^{n-q-1} f^{(n)}(\tau)\, d\tau, \quad n-1 < q < n. \tag{4} $$

For a fractional differential equation which is defined by Caputo derivatives, the initial condition takes on the same form as those for the integer-order ones, which can be measured easily in applications. For this reason, the Caputo derivative will be adopted in the rest of the paper.

2.2. Numerical Methods. Due to the nonlocal property of the operator of fractional calculus, it is not easy to obtain the numerical solutions for a fractional differential equation. Generally speaking, two approximation methods are frequently used, namely, an improved version of Adams-Bashforth-Moulton algorithm based on the predictor-correctors scheme and the frequency domain approximation [25–28]. For the accuracy [29], we will employ the improved predictor-corrector algorithm to solve a fractional differential equation in this paper.

In order to get the approximate solution of a fractional-order chaotic system by the improved predictor-corrector algorithm, the following equation is considered:

$$ \frac{d^q x}{dt^q} = f(t, x), \quad 0 \le t \le T \qquad x^k(0) = x_0^{(k)} \quad k = 0, 1, \cdots, \lceil q \rceil - 1, \tag{5} $$

which is equivalent to the Volterra integral equation

$$ x(t) = \sum_{k=0}^{\lceil q \rceil - 1} x_0^{(k)} \frac{t^k}{k!} + \frac{1}{\Gamma(q)} \int_0^t (t-\tau)^{(q-1)} f(\tau, x(t))\, d\tau. \tag{6} $$

Now, set $h = T/N$, $t_j = jh$, $(j = 0, 1, \cdots, N)$. The corrector formula for (6) can thus be discretized as follows:

$$x_h(t_{n+1}) = \sum_{k=0}^{\lceil q\rceil-1} x_0^{(k)} \frac{t_{n+1}^k}{k!} + \frac{h^q}{\Gamma(q+2)} f\left(t_{n+1}, x_h^p(t_{n+1})\right) + \frac{h^q}{\Gamma(q+2)} \sum_{j=0}^{n} \alpha_{j,n+1} f\left(t_j, x_h(t_j)\right), \tag{7}$$

where predicted values $x_h(t_{n+1})$ are determined by the following formula:

$$x_h^p(t_{n+1}) = \sum_{k=0}^{\lceil q\rceil-1} x_0^{(k)} \frac{t_{n+1}^k}{k!} + \frac{1}{\Gamma(q)} \sum_{j=0}^{n} \beta_{j,n+1} f\left(t_j, x_h(t_j)\right), \tag{8}$$

and

$$\alpha_{j,n+1} = \begin{cases} n^{q+1} - (n-q)(n+1)^q, & j = 0 \\ (n-j+2)^{q+1} + (n-j)^{q+1} - 2(n-j+1)^{q+1}, & 1 \le j \le n \\ 1, & j = n+1. \end{cases} \tag{9}$$

$$\beta_{j,n+1} = \frac{h^q}{q}\left((n-j+1)^q - (n-j)^q\right), \quad 1 \le j \le n$$

The error estimate of this approach is $\max_{j=0,1,\cdots,N}|x(t_j) - x_h(t_j)| = O(h^P)$, where $p = \min(2, 1+q)$.

2.3. The Stability of a Fractional-Order System. For fractional-order systems, the stability analysis of equilibrium points is complex and difficult due to the nonlocal property of fractional calculus. Here, the definitions of commensurate-order and incommensurate-order fractional-order systems will be given firstly.

Definition 1. For a fractional-order system, which can be described by $d^{\mathbf{q}}\mathbf{x}/dt^{\mathbf{q}} = f(\mathbf{x})$, where $\mathbf{x} = (x_1, x_2, \cdots, x_n)^{\mathrm{T}}$ is the state vector, $\mathbf{q} = (q_1, q_2, \cdots, q_n)^{\mathrm{T}}$ is the fractional derivative orders vector, and $q_i > 0$. The fractional-order system is commensurate-order when all the derivative orders satisfy $q_1 = q_2 = \cdots = q_n$; otherwise it is an incommensurate-order system [30].

In order to investigate the stability of equilibrium points for fractional-order systems, the following lemma is used frequently.

Lemma 2. *For a commensurate fractional-order system, the equilibrium points of the system are asymptotically stable if all the eigenvalues at the equilibrium* E^* *satisfy the following condition:*

$$\left|\arg\left(eig(\mathbf{J})\right)\right| = \left|\arg\left(\lambda_j\right)\right| > \frac{\pi}{2}q, \quad j = 1, 2, \cdots, n, \tag{10}$$

where $\mathbf{J}$ *is the Jacobian matrix of the system evaluated at the equilibria* E^* *[31].*

3. A New Fractional-Order System

In this section, a new fractional-order system which consist of three differential equations is proposed and can be denoted as follows:

$$\begin{aligned} D^{q_1}x &= ax - y \\ D^{q_2}y &= x - z - by \\ D^{q_3}z &= ax + 4z(y-2) \end{aligned} \tag{11}$$

where x, y, and z are state variables of the system, a and b the system parameters, and q_1, q_2, and q_3 derivative orders.

When the derivative orders are selected as $q_1 = q_2 = q_3 = q = 0.99$, the system parameters $a = 0.3$ and $b = 0.02$, and initial conditions $(x_0, y_0, z_0) = (-0.5, -1, 1)$, system (11) is chaotic. In Figures 1(a) and 1(b), a chaotic attractor with a one-scroll on three-dimensional space and projected onto $x - y$ plane are depicted. In this case, the corresponding Lyapunov exponents are $\lambda_1 = 0.117$, $\lambda_2 = 0$, and $\lambda_3 = -10.49$. When the derivative order $q = 0.985$ and $q = 0.965$, the corresponding attractors are displayed in Figures 1(c)–1(f).

The equilibrium points of system (11) can be calculated by solving the equations $D^{q_1}x = 0$, $D^{q_2}y = 0$, and $D^{q_3}z = 0$. The system contains two equilibriums, i.e.,

$$\begin{aligned} &\mathrm{E}_1(0, 0, 0) \\ &\mathrm{E}_2\left(\frac{2}{a} - \frac{1}{4(1-ab)}, a\left(\frac{2}{a} - \frac{1}{4(1-ab)}\right), (1-ab)\right. \\ &\quad \left.\cdot\left(\frac{2}{a} - \frac{1}{4(1-ab)}\right)\right). \end{aligned} \tag{12}$$

The equilibrium E_2 exists when the system parameters satisfy the condition $1 - ab \neq 0$ or $1 - ab \neq a$.

The Jacobin matrix for system (11) evaluated at the equilibrium point (x^*, y^*, z^*) is given by

$$J(x^*, y^*, z^*) = \begin{pmatrix} a & -1 & 0 \\ 1 & -b & -1 \\ a & 4z^* & 4(y^* - 2) \end{pmatrix}. \tag{13}$$

Based on the matrix, the characteristic equation at the equilibriums E_1 is

$$\lambda^3 + (8 + b - a)\lambda^2 + [8(b-a) + 1 - ab]\lambda + 8(1-ab) - a = 0. \tag{14}$$

By the Routh-Hurwitz test, the equilibrium point E_1 has three roots with the negative real parts if and only if $8 + b - a > 0$ and $0 < 8(1-ab) - a < (8+b-a)[8(b-a)+1-ab]$. In our case, when the values of the system parameters are taken as $a = 0.3$, $b = 0.02$, the corresponding eigenvalues for the equilibrium point E_1 are $\lambda_1 = -8.0047$ and $\lambda_{2,3} = -0.1576 \pm 1.0089i$. According to Lemma 2, the equilibrium point E_1 is locally stable.

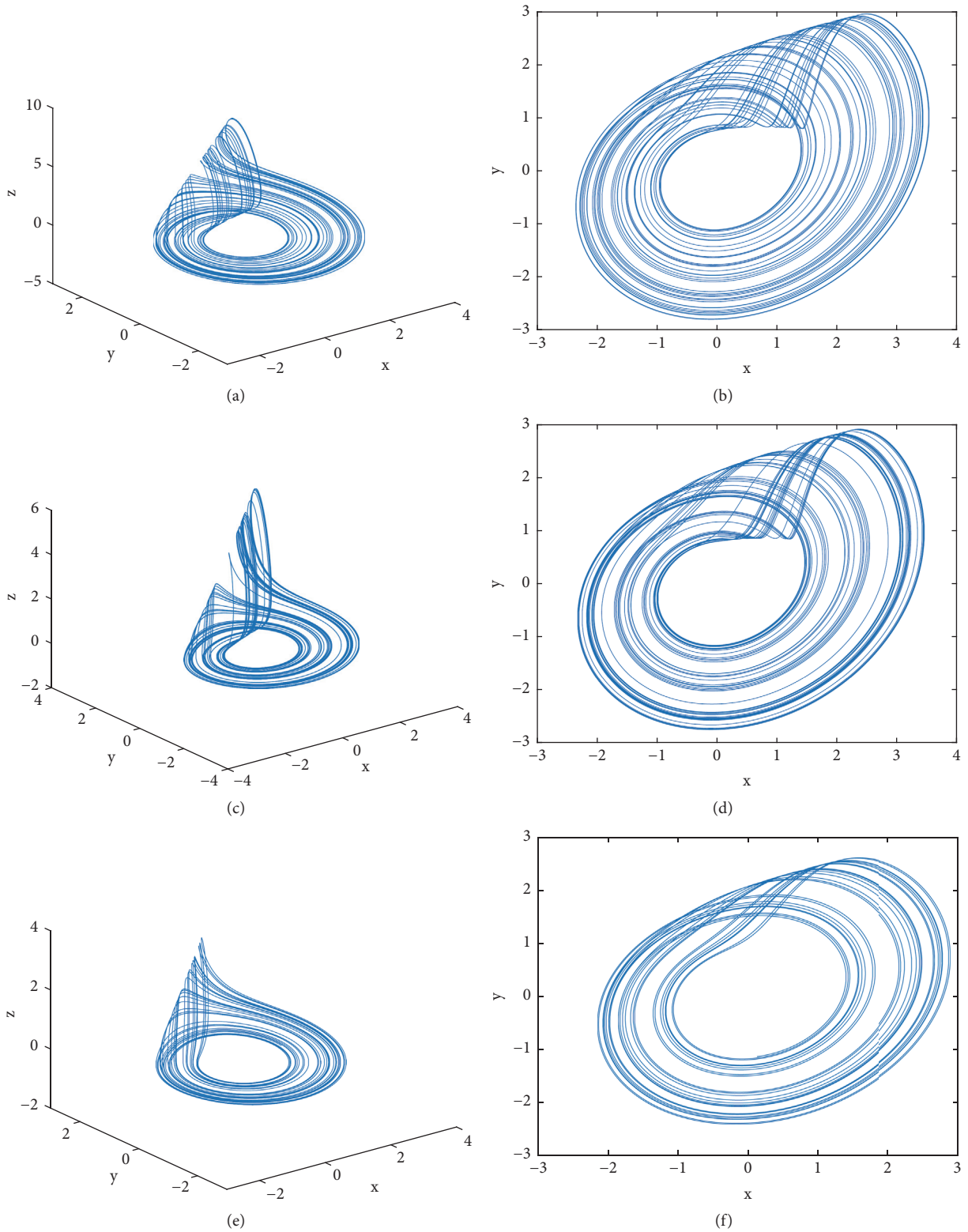

Figure 1: The chaotic attractor of system (11). (a) 3D plot of the attractor when $q = 0.99$; (b) the attractor projected onto $x - y$ plane when $q = 0.99$; (c) 3D plot of the attractor when $q = 0.985$; (d) the attractor projected onto $x - y$ plane when $q = 0.985$; (e) 3D plot of the attractor when $q = 0.965$; (f) the attractor projected onto $x - y$ plane when $q = 0.965$.

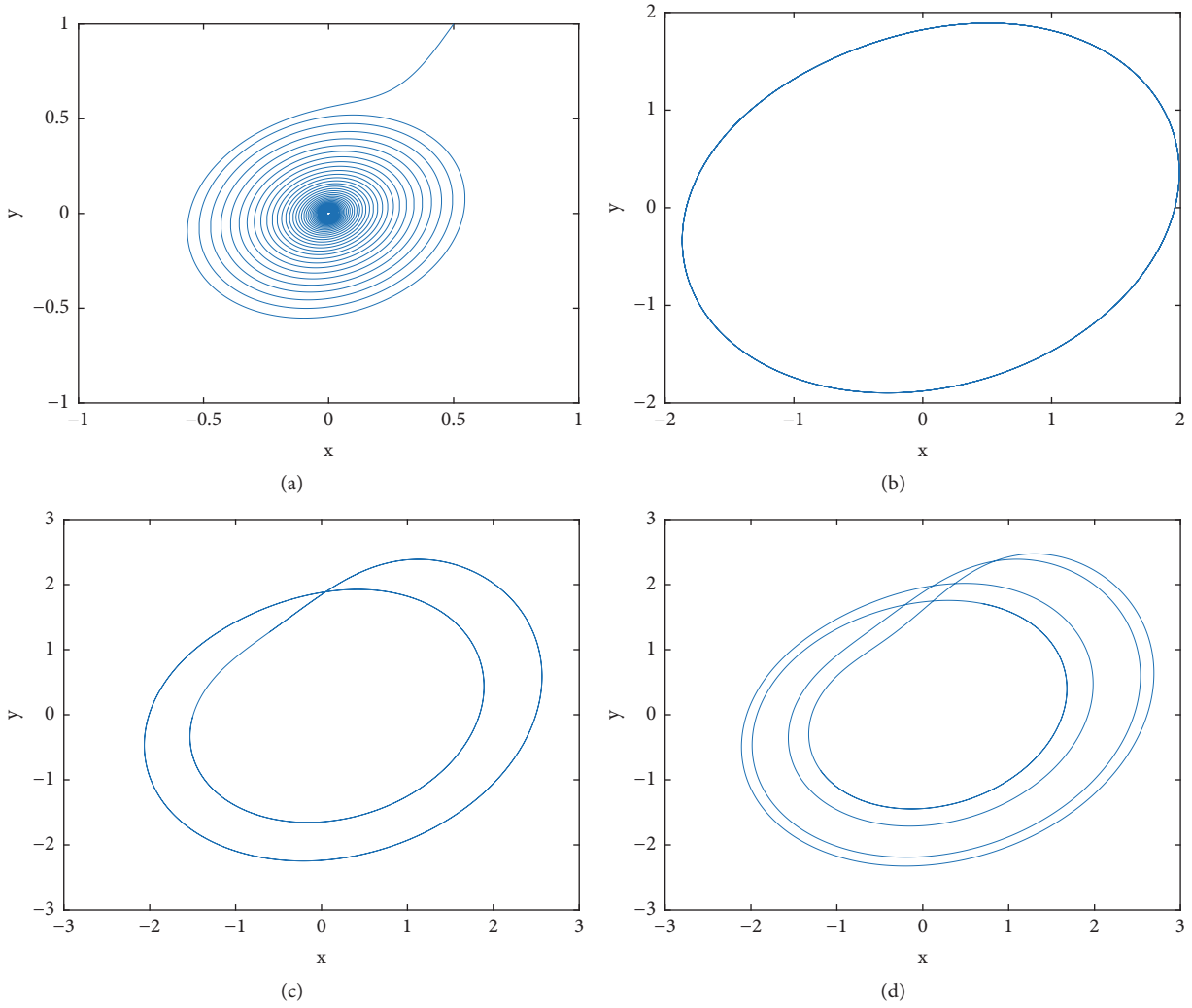

Figure 2: The attractors for different values of the derivative order q. (a) $q = 0.90$; (b) $q = 0.92$; (c) $q = 0.95$; (d) $q = 0.955$.

The characteristic equation at equilibrium E_2 is

$$\lambda^3 + [(b-a) - 4(y-2)]\lambda^2 - [4(y-2)(b-a) + ab - (4z+1)]\lambda + 4(y-2)(ab-1) - a(1+4z) = 0. \quad (15)$$

By the Routh-Hurwitz test, the equilibrium point E_2 has three roots with the negative real parts if and only if $(b-a) - 4(y-2) > 0$ and

$$0 < 4(y-2)(ab-1) - a(1+4z) < [(b-a) - 4(y-2)] \cdot [4(y-2)(b-a) + ab - (4z+1)]. \quad (16)$$

The corresponding eigenvalues for the equilibrium point E_2 are $\lambda_1 = -7.4038$ and $\lambda_{2,3} = 0.1029 \pm 0.9653i$ when the system parameters take the same values as before. Then based on Lemma 2, we can get that the fixed point E_2 is unstable.

In a nonlinear dynamical system, a saddle point is an equilibrium point on which the equivalent linearized model has at least one eigenvalue in the stable region and one eigenvalue in the unstable region. In the same system, a saddle point is called saddle point of index 1 if one of the eigenvalues is unstable and other eigenvalues are stable. Also, a saddle point of index 2 is a saddle point with one stable eigenvalue and two unstable eigenvalues. In chaotic systems, it is proved that scrolls are generated only around the saddle points of index 2. Moreover, saddle points of index 1 are responsible only for connecting scrolls [32, 33].

From the above analysis we can see that the equilibrium point E_2 is a saddle point of index 2. In chaotic systems, it is proved that the scrolls of a chaotic attractor are generated only around the saddle points of index 2. Moreover, the saddle points of index 1 are responsible for connecting the scrolls. In the fractional-order system (11), the equilibrium E_1 is not a saddle point of index 1. The necessary condition for the existence of double-scroll attractor in system (11) cannot be satisfied. Therefore, the chaotic attractor of system (11) is one scroll.

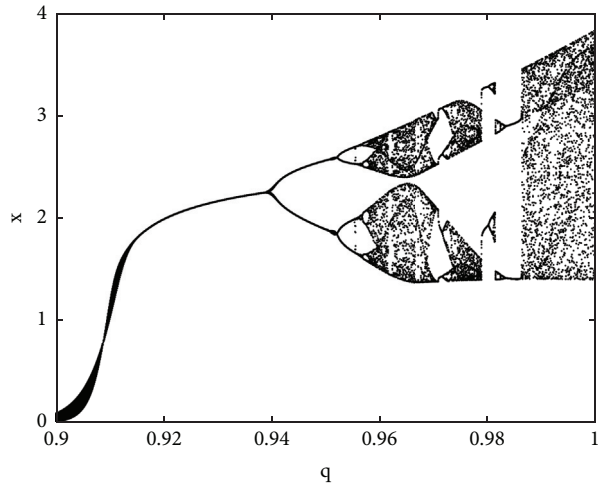

Figure 3: The bifurcation diagram of system (11) with the variation of the derivative order q.

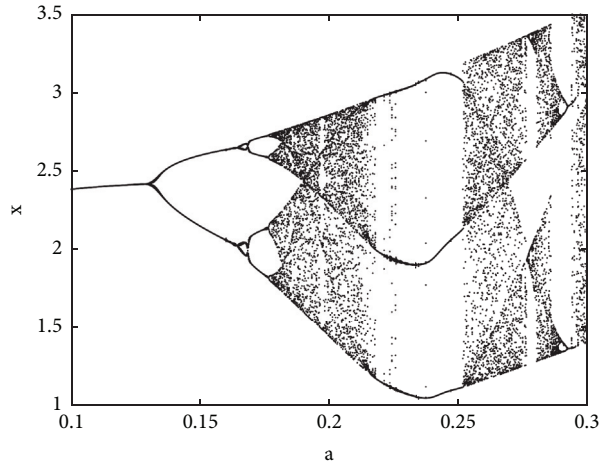

Figure 4: The bifurcation diagram of system (11) with the variation of the system parameter a.

Compared with an integer-order system, the derivative order is an important parameter for a fractional-order system. For system (11), the system parameters and the initial conditions are fixed. The phase diagrams with different values of the derivative order q are employed to demonstrate the behavior of system (11), as shown in Figure 2. From which it can be seen that system (11) converges to a fixed point as $q = 0.90$, and it is period-1 for $q = 0.92$, period-2 for $q = 0.95$, and period-4 for $q = 0.955$.

4. Bifurcations of the New System

Bifurcations play a vital role in dynamics research for fractional-order systems. Therefore, in this section, bifurcation analysis is conducted to study the rich dynamical behavior of the fractional-order system (11) in the two cases of commensurate-order and incommensurate-order, respectively.

4.1. The Commensurate-Order Case. Firstly, with the system parameters fixed and the derivative order varying on the closed interval $q \in [0.9, 1]$, bifurcation diagram for system (11) is depicted in Figure 3. Clearly, the evolution of the period-doubling scenario and saddle-node bifurcation can be observed from this figure. When the order satisfies $q \leq 0.958$, the route of leading to chaos for system (11) is period-doubling bifurcation. When $q = 0.978$, the chaotic solutions disappear suddenly, and two new period-1 solutions appear, which means that the saddle-node bifurcation occurs as the order q varies.

Secondly, bifurcations with the variation of the system parameter a are studied for $q = 0.99$ and $b = 0.02$. In Figure 4, it can be seen that a series of period-doubling bifurcations occurs as the system parameter a decreases from 0.3 to 0.1. Meanwhile, the period-3 and chaos windows can also be observed from the bifurcation diagram.

In order to get a better understanding of the dynamics of system (11), bifurcations with the variation of the parameter a for the different values of derivative order q are given. With the parameter a varying, the corresponding bifurcation diagrams with several specified values of the derivative order like $q = 0.98$, $q = 0.97$, $q = 0.96$, $q = 0.95$, $q = 0.94$, and $q = 0.93$ are plotted in Figure 5 for system (11). Compared these figures, it can be seen that the bifurcation structure

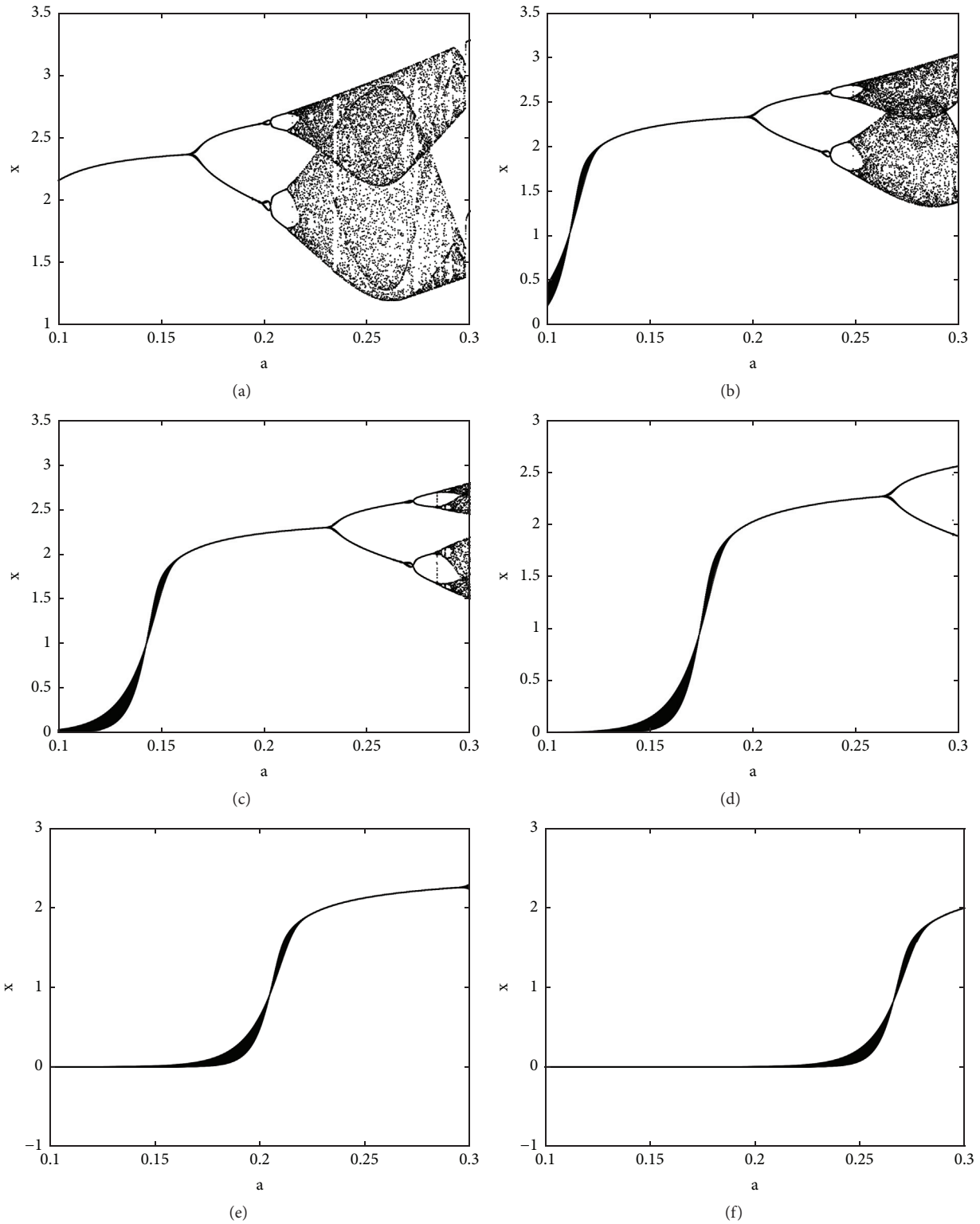

Figure 5: The bifurcation diagrams of system (11) when the parameter a varied with the different values of the order q: (a) $q = 0.98$; (b) $q = 0.97$; (c) $q = 0.96$; (d) $q = 0.95$; (e) $q = 0.94$; (f) $q = 0.93$.

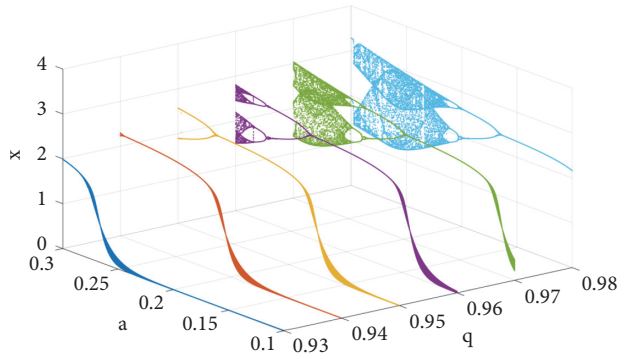

Figure 6: The bifurcation diagram of system (11) in three-dimensional space with the variation of both the parameter a and the order q.

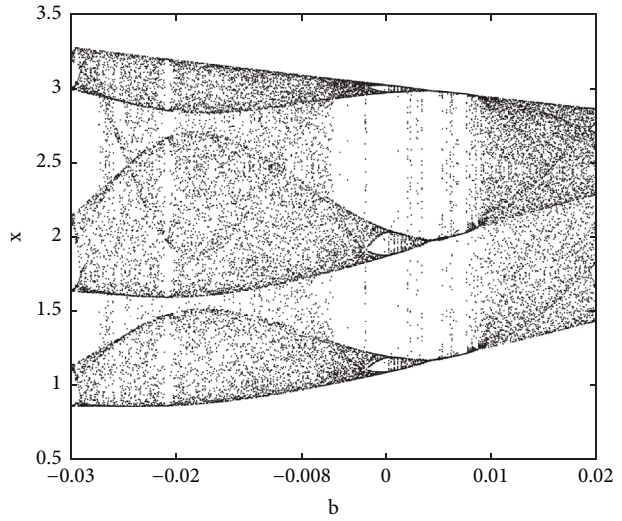

Figure 7: The bifurcation diagram of system (11) with the variation of the parameter b.

of system (11) changes qualitatively with the variation of the parameter a and the order q. The area of the chaotic motion decreases with the augment of the periodic motion as the derivative order decreases. From Figures 5(a)–5(c), it is clear that the route leading to chaos is period-doubling bifurcation. Meanwhile, a typical period-doubling bifurcation, of which numerical solutions change from period-1 to period-2, can be seen clearly from Figures 5(d) and 5(e). The system becomes totally periodic as the order q decreases to 0.93; see Figure 5(f). In order to further discuss the bifurcations with the variation of both the system parameter a and derivative order q, a bifurcation diagram in the three-dimensional space is depicted in Figure 6. It can be seen that dynamics of system (11) becomes simple as the derivative order decreases from 0.98 to 0.93.

Thirdly, the bifurcation of system (11) with the variation of the parameter b is studied for $q = 0.99$ and $a = 0.3$. In Figure 7, there is a long time of the chaotic window for $b \leq -0.008$. Meanwhile, the route leading to chaos is the period-doubling bifurcation for system (11).

Bifurcations with the variation of the parameter b are studied for different values of the derivative order q. When the derivative order q decreases from 0.98 to 0.93, the corresponding bifurcation diagrams are plotted for the fractional-order system (11) when the parameter $b \in [-0.03, 0.02]$; see Figure 8, from which, it is clear that structure of dynamics of system (11) evolves as the order q varies. The interval of the chaotic motion increases and that of the periodic motion decreases. Meanwhile, system (11) is periodic completely when the order $q = 0.94$, and period-4 and period-2 motions can be obtained from Figure 8(e). When the order $q = 0.93$, only period-2 and period-1 motions exist; see Figure 8(f). In order to further discuss the bifurcations with the variation of both the system parameter b and derivative order q, a bifurcation diagram in the three-dimensional space is plotted in Figure 9. It can be seen that dynamics of system (11) becomes complex as the derivative order increases from 0.93 to 0.98.

4.2. The Incommensurate-Order Case. In order to learn more about the characteristics of the new fractional-order system (11), the dynamics of system (11) with the variation of the different derivative orders will be investigated in this subsection. In the following work, the system parameters are taken as $a = 0.3$ and $b = 0.02$.

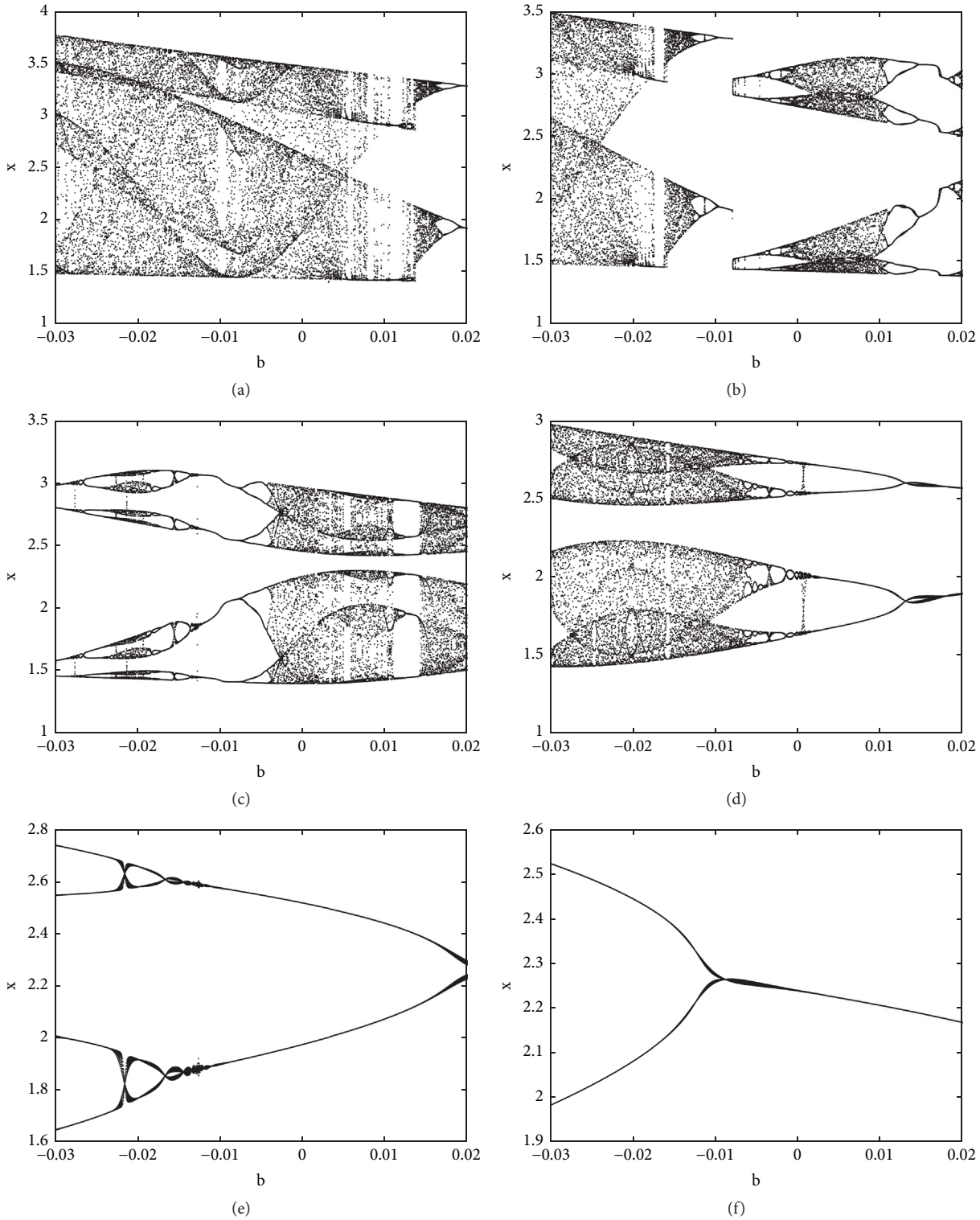

Figure 8: The bifurcation diagrams of system (11) when the parameter b varied with the different values of the order q: (a) $q = 0.98$; (b) $q = 0.97$; (c) $q = 0.96$; (d) $q = 0.95$; (e) $q = 0.94$; (f) $q = 0.93$.

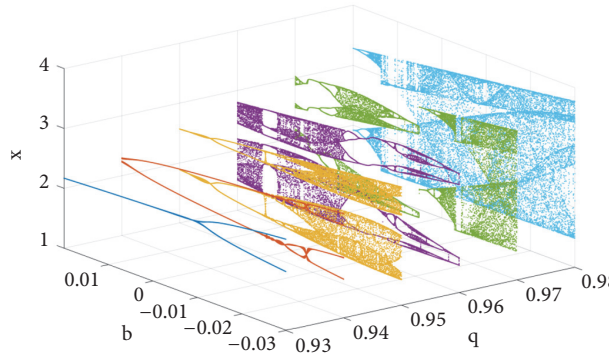

Figure 9: The bifurcation diagram of system (11) in three-dimensional space with the variation of both the parameter b and the order q.

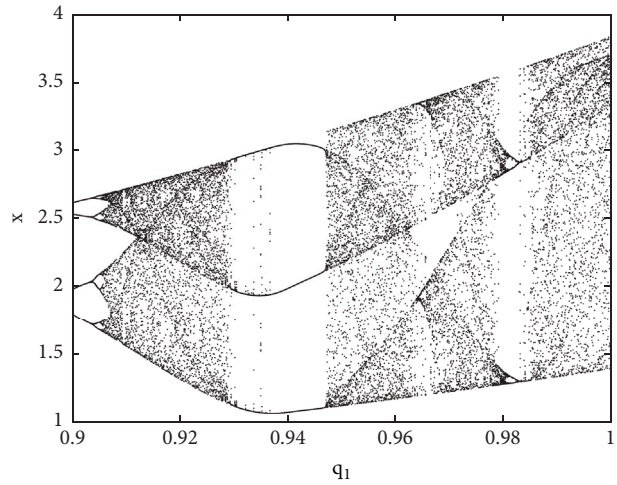

Figure 10: The bifurcation diagram of system (11) with the variation of the order q_1.

Firstly, the bifurcation diagram with the derivative order $q_1 \in [0.9, 1]$ as the others two derivative orders q_2, q_3 are both fixed and $q_2 = q_3 = q = 1$ is plotted. A series of period-doubling bifurcations can be seen in Figure 10. Based on this, bifurcation diagrams versus the order q_1 when the others two derivative orders decrease from 0.98 to 0.93 are given in Figure 11. For Figures 11(a)–11(c), it can be seen that the two branches of the bifurcation gradually decouple, and the area of the chaos gradually decreases with that of the period increases. For Figures 11(d)–11(f), it is clear that the fractional-order system (11) is periodic completely. A bifurcation diagram with the variation of both the order q_1 and derivative order q in the three-dimensional space is plotted in Figure 12. It is clear that dynamics of system (11) becomes simple as the derivative order decreases from 0.98 to 0.93.

Secondly, the bifurcation diagram versus the order $q_2 \in [0.9, 1]$ when the others two derivative orders q_1, q_3 are both fixed and $q_1 = q_3 = q = 1$ is plotted in Figure 13. Meanwhile, a series of bifurcation diagrams versus the order q_2 when the others two derivative orders decrease from 0.98 to 0.85 are given in Figure 14. By comparing Figure 14(a) and Figure 14(b), it is clear that the dynamics of system (11) becomes simple as the order q decreases. For Figures 14(b) and 14(c), it can be observed that the area of chaos increases and that of period decreases. From Figures 14(c) and 14(d), it can be seen that the two branches of the bifurcation gradually couple, and the area of the chaos gradually decreases with that of the period increases. For the rest of the figures in Figure 11, it can be seen that system (11) is totally periodic when the order $q = 0.90$. Meanwhile, the typical period-doubling bifurcation can be seen in Figure 14(g). When the order $q = 0.85$, only period-1 motion for system (11) exists. A bifurcation diagram with the variation of both the order q_2 and derivative order q in the three-dimensional space is plotted in Figure 15. It is clear that dynamics of system (11) becomes simple as the derivative order decreases from 0.98 to 0.85.

The bifurcation diagrams with the variation of the order q_3 when the other two orders q_1, q_2 decrease from 0.98 to 0.93 will not be given in here for the similarity.

5. Conclusions

In this paper, a new fractional-order system is presented. Firstly, the stability of the equilibriums is analyzed. Based on the stability analysis, the reason of the generation for the one scroll of the attractor is analyzed. Phase diagrams for the

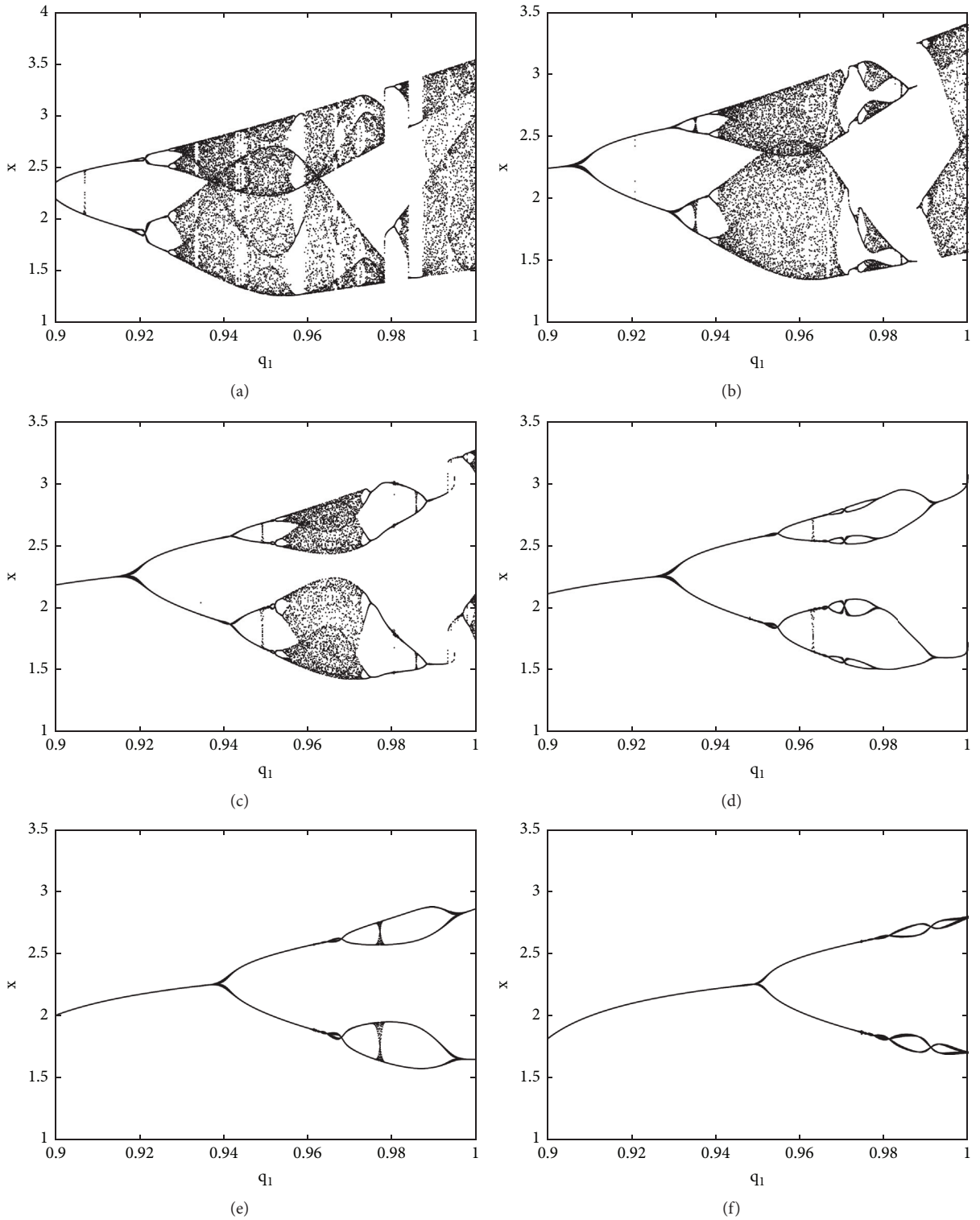

Figure 11: The bifurcation diagram of system (11) when the order q_1 varied with the different values of the order q: (a) $q = 0.98$; (b) $q = 0.97$; (c) $q = 0.96$; (d) $q = 0.95$; (e) $q = 0.94$; (f) $q = 0.93$.

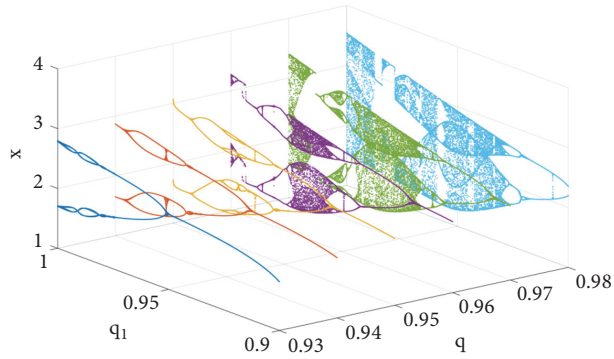

Figure 12: The bifurcation diagram of system (11) in three-dimensional space with the variation of both the orders q_1 and q.

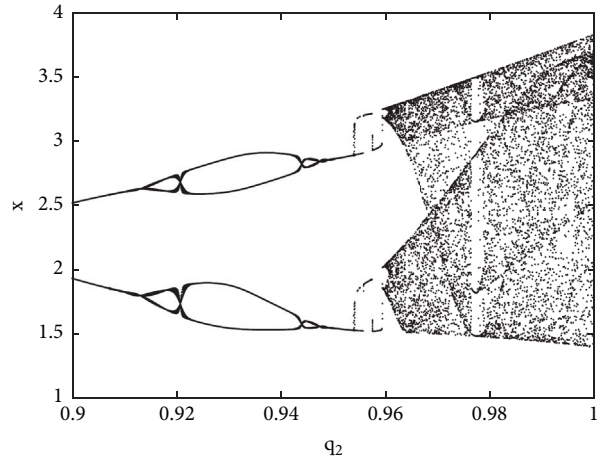

Figure 13: The bifurcation diagram of system (11) with the variation of the derivative order q_2.

different values of the derivative order are obtained to show the rich dynamics of the new fractional-order system.

Bifurcations of the new fractional-order system in commensurate-order and incommensurate-order cases are studied in detail. In the commensurate-order case, when the derivative order decreases from 0.99, bifurcations with the variation of a system parameter are investigated. In the incommensurate-order case, bifurcations with the variation of a derivative order when the other orders decreases from 1 are analyzed. Period-doubling and saddle-node bifurcations can be observed.

What is more, it can be concluded that the dynamics of the new fractional-order system becomes periodic or simple when the derivative order approaches to 0 and chaotic or complex when the order approaches to 1 from a global perspective. These results obtained in this paper can be referenced for the bifurcation control of fractional-order systems. The generalization of the conclusion for other fractional-order systems will be our future work.

Data Availability

The data for the bifurcation diagrams used to support the findings of this study are included within the supplementary information file(s) (available here). In the manuscript, there are 31 bifurcation diagrams. For the large of the data, we will supply the partial bifurcation data calculated by the software Matlab.

Conflicts of Interest

The authors declare that they have no conflicts of interest.

Acknowledgments

This work is supported by the National Natural Science Foundation of China (NSFC) under the Grants nos. 11702194 and 11702195.

Supplementary Materials

(1) adataq093: the bifurcation data of Figure 5(f). (2) adataq094: the bifurcation data of Figure 5(e). (3) adataq095: the bifurcation data of Figure 5(d). (4) adataq096: the bifurcation data of Figure 5(c). (5) adataq097: the bifurcation data of Figure 5(b). (6) adataq098: the bifurcation data of Figure 5(a). (7) q1dataq093: the bifurcation data of Figure 11(f). (8) q1dataq094: the bifurcation data of Figure 11(e). (9) q1dataq095: the bifurcation data of

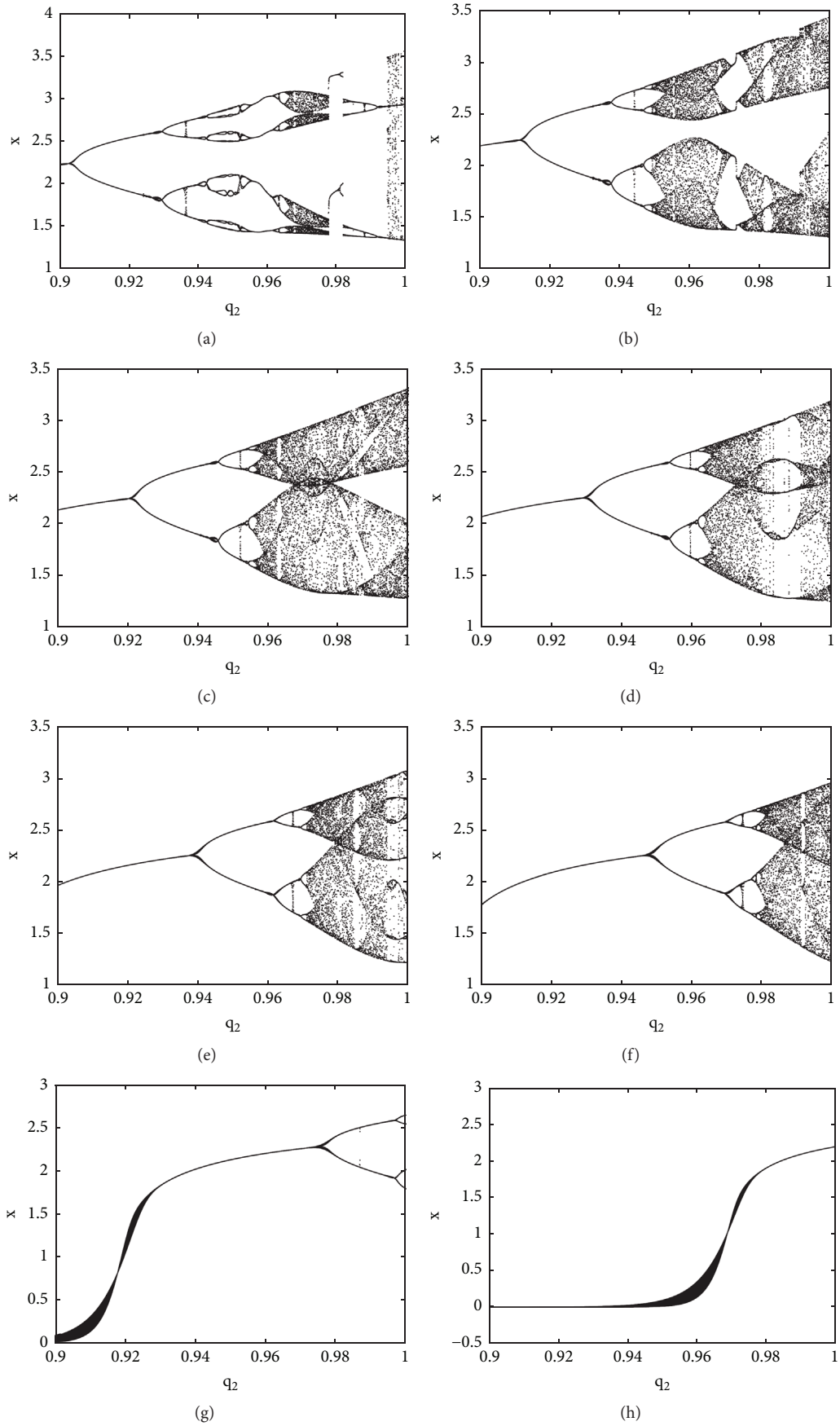

Figure 14: The bifurcation diagram of system (11) when the order q_2 varied with the different values of the order q: (a) $q = 0.98$; (b) $q = 0.97$; (c) $q = 0.96$; (d) $q = 0.95$; (e) $q = 0.94$; (f) $q = 0.93$; (g) $q = 0.90$; (h) $q = 0.85$.

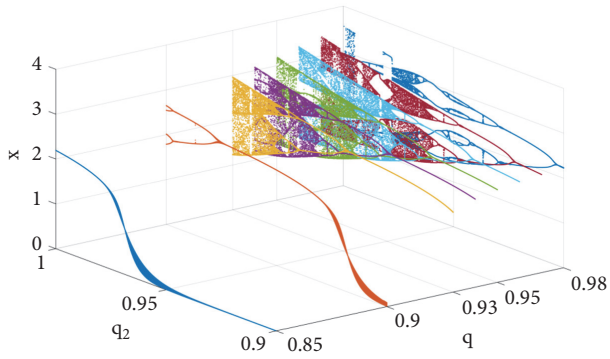

FIGURE 15: The bifurcation diagram of system (11) in three-dimensional space with the variation of both the orders q_2 and q.

Figure 11(d). (10) q1dataq096: the bifurcation data of Figure 11(c). (11) q1dataq097: the bifurcation data of Figure 11(b). (12) q1dataq098: the bifurcation data of Figure 11(a). *(Supplementary Materials)*

References

[1] O. Lyubomudrov, M. Edelman, and G. M. Zaslavsky, "Pseudochaotic systems and their fractional kinetics," *International Journal of Modern Physics B*, vol. 17, no. 22-24, part 1, pp. 4149–4167, 2003.

[2] J. T. Machado and A. M. Galhano, "A fractional calculus perspective of distributed propeller design," *Communications in Nonlinear Science and Numerical Simulation*, vol. 55, Article ID 10075704, pp. 174–182, 2018.

[3] J. A. Tenreiro Machado, M. E. Mata, and A. M. Lopes, "Fractional state space analysis of economic systems," *Entropy*, vol. 17, no. 8, pp. 5402–5421, 2015.

[4] L. J. Sheu, W. C. Chen, Y. C. Chen, and W. T. Weng, "A two-channel secure communication using fractional chaotic systems," *World Academy of Science, Engineering and Technology*, vol. 41, pp. 1057–1061, 2010.

[5] Kiani-B. A., K. Fallahi, N. Pariz, and H. Leung, "A chaotic secure communication scheme using fractional chaotic systems based on an extended fractional Kalman filter(2008)," *Communications in Nonlinear Science and Numerical Simulation*, vol. 22, no. 2, pp. 3709–3720, 2008.

[6] I. Podlubny, *Fractional Differential Equations*, vol. 198 of *Mathematics in Science and Engineering*, Academic Press, San Diego, California, Calif, USA, 1999.

[7] T. T. Hartley, C. F. Lorenzo, and H. K. Qammer, "Chaos in a fractional order Chua's system," *IEEE Transactions on Circuits and Systems I: Fundamental Theory and Applications*, vol. 42, no. 8, pp. 485–490, 1995.

[8] J. H. Chen and W. C. Chen, "Chaotic dynamics of the fractionally damped van der Pol equation," *Chaos, Solitons and Fractals*, vol. 25, p. 188, 2008.

[9] W. C. Chen, "Nonlinear dynamics and chaos in a fractional-order financial system," *Chaos Solitons and Fractals*, vol. 36, pp. 1305–1314, 2008.

[10] X. Gao and J. B. Yu, "Chaos in the fractional-order periodically forced complex Duffing's oscillators," *Chaos, Solitons and Fractals*, vol. 24, no. 4, pp. 1097–1104, 2005.

[11] C. Luo and X. Wang, "Chaos in the fractional-order complex Lorenz system and its synchronization," *Nonlinear Dynamics*, vol. 71, no. 1-2, pp. 241–257, 2013.

[12] X. Liu, L. Hong, and J. Jiang, "Global bifurcations in fractional-order chaotic systems with an extended generalized cell mapping method," *Chaos: An Interdisciplinary Journal of Nonlinear Science*, vol. 26, no. 8, 084304, 7 pages, 2016.

[13] J. C. Sprott, "A proposed standard for the publication of new chaotic systems," *International Journal of Bifurcation and Chaos*, vol. 21, p. 2391, 2011.

[14] S. Jafari, J. C. Sprott, and M. Molaie, "A Simple Chaotic Flow with a Plane of Equilibria," *Chaos: An Interdisciplinary Journal of Nonlinear Science*, vol. 26, no. 6, Article ID 1650098, 2016.

[15] H. Poincaré, *Les Méthodes Nouvelles de la Mécanique Céleste*, Gauthier-Villars, Pairs, France, 1892.

[16] X. J. Liu and L. Hong, "Chaos and adaptive synchronizations in fractional-order systems," *International Journal of Bifurcation and Chaos*, vol. 23, Article ID 1350175, 2013.

[17] D. Cafagna and G. Grassi, "Bifurcation and chaos in the fractional-order Chen system via a time-domain approach," *International Journal of Bifurcation and Chaos*, vol. 18, p. 1845, 2008.

[18] H. A. El-Saka, E. Ahmed, M. I. Shehata, and A. M. A. El-Sayed, "On stability, persistence, and Hopf bifurcation in fractional order dynamical systems," *Nonlinear Dynamics*, vol. 56, no. 1-2, pp. 121–126, 2009.

[19] A. Y. Leung, H. X. Yang, and P. Zhu, "Periodic bifurcation of Duffing-van der Pol oscillators having fractional derivatives and time delay," *Communications in Nonlinear Science and Numerical Simulation*, vol. 19, no. 4, pp. 1142–1155, 2014.

[20] Y. Ji, L. Lai, S. Zhong, and L. Zhang, "Bifurcation and chaos of a new discrete fractional-order logistic map," *Communications in Nonlinear Science and Numerical Simulation*, vol. 57, pp. 352–358, 2018.

[21] J. Palanivel, K. Suresh, S. Sabarathinam, and K. Thamilmaran, "Chaos in a low dimensional fractional order nonautonomous nonlinear oscillator," *Chaos, Solitons & Fractals*, vol. 95, pp. 33–41, 2017.

[22] L. J. Sheu, W. C. Chen, Y. C. Chen, and W. T. Weng, "A two-channel secure communication using fractional chaotic systems," *World Academy of Science, Engineering and Technology*, vol. 65, pp. 1057–1061, 2010.

[23] A. Kiani-B, K. Fallahi, N. Pariz, and H. Leung, "A chaotic secure communication scheme using fractional chaotic systems based on an extended fractional Kalman filter," *Communications in Nonlinear Science and Numerical Simulation*, vol. 14, no. 3, pp. 863–879, 2009.

[24] L. Cheng, *Synchronization and Circuit Implementation for Chaotic and Hyperchaotic Systems*, Northeast Normal University, Chuangchun, China, 2002.

[25] A. A. Kilbas, H. M. Srivastava, and J. J. Trujillo, *Theory and Applications of Fractional Differential Equations*, New York, NY, USA, Elsevier, 2006.

[26] E. Hairer, S. P. Nørsett, and G. Wanner, *Solving Ordinary Differential Equations I: Nonstiff Problems*, vol. 8 of *Springer Series in Computational Mathematics*, Springer, Berlin, Germany, 1993.

[27] E. Hairer and G. Wanner, *Solving Ordinary Differential Equations II: Stiff and Differential- Algebraic Problems*, vol. 14, Springer, Berlin, Germany, 1991.

[28] K. Diethelm, N. J. Ford, and A. D. Freed, "A predictor-corrector approach for the numerical solution of fractional differential equations," *Nonlinear Dynamics*, vol. 29, no. 1–4, pp. 3–22, 2002.

[29] A. Charef, H. H. Sun, Y. Tsao, and B. Onaral, "Fractal system as represented by singularity function," *IEEE Transactions on Automatic Control*, vol. 37, no. 9, pp. 1465–1470, 1992.

[30] M. S. Tavazoei and M. Haeri, "Limitations of frequency domain approximation for detecting chaos in fractional order systems," *Nonlinear Analysis: Theory, Methods & Applications*, vol. 69, no. 4, pp. 1299–1320, 2008.

[31] D. Matignon, "Stability result on fractional differential equations with applications to control processing," in *Proceedings of the IMACS-SMC*, pp. 963–968, 1996.

[32] M. S. Tavazoei and M. Haeri, "A necessary condition for double scroll attractor existence in fractional-order systems," *Physics Letters A*, vol. 367, pp. 102–113, 2007.

[33] A. Nasrollahi and N. Bigdeli, "Extended Chen: a new class of chaotic fractional-order systems," *International Journal of General Systems*, vol. 43, no. 8, pp. 880–896, 2014.

Hindawi
Discrete Dynamics in Nature and Society
Volume 2018, Article ID 3745769, 9 pages
https://doi.org/10.1155/2018/3745769

Research Article

The Impact of User Behavior on Information Diffusion in D2D Communications: A Discrete Dynamical Model

Chenquan Gan, Xiaoke Li, Lisha Wang, and Zufan Zhang

School of Communication and Information Engineering, Chongqing University of Posts and Telecommunications, Chongqing 400065, China

Correspondence should be addressed to Xiaoke Li; lxkever@foxmail.com

Received 6 September 2018; Revised 23 November 2018; Accepted 26 November 2018; Published 9 December 2018

Academic Editor: Guang Zhang

This paper aims to explore the impact of user behavior on information diffusion in D2D (Device-to-Device) communications. A discrete dynamical model, which combines network metrics and user behaviors, including social relationship, user influence, and interest, is proposed and analyzed. Specifically, combined with social tie and user interest, the success rate of data dissemination between D2D users is described, and the interaction factor, user influence, and stability factor are also defined. Furthermore, the state transition process of user is depicted by a discrete-time Markov chain, and global stability analysis of the proposed model is also performed. Finally, some experiments are examined to illustrate the main results and effectiveness of the proposed model.

1. Introduction

The fast development of communication technologies, enhanced devices, and multimedia services will lead to a drastic change in the way of perceiving and interacting with the world around us [1]. The emerging 5G systems would transform current reality into a "connected reality", in which objects and people are interconnected in a unified whole [2]. To realize this vision, the Long Term Evolution (LTE) radio technology is adopted as a lifeline for reality scenarios. As a result, future 5G systems require novel approaches in terms of network design and information dissemination and should provide low latencies and timely connectivity in case of information sharing such as disasters, concerts, and other timely situations [3].

As a key component of 5G systems, D2D communications are proposed as an effective paradigm to reduce information diffusion time [4]. Reference [5] provided a game theoretical formulation for energy minimization in cooperative networks, in which the Nash bargaining solution is derived to achieve a tradeoff between energy reduction and fairness. Indeed, the direct communication between two adjacent user devices is regarded as a promising technology in future 5G systems, which has advantages of coverage extension, high spectrum utilization, and low energy consumption [6, 7]. Obviously, when data must be sent to a group of users through reliable and low latency links, D2D communications are useful for information dissemination. Consequently, the study of information diffusion is of great significance in 5G systems.

In D2D communications, social network is an important carrier of information [8, 9]. Some previous work exploited social metrics to improve information dissemination performance. For instance, [10, 11] gave some extensive analysis of information diffusion approaches, and different quantification models with social relationship were proposed [12–14]. Additionally, Zhang et al. [15] offloaded social network traffic through D2D links to improve the content dissemination time. With consideration of content interests and social network relations, [16] designed a social-aware data sharing strategy, whose effectiveness and functionality is verified through experimental analysis.

In social network, behavior characteristics of different users are crucial factors for information dissemination. Combined with proximity-based communication, rental work investigated the integration of communication and social domains based on user behaviors [17]. References [18, 19] exploited preference features, which indicate how much information the user needs to select seed users for sending information. Furthermore, user selfishness directly affected

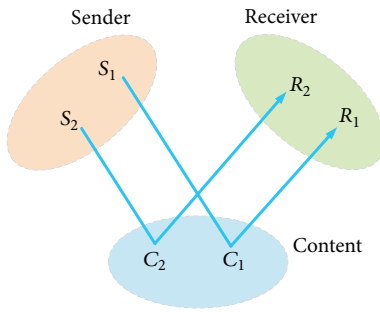

Figure 1: Relationship of three entities in information diffusion process.

the share willingness and the success rate of establishing D2D links [20–22]. Wang et al. [23] constructed a traffic offloading framework, in which a group of user devices were chosen as seeds based on their social influence. In [24], authors focused on maximizing cellular traffic offloading with D2D communications via content caching and users pairing. Reference [25] exploited the social tie and influence among individuals, which is modeled by Indian Buffet Process, to improve the performance and reduce the load on the wireless cellular system. Although the above-mentioned information diffusion approaches provide high data-rate and low latency, they cannot adequately characterize social interaction among users. Besides, they almost only describe the one-hop dissemination so that they fail to characterize the whole diffusion process in the network. In reality, information diffusion is a dynamic process, and its performance is not only affected by the network architecture, but by the social metrics of user as well.

Information diffusion process can be decomposed into multiple end-to-end information transmission cases; each case involves three entities, namely, sender, receiver, and content (see Figure 1). The impact factors of information diffusion include not only the attribute of sender and receiver, but also the content characteristic of information and the mutual relationship between users [26–28]. To overcome the defect of conventional models and inspired by the idea of epidemic models (e.g., [29–34]), this paper proposes a susceptible-infected-recovered (SIR) information diffusion model, which combines network metrics and user behaviors, including social relationship between users, user influence, and interest. Particularly, with consideration of social relationship and user interest, the success rate of data dissemination between D2D users is described, and the interaction factor, user influence, and stability factor are also defined. Additionally, combined with the discrete-time Markov chain, the state transition equation is established to describe the information diffusion process. Finally, global stability analysis and some experiments of the proposed model are also performed.

The subsequent materials of this paper are organized as follows: Section 2 describes mathematical framework. Model analysis and some experiments are examined in Sections 3 and 4, respectively. Finally, Section 5 outlines this work.

2. Mathematical Framework

In this paper, let a graph $G = (V, E)$ with $N > 0$ nodes represent the information propagation network, where V and E denote the set of users and communication links between users, respectively. At any time, a node is in one of the following states.:

(i) S (susceptible): the user who does not receive the information.

(ii) I (infected): the user who has received the information and forwarded it.

(iii) R (recovered): the user who has received the information but never forwards it.

2.1. Notations

(i) inf_i^t: the influence degree of user i at time t, it is effected by the user's relative weight in its neighbors.

(ii) h_{ij}: the success rate of data dissemination that user i sends to user j, whose impact factors include the interest degree, social tie of users and the physical structure of network.

(iii) ω_{ij}: the social tie strength between users i and j, that indirectly characterize the link quality between users.

(iv) r_j: the interest degree of user j for the information.

(v) $p_i^t(X)$: the probability that user i is in state X at time t, $X \in \{S, I, R\}$.

(vi) $p_{XY}^i(t)$: the transition probability of user i from state X to state Y at time t, $X, Y \in \{S, I, R\}$.

(vii) a_{ij}: the element of adjacent matrix indicating whether users i and j are adjacent.

(viii) $IF(i, j)$: the interaction factor of social tie between users i and j, referring to the historical interaction in a certain interval.

(ix) $sf(i, j)$: the stability factor that manifests the numeric fluctuation of social tie between users i and j.

2.2. Model Assumptions

(A1) Only within the scope of D2D communications can users establish communication links to transmit information.

(A2) Considering the interaction behavior which reflects the social relationship between users, and the latter determines the former in turn, an interaction factor is introduced to partly characterize the social relationship. Interaction factor reflects the subjective aspects to establish trustworthy feelings or experiences based on users' historical interactions, and each interaction is judged by a numeric degree to signify the opinion of users. Then,

$$IF(i, j) = \frac{\sum_{k=1}^{n} act(i, j)_k}{n} \times \left(1 - \frac{m}{n}\right)^{1/(n-m)}, \quad (1)$$

where $act(i,j)_k \in [0,1]$ represents the evaluation value of social relationship for the k-th interaction between users i and j and n and m are the numbers of total and negative interactions, respectively.

Obviously, $IF(i,j)$ is the accumulation of historical interactions in a certain time interval and is affected by the number of total negative judgments. The social tie strength will be weakened with the increase of negative judgments. Furthermore, the interaction is bidirectional, so $IF(i,j) = IF(j,i)$.

(A3) Stability factor manifests the numeric fluctuation of social tie between users. Then, it can be calculated based on the time slice aggregation as follows:

$$sf(i,j) = 1 - \sqrt{\frac{\sum_{k=1}^{n}\left[Str(i,j)^{T(k)} - \overline{Str}(i,j)\right]^2}{n}}, \quad (2)$$

where $T(k)$ denotes the k-th time slice, $Str(i,j)^{T(k)}$ is the social tie strength from i to j in the k-th time slice, and $\overline{Str}(i,j)$ indicates the average strength of social tie in all time slices.

The reason for considering the interaction factor and stability factor is to adjust the scenario of this paper. In particular, information transmission over physical link requires reliability and stability to guarantee the successful rate. If the social tie between users is unstable, then the infection probability is accordingly decreased, which will lead to the failure of information transmission. On the contrary, strengthened and stable social tie indicates a reliable interaction and link status, resulting in an improvement of transmission efficiency.

(A4) The social tie strength ω_{ij} is jointly determined by the interaction and stability factors. Then, $\omega_{ij} = IF(i,j) * sf(i,j)$.

(A5) The success rate of data dissemination is proportional to the social tie strength and interest degree of user. Then, it can be expressed as

$$h_{ij} = \left(\beta\omega_{ij} + \gamma r_j\right) a_{ij}, \quad i,j = 1,2,\ldots,N, \quad (3)$$

where $\beta, \gamma > 0$ can be adjusted according to the actual scenario.

(A6) The state transition probability from I to R is determined by the user's spreading ability. A stronger spreading ability corresponds to a longer survival time of information, and this time length is positively correlated to the user influence.

Based on the fact that user influence decays over time and inspired by attenuation models [35, 36], especially the exponential model with a long tail characteristic, the influence of user i at time t is defined as

$$inf_i^t = inf_i^{t_1} * e^{-(t-t_1)}, \quad (4)$$

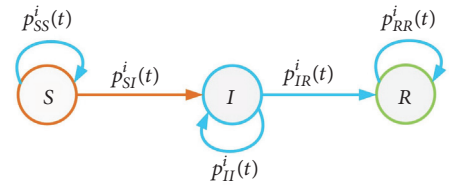

Figure 2: The state transition diagram of user i at time t.

where

$$inf_i^{t_1} = \min\left\{\frac{M(i)}{\sum_{j\in\Gamma(i)} M(j)/M(i)}, 1\right\}, \quad (5)$$

t_1 denotes the initial time, $\Gamma(i)$ is the set of neighbors of user i, and $M(\cdot)$ is the number of user neighbors.

2.3. Model Formulation. Before giving the mathematical expression of the model, let us first introduce some basic information diffusion rules.

(R1) If a node is in state S, it can only receive information from its neighbors at each moment, and once it receives the information, it will transform into state I and never receive the same information from other neighbors. Then, $p_{SS}^i(t) + p_{SI}^i(t) = 1$, and $p_{SI}^i(t) = 1 - \prod_{j\in\Gamma_i}(1 - h_{ij}p_j^t(I))$.

(R2) If a node is in state I, it will forward the information according to its influence, and then will covert to state R after the survival time of information.

(R3) If a node is in state R, it will always maintain state R and will no longer receive and forward the same information. Then, $p_{RR}^i(t) = 1$.

Collecting the foregoing assumptions and information diffusion rules, the state transition diagram of user i at time t can be represented either by Figure 2 or the discrete-time Markov chain:

$$\begin{aligned}
p_i^{t+1}(S) &= p_i^t(S)\, p_{SS}^i(t),\\
p_i^{t+1}(I) &= p_i^t(I)\, p_{II}^i(t) + p_i^t(S)\, p_{SI}^i(t),\\
p_i^{t+1}(R) &= p_i^t(R)\, p_{RR}^i(t) + p_i^t(I)\, p_{IR}^i(t),\\
p_i^t(S) + p_i^t(I) + p_i^t(R) &= 1,\\
& \qquad i = 1,2,\ldots,N.
\end{aligned} \quad (6)$$

3. Model Analysis

The equilibrium and its stability of system (6) will be introduced in this section.

Theorem 1. *Assume that* $E(p_i^*(S), p_i^*(I), p_i^*(R))$, $i = 1,2,\ldots,N$, *is the equilibrium of system (6). Then,* $p_i^*(S) = p_i^*(I) = 0$, *and* $p_i^*(R) = 1$.

Proof. According to the definition of equilibrium, one can get

$$\begin{aligned} &p_i^*(S) = p_i^*(S)\, p_{SS}^i(t), \\ &p_i^*(I) = p_i^*(I)\, p_{II}^i(t) + p_i^*(S)\, p_{SI}^i(t), \\ &p_i^*(R) = p_i^*(R)\, p_{RR}^i(t) + p_i^*(I)\, p_{IR}^i(t), \\ &p_i^*(S) + p_i^*(I) + p_i^*(R) = 1, \\ &\qquad\qquad i = 1, 2, \ldots, N. \end{aligned} \tag{7}$$

Solving system (7), one can obtain $p_i^*(S) = p_i^*(I) = 0$, and $p_i^*(R) = 1$. Thus, the claimed result follows. □

From assumption (A6) and rule (R2), the probability that user stays in state I is positively correlated to its influence. So one might as well make $p_{II}^i(t) = inf_i^t$. Then, $p_{IR}^i(t) = 1 - p_{II}^i(t)$, and system (6) can be rewritten as

$$\begin{aligned} &p_i^{t+1}(I) \\ &\quad = inf_i^t p_i^t(I) \\ &\qquad + \left(1 - \prod_{j\in\Gamma_i}\left(1 - h_{ij}p_j^t(I)\right)\right)\left(1 - p_i^t(I) - p_i^t(R)\right), \\ &p_i^{t+1}(R) = p_i^t(R) + \left(1 - inf_i^t\right) p_i^t(I), \\ &\qquad\qquad i = 1, 2, \ldots, N. \end{aligned} \tag{8}$$

Note that

$$\begin{aligned} &p_i^{t+1}(I) \\ &\quad = inf_i^t p_i^t(I) \\ &\qquad + \left(1 - \prod_{j\in\Gamma_i}\left(1 - h_{ij}p_j^t(I)\right)\right)\left(1 - p_i^t(I) - p_i^t(R)\right) \\ &\quad \le inf_i^t p_i^t(I) + \left(1 - p_i^t(I) - \mathrm{p}_i^t(R)\right) \sum_{j\in\Gamma(i)} h_{ij}p_j^t(I) \\ &\quad \le inf_i^t p_i^t(I) + \sum_{j\in\Gamma(i)} h_{ij}p_j^t(I). \end{aligned} \tag{9}$$

Hence, it suffices to consider the following system:

$$\begin{aligned} &p_i^{t+1}(I) = inf_i^t p_i^t(I) + \sum_{j\in\Gamma(i)} h_{ij}p_j^t(I), \\ &p_i^{t+1}(R) = p_i^t(R) + \left(1 - inf_i^t\right) p_i^t(I), \\ &\qquad\qquad i = 1, 2, \ldots, N. \end{aligned} \tag{10}$$

Besides, systems (10) and (8) have the same equilibrium $E(p_i^*(I) = 0, p_i^*(R) = 1), i = 1, 2, \ldots, N$.

Define

$$\mathbf{p}^t(\cdot) = \left(p_1^t(\cdot), p_2^t(\cdot), \ldots, p_N^t(\cdot)\right)^T, \tag{11}$$

$$\mathbf{I}_N = \begin{pmatrix} 1 & 0 & \cdots & 0 \\ 0 & 1 & \cdots & 0 \\ \vdots & \vdots & \vdots & \vdots \\ 0 & 0 & \cdots & 1 \end{pmatrix}, \tag{12}$$

$$\mathbf{H} = \begin{pmatrix} h_{11} & h_{12} & \cdots & h_{1N} \\ h_{21} & h_{22} & \cdots & h_{2N} \\ \vdots & \vdots & \vdots & \vdots \\ h_{N1} & h_{N2} & \cdots & h_{NN} \end{pmatrix}, \tag{13}$$

$$\mathbf{Inf}_N = \begin{pmatrix} inf_1^t & 0 & \cdots & 0 \\ 0 & inf_2^t & \cdots & 0 \\ \vdots & \vdots & \vdots & \vdots \\ 0 & 0 & \cdots & inf_N^t \end{pmatrix}. \tag{14}$$

Then, $\mathbf{p}^{t+1}(I) = (\mathbf{H} + \mathbf{Inf}_N)\mathbf{p}^t(I)$. It follows from stability theory of autonomous linear systems [37] that the equilibrium of system (10) is globally asymptotically stable if $\lambda_{\max}(\mathbf{H} + \mathbf{Inf}_N) < 1$.

Now, the main result of this paper can be derived as follows.

Theorem 2. *The equilibrium* $E(p_i^*(S), p_i^*(I), p_i^*(R)), i = 1, 2, \ldots, N$, *of system (6) is globally asymptotically stable if* $\lambda_{\max}(\mathbf{H} + \mathbf{Inf}_N) < 1$.

Remark 3. At the stable point, the number of users that have received information (users in state R) represents the transmission range. That is to say, a larger number of users in state correspond to a wider coverage of information. Obviously, the transmission range is affected by the interest degree, social tie, and other factors, which is reasonable in the actual situation.

4. Experiments

To validate the effectiveness of the proposed model, this section simulates the information diffusion process with MATLAB in a random network, in which each node represents a user. At each time point, users take the receiving or forwarding decision according to its own state and the system parameters. Meanwhile, the impact of user influence and information popularity on information diffusion is also illustrated. Here, let us introduce two important indexes in advance.

Max Infection Peak (*MIP*). *MIP* refers to the ratio of the maximum number of infected users to the total number of users. This index characterizes the information diffusion speed, and a larger *MIP* means a wider coverage of information.

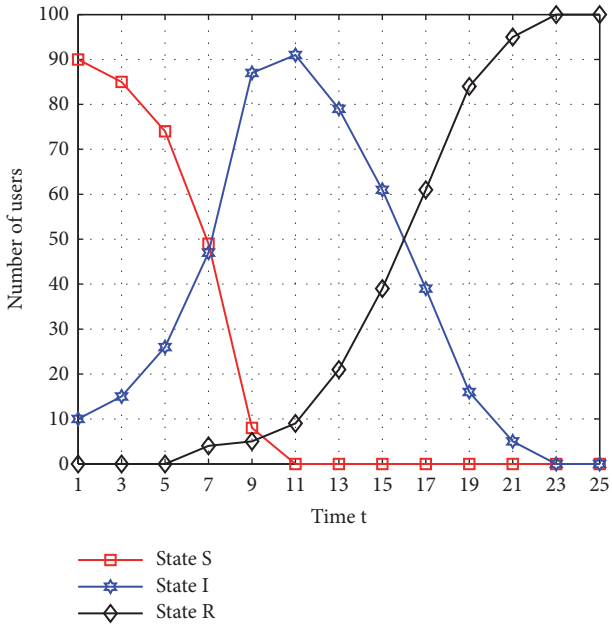

Figure 3: System convergence process.

Average Influence (*AIN*). *AIN* is the average influence of all users in the network, and the influence degree of each user is derived from (4).

Example 4. Consider system (8) with system parameters b=0.6, y=0.4. Meanwhile, take a network with 100 total nodes and 10 seed nodes as the propagation network. Figures 3, 4, 5, 6, and 9 show the model analysis under this condition.

Figure 3 presents the number of users in each state over time. It can be seen that the total number of users at each time point is equal to 100, and the user number in state R is zero at initial time. This is because only the seed users hold the information at initial time, so other users are in state S. Meanwhile, the system converges to a stable state, which is consistent with the theory analysis (i.e., Theorems 1 and 2), and the convergence speed is determined by some parameters, such as the network topology (the adjacent matrix), social tie, and user influence.

Figure 4 illustrates the users state in different time points at t=2, 10, 18, respectively, in which the red, blue, and black circles indicate users in S, I, R state, respectively. It is obvious that the varying number of users in each state of (a), (b), and (c) is consistent with the theoretical analysis.

Figure 5 compares the percentage of each state user between awareness and no awareness. Figures 5(a), 5(b), and 5(c) show the number of susceptible, infected, and recovered users, respectively. It can be observed that the percentage of infected user under the proposed model is larger than that of the model without consideration of social attribute of users and information. This is because the proposed model considers the social tie and user influence, resulting in the fact that information is transmitted with a relative higher successful rate and a wider coverage as shown in Figure 5(c). In addition, it can be found that the model without awareness has higher users in state R over a major part of the time scale. This is because the diffusion model without awareness ignores the impact of influential users, so that the recovery rate is faster than that of the proposed model.

Figure 6 displays the impact of user influence on the number of users in each state. By comparing Figures 6(a), 6(b), and 6(c), it can be concluded that the rate of user transforming from state S to I increases with the *AIN* of user. The reason is that the average influence of users is larger, and the interaction between users will be stronger, so that user is more likely to become infected. Meanwhile, user influence is closely associated with the survival time of information, and a larger *AIN* can extend the length of this time. Therefore, more influential user can expand the diffusion range of information. In addition, with the increase of user influence, the time point that users reach to peak of I state is earlier, so that system converges to a stable state with a fast speed.

Example 5. Consider system (8) with system parameters b=0.6, y=0.4 and 10 initial seed nodes. Figures 7 and 8 illustrate the diffusion model with total nodes 60, 70, and 100, respectively.

Figures 7 and 8 show the evolution of infected and recovered users under different destinations. With the increase of destinations, there is a slightly delay in the time that reaches to peak point of infected users. However, the time delay is quite limited although increasing the number of destinations of almost 67% (from 60 to 100). Furthermore, it should be noted that after almost users are infected, a parallel increase in the number of recovered users is met till all users become recovered, which manifests that a higher number of destinations imply a faster recovery process.

Figure 9 demonstrates a comparison of *MIP* between awareness and no awareness models. Obviously, the *MIP* increasing with the information popularity is independent of model. The reason is that the information popularity is derived from the user interest degree, and a higher interest degree corresponds to a larger popularity. That is to say, if the information is enjoyed by a higher popularity, the transmission probability will increase accordingly, leading to a greater diffusion speed. In this case, most users are in state I before going to state R. Additionally, the *MIP* of the proposed model is higher than that of the model without consideration of social attribute of users. The reason is that the proposed model takes the social tie and user interest degree into account, so that the role of authority user is fully played to expand the diffusion range.

5. Conclusions and Future Work

In this paper, with joint consideration of social tie, user influence, and user interest, a user behavior based information diffusion model for 5G systems has been proposed. By characterizing the state transition probability of each user, a discrete-time Markov chain system has been formulated. Furthermore, the global stability of the system has been

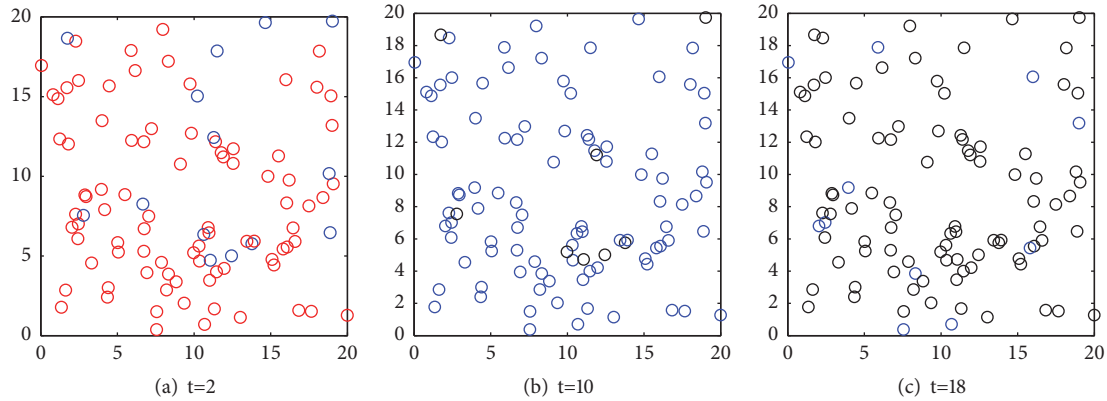

Figure 4: The users state in different time points at t=2, 10, 18.

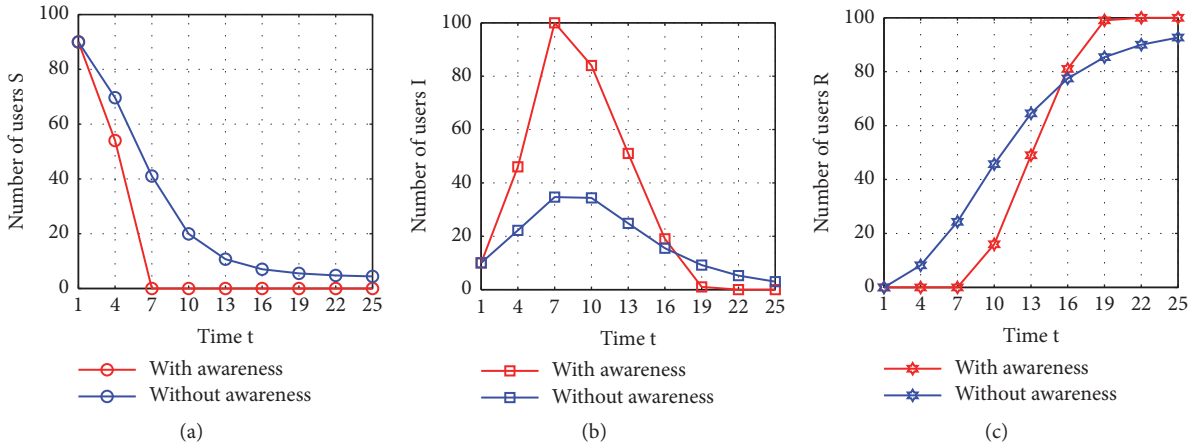

Figure 5: A comparison between awareness and no awareness.

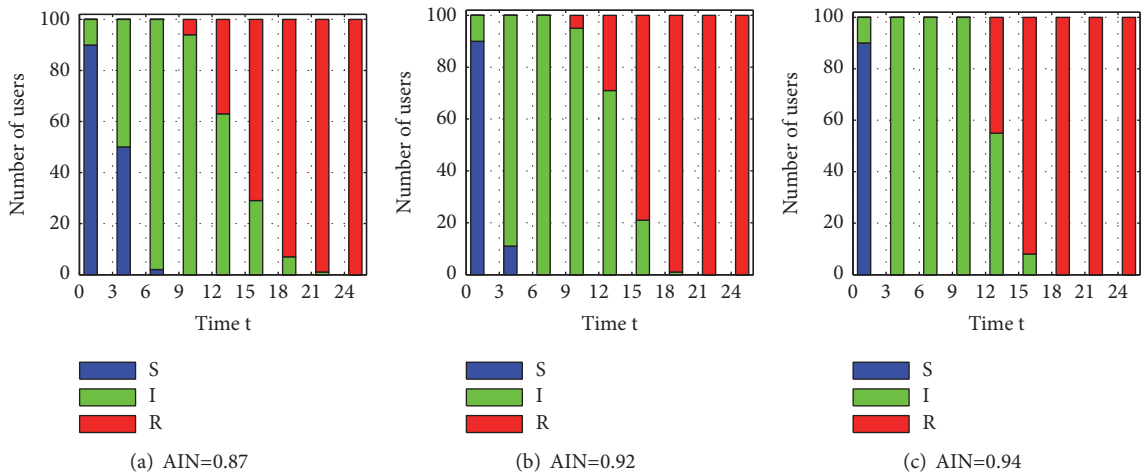

Figure 6: The impact of user influence on information diffusion process.

proved. Finally, some experiments have been performed to illustrate the main results and effectiveness of the proposed model.

The provided insights can guide the development of information diffusion and D2D communications. The discovery of social attributes of user and information improves the effect of information diffusion, which is relevant to advertising, public opinion monitoring, and other scenarios.

In further work, the study can be continued in several directions. On the one hand, we shall apply the theory of discrete dynamics (e.g., [37–40]) to study dynamical behavior of information diffusion and then to study the discrete

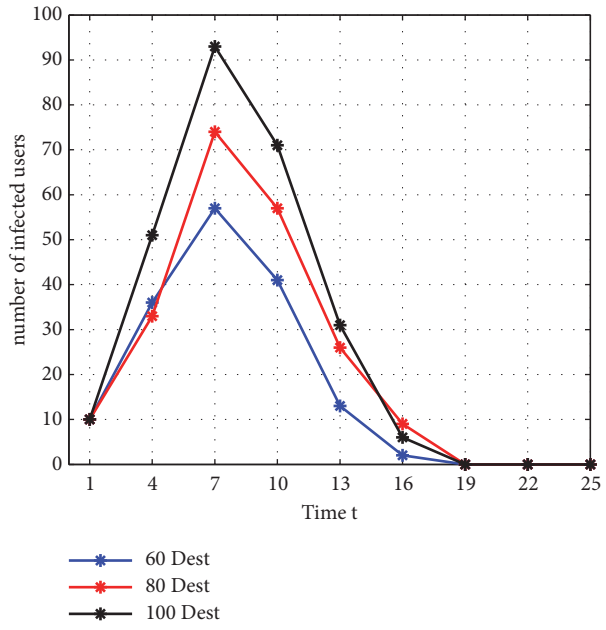

Figure 7: The evolution of infected users over time under different destinations.

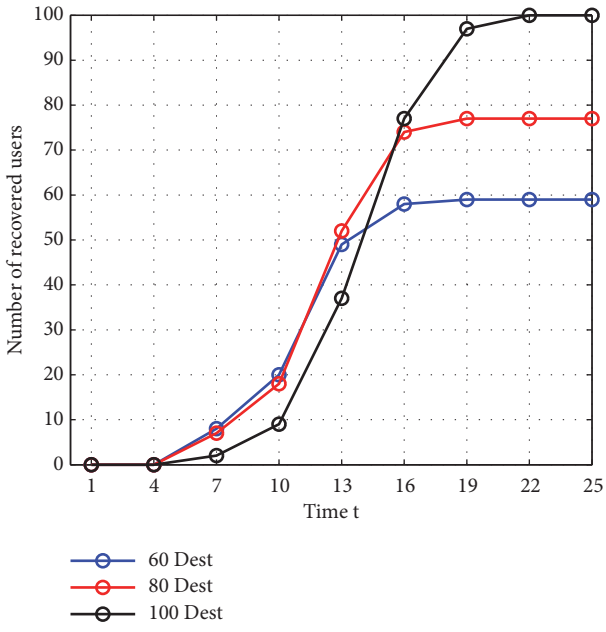

Figure 8: The evolution of recovered users over time under different destinations.

nonautonomous propagation model. On the other hand, the diffusion model should be improved with consideration of user sentiment analysis [41, 42], user mobility, and multitopic scenario.

Data Availability

The data used to support the findings of this study are available from the corresponding author upon request.

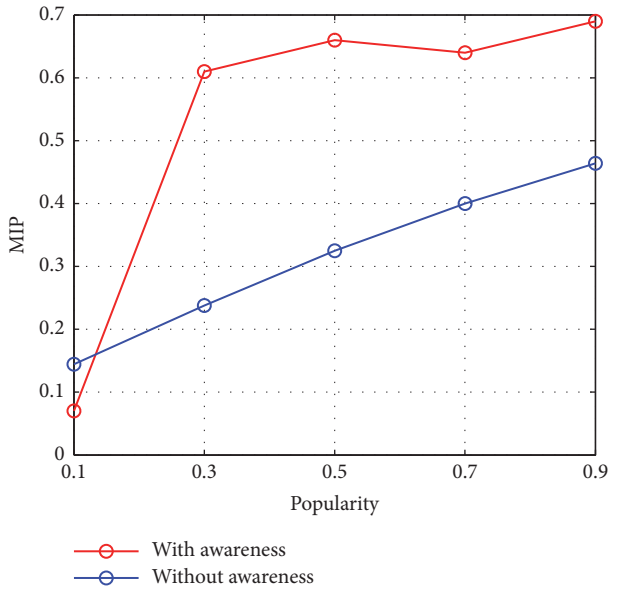

Figure 9: A comparison of *MIP* between awareness and no awareness models.

Conflicts of Interest

The authors declare that there are no conflicts of interest regarding the publication of this paper.

Acknowledgments

This work is supported by Natural Science Foundation of China (Grants nos. 61702066 and 11747125), Scientific and Technological Research Program of Chongqing Municipal Education Commission (Grant no. KJ1704080), Chongqing Research Program of Basic Research and Frontier Technology (Grants nos. cstc2017jcyjAX0256 and cstc2018jcyjAX0154), and Research Innovation Program for Postgraduate of Chongqing (Grants nos. CYS17217 and CYS18238).

References

[1] E. Cianca, M. De Sanctis, and M. Ruggieri, "Convergence towards 4G: A novel view of integration," *Wireless Personal Communications*, vol. 33, no. 3-4, pp. 327–336, 2005.

[2] I. Chih-Lin, S. Han, Y. Chen, and G. Li, "Trillions of nodes for 5G!?" in *Proceedings of the 2014 IEEE/CIC International Conference on Communications in China, ICCC 2014*, pp. 246–250, China, October 2014.

[3] M. A. M. Albreem, "5G wireless communication systems: Vision and challenges," in *Proceedings of the 2nd International Conference on Computer, Communications, and Control Technology, I4CT 2015*, pp. 493–497, Malaysia, April 2015.

[4] A. Pyattaev, O. Galinina, S. Andreev, M. Katz, and Y. Koucheryavy, "Understanding practical limitations of network coding for assisted proximate communication," *IEEE Journal on Selected Areas in Communications*, vol. 33, no. 2, pp. 156–170, 2015.

[5] E. Yaacoub, L. Al-Kanj, Z. Dawy, S. Sharafeddine, F. Filali, and A. Abu-Dayya, "A Nash bargaining solution for energy-efficient

content distribution over wireless networks with mobile-to-mobile cooperation," in *Proceedings of the 4th Joint IFIP Wireless and Mobile Networking Conference (WMNC '11)*, pp. 1–7, Toulouse, France, October 2011.

[6] N. Reider and G. Fodor, "A distributed power control and mode selection algorithm for D2D communications," *Eurasip Journal on Wireless Communications & Networking*, vol. 1, p. 266, 2012.

[7] L. Lei, Z. D. Zhong, C. Lin, and X. M. Shen, "Operator controlled device-to-device communications in LTE-advanced networks," *IEEE Wireless Communications Magazine*, vol. 19, no. 3, pp. 96–104, 2012.

[8] E. Bakshy, I. Rosenn, C. Marlow, and L. Adamic, "The role of social networks in information diffusion," in *Proceedings of the 21st Annual Conference on World Wide Web (WWW '12)*, pp. 519–528, Lyon, France, April 2012.

[9] Y. Zhang, E. Pan, L. Song, W. Saad, Z. Dawy, and Z. Han, "Social network enhanced device-to-device communication underlaying cellular networks in," in *proceedings of the IEEE/CIC International Conference on Communications in China Workshops*, pp. 182–186, 2013.

[10] A. Guille, H. Hacid, C. Favre, and D. A. Zighed, "Information diffusion in online social networks: A survey," *SIGMOD Record*, vol. 42, no. 2, pp. 17–28, 2013.

[11] K. Saito, M. Kimura, K. Ohara, and H. Motoda, "Selecting Information Diffusion Models over Social Networks for Behavioral Analysis," in *Proceedings of the European Conference on Machine Learning and Knowledge Discovery in Databases*, vol. 6323 of *Lecture Notes in Computer Science*, pp. 180–195, Springer.

[12] J. Ho Choi, D. Oh Kang, J. Young Jung, and C. Bae, "Estimating Social Tie Strength for Autonomous D2D Collaborations," *International Journal of Future Computer and Communication*, vol. 4, no. 1, pp. 7–12, 2015.

[13] D. Wu, L. Zhou, Y. Cai, H. Chao, and Y. Qian, "Physical–Social-Aware D2D Content Sharing Networks: A Provider–Demander Matching Game," *IEEE Transactions on Vehicular Technology*, vol. 67, no. 8, pp. 7538–7549, 2018.

[14] Y. Yi, Z. Zhang, and C. Gan, "The effect of social tie on information diffusion in complex networks," *Physica A: Statistical Mechanics and its Applications*, vol. 509, pp. 783–794, 2018.

[15] Y. Zhang, E. Pan, L. Song, W. Saad, Z. Dawy, and Z. Han, "Social network aware device-to-device communication in wireless networks," *IEEE Transactions on Wireless Communications*, vol. 14, no. 1, pp. 177–190, 2015.

[16] L. Aoude, Z. Dawy, S. Sharafeddine, K. Frenn, and K. Jahed, "Social-Aware Device-to-Device Offloading Based on Experimental Mobility and Content Similarity Models," *Wireless Communications and Mobile Computing*, vol. 2018, Article ID 5606829, 16 pages, 2018.

[17] Y. Li, T. Wu, P. Hui, D. Jin, and S. Chen, "Social-aware D2D communications: qualitative insights and quantitative analysis," *IEEE Communications Magazine*, vol. 52, no. 6, pp. 150–158, 2014.

[18] Y. Li, M. Qian, D. Jin, P. Hui, Z. Wang, and S. Chen, "Multiple mobile data offloading through disruption tolerant networks," *IEEE Transactions on Mobile Computing*, vol. 13, no. 7, pp. 1579–1596, 2014.

[19] H.-H. Cheng and K. C.-J. Lin, "Source selection and content dissemination for preference-aware traffic offloading," *IEEE Transactions on Parallel and Distributed Systems*, vol. 26, no. 11, pp. 3160–3174, 2015.

[20] T. Wang, Y. Sun, L. Song, and Z. Han, "Social data offloading in D2D-enhanced cellular networks by network formation games," *IEEE Transactions on Wireless Communications*, vol. 14, no. 12, pp. 7004–7015, 2015.

[21] J. Li, Q. Yang, P. Gong, and K. S. Kwak, "End-to-End Multiservice Delivery in Selfish Wireless Networks under Distributed Node-Selfishness Management," *IEEE Transactions on Communications*, vol. 64, no. 3, pp. 1132–1142, 2016.

[22] C. Wang, X.-Y. Yang, K. Xu, and J.-F. Ma, "SEIR-based model for the information spreading over SNS," *Tien Tzu Hsueh Pao/Acta Electronica Sinica*, vol. 42, no. 11, pp. 2325–2330, 2014.

[23] X. Wang, M. Chen, Z. Han, D. O. Wu, and T. T. Kwon, "TOSS: Traffic offloading by social network service-based opportunistic sharing in mobile social networks," in *Proceedings of the 33rd IEEE Conference on Computer Communications, IEEE INFOCOM 2014*, pp. 2346–2354, Canada, May 2014.

[24] J. Jiang, S. Zhang, B. Li, and B. Li, "Maximized cellular traffic offloading via device-to-device content sharing," *IEEE Journal on Selected Areas in Communications*, vol. 34, no. 1, pp. 82–91, 2016.

[25] Y. Zhang, L. Song, W. Saad, Z. Dawy, and Z. Han, "Exploring social ties for enhanced device-to-device communications in wireless networks," in *Proceedings of the 2013 IEEE Global Communications Conference (GLOBECOM 2013)*, pp. 4597–4602, Atlanta, Ga, USA, December 2013.

[26] H.-F. Zhang, J.-R. Xie, M. Tang, and Y.-C. Lai, "Suppression of epidemic spreading in complex networks by local information based behavioral responses," *Chaos: An Interdisciplinary Journal of Nonlinear Science*, vol. 24, no. 4, 043106, 7 pages, 2014.

[27] K. Paarporn, C. Eksin, J. S. Weitz, and J. S. Shamma, "Epidemic spread over networks with agent awareness and social distancing," in *Proceedings of the 53rd Annual Allerton Conference on Communication, Control, and Computing, Allerton 2015*, pp. 51–57, USA, October 2015.

[28] C. Lagnier, L. Denoyer, E. Gaussier, and P. Gallinari, "Predicting Information Diffusion in Social Networks Using Content and User's Profiles," in *Proceedings of the 35th European Conference on IR Research*, vol. 7814 of *Lecture Notes in Computer Science*, pp. 74–85, Springer, 2013.

[29] Q. Zhu, X. Yang, and J. Ren, "Modeling and analysis of the spread of computer virus," *Communications in Nonlinear Science and Numerical Simulation*, vol. 17, no. 12, pp. 5117–5124, 2012.

[30] C. Gan, X. Yang, W. Liu, Q. Zhu, and X. Zhang, "Propagation of computer virus under human intervention: a dynamical model," *Discrete Dynamics in Nature and Society*, vol. 2012, Article ID 106950, 8 pages, 2012.

[31] L.-X. Yang, X. Yang, J. Liu, Q. Zhu, and C. Gan, "Epidemics of computer viruses: a complex-network approach," *Applied Mathematics and Computation*, vol. 219, no. 16, pp. 8705–8717, 2013.

[32] C. Gan, X. Yang, W. Liu, and Q. Zhu, "A propagation model of computer virus with nonlinear vaccination probability," *Communications in Nonlinear Science and Numerical Simulation*, vol. 19, no. 1, pp. 92–100, 2014.

[33] W. Liu and S. Zhong, "Modeling and analyzing the dynamic spreading of epidemic malware by a network eigenvalue method," *Applied Mathematical Modelling: Simulation and Computation for Engineering and Environmental Systems*, vol. 63, pp. 491–507, 2018.

[34] W. Liu, X. Wu, W. Yang, X. Zhu, and S. Zhong, "Modeling cyber rumor spreading over mobile social networks: A compartment approach," *Applied Mathematics and Computation*, vol. 343, pp. 214–229, 2019.

[35] J. Wallinga and P. Teunis, "Different epidemic curves for severe acute respiratory syndrome reveal similar impacts of control measures," *American Journal of Epidemiology*, vol. 160, no. 6, pp. 509–516, 2004.

[36] S. A. Myers and J. Leskovec, "On the convexity of latent social network inference," in *Proceedings of the 23rd International Conference on Neural Information Processing Systems*, pp. 1741–1749, 2010.

[37] R. C. Robinson, *An Introduction to Dynamical Systems—Continuous and Discrete*, vol. 19 of *Pure and Applied Undergraduate Texts*, American Mathematical Society, Providence, Second edition, 2012.

[38] C. Gan, X. Yang, and W. Liu, "On behavior of two third-order nonlinear difference equations," *Utilitas Mathematica*, vol. 93, pp. 193–203, 2014.

[39] C. Gan, X. Yang, and W. Liu, "Global Behavior of xn+1=(a+βxn+k)(γ+xn)," *Discrete dynamics in nature and society*, vol. 2013, Article ID 963757, 5 pages, 2013.

[40] S. Elaydi, *An Introduction t o Difference Equations*, Springer, New York, NY, USA, 2005.

[41] Z. Zhang, Y. Zou, and C. Gan, "Textual sentiment analysis via three different attention convolutional neural networks and cross-modality consistent regression," *Neurocomputing*, vol. 275, pp. 1407–1415, 2018.

[42] Z. Zhang, L. Wang, Y. Zou, and C. Gan, "The optimally designed dynamic memory networks for targeted sentiment classification," *Neurocomputing*, vol. 309, pp. 36–45, 2018.

Hindawi
Discrete Dynamics in Nature and Society
Volume 2018, Article ID 4945728, 12 pages
https://doi.org/10.1155/2018/4945728

Research Article

Stability Analysis and Control Optimization of a Prey-Predator Model with Linear Feedback Control

Yaning Li,[1] Yan Li,[2] Yu Liu,[3] and Huidong Cheng[1]

[1]*College of Mathematics and Systems Science, Shandong University of Science and Technology, Qingdao 266590, China*
[2]*College of Electrical Engineering and Automation, Shandong University of Science and Technology, Qingdao 266590, China*
[3]*College of Foreign Languages, Shandong University of Science and Technology, Qingdao 266590, China*

Correspondence should be addressed to Huidong Cheng; chd900517@sdust.edu.cn

Received 13 July 2018; Revised 8 November 2018; Accepted 26 November 2018; Published 5 December 2018

Guest Editor: Abdul Qadeer Khan

The application of pest management involves two thresholds when the chemical control and biological control are adopted, respectively. Our purpose is to provide an appropriate balance between the chemical control and biological control. Therefore, a Smith predator-prey system for integrated pest management is established in this paper. In this model, the intensity of implementation of biological control and chemical control depends linearly on the selected control level (threshold). Firstly, the existence and uniqueness of the order-one periodic solution (i.e., OOPS) are proved by means of the subsequent function method to confirm the feasibility of the biological and chemical control strategy of pest management. Secondly, the stability of system is proved by the limit method of the successor points' sequences and the analogue of the Poincaré criterion. Moreover, an optimization strategy is formulated to reduce the total cost and obtain the best level of pest control. Finally, the numerical simulation of a specific model is performed.

1. Introduction

In the practical production, effective control of pests is a very important issue of the world, which catches attention of scholars for pest management method [1–7]. Integrated pest management (IPM), also known as integrated pest control (IPC), is an effective approach that integrates biological, chemical tactics, and physical methods for pests control [8–11]. Due to population dynamics and its related environment, IPM utilize effective methods and techniques comprehensively to reduce the level of economic harm caused by pests. The aim of IPM is to control the density of the insects under the economic threshold by integrated usage of less harmful pesticides and biological control methods for maximizing the protection of the ecosystem.

In mathematics, impulsive differential equations (IDES) is such a powerful tool to describe these phenomena that rapid changes in biological populations are caused by the variety of the pests control by artificial intervention [12–22]. In recent years, the theoretical studies on IDES have produced a lot of good research results [23–34]. Based on the theoretical research, some scholars have introduced impulsive differential equations in Lotka-Volterra system such as the regular release of predators [35–37]; the periodic release of infected pests [38–40]; the periodic release of predators together with regular spray of pesticides [41–43]; the periodic release of predators and infected pests together with regular spray of pesticides [39, 44]. In the practical application, the two control measures can be adopted at two different levels of pest density concerning this case. Nie et al. [45], Tian et al. [46], Zhao et al. [47], and Zhang et al. [48] studied the following predator-prey system and assumed that different control measures were adopted at different thresholds,

$$\begin{aligned} u'(t) &= au\ln\left(\frac{K}{u}\right) - buv, \\ v'(t) &= v(t)(-d + \lambda bu), \\ &\qquad u \neq h_1, h_2, \text{ or } u = h_1,\ v > v^*, \\ \Delta u(t) &= 0, \\ \Delta v(t) &= \gamma, \\ &\qquad u = h_1,\ v = v^*, \end{aligned}$$

$$\Delta u(t) = -\delta u(t),$$
$$\Delta v(t) = -\varrho v(t) + \tau,$$
$$u = h_2, \tag{1}$$

where the intrinsic growth rate of prey is denoted by a, the environment carrying capacity is denoted by K, the predation rate by natural enemies is denoted by b, and the transformation rate and the death rate of predator are denoted by λ and d, respectively. The η is a positive parameter, and the effect of pesticide to predator and prey species is denoted by ϱ and δ, respectively. The releasing quantity of natural enemy $v(t)$ are denoted by γ and τ, respectively.

It is of great practical significance to adopt biological and chemical control strategies based on the different pest thresholds. But an important issue in this process should be pointed out, in which the biological control is carried out when the density of pest denoted by $u(t)$ reaches the threshold h_1, and when the density $u(t)$ reaches the threshold h_2, the integrated control strategy is adopted. But no strategy adopted for the density of pest denoted by $u(t) = h$, where $h_1 < h < h_2$, which is obviously unreasonable. In addition, from an economic and practical point of view, the control taken at threshold h_1 seems to be early and the amount of releasing predators will also be huge, while the control taken at threshold h_2 seems to be late and the intensity of chemical control will also be high. Considering the above problems, we should choose a pest control method between h_1 and h_2.

An outline of this paper is as follows. In next section, a pest management Smith model is formulated. Then the existence, uniqueness, and the asymptotically orbit stability of order-one periodic solution (OOPS) of system (7) are proved in Section 3. In Section 4, an optimization problem is formulated and obtained the minimized total cost in pest control. The theoretical results are verified by numerical simulations in Section 5. Finally, a conclusion is drawn.

2. Model Formulation

In biological mathematics, Logistic model [10]

$$\frac{dx}{dt} = rx\left(1 - \frac{x}{K}\right) \tag{2}$$

is a classical mathematical model, where the predator and prey densities at time t are denoted by $y(t)$ and $x(t)$. r denotes the intrinsic rate of growth and K denotes the maximum environment carrying capacity, while system (2) is based on the assumption that the relative growth rate dx/xdt of the population size is linear function $1 - x/K$. In 1963, F.E.Smith found that the data about the population of Daphnia did not conform to the linear function [49]. Thus, Smith assumed that the relative growth rate of population density at time t is proportional to the amount of remaining food; i.e.,

$$\frac{1}{x}\frac{dx}{dt} = r\left(1 - \frac{H(t)}{T}\right), \tag{3}$$

where $H(t)$ is the rate of food demand of the population at time t; T is the rate of demand for food in a population saturated state. Smith assumed that the food required to keep the population is $c_1x(t)$ and the food required for the population to reproduce is $c_2(dx/dt)$. That is to say,

$$H(x) = c_1x(t) + c_2\frac{dx}{dt}. \tag{4}$$

Then

$$\frac{dx}{dt} = rx\left(1 - \frac{T - c_1x}{T + rc_2x}\right). \tag{5}$$

Considering the demand for food of population reproduction, the Smith model uses the hyperbolic function $(T - c_1x)/(T + rc_2x)$ instead of the linear function in the Logistic model. Thus, the Smith model is a further improvement of Logistic model. With the absence of predators, the per capita growth rate l_{grow} of the pest is assumed to be the Smith growth [49] model.

$$l_{grow} = rx\frac{K - x}{K - (r/c)x}. \tag{6}$$

By the control strategy, the following predator-prey Smith system is investigated in this paper:

$$\frac{dx}{dt} = \frac{mx(t) - rx(t)^2}{K + dx(t)} - qx(t)y(t),$$
$$\frac{dy}{dt} = \mu x(t)y(t) - ly(t),$$
$$x < h, \tag{7}$$
$$\Delta x(t) = -\alpha(x)x(t),$$
$$\Delta y(t) = -\beta(x)y(t) + \sigma(x),$$
$$x = h,\ y \le \overline{y}_h,$$

where the releasing amount of the predator is denoted by $\sigma(x)$ and $\sigma(h_1) = \sigma_{max}$, $\sigma(h_2) = \sigma_{min}$, where $0 \le \sigma_{min} < \sigma_{max}$. The strength of chemical control to the prey is $\alpha(x)$ and that to the predator is $\beta(x)$, where the parameters $\sigma(x), \alpha(x), \beta(x)$ are continuous functions and satisfies $\alpha(h_2) = \alpha_{max}$, $\beta(h_2) = \beta_{max}$. A pest control level h is between h_1 and h_2. $\overline{y}_h$ denotes the level of the predator at a lower density. By calculation we obtain $\overline{y}_h = (\lambda Kq - l)/q(Kq\lambda - dl)$, where $rK \triangleq m, r/c \triangleq d, \lambda q \triangleq \mu < l$ are constants. When the density of predator is below $\overline{y}_h$, the chemical control is taken. Clearly, the control strategy of system (7) changes into the biological control strategy of system (1) when parameters $\alpha(x)$, $\beta(x)$, and $\sigma(x)$, x of system (7), are chosen 0, 0, γ, h_1, respectively. When parameters $\alpha(x)$, $\beta(x)$, and $\sigma(x)$, x of system (7), are chosen δ, ϱ, τ h_2, respectively, the control strategy of system (7) turns into the integrated control strategy of system (1). Therefore, system (7) is the further promotion of system (1).

In our paper, $\sigma(x)$, $\alpha(x)$, and $\beta(x)$ are assumed to have the following linear form [10]

$$\sigma(x) = \sigma_{max} - (\sigma_{max} - \sigma_{min}) \frac{x - h_1}{h_2 - h_1},$$
$$\alpha(x) = \alpha_{max} \frac{x - h_1}{h_2 - h_1} \tag{8}$$
$$\beta(x) = \beta_{max} \frac{x - h_1}{h_2 - h_1}$$

3. Dynamical Analysis of System (7)

In this section, we dynamically analyze system (7) to study the existence, uniqueness and orbital asymptotical stability of the OOPS. For convenience, OOPS is used to represent the order-one periodic solution.

3.1. Qualitative Analysis of System (7). We first study the following continuous system of system (7); i.e.,

$$\frac{dx(t)}{dt} = \frac{mx(t) - rx(t)^2}{K + dx(t)} - qx(t)\, y(t),$$
$$\frac{dy(t)}{dt} = \mu x(t)\, y(t) - ly(t). \tag{9}$$

Let

$$\frac{mx(t) - rx(t)^2}{K + dx(t)} - qx(t)\, y(t) = 0,$$
$$\mu x(t)\, y(t) - ly(t) = 0. \tag{10}$$

Then we get three equilibria $O(0,0)$, $E_0(m/r, 0)$, and $E^*(x^*, y^*)$, where

$$x^* = \frac{l}{\mu},$$
$$y^* = \frac{\mu m - lr}{q(\mu K + dl)}. \tag{11}$$

Let

$$(I): \frac{l}{\mu} > \frac{\sqrt{\Delta} - rK}{rd}, \tag{12}$$

where $\Delta = r^2K^2 + mKrd$. Thus, we get the following theorem.

Theorem 1. *The positive equilibrium point $E^*(x^*, y^*)$ is locally asymptotically stable, if (I) holds.*

Proof. At the point $E^*(x^*, y^*)$, the Jacobian matrix is

$$J(E^*) = \begin{pmatrix} \dfrac{mK - rx^*(dx^* + 2K)}{(K + dx^*)^2} - qy^* & -qx^* \\ \mu y^* & 0 \end{pmatrix}, \tag{13}$$

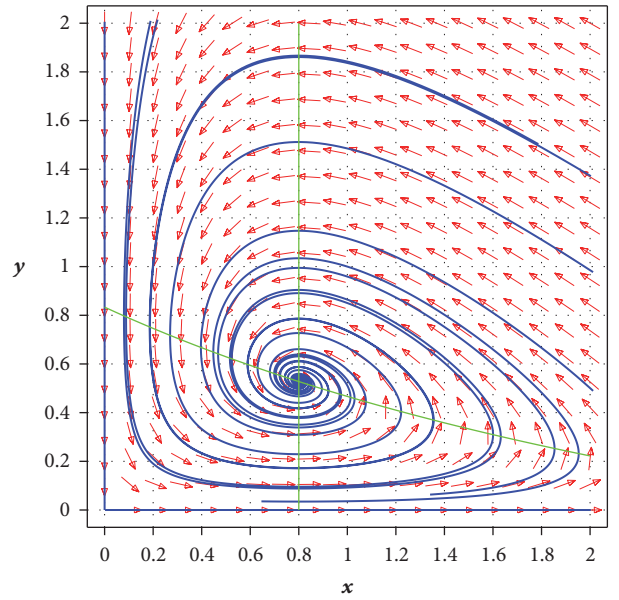

Figure 1: The phase diagram of system (7) with $m = 1$, $r = 0.3$, $K = 2$, $d = 0.5$, $q = 0.6$, $\mu = 0.5$, and $l = 0.4$.

then

$$\det(J(E^*)) = q\mu x^* y^* > 0,$$
$$\operatorname{tr}(J(E^*)) = \frac{mK - rx^*(dx^* + 2K)}{(K + dx^*)^2} - qy^*. \tag{14}$$

When (I) holds, then $\operatorname{tr}(J(E^*)) < 0$. Thus the point E^* is locally asymptotically stable. □

Theorem 2. *If $\mu x \le l$ holds, then the point E^* is globally asymptotically stable.*

Proof. Let $B = 1/x$, then we have

$$D = \frac{\partial(PB)}{\partial x} + \frac{\partial(QB)}{\partial x}$$
$$= \frac{-r(K + dx) - d(m - rx)}{(K + dx)^2} + \mu - \frac{l}{x} \tag{15}$$
$$= \frac{-rK - dm}{(K + dx)^2} + \mu - \frac{l}{x}$$

when $\mu x \le l$, then $D < 0$.

By the method in [48], the point $E^*(x^*, y^*)$ is globally asymptotically stable (see Figure 1.) □

3.2. Existence and Uniqueness of the Periodic Orbit of System (7). For convenience, let $H(x, y) = H_0$ denote the first integral of system (7), where the implicit function $H(x, y) = H(x_0, y_0)$ is divided into upper and lower branches by isoclinic line $dx/dt = 0$ denoted by $y_{H^+}(x, P_0)$ and $y_{H^-}(x, P_0)$, where the starting point is P_0. The impulsive set of system (7) is denoted by $\sum_M = \{(x, y) \mid x = h, 0 \le y \le \overline{y_h}\}$ and the phase set is denoted by $\sum_N = \{(x, y) \mid x = (1 - \alpha(h))h, y \ge 0\}$.

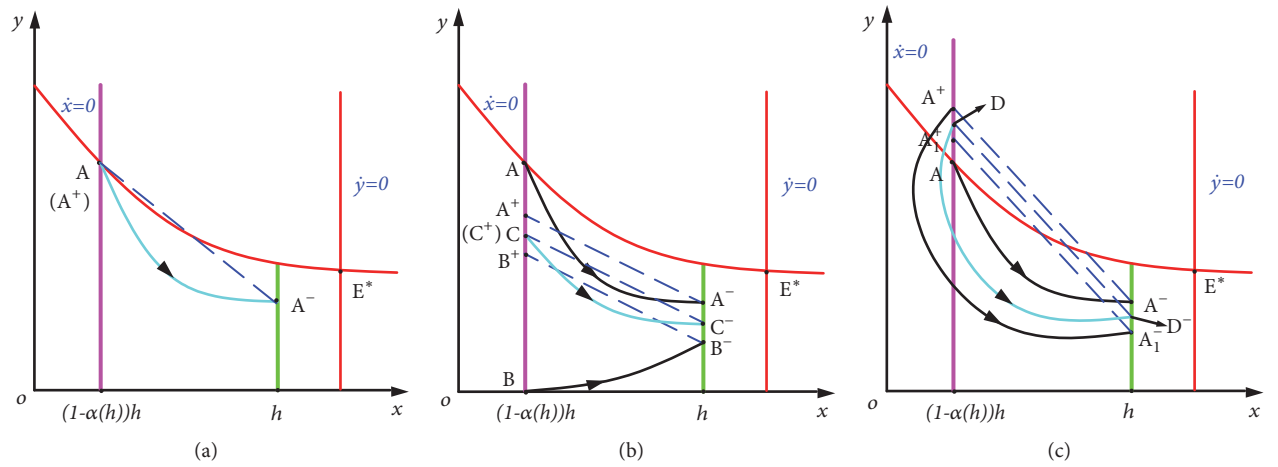

FIGURE 2: The existence of the OOPS of system (7). (a) Discussion in Case (i) if $\sigma(h) = \overline{\sigma}$. (b) Discussion in Case (i) if $\sigma(h) < \overline{\sigma}$. (c) Discussion in Case (ii).

Let $L_1 = \{(x, y) \mid x = l/\mu, y \geq 0\}$ and $L_2 = \{(x, y) \mid 0 \leq x, y = (m - rx)/q(K + dx)\}$ as the isoclinic line $dy/dt = 0$ and $dx/dt = 0$, respectively. For any point $A(x_A, y_A)$, where x_A and y_A are denoted as the abscissa and ordinate of point A, respectively. By the location of the threshold h and positive equilibrium point E^*, we get the following theorem.

Theorem 3. *If $0 < h_1 < h < \min\{x^*, h_2\}$ holds, then a uniqueness OOPS exists in system (7).*

Proof.

Case I ($0 < h_1 < h < \min\{x^*, h_2\}$). In view of Theorems 1 and 2, for any point $Q_0 \in \Omega$ where $\Omega = \{(x, y) \mid 0 \leq x \leq (1 - \alpha(h))h, y \in R\}$ the trajectory $y_{H^-}(x, Q_0)$ has an intersection point with phase set $\sum_N$. Thus, we discuss the trajectory tendency of the initial point on the phase set $\sum_N$.

Assuming the intersection point of phase set $\sum_N$ and isoclinic line $dx/dt = 0$ is point $A(x_A, y_A)$, where $x_A = (1 - \alpha(h))h$ and $y_A = (m - rh(1 - \alpha(h)))/q[K + dh(1 - \alpha)]$. The trajectory $y_{H^-}((1-\alpha)h, A)$ intersects with pulse set Σ_M at point $A^-(x_{A^-}, y_{A^-})$, then the impulsive function can transfer the point $A^-(x_{A^-}, y_{A^-})$ into the point $A^+(x_{A^+}, y_{A^+})$. Thus, we have

$$\begin{aligned} y_{A^+} &= (1 - \beta(h))\, y_{A^-} + \sigma(h) \\ &= (1 - \beta(h))\, y_{H^-}(h, A) + \sigma(h); \end{aligned} \tag{16}$$

define

$$\overline{\sigma}(h) \triangleq y_{A^+} - (1 - \beta(h))\, y_{H^-}(h, A). \tag{17}$$

By the magnitudes between $\sigma(h)$ and $\overline{\sigma}(h)$, one has

(i) $\sigma(h) \leq \overline{\sigma}$.

If $\sigma(h) = \overline{\sigma}$, the subsequent function of point $A(x_A, y_A)$ is $g(A) = 0$, then the trajectory $\widehat{AA^-A^+}$ is an OOPS.

If $\sigma(h) < \overline{\sigma}$, the point $A^+(x_{A^+}, y_{A^+})$ under the point $A(x_A, y_A)$, thus the subsequent function of point A is

$$g(A) = y_{A^+} - y_A < 0. \tag{18}$$

The phase set $\sum_N$ intersects with x-axis at point $B(x_B, 0)$, where $x_B = h(1 - \alpha(h))$. By the orbit tendency, $y_{H^-}(x, B)$ intersects with the impulsive set $\sum_M$ at the point $B^-(x_{B^-}, y_{B^-})$ which jumps to the point $B^+(x_{B^+}, y_{B^+})$. Obviously, the point $B(h(1 - \alpha(h)), 0)$ is under the point $B^+(x_{B^+}, y_{B^+})$. The subsequent function of the point $B(h(1 - \alpha(h)), 0)$ is

$$g(B) = y_{B^+} - y_B > 0. \tag{19}$$

According to the continuity of subsequent function, there must be a point C between point A and B, which makes

$$g(C) = 0. \tag{20}$$

(See Figures 2(a) and 2(b).)

(ii) $\sigma(h) > \overline{\sigma}$

If $\sigma(h) > \overline{\sigma}$, then the point $A^+(x_{A^+}, y_{A^+})$ must be above the point $A(x_A, y_A)$. Thus the subsequent function $g(A) > 0$. The orbit $y_{H^-}(x, A^+)$ will intersect with impulsive set $\sum_M$ at point $A_1^-(x_{A_1^-}, y_{A_1^-})$, then hits phase set $\sum_N$ at point $A_1^+(x_{A_1^+}, y_{A_1^+})$. Clearly, the point $A_1^-(x_{A_1^-}, y_{A_1^-})$ is under the point $A^-(x_{A^-}, y_{A^-})$. Thus the point $A_1^+(x_{A_1^+}, y_{A_1^+})$ must be under the point $A^+(x_{A^+}, y_{A^+})$. The subsequent function of point $A^+(x_{A^+}, y_{A^+})$ is

$$g(A^+) = y_{A_1^+} - y_{A^+} < 0. \tag{21}$$

So there must be a point $D \in \sum_N$, such that $g(D) = 0$ (see Figure 2(c)).

Now, the uniqueness of OOPS of system (7) is to be discussed.

Assuming that $P_1, P_2 \in \widehat{QA}$, then orbit $\widehat{P_1P_1^-P_1^+}$ and $\widehat{P_2P_2^-P_2^+}$ are OOPS, where $y_{P_1} < y_{P_2}$.

$$\begin{aligned} y_{P_1^+} &= (1 - \beta(h))\, h y_{P_1^-} + \sigma(h), \\ y_{P_2^+} &= (1 - \beta(h))\, h y_{P_2^-} + \sigma(h), \end{aligned} \tag{22}$$

Assume

$$\begin{aligned} \delta_{P_1P_2}(x) &= y_{H^-}(x, P_2) - y_{H^-}(x, P_1), \\ &\qquad x \in [(1 - \beta(h))\, h, h], \end{aligned} \tag{23}$$

then

$$\begin{aligned}\delta'_{P_1P_2}(x) &= y'_{H^-}(x,P_2) - y'_{H^-}(x,P_1)\\ &= \frac{\mu xy - ly}{(mx - rx^2)/(K+dx) - qxy}\\ &= \frac{(\mu x - l)(K+dx)}{x}\left[\frac{yP_2}{m - rx - qy_{P_2}(K+dx)}\right.\\ &\left. - \frac{yP_1}{m - rx - qy_{P_1}(K+dx)}\right] = \frac{(\mu x - l)(K+dx)}{x}\\ &\cdot \omega(\xi)\left(y_{P_2} - y_{P_1}\right),\end{aligned} \tag{24}$$

where

$$\omega(y) = \frac{y}{m - rx - qy(K+dx)}, \tag{25}$$

and

$$\omega'(y) = \frac{y(r+dqy)}{[m - rx - qy(K+dx)]^2} > 0. \tag{26}$$

So $\delta_{P_1P_2}(x) < 0$, $x \in [(1-\alpha)h, h]$; that is to say, $\delta_{P_1P_2}(x)$ is a decreasing function. For $x \in [(1-\alpha)h, h]$, then $\delta_{P_1P_2}(h) < \delta_{P_1P_2}((1-\alpha)h)$.

Thus

$$\begin{aligned}\sigma(h) &= y_{P_2^+} - (1-\beta)y_{P_2^-} = y_{P_2} - (1-\beta)y_{P_2^-}\\ &= y_{P_1} + \delta_{P_1P_2}((1-\alpha)h)\\ &\quad - (1-\beta)\left(y_{P_1^-} + \delta_{P_1P_2}(h)\right)\\ &= y_{P_1} - (1-\beta)y_{P_1^-} + \delta_{P_1P_2}((1-\alpha)h)\\ &\quad - (1-\beta)\delta_{P_1P_2}(h) > y_{P_1} - (1-\beta)y_{P_1^-}\\ &= \sigma(h).\end{aligned} \tag{27}$$

which is a contradiction.

When $\sigma(h) > \overline{\sigma}$, then there exists a point $P \in \overline{AA^+}$ such that $y_{P^+} = y_P$. Thus, for any $P' \in \overline{BA^+}$, the subsequent function of point P' is

$$\begin{aligned}g(P') &= y_{P'^+} - y_{P'} = (1-\beta)y_{P'^-} + \sigma(h) - y_{P'}\\ &= (1-\beta)y_{P'^-} - y_{P'} + y_P - (1-\beta)y_{P^-}\\ &= (y_P - y_{P'}) + (1-\beta)(y_{P'^-} - y_{P^-}).\end{aligned} \tag{28}$$

According to the proof above, we have $|y_P - y_{P'}| > |y_P - y_{P'^-}|$. Thus, if $y_{P'} < y_P$, then $g(P') < 0$.

If $y_{P'} > y_P$, then $g(P') > 0$. Thus the uniqueness of OOPS of system (7) in case of $\sigma(h) > \overline{\sigma}$ is proved. The proof is completed. □

Theorem 4. *If $\max\{x^*, h_1\} < h < h_2$ holds, then we have two cases. If $h > h_0$ holds, then system (7) has no OOPS. If $h < h_0$ holds, then system (7) has a unique OOPS, where $h_0 = \max\{x \mid 0 < y_{H^-}(x,B) \le h_2\}$.*

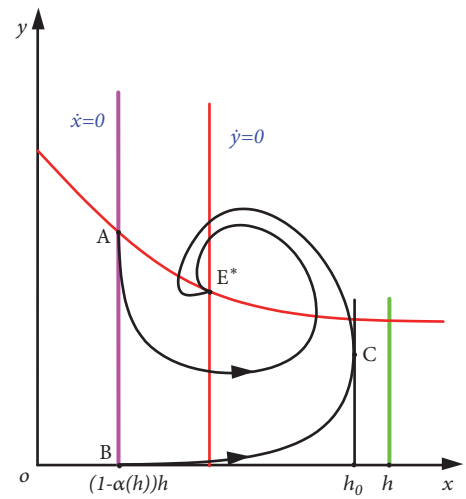

FIGURE 3: The existence of the OOPS of system (2) if $h > h_0$ in Case (II).

Proof.

Case II ($\max\{x^*, h_1 < h \le h_2\}$). Two cases are discussed according the magnitude of h and h_0.

(i) If $h > h_0$, the trajectory $y_{H^-}(x,B)$ tending to point $E^*(x^*, y^*)$ is based on the global asymptotical stability of $E^*(x^*, y^*)$. For any $P(x,y) \in \Omega$, the trajectory $y_{H^-}(x,P)$ tends to $E^*(x^*, y^*)$. (See Figure 3.)

(ii) If $h < h_0$, the trajectory $y_{H^-}(x,B)$ must intersect with the impulsive set $\sum_M$ at the point $B^-(x_{B^-}, y_{B^-})$, which jumps to the point $B^+(x_{B^+}, y_{B^+})$. The subsequent function of point $B(x_B, y_B)$ is $g(B) = y_{B^+} - y_B > 0$. Similar to the proof of Case I, when $\sigma \le \overline{\sigma}$, an OOPS exists in system (7). If $\sigma > \overline{\sigma}$, we also can prove that an OOPS exists in system (7) by same method of Case I. (See Figure 4.) □

4. The Orbital Asymptotical Stability of OOPS of System (7)

According to the discussion above, a unique OOPS exists in system (7), denoted by $\widehat{PP^-P^+}$. Then we get the following theorem.

Theorem 5. *If $\sigma \le \overline{\sigma}$, then the OOPS of system (7) is orbitally asymptotically stable and globally attractive to the point E^*.*

Proof. We choose arbitrary point A_0 on the phase set $\sum_N$. If $A_0 \in N/\overline{AP}$, then after several pulse effects the trajectory will jump to the segment $\overline{AP}$. Thus we assume that $A_0 \in \overline{AP}$; the trajectory $y_{H^-}(x, A_0)$ will hit the impulsive set $\sum_M$ at point A_1^-, which jumps to the point A_1^+. The trajectory $y_{H^-}(x, A_1^+)$ will intersect with impulsive set $\sum_M$ at point A_2^- and then jumps to the point A_2^+. Repeat the process above; we get a point sequences $\{A_k^+\}$, where $k = 1, 2, 3, \cdots$ such that

$$y_A > y_{A_0} > y^+_{A_1} > \cdots > y^+_{A_k} > \cdots \ge y_P. \tag{29}$$

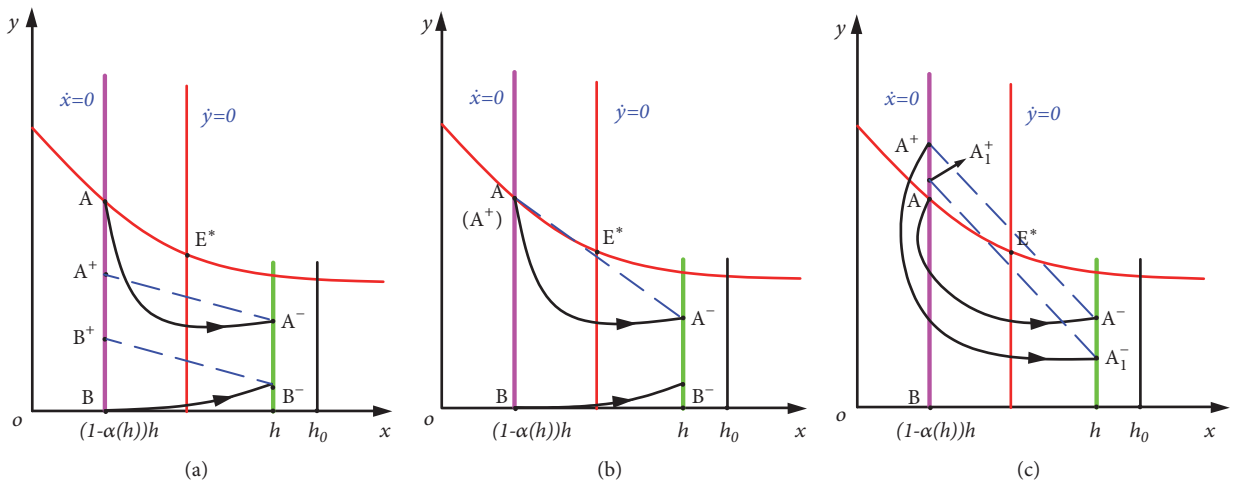

FIGURE 4: The existence of the OOPS of system (7) if $h < h_0$ in Case (II).

The sequence $A_k^+\|_{k=0,1,2,\cdots}$ is a monotonic decreasing sequence with lower bound y_P. According to the monotonic bounded theorem, there must exist a limit $y_{P'}$ such that $\lim_{k\longrightarrow\infty} y_{A_k^+} = y_{P'}$, which means that

$$\begin{aligned} g\left(P'\right) &= g\left(\lim_{k\longrightarrow\infty} y_{A_k^+}\right) = \lim_{k\longrightarrow\infty} g\left(y_{A_k^+}\right) \\ &= \lim_{k\longrightarrow\infty}\left(y_{A_{k+1}^+} - y_{A_k^+}\right) = 0. \end{aligned} \tag{30}$$

Since $g(A) = 0$, if and only if $A = P$, then $P' = P$. That is to say $\lim_{k\longrightarrow\infty} y_{A_k^+} = y_P$.

Similarly, we can use the above method to get an increasing point sequences $B_k^+\|_{k=0,1,2,\cdots}$ such that

$$y_B < y_{B_0} < y_{B_1}^+ < \cdots < y_{B_k}^+ < \cdots \le y_P. \tag{31}$$

There must exist a limit $y_{P'}$ such that $\lim_{k\longrightarrow\infty} y_{B_k^+} = y_{P'}$, which means that

$$\begin{aligned} g\left(P'\right) &= g\left(\lim_{k\longrightarrow\infty} y_{B_k^+}\right) = \lim_{k\longrightarrow\infty} g\left(y_{B_k^+}\right) \\ &= \lim_{k\longrightarrow\infty}\left(y_{B_{k+1}^+} - y_{B_k^+}\right) = 0. \end{aligned} \tag{32}$$

Since $g(B) = 0$, if and only if $B = P$, then $P' = P$. That is to say, $\lim_{k\longrightarrow\infty} y_{B_k^+} = y_P$. By the arbitrariness of the point A_0 and B_0, one has

$$\lim_{k\longrightarrow\infty} y_{A_k^+} = \lim_{k\longrightarrow\infty} y_{B_k^+} = y_P. \tag{33}$$

Thus the OOPS of system (7) is orbitally asymptotically stable and globally attractive (see Figure 5). □

Theorem 6. *If $\sigma > \overline{\sigma}$ and $\gamma_1[m - r\eta_0 - q\gamma_0(K + d\eta_0)](1 - \beta)(K + d\eta_1)/\gamma_0(m - r\eta_1 - q\gamma_1)(K + d\eta_0) < 1$, then the OOPS of system (7) is orbitally asymptotically stable.*

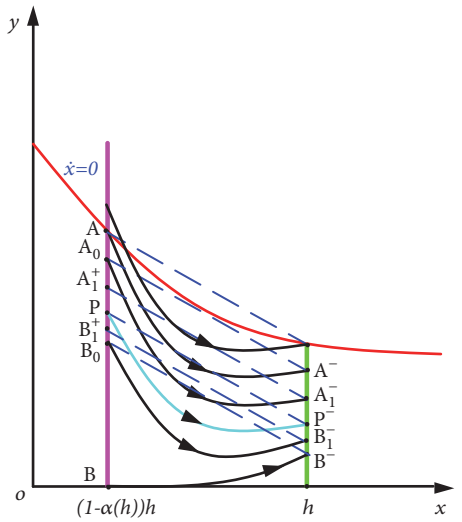

FIGURE 5: The orbitally asymptotically stability of the OOPS of system (7).

Proof. Let $x = \eta(t), y = \gamma(t)$ is a T-periodic orbit of system (7) and $\eta_0 = \eta(0), \gamma_0 = \gamma(0), \eta_1 = \eta(T), \gamma_1 = \gamma(T), \eta_1^+ = \eta(T^+), \gamma_1^+ = \gamma(T^+)$, then

$$\begin{aligned} \eta_1^+ &= \eta_0 = (1 - \alpha)\, h, \\ \gamma_1^+ &= \gamma_0 = (1 - \beta)\, \gamma_1 + \sigma. \end{aligned} \tag{34}$$

Let

$$\begin{aligned} P(x, y) &= \frac{mx - rx^2}{K + dx} - qxy, \\ Q(x, y) &= \mu xy - ly, \\ \zeta(x, y) &= -\alpha x, \\ \xi(x, y) &= -\beta y + \sigma. \end{aligned} \tag{35}$$

Then

$$\begin{aligned}
&\frac{\partial\zeta}{\partial x} = -\alpha,\\
&\frac{\partial\xi}{\partial x} = -\beta,\\
&\frac{\partial\zeta}{\partial y} = 0,\\
&\frac{\partial\xi}{\partial y} = -\beta,\\
&\frac{\partial\varphi}{\partial x} = 1,\\
&\frac{\partial\varphi}{\partial y} = 0
\end{aligned} \tag{36}$$

$$\Delta_1 = \frac{P + ((\partial\xi/\partial y)(\partial\varphi/\partial x) - (\partial\xi/\partial x)(\partial\varphi/\partial y) + \partial\varphi/\partial x) + Q + ((\partial\zeta/\partial x)(\partial\varphi/\partial y) - (\partial\zeta/\partial y)(\partial\varphi/\partial x) + \partial\varphi/\partial y)}{P(\partial\varphi/(\partial x + Q(\partial\varphi/\partial y)))},$$

$$= \frac{P(\eta_1^+, \gamma_1^+)(-\beta - 0 + 1) + Q(\eta_1^+, \gamma_1^+)(-\alpha \times 0 - r \times 0 + 0)}{P(\eta_1, \gamma_1) \times 1 + Q(\eta_1, \gamma_1) \times 0} = \frac{\eta_0[(m - r\eta_0)/(K + d\eta_0) - q\gamma_0](1 - \beta)}{\eta_1[(m - r\eta_1)/(K + d\eta_1) - q\gamma_1]}.$$

and

$$\int_0^T \left(\frac{\partial P}{\partial x} + \frac{\partial Q}{\partial y}\right) dt = \int_0^T \left[\frac{m - 2rx}{K + dx} - \frac{d\left(mx - rx^2\right)}{(K + dx)^2}\right.$$

$$\left. - qy + \mu x - l\right] dt = \int_0^T \left[\frac{m - rx}{K + dx} - \frac{rx}{K + dx}\right.$$

$$\left. - \frac{d\left(mx - rx^2\right)}{(K + dx)^2} - qy + \mu x - l\right] dt$$

$$= \int_0^T \left[\frac{\dot{x}}{x(t)} + \frac{\dot{y}}{y(t)}\right] - \left[\int_0^T \frac{rx}{K + dx}\right.$$

$$\left. + \frac{d\left(mx - rx^2\right)}{(K + dx)^2}\right] dt = \ln\frac{x(T)\, y(T)}{x(0)\, y(0)}$$

$$- \int_0^T \frac{rx(K + dx) + d\left(mx - rx^2\right)}{(K + dx)^2} dt$$

$$= \ln\frac{x(T)\, y(T)}{x(0)\, y(0)} - \int_0^T \frac{dmx + rKx}{(K + dx)^2} dt.$$

$$\mu_2 = \Delta_1 \int_0^T \left(\frac{\partial P}{\partial x} + \frac{\partial Q}{\partial y}\right) dt$$

$$= \frac{\left[m\eta_0 - r\eta_0^2 - q\eta_0\gamma_0(K + d\eta_0)\right](1 - \beta)}{K + d\eta_0}$$

$$\cdot \frac{K + d\eta_1}{m\eta_1 - r\eta_1^2 - q\eta_1\gamma_1} \frac{\eta_1\gamma_1}{\eta_0\gamma_0} \exp\int_0^T \frac{-dmx - rKx}{(K + dx)^2}$$

$$= \frac{\gamma_1[m - r\eta_0 - q\gamma_0(K + d\eta_0)](1 - \beta)(K + d\eta_1)}{\gamma_0(m - r\eta_1 - q\gamma_1)(K + d\eta_0)}$$

$$\cdot \exp\int_0^T \frac{-dmx - rKx}{(K + dx)^2}. \tag{37}$$

Thus, when $\sigma > \overline{\sigma}$ and $\gamma_1[m - r\eta_0 - q\gamma_0(K + d\eta_0)](1 - \beta)(K + d\eta_1)/\gamma_0(m - r\eta_1 - q\gamma_1)(K + d\eta_0) < 1$, $|\mu_2| < 1$. Therefore, the OOPS is orbitally asymptotically stable. □

5. Numerical Simulations and Optimization of Pest Control Level

5.1. Numerical Simulations. In this section, the feasibility of our conclusions is verified by an example. Let $m = 1$, $r = 0.3$, $K = 2$, $d = 0.5$, $q = 0.6$, $\mu = 0.5$, and $l = 0.4$. By calculation, the equilibrium point E^* of system (7) is $E^*(0.8, 0.528)$. Parameter values are taken into system (7), then

$$\begin{aligned}
&\frac{dx}{dt} = \frac{x(t) - 0.3x(t)^2}{2 + 0.5x(t)} - 0.6x(t)\, y(t),\\
&\frac{dy}{dt} = 0.5x(t)\, y(t) - 0.4y(t),
\end{aligned}$$

$$x < h,$$

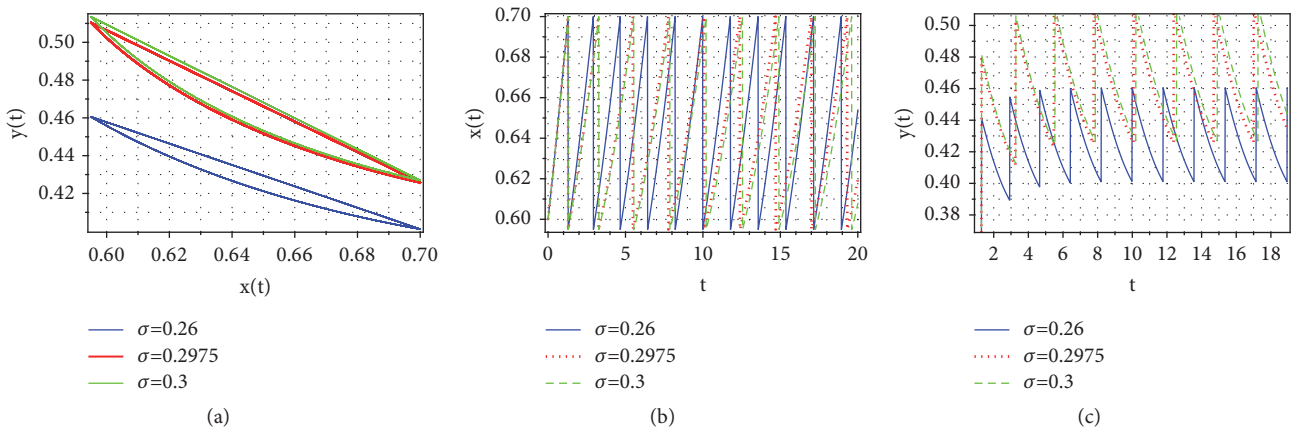

FIGURE 6: Numerical simulations in case $0 < h_1 < h < \min\{x^*, h_2\}$. (a) Phase portrait of $x(t)$ and $y(t)$ on $h = 0.7$. (b) Time series of $x(t)$. (c) Time series of $y(t)$.

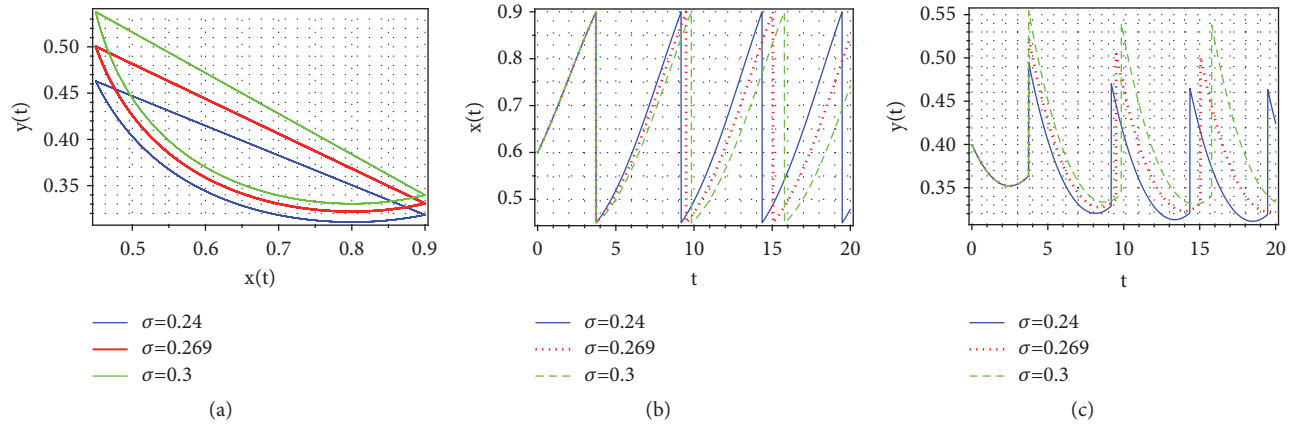

FIGURE 7: Numerical simulations in case $0 < \max\{x^*, h_1\} < h < h_0 < h_2$. (a) Phase portrait of $x(t)$ and $y(t)$ on $h = 0.9$. (b) Time series of $x(t)$. (c) Time series of $y(t)$.

$$\Delta x(t) = -\alpha(x)\, x(t),$$
$$\Delta y(t) = -\beta(x)\, y(t) + \sigma(x),$$
$$x = h, \quad y \le \overline{y}_h \tag{38}$$

Let $h = 0.7$ satisfy the condition $0 < h_1 < h < \min\{x^*, h_2\}$ and the initial value be $(0.4, 0.4)$. Let $\sigma_{max} = 1.5$, $\delta_{min} = 0.1$, $\alpha_{max} = 1.75$, $\beta_{max} = 2$, $h_1 = 0$, and $h_2 = 2$. A directed calculation yields that $\alpha_{0.7} = 0.15$, $\beta_{0.7} = 0.5$, and $\overline{\sigma_{0.7}} = 0.2975$. Let $\sigma = 0.26$, $\sigma = \overline{\sigma_{0.7}} = 0.2975$, and $\sigma = 0.3$. Figures 6(a), 6(b), and 6(c) show that a unique and asymptotically stable OOPS exists in system (7).

Let $h = 0.9$ satisfy the condition $0 < \max\{x^*, h_1\} < h < h_0 < h_2$ and the initial value be $(0.5, 1)$. A directed calculation yields that $\alpha_{0.9} = 0.5$, $\beta_{0.9} = 0.3$, and $\overline{\sigma_{0.9}} = 0.269$. Let $\sigma = 0.24$, $\sigma = \overline{\sigma_{0.9}} = 0.269$, and $\sigma = 0.3$. Figures 7(a), 7(b), and 7(c) show that system (7) has a unique and asymptotically stable OOPS.

For the case of $0 < \max\{x^*, h_1\} < h_0 < h \le h_2$, for example, $h = 1.5$ and the orbit of system (7) starts from $(0.5, 1)$, we get $\alpha_{1.5} = 0.5$, $\beta_{0.9} = 0.3$ and $\sigma_{1.5} = 0.24$ by calculation. Figures 8(a), 8(b), and 8(c) show that system (7) has no OOPS.

5.2. Determination and Optimization of Pest Control Level. The goal to investigate the existence of OOPS of system (7) lies in that it can obtain the possibility of determining the frequency of releasing predators and spraying pesticides, which makes the density of pest below the damage level. Although the density of prey is inaccurate or biased, the system will eventually undergo periodic changes under the effective control. The following problems are considered to determine the optimal frequency for releasing predators and chemical controls.

Assuming that unit cost of releasing predator is denoted by ι_1 and the unit cost of spraying pesticides is denoted by ι_2, which include the price of chemical agent and the price of the damage to environment. Our goal is to reduce the unit cost in this process. In one period, the total cost is denoted by F_t, which is a function about $\alpha(h)$ (i.e., chemical control strength) and $\sigma(h)$ (i.e., yield of releases of predator).

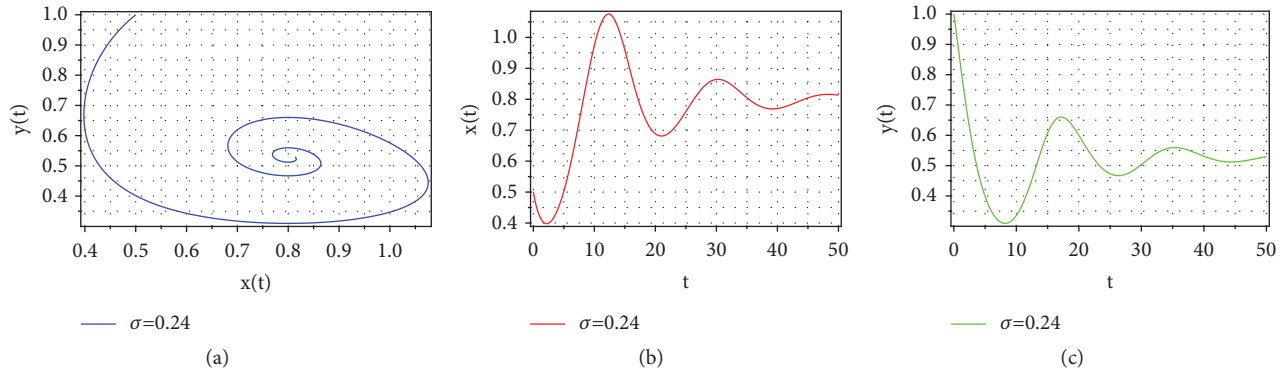

FIGURE 8: Numerical simulations in case $< \max\{x^*, h_1\} < h_0 < h \le h_2$. (a) Phase portrait of $x(t)$ and $y(t)$ on $h = 1.5$. (b) Time series of $x(t)$. (c) Time series of $y(t)$.

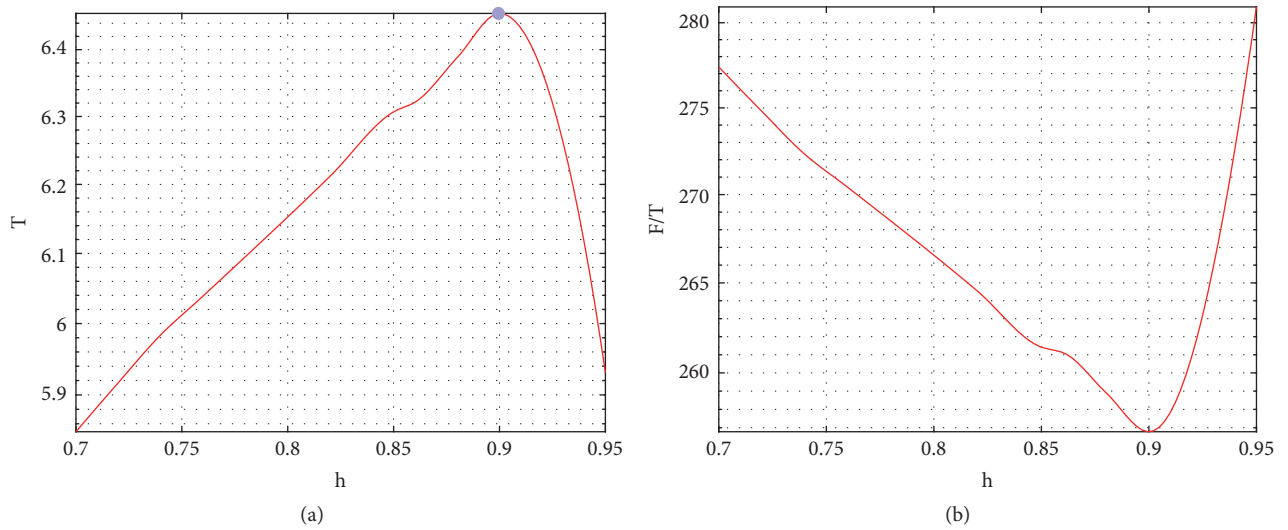

FIGURE 9: The variety in the period T and the profit per unit time F/T on the threshold h. (a) The variety in the period T on the threshold h. (b) The profits per unit time F/T on the threshold h.

Then $F_\iota(h) = \iota_1\sigma(h) + \iota_2\alpha(h)$. So the optimization model is formulated as

$$\max \quad \frac{F_\iota(h)}{T(h)} \qquad \text{s.t.} \quad h_1 \le h \le h_2 \tag{39}$$

The optimization problem is solved to yield the optimal pest level h^*, which the optimal release rate of predator is $\sigma^* = \sigma_{h^*}$, the optimal strength of chemical control is $\alpha^* = \alpha_{h^*}$, and the optimal impulse period of chemical control is $T^* = T(\sigma^*, \alpha^*)$. However, the optimum pest control level h^* is dependent on the ratio of $\omega \triangleq \iota_2/\iota_1$. The impulse period T varies with the threshold h, as shown in Figure 9(a). And Figure 9(b) shows the variation of cost per unit time F/T and the period T with the pest control level h, where $\iota_1 = 1000$, $\iota_2 = 1000$, i.e., $\omega = 1$. The optimal pest level is $h^* = 0.9$, the optimal strength of chemical control is $\alpha_{h^*} = 0.788$, and the optimal release rate of predator is $\sigma_{h^*} = 0.87$. It is important to note that the optimum economic threshold h is dependent on ω, as is illustrated in Figure 10.

6. Conclusion

A Smith prey-predator system with linear feedback control for integrated pest management is investigated in this paper. Integrated control strategy is more practical which can maximize the protection of the ecological environment and reduce the cost of pest management. First, the method of subsequent function and differential equation geometry theory are used to prove the existence, uniqueness, and stability of the OOPS of system (7). Second, a specific example is given to verify the conclusion of the impulsive strategy. Last, an optimized problem is formulated and the minimized total cost in pest control is obtained. However, the optimized results have some deviations which need to be further improved.

Data Availability

We agree to share the data underlying the findings of the manuscript. Data sharing allows researchers to verify the results of an article, replicate the analysis, and conduct secondary analyses.

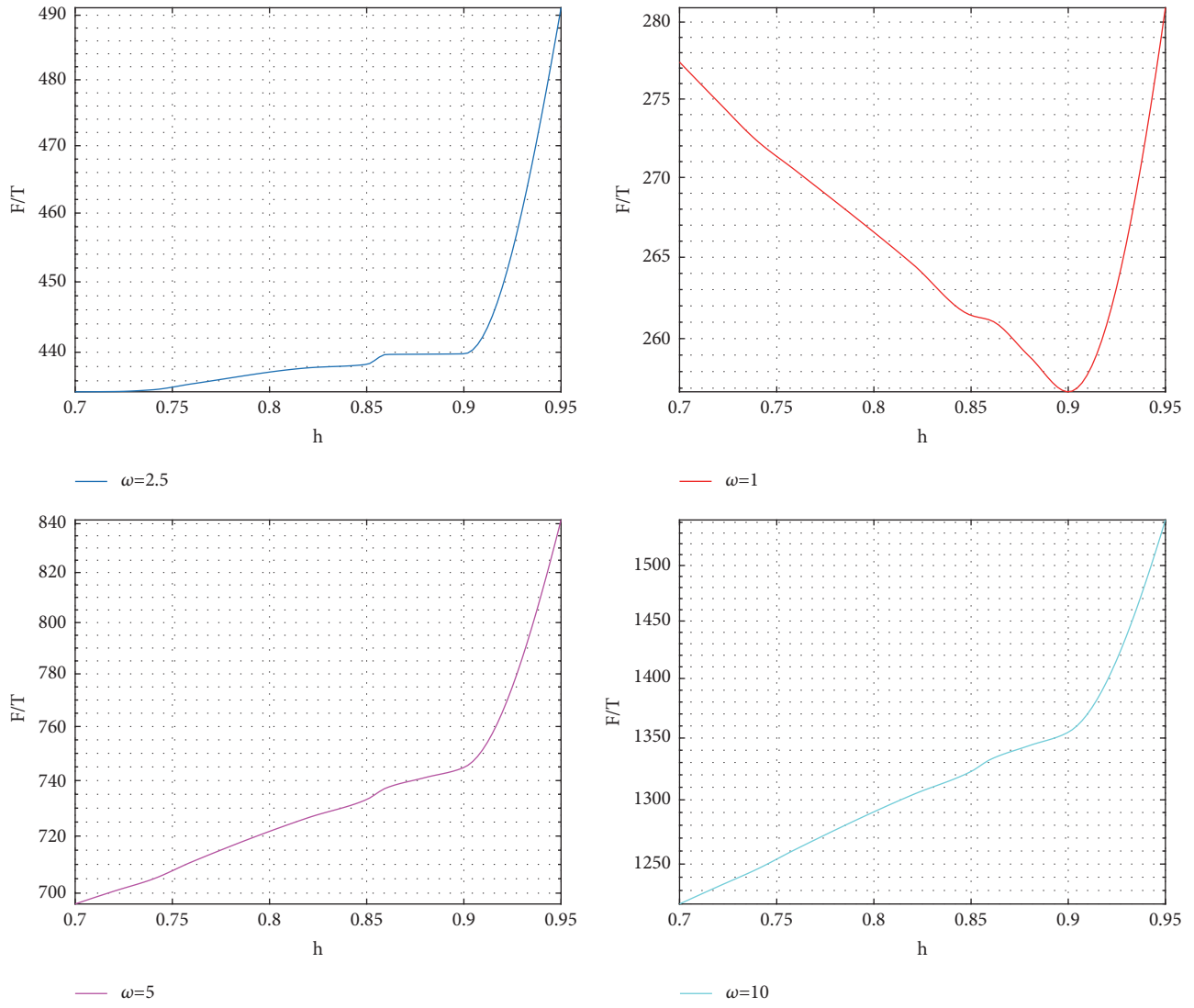

FIGURE 10: The change in the cost per unit time F/T on the control level h for $\iota_2/\iota_1 = 2.5, 1, 5, 10$.

Conflicts of Interest

The authors declare that they have no conflicts of interest.

Acknowledgments

This work was supported by the National Natural Science Foundation of China (11371230 and 11501331), the SDUST Research Fund (2014TDJH102), Shandong Provincial Natural Science Foundation, China (ZR2015AQ001 and BS2015SF002), Joint Innovative Center for Safe and Effective Mining Technology and Equipment of Coal Resources, the Open Foundation of the Key Laboratory of Jiangxi Province for Numerical Simulation and Emulation Techniques, Gannan Normal University, China, and SDUST Innovation Fund for Graduate Students (no. SDKDYC170225).

References

[1] M. Huang and X. Song, "Periodic Solutions and Homoclinic Bifurcations of Two Predator-Prey Systems with Nonmonotonic Functional Response and Impulsive Harvesting," *Journal of Applied Mathematics*, vol. 2014, Article ID 803764, 11 pages, 2014.

[2] C. J. Wei and L. S. Chen, "Periodic solution and heteroclinic bifurcation in a predator-prey system with Allee effect and impulsive harvesting," *Nonlinear Dynamics*, vol. 76, no. 2, pp. 1109–1117, 2014.

[3] Y. Li, H. Cheng, and Y. Wang, "A Lycaon pictus impulsive state feedback control model with Allee effect and continuous time delay," *Advances in Difference Equations*, Paper No. 367, 17 pages, 2018.

[4] B. Liu, Y. Tian, and B. Kang, "Dynamics on a Holling II predator-prey model with state-dependent impulsive control," *International Journal of Biomathematics*, vol. 5, no. 3, Article ID 1260006, pp. 93–110, 2012.

[5] M. Zhang, G. Song, and L. Chen, "A state feedback impulse model for computer worm control," *Nonlinear Dynamics*, vol. 85, no. 3, pp. 1561–1569, 2016.

[6] X. Z. Meng, S. N. Zhao, T. Feng, and T. H. Zhang, "Dynamics of a novel nonlinear stochastic SIS epidemic model with double

epidemic hypothesis," *Journal of Mathematical Analysis and Applications*, vol. 433, no. 1, pp. 227–242, 2016.

[7] T. Zhang, T. Zhang, and X. Meng, "Stability analysis of a chemostat model with maintenance energy," *Applied Mathematics Letters*, vol. 68, pp. 1–7, 2017.

[8] Huidong Cheng, Tongqian Zhang, and Fang Wang, "Existence and Attractiveness of Order One Periodic Solution of a Holling I Predator-Prey Model," *Abstract and Applied Analysis*, vol. 2012, Article ID 126018, 18 pages, 2012.

[9] H. Liu and H. Cheng, "Dynamic analysis of a prey–predator model with state-dependent control strategy and square root response function," *Advances in Difference Equations*, Paper No. 63, 13 pages, 2018.

[10] K. B. Sun, T. H. Zhang, and Y. Tian, "Theoretical study and control optimization of an integrated pest management predator-prey model with power growth rate," *Mathematical Biosciences*, vol. 279, pp. 13–26, 2016.

[11] G. Liu, X. Wang, X. Meng, and S. Gao, "Extinction and Persistence in Mean of a Novel Delay Impulsive Stochastic Infected Predator-Prey System with Jumps," *Complexity*, vol. 2017, Article ID 1950970, 15 pages, 2017.

[12] H. Zhang, J. Jiao, and L. Chen, "Pest management through continuous and impulsive control strategies," *BioSystems*, vol. 90, no. 2, pp. 350–361, 2007.

[13] F. Wang, B. Chen, Y. Sun, and C. Lin, "Finite time control of switched stochastic nonlinear systems," *Fuzzy Sets and Systems*, 2018.

[14] G. Pang and L. Chen, "Periodic solution of the system with impulsive state feedback control," *Nonlinear Dynamics*, vol. 78, no. 1, pp. 743–753, 2014.

[15] W. Lv, F. Wang, and Y. Li, "Adaptive finite-time tracking control for nonlinear systems with unmodeled dynamics using neural networks," *Advances in Difference Equations*, Paper No. 159, 17 pages, 2018.

[16] T. Zhang, W. Ma, and X. Meng, "Global dynamics of a delayed chemostat model with harvest by impulsive flocculant input," *Advances in Difference Equations*, Paper No. 115, 17 pages, 2017.

[17] W. Lv and F. Wang, "Adaptive tracking control for a class of uncertain nonlinear systems with infinite number of actuator failures using neural networks," *Advances in Difference Equations*, Paper No. 374, 16 pages, 2017.

[18] F. Liu, "Continuity and approximate differentiability of multisublinear fractional maximal functions," *Mathematical Inequalities & Applications*, vol. 21, no. 1, pp. 25–40, 2018.

[19] F. Liu, Q. Xue, and K. Yabuta, "Rough maximal singular integral and maximal operators supported by subvarieties on Triebel-Lizorkin spaces," *Nonlinear Analysis. Theory, Methods & Applications. An International Multidisciplinary Journal*, vol. 171, pp. 41–72, 2018.

[20] Y. Li, H. Cheng, J. Wang, and Y. Wang, "Dynamic analysis of unilateral diffusion Gompertz model with impulsive control strategy," *Advances in Difference Equations*, Paper No. 32, 14 pages, 2018.

[21] T. Zhang, X. Liu, X. Meng, and T. Zhang, "Spatio-temporal dynamics near the steady state of a planktonic system," *Computers & Mathematics with Applications*, vol. 75, no. 12, pp. 4490–4504, 2018.

[22] F. Wang, B. Chen, C. Lin, J. Zhang, and X. Meng, "Adaptive Neural Network Finite-Time Output Feedback Control of Quantized Nonlinear Systems," *IEEE Transactions on Cybernetics*, vol. 48, no. 6, pp. 1839–1848, 2017.

[23] A. Miao, T. Zhang, J. Zhang, and C. Wang, "Dynamics of a stochastic SIR model with both horizontal and vertical transmission," *Journal of Applied Analysis and Computation*, vol. 8, no. 4, pp. 1108–1121, 2018.

[24] X. Fan, Y. Song, and W. Zhao, "Modeling Cell-to-Cell Spread of HIV-1 with Nonlocal Infections," *Complexity*, vol. 2018, pp. 1–10, 2018.

[25] Z. Zhao, L. Pang, and X. Song, "Optimal control of phytoplankton-fish model with the impulsive feedback control," *Nonlinear Dynamics*, vol. 88, no. 3, pp. 2003–2011, 2017.

[26] H. Guo, L. Chen, and X. Song, "Dynamical properties of a kind of SIR model with cnstant vaccination rate and impulsive state feedback control," *International Journal of Biomathematics*, vol. 10, no. 7, 1750093, 21 pages, 2017.

[27] G. Z. Zeng, L. S. Chen, and J. F. Chen, "Persistence and periodic orbits for two-species nonautonomous diffusion Lotka-Volterra models," *Mathematical and Computer Modelling*, vol. 20, no. 12, pp. 69–80, 1994.

[28] F. Liu, "A note on Marcinkiewicz integrals associated to surfaces of revolution," *Journal of the Australian Mathematical Society*, vol. 104, no. 3, pp. 380–420, 2018.

[29] M. Chi and W. Zhao, "Dynamical analysis of multi-nutrient and single microorganism chemostat model in a polluted environment," *Advances in Difference Equations*, Paper No. 120, 16 pages, 2018.

[30] M. Huang, X. Song, and J. Li, "Modelling and analysis of impulsive releases of sterile mosquitoes," *Journal of Biological Dynamics*, vol. 11, no. 1, pp. 147–171, 2017.

[31] A. Miao, J. Zhang, T. Zhang, and P. Aruna, "Threshold dynamics of a stochastic SIR model with vertical transmission and vaccination," *Computational and Mathematical Methods in Medicine*, vol. 2017, Article ID 4820183, 10 pages, 2017.

[32] F. Liu and H. Wu, "Singular integrals related to homogeneous mappings in Triebel-Lizorkin spaces," *Journal of Mathematical Inequalities*, vol. 11, no. 4, pp. 1075–1097, 2017.

[33] Y. Song, A. Miao, T. Zhang, X. Wang, and J. Liu, "Extinction and persistence of a stochastic SIRS epidemic model with saturated incidence rate and transfer from infectious to susceptible," *Advances in Difference Equations*, Paper No. 293, 11 pages, 2018.

[34] Y. Li and X. Liu, "H-index for nonlinear stochastic systems with state and input dependent noises," *International Journal of Fuzzy Systems*, vol. 20, no. 3, pp. 759–768, 2018.

[35] X. Meng and L. Zhang, "Evolutionary dynamics in a Lotka-Volterra competition model with impulsive periodic disturbance," *Mathematical Methods in the Applied Sciences*, vol. 39, no. 2, pp. 177–188, 2016.

[36] H. Cheng and T. Zhang, "A new predator-prey model with a profitless delay of digestion and impulsive perturbation on the prey," *Applied Mathematics and Computation*, vol. 217, no. 22, pp. 9198–9208, 2011.

[37] Y. Li, W. Zhang, and X.-K. Liu, "H-index for discrete-time stochastic systems with markovian jump and multiplicative noise," *Automatica*, vol. 90, pp. 286–293, 2018.

[38] J. Wang, H. Cheng, X. Meng, and B. G. Pradeep, "Geometrical analysis and control optimization of a predator-prey model with multi state-dependent impulse," *Advances in Difference Equations*, Paper No. 252, 17 pages, 2017.

[39] Q. Liu, L. Huang, and L. Chen, "A pest management model with state feedback control," *Advances in Difference Equations*, vol. 2016, no. 1, 292 pages, 2016.

[40] T. Zhang, W. Ma, X. Meng, and T. Zhang, "Periodic solution of a prey-predator model with nonlinear state feedback control," *Applied Mathematics and Computation*, vol. 266, pp. 95–107, 2015.

[41] L. Chen, "Pest control and geometric theory of semi-continuous dynamical system," *Journal of Beihua University*, vol. 12, no. 1, 2011.

[42] J. Wang, H. Cheng, H. Liu, and Y. Wang, "Periodic solution and control optimization of a prey-predator model with two types of harvesting," *Advances in Difference Equations*, Paper No. 41, 14 pages, 2018.

[43] H. Cheng, F. Wang, and T. Zhang, "Multi-state dependent impulsive control for pest management," *Journal of Applied Mathematics*, vol. 2012, Article ID 381503, 25 pages, 2012.

[44] J. Wang, H. Cheng, Y. Li, and X. Zhang, "The geometrical analysis of a predator-prey model with multi-state dependent impulses," *Journal of Applied Analysis and Computation*, vol. 8, no. 2, pp. 427–442, 2018.

[45] L. Nie, Z. Teng, L. Hu, and J. Peng, "The dynamics of a Lotka-Volterra predator-prey model with state dependent impulsive harvest for predator," *BioSystems*, vol. 98, no. 2, pp. 67–72, 2009.

[46] Y. Tian, T. Zhang, and K. Sun, "Dynamics analysis of a pest management prey-predator model by means of interval state monitoring and control," *Nonlinear Analysis: Hybrid Systems*, vol. 23, pp. 122–141, 2017.

[47] L. Zhao, L. Chen, and Q. Zhang, "The geometrical analysis of a predator-prey model with two state impulses," *Mathematical Biosciences*, vol. 238, no. 2, pp. 55–64, 2012.

[48] T. Q. Zhang, X. Z. Meng, R. Liu, and T. H. Zhang, "Periodic solution of a pest management Gompertz model with impulsive state feedback control," *Nonlinear Dynamics*, vol. 78, no. 2, pp. 921–938, 2014.

[49] F. E. Smith, "Population dynamics in *Daphnia magna* and a new model for population growth," *Ecology*, vol. 44, no. 4, pp. 651–663, 1963.

Hindawi
Discrete Dynamics in Nature and Society
Volume 2018, Article ID 6935095, 10 pages
https://doi.org/10.1155/2018/6935095

Research Article

Stochastic P-Bifurcation of a Bistable Viscoelastic Beam with Fractional Constitutive Relation under Gaussian White Noise

Yajie Li,[1,2] **Zhiqiang Wu**,[1,2] **Guoqi Zhang**,[1,2] **and Feng Wang**[1,2]

[1]*Department of Mechanics, School of Mechanical Engineering, Tianjin University, Tianjin 300072, China*
[2]*Tianjin Key Laboratory of Nonlinear Dynamics and Chaos Control, Tianjin University, Tianjin 300072, China*

Correspondence should be addressed to Zhiqiang Wu; zhiqwu@tju.edu.cn

Received 28 July 2018; Revised 26 October 2018; Accepted 5 November 2018; Published 2 December 2018

Academic Editor: Dorota Mozyrska

In this paper, we study the stochastic P-bifurcation problem for axially moving of a bistable viscoelastic beam with fractional derivatives of high order nonlinear terms under Gaussian white noise excitation. First, using the principle for minimum mean square error, we show that the fractional derivative term is equivalent to a linear combination of the damping force and restoring force, so that the original system can be simplified to an equivalent system. Second, we obtain the stationary Probability Density Function (PDF) of the system's amplitude by stochastic averaging, and using singularity theory, we find the critical parametric condition for stochastic P-bifurcation of amplitude of the system. Finally, we analyze the types of the stationary PDF curves of the system qualitatively by choosing parameters corresponding to each region within the transition set curve. We verify the theoretical analysis and calculation of the transition set by showing the consistency of the numerical results obtained by Monte Carlo simulation with the analytical results. The method used in this paper directly guides the design of the fractional order viscoelastic material model to adjust the response of the system.

1. Introduction

Fractional calculus is a generalization of integer-order calculus, it extends the order of calculus operation from the traditional integer order to the case of noninteger order, and it has a history of more than 300 years as so far. Due to the limitation of the definition of integer-order derivative, it cannot express the memory property of viscoelastic substances. The definition of fractional derivative contains convolution, which can well express the memory effect and show the cumulative effect over time. Compared with the traditional integer-order calculus, fractional calculus has more advantages and is a suitable mathematical tool for describing the memory characteristics [1–11] and in recent years, it has become the powerful mathematical tool in many disciplines, especially in the study of viscoelastic materials.

The fractional derivative can accurately describe the constitutive relation of viscoelastic materials with fewer parameters, so the studies of fractional differential equations on the typical mechanical properties and the influences of fractional order parameters on the system are very necessary and have important significance. In recent years, many scholars have done a lot of work and achieved fruitful results in this field: Li and Tang studied the nonlinear parametric vibration of an axially moving string made by rubber-like materials, a new nonlinear fractional mathematical model governing transverse motion of the string is derived based on Newton's second law, the Euler beam theory, and the Lagrangian strain, and the principal parametric resonance is analytically investigated via applying the direct multiscale method [12]. Liu et al. introduced a transfer entropy and surrogate data algorithm to identify the nonlinearity level of the system by using a numerical solution of nonlinear response of beams, the Galerkin method was applied to discretize the dimensionless differential governing equation of the forced vibration, and then the fourth-order Runge-Kutta method was used to obtain the time history response of the lateral displacement [13]. Liu et al. investigated the stochastic stability of coupled viscoelastic system with nonviscously damping driven by white noise through moment Lyapunov exponents and Lyapunov exponents, obtained the coupled Itô stochastic differential equations of the norm of

the response and angles process by using the coordinate transformation, and discussed the effects of various physical quantities of stochastic coupled system on the stochastic stability [14]. Nutting, Gemant and Scott-Blair et al. [15–17] first proposed the fractional derivative models to study the constitutive relation of viscoelastic materials and the research on the viscoelastic materials with fractional derivative is also increasing, and so far, it is still a research hotspot [18–25]. Rodr Guez et al. calculated the correlation function of transverse wave in linear and homogeneous viscoelastic liquid by the Generalized Langevin Equation (GLE) method and the influence of fractional correlation function on the dynamic behavior of the system is analyzed [26]. Bagley and Torvik used fractional calculus to study the dynamic behavior of viscoelastic damping structure and the responses of the system under general load as well as step load are analyzed respectively [27, 28]. Pakdemirli and Ulsoy studied the primary parametric resonance and combined resonance of the axial acceleration rope based on the discrete perturbation method and the multiscale method [29]. Zhang and Zhu analyzed the stability and dynamic response of viscoelastic belt under parametric excitation by the multiscale method [30, 31]. Chen et al. studied the dynamic behavior and steady-state response of axially accelerating viscoelastic beam by the Galerkin method [32–35], derived the differential equation of nonlinear vibration for axially moving viscoelastic rope, and then pointed out that the damping of viscoelastic rope only exists in the nonlinear term [36, 37]. Leung et al. studied the steady-state response of a simply supported viscoelastic column under the axial harmonic excitation based on the fractional derivative constitutive model of cubic nonlinear and derived the generalized Mathieu-Duffing equation with time delay by the Galerkin discrete method, then the bifurcation behavior of the system caused by the order of the fractional derivative is analyzed [38]. Ghayesh and Moradian developed the Kelvin-Voigt viscoelastic model of the axially moving and the tensile belt, and then found the existence of nontrivial limit cycle in this system [39]. Liu et al. studied the dynamic response of an axially moving viscoelastic beam under random disorder periodic excitation, the first order expression of the solution is obtained by the multiscale method, and the stochastic jump phenomenon between the steady-state solutions is carried out [40]. Yang and Fang derived the system equation based on Newton's second law and the fractional Kelvin constitutive relation and then studied the stability of the axially moving beam under the parametric resonance condition [41]. Leung et al. studied the single mode dynamic characteristics of the nonlinear arch with the fractional derivative, the steady-state solution of the system is obtained based on the residual harmonic homotopy method, and the influence of the parametric variation on the dynamic behaviors of the viscoelastic damping material is analyzed [42]. Galucio et al. obtained the fractional derivative model to describe the viscoelasticity of the system based on the Timoshenko theory and Euler-Bernoulli hypothesis and proposed a finite element formula for analyzing the sandwich beam of viscoelastic material with fractional derivative and the results were verified numerically [43].

Due to the complexity of fractional derivative, the analysis method of it becomes more difficult, the study on the vibration characteristics of the parameters can only be qualitatively analyzed, and the critical conditions of the parametric influences cannot be found, which affect the analysis and design of such systems, as well as the stochastic P-bifurcation of bistability for the viscoelastic beam with fractional derivatives of high order nonlinear terms under random noise excitation has not been reported. In view of the above situation, the nonlinear vibration of viscoelastic beam with fractional constitutive relation under Gaussian white noise excitation is taken as an example, the transition set curve of the fractional order system as well as the critical parametric condition for stochastic P-bifurcation of the system is obtained by the singularity theory, and then the types of stationary PDF curves of the system in each region in the parametric plane divided by the transition set are analyzed. By the method of Monte Carlo simulation, the numerical results are compared with the analytical results obtained in this paper, it can be seen that the numerical solutions are in good agreements with the analytical solutions, and thus the correctness of the theoretical analysis in this paper is verified.

2. Equation of Axially Moving Viscoelastic Beam

There are many definitions of fractional derivatives, and the Riemann-Liouville derivative and Caputo derivative are commonly used. The initial conditions corresponding to the Riemann-Liouville derivative have no physical meanings, however, the initial conditions of the systems described by the Caputo derivative have clear physical meanings and their forms are the same as the initial conditions for the differential equations of integer order. So in this paper, the Caputo-type fractional derivative is adopted as follows:

$$ {}_{a}^{C}D^{p}\left[x\left(t\right)\right] = \frac{1}{\Gamma\left(m-p\right)}\int_{a}^{t}\frac{x^{(m)}\left(u\right)}{\left(t-u\right)^{1+p-m}}du, \tag{1} $$

where $m-1 < p \le m, m \in N, t \in [a,b]$, $\Gamma(m)$ is the Euler Gamma function, and $x^{(m)}(t)$ is the m order derivative of $x(t)$.

For a given physical system, due to the fact that the initial moment of the oscillator is $t = 0$, the following form of the Caputo derivative is often used:

$$ {}_{0}^{C}D^{p}\left[x\left(t\right)\right] = \frac{1}{\Gamma\left(m-p\right)}\int_{0}^{t}\frac{x^{(m)}\left(u\right)}{\left(t-u\right)^{1+p-m}}du, \tag{2} $$

In this paper, the transverse vibration $y(x,t)$ of a viscoelastic simply supported beam under lateral excitation $F(x,t)$ as shown in Figure 1 is considered; applying the d'Alambert principle, the governing equation can be written as [42]

$$ \begin{aligned} \frac{\partial \mathrm{Q}}{\partial x} &= F\left(x,t\right) - \rho A\frac{\partial^{2} y}{\partial t^{2}} \\ \frac{\partial M}{\partial x} &= \mathrm{Q} - N\frac{\partial y}{\partial x}, \end{aligned} \tag{3} $$

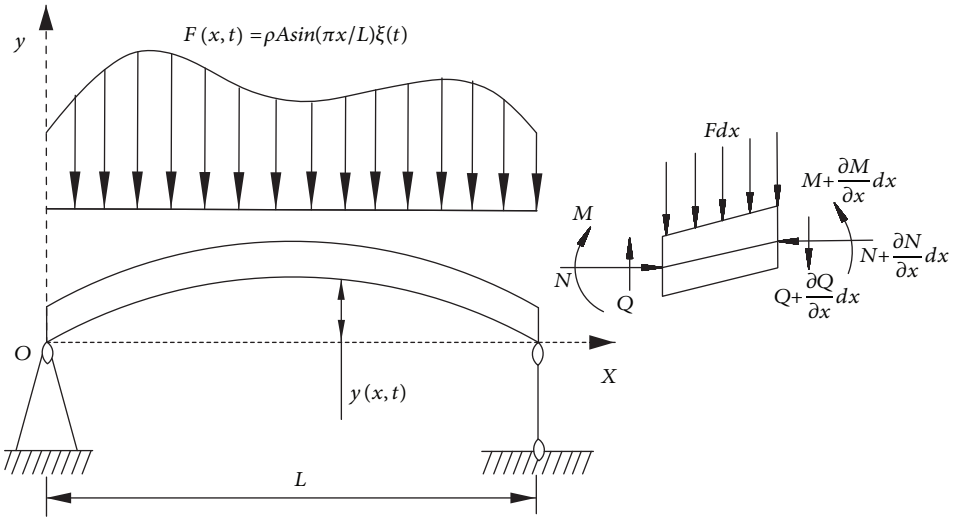

Figure 1: Schematic stress diagram of viscoelastic beam.

where ρ is the mass density of the beam, A is the area of cross-section, M is the bending moment, Q is the lateral force, and N is the horizontal force. From (3), we have

$$\frac{\partial^2 M}{\partial x^2} + N\frac{\partial^2 y}{\partial x^2} + \rho A\frac{\partial y^2}{\partial t^2} - F(x,t) = 0. \tag{4}$$

Assuming the material of the beam obeys a fractional derivative viscoelastic constitutive relation:

$$\begin{aligned}\sigma(x,z,t) &= E_0\varepsilon(x,z,t) + E_1\,{}_0^C D^p\left[\varepsilon(x,z,t)\right] \\ &= E_0\left(1+\eta\,{}_0^C D^p\right)\varepsilon(x,z,t) \triangleq S\varepsilon(x,z,t),\end{aligned} \tag{5}$$

where p is the order of fractional derivative ${}_0^C D^p[\varepsilon(x,z,t)]$ as is defined in (2), $\eta = E_1/E_0$ is the material modulus ratio, and $\varepsilon(x,z,t)$ is axial strain component.

When the deformation of the beam is small, the axial strain ε and lateral displacement $y(x,t)$ satisfy the relationship as follows:

$$\varepsilon(x,z,t) = -z\frac{\partial^2 y(x,t)}{\partial x^2}. \tag{6}$$

Substituting (6) into (5) yields

$$\sigma(x,z,t) = S\left[-z\frac{\partial^2 y(x,t)}{\partial x^2}\right]. \tag{7}$$

The relationship between bending moment $M(x,t)$ and axial stress $\sigma(x,z,t)$ of the beam can be expressed as follows:

$$M(x,t) = \int_{-h/2}^{h/2} z\sigma(x,z,t)\,dz, \tag{8}$$

where h is the thickness of the beam.

From (7) and (8), the expression of the bending moment M can be obtained as follows:

$$\begin{aligned}M(x,t) &= I\left[E_0\left(\frac{\partial^2 y}{\partial x^2}\right) + E_1\cdot{}_0^C D^p\left(\frac{\partial^2 y}{\partial x^2}\right)\right] \\ &= IS\left(\frac{\partial^2 y}{\partial x^2}\right),\end{aligned} \tag{9}$$

where $I = h^3/12$.

The expression of the horizontal tension is

$$\begin{aligned}N &= \frac{E_0 A}{2L}\int_0^L\left[\left(\frac{\partial y}{\partial x}\right)^2 - \left(\frac{\partial y}{\partial x}\right)^4\right]dx \\ &\quad + \frac{E_1 A}{2L}\int_0^L {}_0^C D^p\left[\left(\frac{\partial y}{\partial x}\right)^2 - \left(\frac{\partial y}{\partial x}\right)^4\right]dx \\ &= \frac{A}{2L}S\int_0^L\left[\left(\frac{\partial y}{\partial x}\right)^2 - \left(\frac{\partial y}{\partial x}\right)^4\right]dx.\end{aligned} \tag{10}$$

Substituting (9) and (10) into system (4), system (4) can be rewritten as

$$\begin{aligned}&IS\left(\frac{\partial^4 y}{\partial x^4}\right) \\ &\quad + S\frac{A}{2L}\frac{\partial^2 y}{\partial x^2}\int_0^L {}_0^C D^p\left[\left(\frac{\partial y}{\partial x}\right)^2 - \left(\frac{\partial y}{\partial x}\right)^4\right]dx \\ &\quad + \rho A\frac{\partial^2 y}{\partial t^2} - F(x,t) = 0.\end{aligned} \tag{11}$$

The boundary conditions are

$$\frac{\partial^2 y}{\partial x^2} = 0, \quad \text{when } x = 0,\ x = L. \tag{12}$$

According to the boundary conditions (12), the solution of system (11) can be expressed as the Fourier series:

$$y(x,t) = \sum_{n=1}^{\infty} u_n(t)\sin\left(\frac{n\pi}{L}x\right). \tag{13}$$

Assume that the initial transverse vibration of the system is $y_0(x) = 0$ and the transverse load of the system satisfies the following form:

$$F(x,t) = \rho A \cdot \sin\left(\frac{\pi}{L}x\right)\xi(t), \tag{14}$$

where $\xi(t)$ is the Gaussian white noise, which satisfies $E[\xi(t)] = 0$, $E[\xi(t)\xi(t-\tau)] = 2D\delta(\tau)$, D represents the noise intensity, and $\delta(\tau)$ is the Dirac function.

By the discrete format based on Galerkin method, system (11) can be reduced to the fractional differential equation as follows:

$$\begin{aligned}\ddot{u} + k_1 u + \eta k_1 {}_0^C D^p u - k_3 u^3 - \eta k_3 u {}_0^C D^p\left(u^2\right) + k_5 u^5 \\ + \eta k_5 u {}_0^C D^p\left(u^4\right) = \xi(t),\end{aligned} \tag{15}$$

where ${}_0^C D_t^p u$ is the p $(0 < p < 1)$ order Caputo derivative of $u(t)$ as is defined in (2), and

$$\begin{aligned}k_1 &= \left(\frac{\pi}{L}\right)^4 \frac{IE_0}{\rho A}, \\ k_3 &= \left(\frac{\pi}{L}\right)^4 \frac{E_0}{4\rho}, \\ k_5 &= \left(\frac{\pi}{L}\right)^6 \frac{3E_0}{16\rho}.\end{aligned} \tag{16}$$

For convenience, system (15) can be represented as follows:

$$\begin{aligned}\ddot{u} + w^2 u + \eta w^2 {}_0^C D^p u - k_3 u^3 - \eta k_3 u {}_0^C D^p\left(u^2\right) \\ + k_5 u^5 + \eta k_5 u {}_0^C D^p\left(u^4\right) = \xi(t),\end{aligned} \tag{17}$$

where $w = \sqrt{k_1}$.

The fractional derivative term has contributions to both damping and restoring forces [44–47], hence, introducing the following equivalent system:

$$\begin{aligned}\ddot{u} + w^2 u + \eta w^2\left[c(a)\dot{u} + w^2(a)u\right] - k_3 u^3 \\ - \eta k_3 u {}_0^C D^p\left(u^2\right) + k_5 u^5 + \eta k_5 u {}_0^C D^p\left(u^4\right) \\ = \xi(t),\end{aligned} \tag{18}$$

where $c(a)$, $w^2(a)$ are the coefficients of equivalent damping and restoring forces of fractional derivative ${}_0^C D^p u$, respectively.

The error between system (17) and (18) is

$$e = \eta w^2\left[c(a)\dot{u} + w^2(a)u - {}_0^C D^p u\right]. \tag{19}$$

The necessary conditions for minimum mean square error are [48]

$$\begin{aligned}\frac{\partial E\left[e^2\right]}{\partial\left(c(a)\right)} &= 0, \\ \frac{\partial E\left[e^2\right]}{\partial\left(w(a)\right)} &= 0.\end{aligned} \tag{20}$$

Substituting (19) into (20) yields

$$\begin{aligned}&E\left[c(a)\dot{u}^2 + w^2(a)u\dot{u} - \dot{u}\,{}_0^C D^p u\right] \\ &= \lim_{T\to\infty}\frac{1}{T}\int_0^T\left(c(a)\dot{u}^2 + w^2(a)u\dot{u} - \dot{u}\,{}_0^C D^p u\right)dt \\ &= 0 \\ &E\left[c(a)\dot{u}u + w^2(a)u^2 - u\,{}_0^C D^p u\right] \\ &= \lim_{T\to\infty}\frac{1}{T}\int_0^T\left(c(a)\dot{u}u + w^2(a)u^2 - u\,{}_0^C D^p u\right)dt \\ &= 0.\end{aligned} \tag{21}$$

Assume that the solution of system (18) has the following form:

$$\begin{aligned}u(t) &= a(t)\cos\varphi(t) \\ \varphi(t) &= wt + \theta,\end{aligned} \tag{22}$$

where w is the natural frequency of system (17).

Based on (22), we can obtain

$$\dot{u}(t) = -a(t)w\sin\varphi(t). \tag{23}$$

Substituting (22) and (23) into (21) yields

$$\begin{aligned}&\lim_{T\to\infty}\frac{1}{T}\int_0^T\left(c(a)\dot{u}^2 + w^2(a)u\dot{u} - \dot{u}\,{}_0^C D^p u\right)dt \\ &= \lim_{T\to\infty}\frac{1}{T}\int_0^T\left(c(a)a^2w^2\sin^2\varphi - a^2ww^2(a)\sin\varphi\right. \\ &\left.\cdot\cos\varphi - aw\sin\varphi\,{}_0^C D^p u\right)dt \approx \frac{c(a)a^2w^2}{2} \\ &+ \frac{1}{\Gamma(1-p)}\lim_{T\to\infty}\frac{1}{T}\int_o^T\left[(aw\sin\varphi)\right. \\ &\left.\cdot\int_0^t\frac{\dot{x}(t-\tau)}{\tau^\alpha}d\tau\right]dt = \frac{c(a)a^2w^2}{2} \\ &- \frac{1}{\Gamma(1-p)}\lim_{T\to\infty}\frac{1}{T}\int_o^T\left(a^2w^2\sin\varphi\right. \\ &\left.\cdot\int_0^t\frac{\sin\varphi\cos(w\tau) - \cos\varphi\sin(w\tau)}{\tau^\alpha}\right)dt = 0 \\ &\lim_{T\to\infty}\frac{1}{T}\int_0^T\left(c(a)\dot{u}u + w^2(a)uu - u\,{}_0^C D^p u\right)dt \\ &= \lim_{T\to\infty}\frac{1}{T}\int_0^T\left(-c(a)a^2w\sin\varphi\cos\varphi + a^2w^2(a)\right. \\ &\left.\cdot\cos^2\varphi - a\cos\varphi\,{}_0^C D^p u\right)dt \approx \frac{a^2w^2(a)}{2}\end{aligned} \tag{24}$$

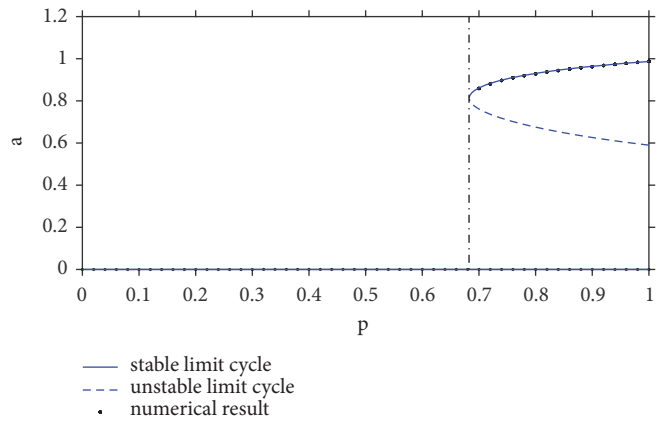

Figure 2: Bifurcation diagram of amplitude of system (28) at $D = 0$.

$$
\begin{aligned}
&-\frac{1}{\Gamma(1-p)}\lim_{T\to\infty}\frac{1}{T}\int_o^T\left[(a\cos\varphi)\right.\\
&\cdot\left.\int_0^t\frac{\dot{x}(t-\tau)}{\tau^{\alpha}}d\tau\right]dt=\frac{a^2w^2(a)}{2}+\frac{1}{\Gamma(1-p)}\\
&\cdot\lim_{T\to\infty}\frac{1}{T}\int_o^T\left(a^2w\cos\varphi\right.\\
&\cdot\left.\int_0^t\frac{\sin\varphi\cos(w\tau)-\cos\varphi\sin(w\tau)}{\tau^{\alpha}}\right)dt=0.
\end{aligned}
\tag{25}
$$

To simplify (24) and (25) further, asymptotic integrals are introduced as follows:

$$
\begin{aligned}
\int_0^t\frac{\cos(w\tau)}{\tau^p}d\tau&=w^{p-1}\left(\Gamma(1-p)\sin\left(\frac{p\pi}{2}\right)\right.\\
&\left.+\frac{\sin(wt)}{(wt)^p}+o\left((wt)^{-p-1}\right)\right)\\
\int_0^t\frac{\sin(w\tau)}{\tau^p}d\tau&=w^{p-1}\left(\Gamma(1-p)\cos\left(\frac{p\pi}{2}\right)\right.\\
&\left.-\frac{\cos(wt)}{(wt)^p}+o\left((wt)^{-p-1}\right)\right).
\end{aligned}
\tag{26}
$$

Substituting (26) into (24) and (25) and averaging them across φ produce the ultimate forms of $c(a)$ and $w^2(a)$ as follows:

$$
\begin{aligned}
c(a)&=w^{p-1}\sin\left(\frac{p\pi}{2}\right),\\
w^2(a)&=w^p\cos\left(\frac{p\pi}{2}\right).
\end{aligned}
\tag{27}
$$

Therefore, the equivalent system associated with system (18) can be expressed as follows:

$$
\begin{aligned}
&\ddot{u}+w_0^2u+\gamma\dot{u}-k_3u^3-\eta k_3u\,{}_0^C D^p\left(u^2\right)+k_5u^5\\
&+\eta k_5u\,{}_0^C D^p\left(u^4\right)=\xi(t),
\end{aligned}
\tag{28}
$$

where $w_0^2=w^2[1+\eta w^p\cos(p\pi/2)]$ and $\gamma=\eta w^{p+1}\sin(p\pi/2)$.

Next, we consider the stochastic P-bifurcation of system (28) which comprises the fractional derivatives of high order nonlinear terms and analyze the influence of parametric variation on the system response.

3. The Stationary PDF of Amplitude

For the system (28), the material modulus ratio is given as $\eta = 0.5$, coefficients of nonlinear terms are given as $k_3 = 7.8$, $k_5 = 5.9$, respectively, and nature frequency is given as $w = 1$. For the convenience to discuss the parametric influence, the bifurcation diagram of amplitude of the limit cycle along with variation of the fractional order p is shown in Figure 2 when $D = 0$.

As can be seen from Figure 2, the solution corresponding to the solid line is almost completely coincided with the numerical solution, which proves the correctness and accuracy of the approximate analytical result of the deterministic system; at the same time, it shows that the solution corresponding to the solid line is stable and the solution corresponding to the dotted line is unstable. And it also can be seen that there is 1 attractor in the system when p changes in the interval $[0, 0.6817]$: equilibrium, as shown in Figure 3(a); there are 2 attractors when p changes in the interval $[0.6818, 1]$: equilibrium and limit cycle, as shown in Figure 3(b).

In order to obtain the stationary PDF of the amplitude of system (28), the following transformation is introduced:

$$
\begin{aligned}
u(t)&=a(t)\cos\Phi(t)\\
\dot{u}(t)&=-a(t)w_0\sin\Phi(t)\\
\Phi(t)&=w_0t+\theta(t),
\end{aligned}
\tag{29}
$$

where w_0 is the natural frequency of the equivalent system (28), $a(t)$ and $\theta(t)$ represent the amplitude process and the phase process of the system response, respectively, and they are all random processes.

Substituting (29) into (28), we can obtain

$$
\frac{da}{dt}=F_{11}(a,\theta)+G_{11}(a,\theta)\xi(t)
$$

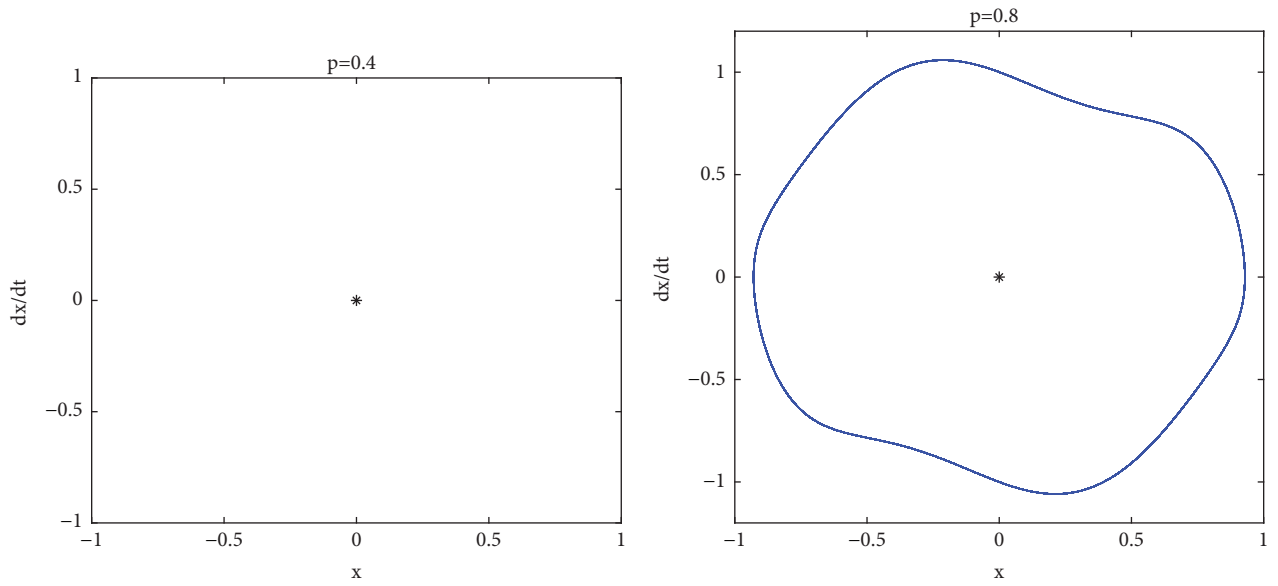

(a) Equilibrium (b) Equilibrium and limit cycle

Figure 3: Phase diagrams of system (28) at $D = 0$.

$$\frac{d\theta}{dt} = F_{21}(a,\theta) + G_{21}(a,\theta)\,\xi(t), \tag{30}$$

in which

$$\begin{aligned} F_{11} &= -\frac{\Delta \sin\Phi}{w_0} \\ F_{21} &= -\frac{\Delta \cos\Phi}{aw_0} \\ G_{11} &= -\frac{\sin\Phi}{w_0} \\ G_{21} &= -\frac{\cos\Phi}{aw_0}, \end{aligned} \tag{31}$$

and

$$\begin{aligned} \Delta = {} & \eta w^{p+1} a w_0 \sin\left(\frac{p\pi}{2}\right)\sin\Phi - k_3 a^3 \cos^3\Phi - \eta k_3 \\ & \cdot \frac{a^3}{2}(2w_0)^p \cos\Phi\cos\left(2\Phi + \frac{p\pi}{2}\right) - k_5 a^5 \cos^5\Phi \\ & - \eta k_5 a^5 \cos\Phi\left[\frac{1}{8}(4w_0)^p \cos\left(4\Phi + \frac{p\pi}{2}\right)\right. \\ & \left. + \frac{1}{2}(2w_0)^p \cos\left(2\Phi + \frac{p\pi}{2}\right)\right]. \end{aligned} \tag{32}$$

Equation (30) can be regarded as a Stratonovich stochastic differential equation, by adding the corresponding Wong-

Zakai correction term: it can be transformed into the following Itô stochastic differential equation:

$$\begin{aligned} da = {} & \left[F_{11}(a,\theta) + F_{12}(a,\theta)\right]dt \\ & + \sqrt{2D}\,G_{11}(a,\theta)\,dB(t) \\ d\theta = {} & \left[F_{21}(a,\theta) + F_{22}(a,\theta)\right]dt \\ & + \sqrt{2D}\,G_{21}(a,\theta)\,dB(t), \end{aligned} \tag{33}$$

where $B(t)$ is a standard Wiener process and

$$\begin{aligned} F_{12}(a,\theta) &= D\frac{\partial G_{11}}{\partial a}G_{11} + D\frac{\partial G_{11}}{\partial \theta}G_{21} \\ F_{22}(a,\theta) &= D\frac{\partial G_{21}}{\partial a}G_{11} + D\frac{\partial G_{21}}{\partial \theta}G_{21}. \end{aligned} \tag{34}$$

By the stochastic averaging method, averaging (33) regarding Φ, the following averaged Itô equation can be obtained as follows:

$$\begin{aligned} da &= m_1(a)\,dt + \sigma_1(a)\,dB(t) \\ d\theta &= m_2(a)\,dt + \sigma_2(a)\,dB(t), \end{aligned} \tag{35}$$

where

$$\begin{aligned} m_1(a) = {} & -\frac{\eta k_5 2^p w_0^{p-1} a^5 \sin(p\pi/2)}{8} \\ & - \frac{\eta k_3 2^p w_0^{p-1} a^3 \sin(p\pi/2)}{8} \\ & - \frac{\eta w^{p+1} a \sin(p\pi/2)}{2} + \frac{D}{2aw_0^2} \\ \sigma_1{}^2(a) = {} & \frac{D}{w_0^2} \\ m_2(a) = {} & \frac{k_5\left(2\eta \cdot 2^p w_0^p \cos(p\pi/2) + 5\right)a^4}{16w_0} \end{aligned}$$

$$+\frac{k_3\left(\eta\cdot 2^p w_0^p\cos\left(p\pi/2\right)+3\right)a^2}{8w_0}$$

$$\sigma_2{}^2(a)=\frac{D}{a^2w_0^2}. \tag{36}$$

Equations (35) and (36) show that the averaged Itô equation for $a(t)$ is independent of $\theta(t)$ and the random process $a(t)$ is a one-dimensional diffusion process. The corresponding FPK equation associated with $a(t)$ can be written as

$$\frac{\partial p}{\partial t}=-\frac{\partial}{\partial a}\left[m_1(a)\,p\right]+\frac{1}{2}\frac{\partial^2}{\partial a^2}\left[\sigma_1{}^2(a)\,p\right]. \tag{37}$$

The boundary conditions are

$$p=c,\ c\in(-\infty,+\infty)\quad \text{when } a=0$$

$$p\longrightarrow 0,\ \frac{\partial p}{\partial a}\longrightarrow 0\quad \text{when } a\longrightarrow\infty. \tag{38}$$

Thus, based on these boundary conditions (38), we can obtain the stationary PDF of amplitude a as follows:

$$p(a)=\frac{C}{\sigma_1{}^2(a)}\exp\left[\int_0^a\frac{2m_1(u)}{\sigma_1{}^2(u)}du\right], \tag{39}$$

where C is a normalized constant, which satisfies

$$C=\left[\int_0^\infty\left(\frac{1}{\sigma_1{}^2(a)}\exp\left[\int_0^a\frac{2m_1(u)}{\sigma_1{}^2(u)}du\right]\right)da\right]^{-1}. \tag{40}$$

Substituting (36) into (39), the explicit expression for the stationary PDF of amplitude a can be obtained as follows:

$$p(a)=\frac{Caw_0^2}{D}\exp\left[-\frac{\eta a^2\sin\left(p\pi/2\right)\left(k_5 2^{p+1}a^4w_0^{p+1}+3k_3 2^p a^2 w_0^{p+1}+24w_0^2w^{p+1}\right)}{48D}\right], \tag{41}$$

where $w_0^2=w^2[1+\eta w^p\cos(p\pi/2)]$.

4. Stochastic P-Bifurcation

Stochastic P-bifurcation refers to the changes of the number of peaks in the PDF curve; in order to obtain the critical parametric condition for stochastic P-bifurcation, the influences of the parameters for stochastic P-bifurcation of the system are analyzed by using the singularity theory below.

For the sake of convenience, we can write $p(a)$ as follows:

$$p(a)=CR\left(a,D,w,\eta,p,k_3,k_5\right)\cdot\exp\left[Q\left(a,D,w,\eta,p,k_3,k_5\right)\right], \tag{42}$$

in which

$$R\left(a,D,w,\eta,p,k_3,k_5\right)=\frac{aw_0^2}{D}$$

$$Q\left(a,D,w,\eta,p,k_3,k_5\right)=-\frac{\eta a^2\sin\left(p\pi/2\right)\left(k_5 2^{p+1}a^4w_0^{p+1}+3k_3 2^p a^2 w_0^{p+1}+24w_0^2w^{p+1}\right)}{48D}. \tag{43}$$

According to the singularity theory, the stationary PDF needs to satisfy the following two conditions:

$$\frac{\partial p(a)}{\partial a}=0,\qquad \frac{\partial^2 p(a)}{\partial a^2}=0. \tag{44}$$

Substituting (42) into (44), we can obtain the following condition [49]:

$$H=\left\{R'+RQ'=0,R''+2R'Q'+RQ''+RQ'^2=0\right\}, \tag{45}$$

where H represents the critical condition for the changes of the number of peaks in the PDF curve.

Substituting (43) into (45), we can get the critical parametric condition for stochastic P-bifurcation of the system as follows:

$$D=\frac{1}{8}\eta k_5 2^{p+1}w_0^{p+1}\sin\left(\frac{p\pi}{2}\right)a^6+\frac{1}{8}\eta k_3 2^{p+1}w_0^{p+1}\sin\left(\frac{p\pi}{2}\right)a^4+\eta w_0^2w^{p+1}\sin\left(\frac{p\pi}{2}\right)a^2, \tag{46}$$

where $w_0^2=w^2[1+\eta w^p\cos(p\pi/2)]$.

And amplitude a satisfies

$$3k_5 2^p w_0^{p+1}a^4+2k_3 2^p w_0^{p+1}a^2+4w_0^2w^{p+1}=0. \tag{47}$$

Taking the parameters as $\eta=0.5$, $k_3=7.8$, $k_5=5.9$, and $w=1$, according to (46) and (47), the transition set for stochastic P-bifurcation of the system with the unfolding parameters p and D can be obtained, as shown in Figure 4.

According to the singularity theory, the topological structures of the stationary PDF curves of different points (p,D) in the same region are qualitatively the same. Taking a point (p,D) in each region, all varieties of the stationary PDF curves which are qualitatively different could be obtained. It can be seen that the unfolding parameter $p-D$ plane is divided into two subregions by the transition set curve;

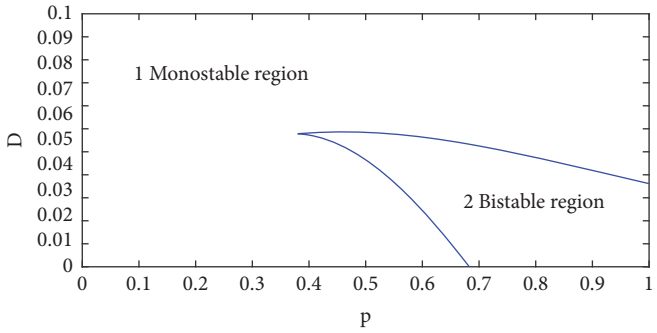

Figure 4: The transition set curve of system (28).

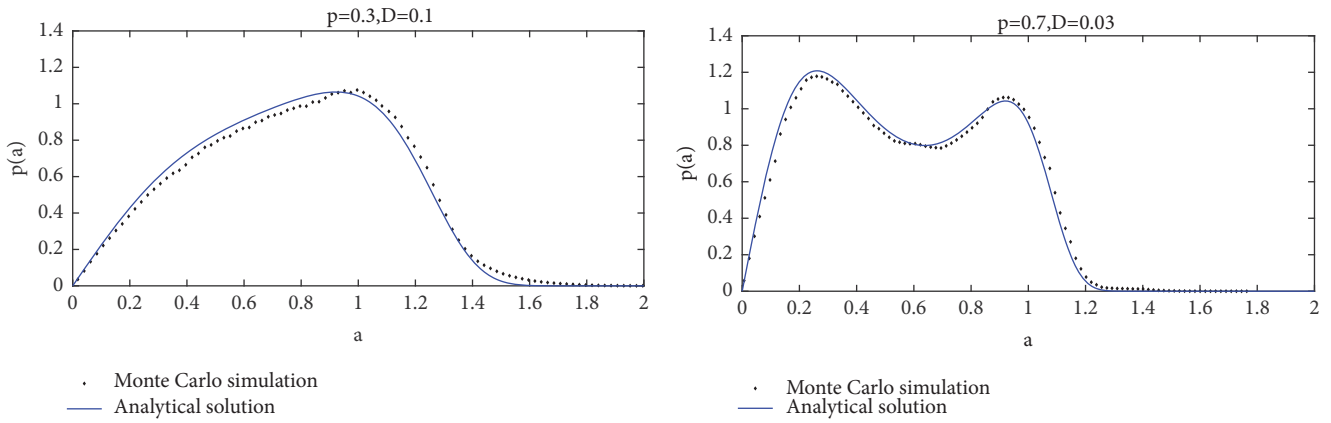

(a) parameter (p, D) in region 1 of Figure 4

(b) parameter (p, D) in region 2 of Figure 4

Figure 5: The stationary PDF curves for the amplitude of system (28).

for convenience, each region in Figure 4 is marked with a number.

Taking a given point (p, D) in each of the two subregions of Figure 4, the characteristics of stationary PDF curves are analyzed, and the corresponding results are shown in Figure 5.

As can be seen from Figure 4, the parametric region where the PDF curve appears bimodal is surrounded by an approximately triangular region. When the parameter (p, D) is taken in the region 1, the PDF curve has only a distinct peak, as shown in Figure 5(a); in region 2, the PDF curve has a distinct peak near the origin, but the probability is obviously not zero far away from the origin; there are both the equilibrium and limit cycle in the system simultaneously, as shown in Figure 5(b).

The analysis results above show that the stationary PDF curves of the system amplitude in any two adjacent regions in Figure 4 are qualitatively different. No matter the values of the unfolding parameters cross any line in the figure, the system will occur stochastic P-bifurcation behaviors, so the transition set curve is just the critical parametric condition for the stochastic P-bifurcation of the system, and the analytic results in Figure 5 are in good agreement with the numerical results by Monte Carlo simulation, which further verify the correctness of the theoretical analysis.

5. Conclusion

In this paper, we studied the stochastic P-bifurcation for axially moving of a bistable viscoelastic beam model with fractional derivatives of high order nonlinear terms under Gaussian white noise excitation. According to the minimum mean square error principle, we transformed the original system into an equivalent and simplified system and obtained the stationary PDF of the system amplitude using stochastic averaging. In addition, we obtained the critical parametric condition for stochastic P-bifurcation of the system using singularity theory; based on this, the system response can be maintained at the monostability or small amplitude near the equilibrium by selecting the appropriate unfolding parameters, providing theoretical guidance for system design in practical engineering, and avoiding the instability and damage caused by the large amplitude vibration or nonlinear jump phenomenon of the system. Finally, the numerical results by Monte Carlo simulation of the original system also verify the theoretical results obtained in this paper. We conclude that the order p of fractional derivative and the noise intensity D can both cause stochastic P-bifurcation of the system and the number of peaks in the stationary PDF curve of system amplitude can change from 2 to 1 by selecting the appropriate unfolding parameters (p, D); it also shows that the method used in this paper is feasible to analyze

the stochastic P-bifurcation behaviors of viscoelastic material system with fractional constitutive relation.

Data Availability

Data that support the findings of this study are included within the article (and its additional files). All other data are available from the corresponding author upon reasonable request.

Conflicts of Interest

The authors declare that there are no conflicts of interest regarding the publication of this paper.

Acknowledgments

This work was supported by the National 973 Project of China (Grant no. 2014CB046805) and the Natural Science Foundation of China (Grant no. 11372211).

References

[1] W. Tan and M. Xu, "Plane surface suddenly set in motion in a viscoelastic fluid with fractional Maxwell model," *Acta Mechanica Sinica. English Series. The Chinese Society of Theoretical and Applied Mechanics*, vol. 18, no. 4, pp. 342–349, 2002.

[2] J. Sabatier, O. P. Agrawal, and J. A. Machado, *Advance in Fractional Calculus: Theoretical Developments and Applications in Physics and Engineering*, Springer, Dordrecht, The Netherlands, 2007.

[3] I. Podlubny, "Fractional order systems and PID controller," *IEEE Transactions on Automatic Control*, vol. 44, no. 1, pp. 208–214, 1999.

[4] C. A. Monje, Y. Chen, B. M. Vinagre, D. Xue, and V. Feliu, *Fractional-Order Systems and Controls: Fundamentals and Applications*, Advances in Industrial Control, Springer, London, UK, 2010.

[5] Q. Li, Y. L. Zhou, X. Q. Zhao, and X. Y. Ge, "Fractional order stochastic differential equation with application in European option pricing," *Discrete Dynamics in Nature and Society*, vol. 2014, Article ID 621895, 12 pages, 2014.

[6] S. Nie, H. Sun, Y. Zhang et al., "Vertical distribution of suspended sediment under steady flow: existing theories and fractional derivative model," *Discrete Dynamics in Nature and Society*, vol. 2017, Article ID 5481531, 11 pages, 2017.

[7] X. Liu, L. Hong, H. Dang, and L. Yang, "Bifurcations and synchronization of the fractional-order Bloch system," *Discrete Dynamics in Nature and Society*, vol. 2017, Article ID 4694305, 10 pages, 2017.

[8] W. Li and Y. Pang, "Asymptotic solutions of time-space fractional coupled systems by residual power series method," *Discrete Dynamics in Nature and Society*, vol. 2017, Article ID 7695924, 10 pages, 2017.

[9] Z. Liu, T. Xia, and J. Wang, "Image encryption technology based on fractional two-dimensional triangle function combination discrete chaotic map coupled with Menezes-Vanstone elliptic curve cryptosystem," *Discrete Dynamics in Nature and Society*, vol. 2018, Article ID 4585083, 24 pages, 2018.

[10] C. Sánchez-López, V. H. Carbajal-Gómez, M. A. Carrasco-Aguilar, and I. Carro-Pérez, "Fractional-Order Memristor Emulator Circuits," *Complexity*, vol. 2018, Article ID 2806976, 10 pages, 2018.

[11] K. Rajagopal, A. Karthikeyan, P. Duraisamy, and R. Weldegiorgis, "Bifurcation and Chaos in Integer and Fractional Order Two-Degree-of-Freedom Shape Memory Alloy Oscillators," *Complexity*, vol. 2018, 9 pages, 2018.

[12] Ying Li and Ye Tang, "Analytical Analysis on Nonlinear Parametric Vibration of an Axially Moving String with Fractional Viscoelastic Damping," *Mathematical Problems in Engineering*, vol. 2017, Article ID 1393954, 9 pages, 2017.

[13] G. Liu, C. Ye, X. Liang, Z. Xie, and Z. Yu, "Nonlinear Dynamic Identification of Beams Resting on Nonlinear Viscoelastic Foundations BASed on the Time-DELayed TRAnsfer Entropy and IMProved Surrogate DATa Algorithm," *Mathematical Problems in Engineering*, vol. 2018, Article ID 6531051, 14 pages, 2018.

[14] D. Liu, Y. Wu, and X. Xie, "Stochastic Stability Analysis of Coupled Viscoelastic SYStems with Nonviscously Damping DRIven by White NOIse," *Mathematical Problems in Engineering*, vol. 2018, Article ID 6532305, 16 pages, 2018.

[15] P. G. Nutting, "A new general law of deformation," *Journal of The Franklin Institute*, vol. 191, no. 5, pp. 679–685, 1921.

[16] A. Gemant, "A method of analyzing experimental results obtained from elasto-viscous bodies," *Journal of Applied Physics*, vol. 7, no. 8, pp. 311–317, 1936.

[17] G. S. Blair and J. Caffyn, "VI. An application of the theory of quasi-properties to the treatment of anomalous strain-stress relations," *The London, Edinburgh, and Dublin Philosophical Magazine and Journal of Science*, vol. 40, no. 300, pp. 80–94, 2010.

[18] C. Mote, "Dynamic Stability of Axially Moving Materals," *Shock and Vibration*, vol. 4, no. 4, pp. 2–11, 1972.

[19] A. Ulsoy and C. Mote, "Band Saw Vibration and Stability," *Shock and Vibration*, vol. 10, no. 11, pp. 3–15, 1978.

[20] J. A. Wickert and C. D. Mote Jr., "Current research on the vibration and stability of axially-moving materials," *Shock and Vibration*, vol. 20, no. 1, pp. 3–13, 1988.

[21] K. W. Wang and S. P. Liu, "On the noise and vibration of chain drive systems," *Shock and Vibration Digest*, vol. 23, no. 4, pp. 8–13, 1991.

[22] F. Pellicano and F. Vestroni, "Complex dynamics of high-speed axially moving systems," *Journal of Sound and Vibration*, vol. 258, no. 1, pp. 31–44, 2002.

[23] N.-H. Zhang and L.-Q. Chen, "Nonlinear dynamical analysis of axially moving viscoelastic strings," *Chaos, Solitons & Fractals*, vol. 24, no. 4, pp. 1065–1074, 2005.

[24] M. H. Ghayesh, H. A. Kafiabad, and T. Reid, "Sub- and supercritical nonlinear dynamics of a harmonically excited axially moving beam," *International Journal of Solids and Structures*, vol. 49, no. 1, pp. 227–243, 2012.

[25] M. H. Ghayesh, "Stability and bifurcations of an axially moving beam with an intermediate spring support," *Nonlinear Dynamics*, vol. 69, no. 1-2, pp. 193–210, 2012.

[26] R. Rodríguez, E. Salinas-Rodríguez, and J. Fujioka, "Fractional Time Fluctuations in Viscoelasticity: A Comparative Study of Correlations and Elastic Moduli," *Entropy*, vol. 20, no. 1, p. 28, 2018.

[27] R. L. Bagley and P. J. Torvik, "Fractional calculus-a different approach to the analysis of viscoelastically damped structures," *AIAA Journal*, vol. 21, no. 5, pp. 741–748, 2012.

[28] R. L. Bagley and P. J. Torvik, "Fractional calculus in the transient analysis of viscoelastically damped structures," *AIAA Journal*, vol. 23, no. 6, pp. 918–925, 1985.

[29] M. Pakdemirli and A. G. Ulsoy, "Stability analysis of an axially accelerating string," *Journal of Sound and Vibration*, vol. 203, no. 5, pp. 815–832, 1997.

[30] L. Zhang and J. W. Zu, "Nonlinear vibration of parametrically excited moving belts, part I: Dynamic response," *Journal of Applied Mechanics*, vol. 66, no. 2, pp. 396–402, 1999.

[31] L. Zhang and J. W. Zu, "Nonlinear vibration of parametrically excited viscoelastic moving belts, part II: Stability analysis," *Journal of Applied Mechanics*, vol. 66, no. 2, pp. 403–409, 1999.

[32] L. Q. Chen, X. D. Yang, and C. J. Cheng, "Dynamic stability of an axially accelerating viscoelastic beam," *European Journal of Mechanic*, vol. 23, no. 4, pp. 659–666, 2004.

[33] L. Q. Chen and X. D. Yang, "Steady-state response of axially moving viscoelastic beams with pulsating speed: comparison of two nonlinear models," *International Journal of Solids and Structures*, vol. 42, no. 1, pp. 37–50, 2005.

[34] L. Q. Chen and X. D. Yang, "Transverse nonlinear dynamics of axially accelerating viscoelastic beams based on 4-term Galerkin truncation," *Chaos Soliton and Fractal*, vol. 27, no. 3, pp. 748–757, 2006.

[35] H. Ding and L.-Q. Chen, "Galerkin methods for natural frequencies of high-speed axially moving beams," *Journal of Sound and Vibration*, vol. 329, no. 17, pp. 3484–3494, 2010.

[36] L.-Q. Chen, J. Wu, and J. W. Zu, "Asymptotic nonlinear behaviors in transverse vibration of an axially accelerating viscoelastic string," *Nonlinear Dynamics*, vol. 35, no. 4, pp. 347–360, 2004.

[37] L.-Q. Chen, N.-H. Zhang, and J. W. Zu, "The regular and chaotic vibrations of an axially moving viscoelastic string based on fourth order Galerkin truncation," *Journal of Sound and Vibration*, vol. 261, no. 4, pp. 764–773, 2003.

[38] A. Y. T. Leung, H. X. Yang, and J. Y. Chen, "Parametric bifurcation of a viscoelastic column subject to axial harmonic force and time-delayed control," *Computers & Structures*, vol. 136, pp. 47–55, 2014.

[39] M. H. Ghayesh and N. Moradian, "Nonlinear dynamic response of axially moving, stretched viscoelastic strings," *Archive of Applied Mechanics*, vol. 81, no. 6, pp. 781–799, 2011.

[40] D. Liu, W. Xu, and Y. Xu, "Dynamic responses of axially moving viscoelastic beam under a randomly disordered periodic excitation," *Journal of Sound and Vibration*, vol. 331, no. 17, pp. 4045–4056, 2012.

[41] T. Z. Yang and B. Fang, "Stability in parametric resonance of an axially moving beam constituted by fractional order material," *Archive of Applied Mechanics*, vol. 82, no. 12, pp. 1763–1770, 2012.

[42] A. Y. T. Leung, H. X. Yang, P. Zhu, and Z. J. Guo, "Steady state response of fractionally damped nonlinear viscoelastic arches by residue harmonic homotopy," *Computers & Structures*, vol. 121, pp. 10–21, 2013.

[43] A. C. Galucio, J.-F. Deüi, and R. Ohayon, "Finite element formulation of viscoelastic sandwich beams using fractional derivative operators," *Computational Mechanics*, vol. 33, no. 4, pp. 282–291, 2004.

[44] L. Chen, W. Wang, Z. Li, and W. Zhu, "Stationary response of Duffing oscillator with hardening stiffness and fractional derivative," *International Journal of Non-Linear Mechanics*, vol. 48, pp. 44–50, 2013.

[45] L. C. Chen, Z. S. Li, Q. Zhuang, and W. Q. Zhu, "First-passage failure of single-degree-of-freedom nonlinear oscillators with fractional derivative," *Journal of Vibration and Control*, vol. 19, no. 14, pp. 2154–2163, 2013.

[46] Y. Shen, S. Yang, H. Xing, and G. Gao, "Primary resonance of Duffing oscillator with fractional-order derivative," *Communications in Nonlinear Science and Numerical Simulation*, vol. 17, no. 7, pp. 3092–3100, 2012.

[47] Y. G. Yang, W. Xu, Y. H. Sun, and X. D. Gu, "Stochastic response of van der Pol oscillator with two kinds of fractional derivatives under Gaussian white noise excitation," *Chinese Physics B*, vol. 25, no. 2, pp. 13–21, 2016.

[48] L. Chen and W. Zhu, "Stochastic response of fractional-order van der Pol oscillator," *Theoretical & Applied Mechanics Letters*, vol. 4, no. 1, pp. 68–72, 2014.

[49] W. Li, M. Zhang, and J. Zhao, "Stochastic bifurcations of generalized Duffing–van der Pol system with fractional derivative under colored noise," *Chinese Physics B*, vol. 26, no. 9, pp. 62–69, 2017.

Hindawi
Discrete Dynamics in Nature and Society
Volume 2018, Article ID 7052935, 22 pages
https://doi.org/10.1155/2018/7052935

Research Article

Global Asymptotic Stability and Naimark-Sacker Bifurcation of Certain Mix Monotone Difference Equation

M. R. S. Kulenović,[1] S. Moranjkić,[2] M. Nurkanović,[2] and Z. Nurkanović[2]

[1]*Department of Mathematics, University of Rhode Island, Kingston, RI 02881, USA*
[2]*Department of Mathematics, University of Tuzla, 75000 Tuzla, Bosnia and Herzegovina*

Correspondence should be addressed to M. R. S. Kulenović; mkulenovic@mail.uri.edu

Received 18 July 2018; Accepted 17 October 2018; Published 8 November 2018

Guest Editor: Abdul Qadeer Khan

We investigate the global asymptotic stability of the following second order rational difference equation of the form $x_{n+1} = (Bx_nx_{n-1} + F)/(bx_nx_{n-1} + cx_{n-1}^2)$, $n = 0, 1, \ldots$, where the parameters B, F, b, and c and initial conditions x_{-1} and x_0 are positive real numbers. The map associated with this equation is always decreasing in the second variable and can be either increasing or decreasing in the first variable depending on the parametric space. In some cases, we prove that local asymptotic stability of the unique equilibrium point implies global asymptotic stability. Also, we show that considered equation exhibits the Naimark-Sacker bifurcation resulting in the existence of the locally stable periodic solution of unknown period.

1. Introduction and Preliminaries

In this paper, we investigate the local and global dynamics of the following difference equation:

$$x_{n+1} = \frac{Bx_nx_{n-1} + F}{bx_nx_{n-1} + cx_{n-1}^2} \quad n = 0, 1, \ldots \tag{1}$$

where the parameters B, F, b, c are positive real numbers and initial conditions x_{-1} and x_0 are arbitrary positive real numbers. Equation (1) is the special case of a general second order quadratic fractional equation of the form

$$x_{n+1} = \frac{Ax_n^2 + Bx_nx_{n-1} + Cx_{n-1}^2 + Dx_n + Ex_{n-1} + F}{ax_n^2 + bx_nx_{n-1} + cx_{n-1}^2 + dx_n + ex_{n-1} + f}, \quad n = 0, 1, \ldots, \tag{2}$$

with nonnegative parameters and initial conditions such that $A+B+C > 0, a+b+c+d+e+f > 0$ and $ax_n^2+bx_nx_{n-1}+cx_{n-1}^2+dx_n + ex_{n-1} + f > 0$, $n = 0, 1, \ldots$. Several global asymptotic results for some special cases of Equation (2) were obtained in [1–11]. Also, Equation (1) is a special case of the equation

$$x_{n+1} = \frac{Bx_nx_{n-1} + Cx_{n-1}^2 + F}{bx_nx_{n-1} + cx_{n-1}^2 + f}, \quad n = 0, 1, \ldots, \tag{3}$$

with positive parameters and nonnegative initial conditions x_{-1}, x_0. Local and global dynamics of Equation (3) was investigated in [12].

The special case of Equation (3) when $B = C = 0$, i.e.,

$$x_{n+1} = \frac{F}{bx_nx_{n-1} + cx_{n-1}^2 + f}, \quad n = 0, 1, \ldots \tag{4}$$

was studied in [8]. The authors performed the local stability analysis of the unique equilibrium point and gave the necessary and sufficient conditions for the equilibrium to be locally asymptotically stable, a repeller or nonhyperbolic equilibrium. Also, it was shown that Equation (4) exhibits the Naimark-Sacker bifurcation.

The special case of Equation (3) (when $B = F = 0$ and $C = 1$) is the following equation:

$$x_{n+1} = \frac{x_{n-1}^2}{bx_nx_{n-1} + cx_{n-1}^2 + f}, \quad n = 0, 1, \ldots, \tag{5}$$

where the parameters b, c, and f are nonnegative numbers with condition $b + c > 0$, $f \neq 0$ and the initial conditions x_{-1}, x_0 arbitrary nonnegative numbers such that $x_{-1}+x_0 > 0$. Equation (5) is a perturbed Sigmoid Beverton-Holt difference

equation and it was studied in [9]. The special case of Equation (5) for $b = 0$ is the well-known Thomson equation

$$x_{n+1} = \frac{x_{n-1}^2}{cx_{n-1}^2 + f}, \quad n = 0, 1, \ldots, \tag{6}$$

where the parameters c and f are positive numbers and the initial conditions x_{-1}, x_0 are arbitrary nonnegative numbers, is used in the modelling of fish population [13].

The dynamics of (6) is very interesting and follows from the dynamics of related equation

$$x_{n+1} = \frac{x_n^2}{cx_n^2 + f}, \quad n = 0, 1, \ldots. \tag{7}$$

Indeed (6) is delayed version of (7) and so it exhibits the existence of period-two solutions.

Two interesting special cases of Equation (2) are the following difference equations:

$$x_{n+1} = \frac{\alpha + \gamma x_{n-1}}{Bx_n + Dx_n x_{n-1} + x_{n-1}}, \quad n = 0, 1, \ldots, \tag{8}$$

studied in [14], and

$$x_{n+1} = \frac{x_n x_{n-1} + \alpha x_n + \beta x_{n-1}}{ax_n x_{n-1} + bx_{n-1}}, \quad n = 0, 1, \ldots, \tag{9}$$

studied in [5]. In both equations, (8) and (9), the associated map changes its monotonicity with respect to its variable.

In this paper, in some cases when the associated map changes its monotonicity with respect to the first variable in an invariant interval, we will use Theorems 1 and 2 below in order to obtain the convergence results. However, if $F = F_g = (B/b)^3 c$, we would not be able to use this method, so we will use the semicycle analysis; see [15] to show that each of the following four sequences $\{x_{4k}\}_{k=1}^{\infty}$, $\{x_{4k+1}\}_{k=0}^{\infty}$, $\{x_{4k+2}\}_{k=0}^{\infty}$, $\{x_{4k+3}\}_{k=0}^{\infty}$ converges to the unique equilibrium point.

Also, we will show that Equation (1) exhibits the Naimark-Sacker bifurcation resulting in the existence of the locally stable periodic solution of unknown period.

Note that the problem of determining invariant intervals in the case when the associated map changes its monotonicity with respect to its variable has been considered in [17, 18].

In this paper, we will use the following well-known results, Theorem 2.22, in [16], and Theorem 1.4.7 in [19].

Theorem 1. *Let $[a, b]$ be a compact interval of real numbers and assume that $f : [a, b] \times [a, b] \longrightarrow [a, b]$ is a continuous function satisfying the following properties:*

(a) *$f(x, y)$ is nondecreasing in $x \in [a, b]$ for each $y \in [a, b]$, and $f(x, y)$ is nonincreasing in $y \in [a, b]$ for each $x \in [a, b]$;*

(b) *If $(m, M) \in [a, b] \times [a, b]$ is a solution of the system*

$$f(m, M) = m \quad \text{and} \quad f(M, m) = M, \tag{10}$$

then $m = M$.

Then

$$x_{n+1} = f(x_n, x_{n-1}), \quad n = 0, 1, \cdots \tag{11}$$

has a unique equilibrium $\overline{x} \in [a, b]$ and every solution of Equation (11) converges to $\overline{x}$.

Theorem 2. *Let $[a, b]$ be an interval of real numbers and assume that $f : [a, b] \times [a, b] \longrightarrow [a, b]$ is a continuous function satisfying the following properties:*

(a) *$f(x, y)$ is nonincreasing in both variables*

(b) *If $(m, M) \in [a, b] \times [a, b]$ is a solution of the system*

$$f(m, m) = M \quad \text{and} \quad f(M, M) = m, \tag{12}$$

then $m = M$.

Then, (11) has a unique equilibrium $\overline{x} \in [a, b]$ and every solution of Equation (11) converges to $\overline{x}$.

Remark 3. As is shown in [20] the unique equilibrium in Theorems 1 and 2 is globally asymptotically stable.

The rest of this paper is organized as follows. The second section presents the local stability of the unique positive equilibrium solution and the nonexistence of the minimal period-two solution. The third section gives global dynamics in certain regions of the parametric space. The results and techniques depend on monotonic character of the transition function $f(x, y)$ which is either decreasing in both arguments or increasing in first and decreasing in second argument. In simpler situations Theorems 1 and 2 are sufficient to prove global stability of the unique equilibrium. In more complicated situations we use the semicycle analysis, which is extensively used in [15, 19] for many linear fractional equations, to prove that every solution has four convergent subsequences, which leads to the conclusion that every solution converges to period-four solution. In some parts of parametric space we prove that there is no minimal period-four solution and so every solution converges to the equilibrium, while in other parts of parametric space we prove that the period-four solution exists. The semicycle analysis presented here uses innovative techniques based on analysis of systems of polynomial equations which coefficients depend on four parameters. Finally in the region of parameters complementary to the one where the period-four solution exists we prove that the Naimark-Sacker bifurcation takes place which produces locally stable periodic solution. All numerical simulations indicate that the equilibrium solution is globally asymptotically stable whenever it is locally asymptotically stable and that the dynamics is chaotic whenever the equilibrium is repeller. An interesting feature of Equation (1) is that it gives an example of second order difference equation with period-four solution for which period-two solution does not exist. The global dynamics of Equation (11) when the transition function $f(x, y)$ is either increasing in both arguments or decreasing in the first and increasing in the second argument is fairly simple as every solution $\{x_n\}$ breaks into two eventually monotonic subsequences $\{x_{2n}\}$ and $\{x_{2n+1}\}$; see [21–23]. The global dynamics of Equation (11) when the transition function $f(x, y)$ is either decreasing

in both arguments or increasing in the first and decreasing in the second argument could be quite complicated ranging from global asymptotic stability of the equilibrium, see [19, 21, 22, 24–26] to conservative and nonconservative chaos, see [3, 19, 26]. Interesting applications can be found in [27].

2. Linearized Stability

In this section, we present the local stability of the unique positive equilibrium of Equation (1) and the nonexistence of the minimal period-two solution of Equation (1).

In view of the above restriction on the initial conditions of Equation (1), the equilibrium points of Equation (1) are the positive solutions of the equation

$$\overline{x} = \frac{B\overline{x}^2 + F}{(b+c)\,\overline{x}^2}, \tag{13}$$

or equivalently

$$(b+c)\,\overline{x}^3 - B\overline{x}^2 - F = 0. \tag{14}$$

Equation (1) has the unique positive solution $\overline{x}$ given as

$$\overline{x} = \frac{B}{3(b+c)} + \frac{\sqrt[3]{2}B^2}{3(b+c)\sqrt[3]{\Delta + \sqrt{\Delta^2 - 4B^6}}} + \frac{\sqrt[3]{\Delta + \sqrt{\Delta^2 - 4B^6}}}{3\sqrt[3]{4}}, \tag{15}$$

where

$$\Delta = 2B^3 + 27F(b+c)^2. \tag{16}$$

Now, we investigate the stability of the positive equilibrium of Equation (1). Set

$$f(u,v) = \frac{Buv + F}{buv + cv^2} = \frac{Buv + F}{v(bu + cv)}, \tag{17}$$

and observe that

$$f'_u = \frac{Bcv^2 - bF}{v(bu+cv)^2}, \qquad f'_v = -\frac{Bcuv^2 + 2cFv + bFu}{v^2(bu+cv)^2} < 0. \tag{18}$$

The linearized equation associated with Equation (1) about the equilibrium point $\overline{x}$ is

$$z_{n+1} = sz_n + tz_{n-1} \tag{19}$$

where

$$s = f'_u(\overline{x},\overline{x}) \quad \text{and} \quad t = f'_v(\overline{x},\overline{x}). \tag{20}$$

Theorem 4. *Let $F_0 = (B/c)^3 b$. The unique equilibrium point $\overline{x}$ of Equation (1) given by (15) is*

(i) *locally asymptotically stable if $F < F_0$,*

(ii) *a repeller if $F > F_0$,*

(iii) *a nonhyperbolic point of elliptic type if $F = F_0$.*

Proof. In view of

$$s = f'_u(\overline{x},\overline{x}) = \frac{Bc\overline{x}^2 - bF}{\overline{x}^3(b+c)^2} = \frac{c}{b+c} - \frac{F}{(b+c)\,\overline{x}^3},$$

$$t = f'_v(\overline{x},\overline{x}) = -\frac{Bc\overline{x}^2 + 2cF + bF}{\overline{x}^3(b+c)^2} = -s - \frac{2F}{(b+c)\,\overline{x}^3} = -\frac{c}{b+c} - \frac{F}{(b+c)\,\overline{x}^3} < 0, \tag{21}$$

we have that

$$s + t = -\frac{2F}{\overline{x}^3(b+c)} < 0 \tag{22}$$

and

$$s^2 - (1-t)^2 = \left(\frac{Bc\overline{x}^2 - bF}{\overline{x}^3(b+c)^2}\right)^2 - \left(1 + \frac{Bc\overline{x}^2 + 2cF + bF}{\overline{x}^3(b+c)^2}\right)^2$$
$$= \frac{\left(Fb - Bc\overline{x}^2\right)^2}{\overline{x}^6(b+c)^4} - \frac{\left(b^2\overline{x}^3 + 2bc\overline{x}^3 + Fb + c^2\overline{x}^3 + Bc\overline{x}^2 + 2Fc\right)^2}{\overline{x}^6(b+c)^4}$$
$$= -\frac{\left(2F + b\overline{x}^3 + c\overline{x}^3\right)\left(b^2\overline{x}^3 + 2bc\overline{x}^3 + c^2\overline{x}^3 + 2Bc\overline{x}^2 + 2Fc\right)}{\overline{x}^6(b+c)^3} < 0, \tag{23}$$

and so $|s| < |1-t|$.

Also, we have

$$1 - t = 1 + \frac{Bc\overline{x}^2 + 2cF + bF}{\overline{x}^3(b+c)^2} > 0 \Longrightarrow t < 1. \tag{24}$$

Since $|s| < |1-t|$, the equilibrium point $\overline{x}$ will be nonhyperbolic if $t = -1$ and $|s| < 2$. From $t = -1$ we obtain

$$-\frac{c}{b+c} - \frac{F}{(b+c)\,\overline{x}^3} = -1 \Longleftrightarrow \overline{x} = \sqrt[3]{\frac{F}{b}}, \tag{25}$$

and by using (14), we have

$$(b+c)\left(\sqrt[3]{\frac{F}{b}}\right)^3 - B\left(\sqrt[3]{\frac{F}{b}}\right)^2 - F = 0 \Longleftrightarrow F = F_0 = \left(\frac{B}{c}\right)^3 b. \tag{26}$$

Now,

$$s = \frac{c}{b+c} - \frac{F}{(b+c)(F/b)} = -\frac{b-c}{b+c} \tag{27}$$

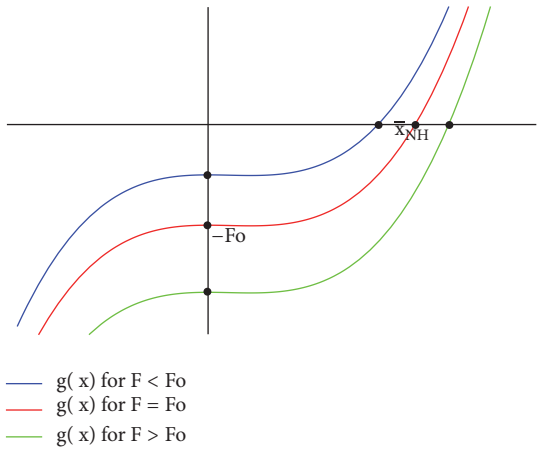

FIGURE 1: If $F < F_0$, then $\overline{x} < \overline{x}_{nh}$, i.e., $\overline{x}$ is LAS, and if $F > F_0$, then $\overline{x} > \overline{x}_{nh}$, i.e., $\overline{x}$ is repeller.

and the characteristic equation of (19) is of the form

$$\lambda^2 + \frac{b-c}{b+c}\lambda + 1 = 0, \tag{28}$$

from which

$$\lambda_{1,2} = \frac{c - b \pm i\sqrt{(b+3c)(3b+c)}}{2(b+c)} \quad \text{and} \quad |\lambda_{1,2}| = 1, \tag{29}$$

that is, $\overline{x}$ is nonhyperbolic equilibrium point. Let us denote

$$g(x) = (b+c)x^3 - Bx^2 - F. \tag{30}$$

Then,

$$g(\overline{x}_{nh}) = 0 \Longleftrightarrow F = F_0, \quad \text{and } g(0) = -F = -F_0. \tag{31}$$

The condition $|s| < |1 - t| = 1 - t$ is always satisfied. Hence, it holds: the equilibrium solution $\overline{x}$ is locally asymptotically stable if

$$t < -1 \Longleftrightarrow -\frac{c}{b+c} - \frac{F}{(b+c)\overline{x}^3} < -1 \Longleftrightarrow \overline{x} < \sqrt[3]{\frac{F}{b}} = \overline{x}_{nh}, \tag{32}$$

i.e., $F < F_0$ and a repeller if $t > -1$, which is equivalent with $\overline{x} > \sqrt[3]{F/b} = \overline{x}_{nh}$, i.e., $F > F_0$. See Figure 1. □

Lemma 5. *Equation (1) has no minimal period-two solution.*

Proof. Otherwise Equation (1) has a minimal period-two solution $\ldots x, y, x, y, \ldots$ which satisfies

$$x = \frac{Byx + F}{byx + cx^2}, \quad y = \frac{Bxy + F}{bxy + cy^2}. \tag{33}$$

Then,

$$bx^2 y + cx^3 = Bxy + F, \quad bxy^2 + cy^3 = Bxy + F, \tag{34}$$

which yields

$$(x - y)\left(bxy + c\left(x^2 + xy + y^2\right)\right) = 0, \tag{35}$$

which implies $x = y$. So, there is no a minimal period-two solution. □

3. Global Results

In this section, we prove several global attractivity results in the parts of parametric space.

We notice that the function $f(u, v)$ is always decreasing with respect to the second variable and can be either decreasing or increasing with respect to the first variable, depending on the sign of the nominator of f'_u. Therefore,

$$f'_u = 0 \Longleftrightarrow v = \sqrt{\frac{bF}{Bc}}, \tag{36}$$

and the function $f(u, v)$ is nonincreasing in both variables if $v \leq \sqrt{bF/Bc}$, and nondecreasing with respect to the first variable and nonincreasing with respect to the second variable if $v \geq \sqrt{bF/Bc}$. Since

$$f\left(\sqrt{\frac{bF}{Bc}}, \sqrt{\frac{bF}{Bc}}\right) = \frac{B}{b}, \tag{37}$$

if we denote $F_g = (B/b)^3 c$, we can have three possible cases:

$$\frac{B}{b} > \sqrt{\frac{bF}{Bc}} \Longleftrightarrow F < F_g, \quad \frac{B}{b} = \sqrt{\frac{bF}{Bc}} \Longleftrightarrow F = F_g, \quad \frac{B}{b} < \sqrt{\frac{bF}{Bc}} \Longleftrightarrow F > F_g. \tag{38}$$

As we have been seen, the nature of the local stability of the equilibrium point depends on the parameter F_0, so we distinguish the following scenarios:

(1) $F_g \le F_0$,

(2) $F_g > F_0$.

Case 1 ($F_g \le F_0$). Notice first that $F_g < F_0$ implies $c < b$ and that $F_g = F_0$ implies $c = b$. Now, we observe three subcases.

(a) $F < F_g \le F_0$. If $F < F_g \le F_0$, the function $f(u, v)$ is nondecreasing with respect to the first variable and nonincreasing with respect to the second variable on the invariant interval of Equation (1) which is given by

$$[L,U] = \left[\sqrt{\frac{bF}{Bc}}, \frac{B}{b}\right], \tag{39}$$

i.e., it holds

$$f : \left[\sqrt{\frac{bF}{Bc}}, \frac{B}{b}\right]^2 \longrightarrow \left[\sqrt{\frac{bF}{Bc}}, \frac{B}{b}\right]. \tag{40}$$

Indeed, since

$$\begin{aligned} &\max_{(x,y)\in[L,U]^2} f(x,y) = f(U,L) \\ &\text{and } \min_{(x,y)\in[L,U]^2} f(x,y) = f(L,U) \end{aligned} \tag{41}$$

we have that

$$\begin{aligned} f(U,L) &= f\left(\frac{B}{b}, \sqrt{\frac{bF}{Bc}}\right) \\ &= \frac{F + \left(B^2/b\right)\sqrt{(1/B)F(b/c)}}{B\sqrt{(1/B)F(b/c)} + (1/B)Fb} = \frac{B}{b} = U, \end{aligned} \tag{42}$$

and

$$\begin{aligned} &f(L,U) \ge L \Longleftrightarrow \\ &f\left(\sqrt{\frac{bF}{Bc}}, \frac{B}{b}\right) = \frac{F + \left(B^2/b\right)\sqrt{(1/B)F(b/c)}}{B\sqrt{(1/B)F(b/c)} + \left(B^2/b^2\right)c} \\ &\ge \sqrt{\frac{bF}{Bc}} \Longleftrightarrow \\ &F + \frac{B^2}{b}\sqrt{\frac{1}{B}F\frac{b}{c}} \ge B\left(\frac{bF}{Bc}\right) + \frac{B^2}{b^2}c\sqrt{\frac{bF}{Bc}} \Longleftrightarrow \\ &Fb^2c + bcB^2\sqrt{\frac{bF}{Bc}} \ge b^3F + B^2c^2\sqrt{\frac{bF}{Bc}} \Longleftrightarrow \\ &Fb^2(c-b) \ge (c-b)cB^2\sqrt{\frac{bF}{Bc}} \end{aligned} \tag{43}$$

which is true for $c \le b$ and $F < F_g$.

Also, since $F < (B^3/b^3)c = F$, we obtain

$$\begin{aligned} &g\left(\sqrt{\frac{bF}{Bc}}\right) g\left(\frac{B}{b}\right) \\ &= -\frac{(b+c)\left(B^3c - Fb^3\right)\left(F - c\sqrt{(bF/Bc)^3}\right)}{b^3c} < 0. \end{aligned} \tag{44}$$

This means that the equilibrium point $\overline{x}$ belongs to the invariant interval $[L,U]$.

Theorem 6. *If $F < F_g \le F_0$, then the equilibrium point $\overline{x}$ is globally asymptotically stable.*

Proof. The system of algebraic equations

$$\begin{aligned} f(m,M) &= m, \\ f(M,m) &= M, \end{aligned} \tag{45}$$

is reduced to the system

$$\begin{aligned} F + BMm &= m\left(cM^2 + bmM\right), \\ F + BMm &= M\left(cm^2 + Mbm\right), \end{aligned} \tag{46}$$

which yields

$$Mm(b-c)(M-m) = 0. \tag{47}$$

Since $c \ne b$, then it implies that $m = M = \overline{x}$. Now, by using Theorems 1 and 4, the conclusion follows. □

For some numerical values of parameters we give a visual evidence for Theorem 6 which indicates that in the case when $F < F_g < F_0$, the corresponding orbit converges very quickly (see Figure 2(a)), and in the case when $F < F_g = F_0$, the corresponding orbit converges significantly slower (see Figure 2(b)).

(b) $F_g < F < F_0$

Lemma 7. *If $F < F_d = 4B^3/(b+c)^2$, then the system of algebraic equations*

$$\begin{aligned} f(m,m) &= M \\ \text{and } f(M,M) &= m, \end{aligned} \tag{48}$$

has the unique solution $(m,M) = (\overline{x}, \overline{x})$

Proof. From (48) we have that

$$\begin{aligned} Bm^2 + F &= Mm^2(b+c), \\ BM^2 + F &= mM^2(b+c), \end{aligned} \tag{49}$$

that is,

$$\begin{aligned} &M\left(bm^2 + cm^2\right) - Bm^2 - m\left(bM^2 + cM^2\right) + BM^2 \\ &= 0 \\ &(M-m)\left[B(m + M - (b+c)mM)\right] = 0, \end{aligned} \tag{50}$$

from which $m = M = \overline{x}$ or $B(m + M - (b+c)mM) = 0$.

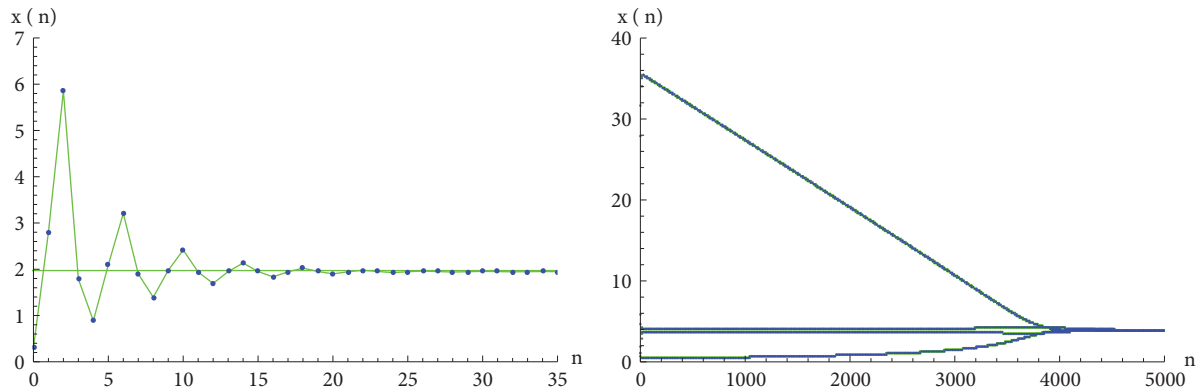

(a) $F < F_g < F_0$ (b) $F < F_g = F_0$

FIGURE 2: The orbit for (a) $b = 2$, $c = 1$, $B = 4$, $F = 7$, $F_g = 8$, $F_0 = 128$, and $(x_0, x_{-1}) = (0.3, 2.8)$ and (b) $b = 0.5$, $c = 0.5$, $B = 2$, $F = 30$, $F_g = F_0 = 32$, and $(x_0, x_{-1}) = (1.1, 1)$ generated by Dynamica 4 [16].

If $B(m + M - (b+c)mM) = 0$, then $m = BM/(-B + M(b+c))$. Since $M = (Bm^2 + F)/m^2(b+c) > B/(b+c)$ (see the first equation of system (49)), then $m > 0$. After substituting m in the second equation of system (49), we get

$$BM^2 + F = M^2\left(b + c^2\right)\frac{BM}{-B + M\,(b+c)} \Longleftrightarrow$$
$$B^2M^2 + F\,(b+c)\,M + BF = 0, \tag{51}$$

from which we have that

$$M_{1,2} = \frac{1}{2B^2}\left(F\,(b+c) \pm \sqrt{F^2\,(b+c)^2 - 4B^3F}\right) > 0. \tag{52}$$

Straightforward calculation show that $m_1 = M_2$ and $m_2 = M_1$. Notice that the solution (m_2, M_2) is exactly the same as the solution (M_1, m_1), and that system (48) has a unique solution $m = M = \overline{x}$ if $F \le 4B^3/(b+c)^2 = F_d$. □

Theorem 8. *If $F_g < F \le F_d < F_0$, where $F_d = 4B^3/(b+c)^2$, then the equilibrium $\overline{x}$ is globally asymptotically stable.*

Proof. If $F_g < F < B^3/bc$, then

$$f : \left[\frac{B}{b}, \sqrt{\frac{bF}{Bc}}\right]^2 \longrightarrow \left[\frac{B}{b}, \sqrt{\frac{bF}{Bc}}\right], \tag{53}$$

which means that the interval $[L, U] = [B/b, \sqrt{bF/Bc}]$ is an invariant interval.

Indeed, since the function f is nonincreasing in both variables on the invariant interval, then

$$\max_{(x,y)\in[L,U]^2} f\,(x,y) = f\,(L,L)$$
$$\text{and} \quad \min_{(x,y)\in[L,U]^2} f\,(x,y) = f\,(U,U), \tag{54}$$

and we obtain that

$$f\,(U,U) = f\left(\sqrt{\frac{bF}{Bc}}, \sqrt{\frac{bF}{Bc}}\right)$$
$$= \frac{F\,(b/c) + F}{(1/B)\,F\left(b^2/c\right) + (1/B)\,Fb} = \frac{B}{b} = L, \tag{55}$$

and

$$f\,(L,L) \le U \Longleftrightarrow$$
$$f\left(\frac{B}{b}, \frac{B}{b}\right) = \frac{B^3 + Fb^2}{B^2\,(b+c)} \le \sqrt{\frac{bF}{Bc}} \Longleftrightarrow$$
$$\left(\frac{B^3 + Fb^2}{B^2\,(b+c)}\right)^2 - \frac{bF}{Bc} < 0 \Longleftrightarrow$$
$$\left(B^3c - Fb^3\right)\left(B^3 - Fbc\right) < 0 \Longleftrightarrow \tag{56}$$
$$F_g = \frac{B^3}{b^3}c < F < \frac{B^3}{bc}.$$

Hence,

$$f\left(\frac{B}{b}, \frac{B}{b}\right) = \frac{Fb^2 + B^3}{B^2\,(b+c)} \in \left[\frac{B}{b}, \sqrt{\frac{bF}{Bc}}\right],$$
$$\text{if } c < b \text{ and } F_g = \frac{B^3}{b^3}c < F < \frac{B^3}{bc}. \tag{57}$$

The following calculation will show that $F_d < B^3/bc$. Indeed,

$$\frac{4B^3}{(b+c)^2} < \frac{B^3}{bc} \Longleftrightarrow$$
$$-B^3\frac{(b-c)^2}{bc\,(b+c)^2} < 0, \tag{58}$$

which is true.

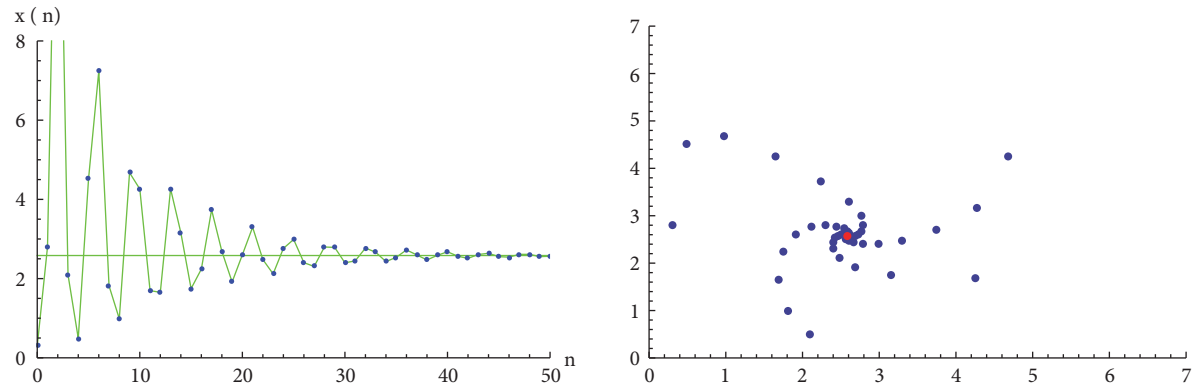

FIGURE 3: The orbit and the phase portrait for $b = 2$, $c = 1$, $B = 4$, $F = 28$, $F_g = 8$, $F_0 = 128$, and $(x_0, x_{-1}) = (0.3, 2.8)$ generated by Dynamica 4 [16].

Also, since $g(\sqrt{bF/Bc})g(B/b) < 0$, it means that the equilibrium point $\overline{x}$ belongs to the invariant interval $[L, U]$.

Now, by using Lemma 7, Theorems 2 and 4, we get the conclusion that the equilibrium $\overline{x}$ is globally asymptotically stable. □

For some numerical values of parameters we give a visual evidence for Theorem 8. See Figure 3.

Lemma 9. *Assume that $F \neq F_g$.*

(i) *If $x_{n-1} < \sqrt{bF/Bc}$, then $x_{n+1} > B/b$.*

(ii) *If $x_{n-1} > \sqrt{bF/Bc}$, then $x_{n+1} < B/b$.*

(iii) *If $x_{n-1} = \sqrt{bF/Bc}$, then $x_{n+1} = B/b$.*

Proof. Since the map associated with the right-hand side of Equation (1) is always decreasing in the second variable, we have that

$$x_{n-1} \left\{ \begin{matrix} < \\ > \\ = \end{matrix} \right\} \sqrt{\frac{bF}{Bc}} \Longrightarrow$$

$$x_{n+1} = \frac{Bx_nx_{n-1} + F}{bx_nx_{n-1} + cx_{n-1}^2} \left\{ \begin{matrix} > \\ < \\ = \end{matrix} \right\} \frac{Bx_n\sqrt{bF/Bc} + F}{bx_n\sqrt{bF/Bc} + bF/B} \tag{59}$$

$$= \frac{B}{b}.$$

□

Note that under assumption of Lemma 9, the following inequality holds:

$$\min\left\{\sqrt{\frac{bF}{Bc}}, \frac{B}{b}\right\} < \overline{x} < \max\left\{\sqrt{\frac{bF}{Bc}}, \frac{B}{b}\right\}. \tag{60}$$

(c) $F = F_g < F_0$. By substituting parameter $F = F_g = (B/b)^3 c = E^3 c$, where $\overline{x} = E = B/b$, in Equation (1), we obtain

$$\begin{aligned} x_{n+1} &= \frac{Bx_nx_{n-1} + \left(B^3/b^3\right)c}{bx_nx_{n-1} + cx_{n-1}^2} \\ &= \frac{(B/b)\,x_nx_{n-1} + (B/b)^3\,(c/b)}{x_nx_{n-1} + (c/b)\,x_{n-1}^2} \\ &= \frac{Ex_nx_{n-1} + E^3\,(c/b)}{x_nx_{n-1} + (c/b)\,x_{n-1}^2}. \end{aligned} \tag{61}$$

Lemma 10. *(i) Assume that $F = F_g < F_0$, i.e., $c < b$. Then Equation (61) does not possess a minimal period-four solution.*

(ii) Assume that $F = F_g = F_0$, i.e., $c = b$. Then Equation (61) has the minimal period-four solutions of the form

$$\ldots, E, \frac{E^2}{t}, E, t, E, \frac{E^2}{t}, E, t, \ldots \tag{62}$$

where $E = \overline{x} = (B/b)(= B/c)$ and $t > 0$ is an arbitrary number depending on initial conditions x_0 and x_{-1}.

Proof. Suppose that Equation (61) has a minimal period-four solution $\ldots x, y, z, t, x, y, z, t, \ldots$; then it holds

$$\begin{aligned} x &= \frac{Etz + E^3\,(c/b)}{tz + (c/b)\,z^2}, \\ y &= \frac{Ext + E^3\,(c/b)}{xt + (c/b)\,t^2}, \\ z &= \frac{Exy + E^3\,(c/b)}{xy + (c/b)\,x^2}, \\ t &= \frac{Eyz + E^3\,(c/b)}{yz + (c/b)\,y^2}, \end{aligned} \tag{63}$$

where $E = \overline{x}$. By eliminating x and y we obtain

$$\begin{aligned} z\,(z - E)\,W\,(t, z) &= 0, \\ t\,(t - E)\,U\,(t, z) &= 0, \end{aligned} \tag{64}$$

where the functions $W(t,z)$ and $U(t,z)$ can be written in the polynomial form as

$$W(t,z) = \beta_4 z^4 + \beta_3 z^3 + \beta_2 z^2 + \beta_1 z + \beta_0, \tag{65}$$

$$U(t,z) = \alpha_5 z^5 + \alpha_4 z^4 + \alpha_3 z^3 + \alpha_2 z^2 + \alpha_1 z + \alpha_0, \tag{66}$$

where

$$\begin{aligned}
\beta_4 &= c^3 tE\left(b^2E - c^2t\right),\\
\beta_3 &= c\left(bc^3E^4 - c^4t^2E^2 + b^2c^2t^4 - b^2c^2t^2E^2\right.\\
&\quad \left. + 2b^3ct^2E^2 - 3bc^3t^3E + b^4t^3E\right),\\
\beta_2 &= b^5t^4E - c^5t^2E^3 + b^3c^2t^5 - bc^4t^3E^2 + 2b^2c^3tE^4\\
&\quad - 2b^2c^3t^4E + b^4ct^3E^2 - b^2c^3t^2E^3 + 2b^3c^2t^2E^3\\
&\quad - 2b^3c^2t^3E^2 - bc^4tE^4 + b^4ct^4E,\\
\beta_1 &= bctE^3\left(-c^3E^2 + 2b^3t^2 - c^3t^2 + bc^2E^2 + b^2ct^2\right.\\
&\quad \left. - 3bc^2tE + b^2ctE\right),\\
\beta_0 &= bc^2tE^5\left(b^2t - c^2E\right),\\
\alpha_5 &= bc^4tE > 0,\\
\alpha_4 &= c^2\left(b^2t^2(cE + bt) - c^3E^3 + \left(b^3 - c^3\right)tE^2\right.\\
&\quad \left. + \left(b^2 - c^2\right)ct^2E\right),\\
\alpha_3 &= b\left(bc^3E^4 + b^4t^3E - 2c^4tE^3 - 2c^4t^3E - 2c^4t^2E^2\right.\\
&\quad \left. + b^3ct^4 - bc^3t^2E^2 + b^2c^2t^3E + b^3ct^2E^2\right),\\
\alpha_2 &= bctE\left(-2c^3E^3 + b^2cE^3 + 2b^3tE^2 + b^3t^2E\right.\\
&\quad \left. - bc^2t^2E - bc^2t^3 - bc^2tE^2 - b^2ct^2E\right),\\
\alpha_1 &= b^2c^2tzE^4(bE + 2t(b-c)) > 0,\\
\alpha_0 &= b^2c^3tE^6 > 0.
\end{aligned} \tag{67}$$

Since $z \neq 0$ and $t \neq 0$, from system (64), we obtain the following four cases:

(1) The system

$$\begin{aligned} z - E &= 0,\\ t - E &= 0, \end{aligned} \tag{68}$$

implies $z = t = E$, and by using (63), we get $x = y = E$.

(2) The system

$$\begin{aligned} z - E &= 0,\\ U(t,z) &= 0, \end{aligned} \tag{69}$$

implies $z = E$ and

$$\begin{aligned} U(t,E) &= E^3(b-c)(b+c)\left(ct^2 + tE(b+c) + cE^2\right)\\ &\quad \cdot (cE + bt)^2 > 0 \end{aligned} \tag{70}$$

if $c < b$. If $b = c$, then $U(t,z) = 0$ is satisfied for every $t > 0$, and by using system (63), it follows that the periodic solution of the minimal period four is of the form (62).

(3) The system

$$\begin{aligned} W(t,z) &= 0,\\ t - E &= 0, \end{aligned} \tag{71}$$

implies $t = E$ and

$$\begin{aligned} W(E,z) &= E^3(b-c)(b+c)\left(cz^2 + zE(b+c) + cE^2\right)\\ &\quad \cdot \left(c^2z^2 + bzE(b+c) + bcE^2\right) > 0, \end{aligned} \tag{72}$$

so the conclusion is the same as in the previous case.

(4) The system

$$\begin{aligned} W(t,z) &= 0,\\ U(t,z) &= 0, \end{aligned} \tag{73}$$

demands more detailed analysis.

(a) Assume that $b > c$. Then we can write $b = c + \xi$, $\xi > 0$. Consider the polynomials $W(t,z)$ and $U(t,z)$ as polynomials in one variable t:

$$\begin{aligned} W(t,z) &= a_5t^5 + a_4t^4 + a_3t^3 + a_2t^2 + a_1t + a_0,\\ U(t,z) &= b_4t^4 + b_3t^3 + b_2t^2 + b_1t + b_0, \end{aligned} \tag{74}$$

where

$$\begin{aligned}
a_5 &= c^2z^2(c+\xi)^3,\\
a_4 &= z^2(c+\xi)^2\left(c^3z + \xi^3E + 4c\xi^2E + 5c^2\xi E\right),\\
a_3 &= 2c^5zE\left(E^2 - zE - z^2\right) + c^4z\xi E\left(10E^2 - 3zE\right.\\
&\quad \left. + z^2\right) + 3c^3z\xi^2E\left(5E^2 + 2z^2\right) + c^2z\xi^3E\left(2zE\right.\\
&\quad \left. + 9E^2 + 4z^2\right) + cz\xi^4E\left(zE + 2E^2 + z^2\right),\\
a_2 &= c^5E\left(E^4 - 2zE^3 - z^4\right) + c^4\xi E^2\left(3E^3 - 3zE^2\right.\\
&\quad \left. + 4z^2E + 4z^3\right) + c^3\xi^2E^2\left(3E^3 + 5z^2E + 5z^3\right)\\
&\quad + c^2\xi^3E^2(z+E)\left(E^2 + 2z^2\right),\\
a_1 &= c^3E^2(c+\xi)\left(c\left(z^4 - E^4\right) + z^4\xi + cz^2E^2 + 2z^2\xi E^2\right.\\
&\quad \left. + z\xi E^3\right),\\
a_0 &= c^4z^3E^4(c+\xi),
\end{aligned}$$

$$
\begin{aligned}
b_4 &= cz^2(c+\xi)^2\left(z(c+\xi)^2 - c^2E\right),\\
b_3 &= z^2E(c+\xi)^3\left(z(c+\xi)^2 - c^2E\right) + cz^2\xi E^2(2c+\xi)\\
&\quad\cdot(c+\xi)^2 + c^2z^3(c+\xi)\left(\xi^2E + 2c\xi E + z(c+\xi)^2\right.\\
&\quad\left. - c^2E\right),\\
b_2 &= c^5z^2E(E-z)^2 + 2c^4zE\xi\left(E^3 + 3zE^2 + 2z^3\right)\\
&\quad + c^3zE\xi^2\left(4E^3 + 11zE^2 + 5z^2E + 2z^3\right)\\
&\quad + 2c^2zE^2\xi^3\left(4zE + E^2 + 2z^2\right) + cz^2E^2\xi^4(z+2E),\\
b_1 &= c^5E(E-z)(z+E)\left(E^3 + z\left(E^2 - z^2\right)\right)\\
&\quad + c^4\xi E\left(z^2E^3 + 2\left(E^3 - z^3\right)E^2 + 3zE^4 + 3z^4E\right.\\
&\quad\left. + z^5\right) + c^3\xi^2E^2\left(3z^2E^2 + E^4 + 3zE^3 + 3z^4\right)\\
&\quad + c^2z\xi^3E^2\left(E^3 + zE^2 + z^3\right),\\
b_0 &= c^3z^3E^3\left(E(c+\xi)^2 - c^2z\right).
\end{aligned}
\tag{75}
$$

If $z \in [c^2E/(c+\xi)^2, E]$, then $b_i \geqslant 0$, for $i = 0, 1, 4$ and $b_2 > 0, b_3 > 0$, so we have that

$$
U(t,z) > 0 \quad \text{for } z \in \left[\frac{c^2E}{(c+\xi)^2}, E\right]. \tag{76}
$$

Since $W(t,z)$ and $U(t,z)$ are polynomials of the fifth and fourth degrees, respectively, the resultant of these polynomials is the determinant of the ninth degree:

$$
\begin{aligned}
&res_t(W,U)\\
&= \det\begin{bmatrix}
a_5 & a_4 & a_3 & a_2 & a_1 & a_0 & 0 & 0 & 0\\
0 & a_5 & a_4 & a_3 & a_2 & a_1 & a_0 & 0 & 0\\
0 & 0 & a_5 & a_4 & a_3 & a_2 & a_1 & a_0 & 0\\
0 & 0 & 0 & a_5 & a_4 & a_3 & a_2 & a_1 & a_0\\
b_4 & b_3 & b_2 & b_1 & b_0 & 0 & 0 & 0 & 0\\
0 & b_4 & b_3 & b_2 & b_1 & b_0 & 0 & 0 & 0\\
0 & 0 & b_4 & b_3 & b_2 & b_1 & b_0 & 0 & 0\\
0 & 0 & 0 & b_4 & b_3 & b_2 & b_1 & b_0 & 0\\
0 & 0 & 0 & 0 & b_4 & b_3 & b_2 & b_1 & b_0
\end{bmatrix},
\end{aligned}
\tag{77}
$$

from which we obtain

$$
\begin{aligned}
res_t(W,U) &= (z-E)^4\Upsilon_1(z)\Upsilon_2(z)\Upsilon_3(z)\Upsilon_4(z)\\
&\quad\cdot\Phi(z,E,c+\xi,c),
\end{aligned}
\tag{78}
$$

where

$$
\begin{aligned}
\Upsilon_1(z) &= \xi z^2 + \xi Ez - cE^2,\\
\Upsilon_2(z) &= \left(c^2z^2 + \xi bEz - (c+\xi)cE^2\right)^2,\\
\Upsilon_3(z) &= (c+\xi)^9c^{17}z^9E^{10}(z+E)^6\left((2c+\xi)z^2\right.\\
&\quad\left. + c(z+E)E\right) > 0,\\
\Upsilon_4(z) &= c^2z^2 + z(2c+\xi)bE + (c+\xi)cE^2 > 0,\\
\Phi(z,E,c+\xi,c) &= c_4z^4 + c_3z^3 + c_2z^2 + c_1z + c_0,\\
c_4 &= 8c^2\left(2c\xi + \xi^2 + 2c^2\right)(c+\xi)^7,\\
c_3 &= -2E\left(2c\xi + \xi^2 + 2c^2\right)\left(-55c^2\xi^4 - 50c^3\xi^3 + 2c^4\xi^2\right.\\
&\quad\left. - 4\xi^6 - 24c\xi^5 + 32c^5\xi + 16c^6\right)(c+\xi)^3,\\
c_2 &= 96c^{11}E^2 + 512c^{10}\xi E^2 + 1208c^9\xi^2E^2\\
&\quad + 1512c^8\xi^3E^2 + 768c^7\xi^4E^2 - 644c^6\xi^5E^2\\
&\quad - 1600c^5\xi^6E^2 - 1542c^4\xi^7E^2 - 903c^3\xi^8E^2\\
&\quad - 338c^2\xi^9E^2 - 76c\xi^{10}E^2 - 8\xi^{11}E^2,\\
c_1 &= -2cE^3\left(2c\xi + \xi^2 + 2c^2\right)\left(31c^2\xi^4 + 48c^3\xi^3\right.\\
&\quad\left. + 62c^4\xi^2 + 4\xi^6 + 16c\xi^5 + 48c^5\xi + 16c^6\right)(c+\xi)^2,\\
c_0 &= 16c^3E^4(c+\xi)^8.
\end{aligned}
\tag{79}
$$

If the equation $res_t(W,U) = 0$ has solutions for variable z, then they are the common roots of both equations in system (73) for a fixed value of t. One of these positive roots is $z_1 = E$, but for $z = E$ and $t > 0$ system (73) has no solutions since $U(t,E) > 0$, see (76). Therefore, in this case, Equation (61) has no minimal period-four solution.

The positive solution of the equation $\Upsilon_1(z) = 0$ is

$$
z_2 = \frac{E\left(-\xi + \sqrt{\xi(\xi+4c)}\right)}{2\xi}. \tag{80}
$$

We will show later that z_2 can not be a component of any positive solutions of system (73).

The positive solution of the equation $\Upsilon_2(z) = 0$ is

$$
\begin{aligned}
&z_3\\
&= \frac{E\left(-(c+\xi)\xi + \sqrt{(2c+\xi)(c+\xi)\left(\xi^2 - c\xi + 2c^2\right)}\right)}{2c^2},
\end{aligned}
\tag{81}
$$

and $z_3 \in (c^2E/(c+\xi)^2, E)$. Namely,

$$
\begin{aligned}
&z_3 < E \Longleftrightarrow\\
&4c^2\xi^2 > 0,
\end{aligned}
\tag{82}
$$

which is true, and

$$
\begin{aligned}
&\frac{c^2}{(c+\xi)^2}E < z_3 \Longleftrightarrow\\
&\frac{c^2E}{(c+\xi)^2}
\end{aligned}
$$

$$-\frac{E\left(-(c+\xi)\xi+\sqrt{(2c+\xi)(c+\xi)(\xi^2-c\xi+2c^2)}\right)}{2c^2}$$
$$<0 \Longleftrightarrow$$
$$-4c^3\xi\left(4c\xi^3+7c^3\xi+7c^2\xi^2+4c^4+\xi^4\right)<0, \tag{83}$$

which is also true. So, system (73) has no solutions since $U(t,E)>0$, see (76).

Now, we prove that the eventually positive roots of the equation $\Phi(z,E,c+\xi,c)=0$ for variable z can belong only to the interval $(c^2E/(c+\xi)^2,E)$ and that every $z\in(c^2E/(c+\xi)^2,E)$ can not be a component of any positive solution of system (73). First, we prove that $\Phi(z,E,c+\xi,c)>0$ for $z>E$. Let $z=E+\gamma$, $\gamma>0$; then we obtain

$$\begin{aligned}\Phi(E+\gamma,E,c+\xi,c)&=16c^{11}\gamma^4+128c^{10}\gamma^2\xi\left(\gamma^2+E^2+\gamma E\right)+8c^9\xi^2\left(57\gamma^4+16E^4+142\gamma^2E^2+48\gamma E^3+111\gamma^3E\right)+8c^8\xi^3\left(119\gamma^4+76E^4+522\gamma^2E^2+256\gamma E^3+349\gamma^3E\right)+8c^7\xi^4\left(161\gamma^4+162E^4+1101\gamma^2E^2+627\gamma E^3+657\gamma^3E\right)+4c^6\xi^5\left(294\gamma^4+402E^4+3013\gamma^2E^2+1839\gamma E^3+1646\gamma^3E\right)+2c^5\xi^6\left(364\gamma^4+636E^4+5653\gamma^2E^2+3550\gamma E^3+2879\gamma^3E\right)+2c^4\xi^7\left(148\gamma^4+330E^4+3708\gamma^2E^2+2333\gamma E^3+1789\gamma^3E\right)+c^3\xi^8\left(72\gamma^4+221E^4+3375\gamma^2E^2+2082\gamma E^3+1570\gamma^3E\right)+2c^2\xi^9(\gamma+E)\left(4\gamma^3+22E^3+281\gamma E^2+231\gamma^2E\right)+4c\xi^{10}E(\gamma+E)\left(22\gamma^2+E^2+25\gamma E\right)+8\gamma\xi^{11}E(\gamma+E)^2,\end{aligned} \tag{84}$$

i.e., $\Phi(E+\gamma,E,c+\xi,c)>0$. It means that the function $\Phi(z,E,c+\xi,c)$ eventually has the positive roots in the interval $(0,E]$. Since we already considered the case when $z=E$, now we investigate the existence of the positive roots of the equation $\Phi(z,E,b,c)=0$ for $0<z<E$. As we have seen, $U(t,z)>0$ for $c^2E/(c+\xi)^2<z<E$ and $t>0$, so system (73) has no solution in the case when the equation $\Phi(z,E,c+\xi,c)=0$ has the positive roots in the interval $(c^2E/(c+\xi)^2,E)$. This implies that Equation (61) has no minimal period-four solution whenever any root of equation $res_t(W,U)=0$ lies in the interval $(c^2E/(c+\xi)^2,E)$.

Now, we prove that the equation $\Phi(z,E,c+\xi,c)=0$ has no root for variable z if $z\in(0,c^2E/(c+\xi)^2)$ and $\xi>0$. It is easy to see the following:

$$\Phi_0=\Phi(0,E,c+\xi,c)=16c^3E^4(c+\xi)^8>0. \tag{85}$$

For $\Phi_1=\Phi(c^2E/(c+\xi)^2,E,c+\xi,c)$ we have

$$\Phi_1=\frac{c^3\xi^2E^4\left(72c\xi^7+184c^7\xi+278c^2\xi^6+618c^3\xi^5+877c^4\xi^4+820c^5\xi^3+500c^6\xi^2+32c^8+8\xi^8\right)(2c+\xi)^2}{(c+\xi)^4}>0, \tag{86}$$

and

$$\begin{aligned}&\Phi_0-\Phi_1\\&=\frac{c^3E^4\left(2c\xi+2c^2+\xi^2\right)\left(5c\xi^2+4c^2\xi+2c^3+2\xi^3\right)\left(26c\xi^6+36c^6\xi+76c^2\xi^5+135c^3\xi^4+154c^4\xi^3+104c^5\xi^2+4c^7+4\xi^7\right)}{(c+\xi)^4}\\&>0.\end{aligned} \tag{87}$$

Now, it is sufficient to prove $d\Phi(z,E,b,c)/dz<0$ in $(0,c^2E/(c+\xi)^2),\xi>0$. Since

$$\frac{d\Phi(z,E,c+\xi,c)}{dz}=2\left((c+\xi)^2+c^2\right)P(z,E,c+\xi,c), \tag{88}$$

where

$$\begin{aligned}&P(z,E,c+\xi,c)\\&=16c^9(z-E)^3+16c^8\xi(z-E)\left(-8zE+5E^2+7z^2\right)+6c^7\xi^2\left(-29E^3+62zE^2-73z^2E+56z^3\right)+4c^6\xi^3\left(-55E^3+70zE^2-51z^2E+140z^3\right)+c^5\xi^4\left(-189E^3-82zE^2+501z^2E+560z^3\right)\end{aligned}$$

$$
\begin{aligned}
&+ c^4\xi^5\left(-126E^3 - 380zE^2 + 1011z^2E + 336z^3\right)\\
&+ c^3\xi^6\left(-67E^3 - 379zE^2 + 873z^2E + 112z^3\right)\\
&+ c^2\xi^7\left(-24E^3 - 202zE^2 + 417z^2E + 16z^3\right)\\
&+ 4c\xi^8E\left(-15zE - E^2 + 27z^2\right)\\
&+ 4z\xi^9E\left(3z - 2E\right),
\end{aligned}
\tag{89}
$$

then for $z = c^2E/k(c+\xi)^2$, $\xi > 0$, $k > 1$ we obtain

$$
P\left(\frac{c^2E}{k\left(c+\xi\right)^2}, E, c+\xi, c\right) = cE^3\frac{\Omega\left(c,\xi,k\right)}{k^3\left(c+\xi\right)^2} < 0, \tag{90}
$$

with

$$
\begin{aligned}
&\Omega\left(c,\xi,k\right)\\
&\quad = -16c^{10}\left(k-1\right)^3\\
&\qquad - 16c^9\xi\left(k-1\right)\left(6k\left(k-1\right) + k^2 + 3\right)\\
&\qquad - 2c^8\xi^2\left(51k - 186k^2 + 175k^3 - 24\right)\\
&\qquad - 8c^7\xi^3\left(\left(k-1\right)\left(20k + 55k^2 + 2\right) + 26k^3\right)\\
&\qquad - c^6\xi^4k\left(82k + 488k^2 + 315\left(k^2-1\right)\right)\\
&\qquad - c^5\xi^5k\left(380k + 487k^2 + 237\left(k^2-1\right)\right)\\
&\qquad - c^4\xi^6k\left(379k + 424k^2 + 84\left(k^2-1\right)\right)\\
&\qquad - 2c^3\xi^7k\left(101k + 136k^2 + 6\left(k^2-1\right)\right)\\
&\qquad - c^2\xi^8k^2\left(119k + 60\right) - 8c\xi^9k^2\left(4k+1\right)\\
&\qquad - 4\xi^{10}k^3 < 0.
\end{aligned}
\tag{91}
$$

Similarly, now we will consider $W(t,z)$ and $U(t,z)$ as polynomials in the variable t (with the coefficients α_i, β_j, $i \in \{0,1,\ldots,5\}$, $j \in \{0,1,\ldots,4\}$). The resultant of these polynomials is

$$
\begin{aligned}
res_z\left(W,U\right) &= \left(t-E\right)^2\left(t+E\right)^4\left(\left(c+\xi\right)t - cE\right)^6\Lambda_1\left(t\right)\\
&\quad\cdot\Lambda_2\left(t\right)\Phi\left(t,E,c+\xi,c\right),
\end{aligned}
\tag{92}
$$

where

$$
\begin{aligned}
\Lambda_1\left(t\right) &= \left(c+\xi\right)^4c^{18}t^4E^{15}\left(\left(2c+\xi\right)t^2 + cE\left(t+E\right)\right)\\
&\quad\cdot\left(cE + \left(c+\xi\right)t\right)^4 > 0,\\
\Lambda_2\left(t\right) &= \xi t^2 + \xi Et - cE^2.
\end{aligned}
\tag{93}
$$

If the equation $res_z(W,U) = 0$ has solutions for variable t, then they are the common roots of both equations in system (73) for a fixed value of z. One of these positive roots is $t_1 = E$, and for $t = E$ and $z > 0$ system (73) has no solutions since

$$
\begin{aligned}
W\left(E,z,c+\xi,c\right) &= \xi E^3\left(2c+\xi\right)\\
&\quad\cdot\left(cz^2 + zE\left(2c+\xi\right) + cE^2\right)\\
&\quad\cdot\left(c^2z^2 + \left(z\left(2c+\xi\right) + cE\right)\left(c+\xi\right)E\right) > 0
\end{aligned}
\tag{94}
$$

for $\xi > 0$. It means that Equation (61) has no minimal period-four solution.

Similarly, for the second root $t_2 = cE/(c+\xi)$, $\xi > 0$ we obtain $\widetilde{U} = U(cE/(c+\xi), z, c+\xi, c)$,

$$
\begin{aligned}
&\widetilde{U}\\
&= \frac{c^3E^2\left(z+E\right)^2\left(c^4\left(z+E\right)\left(z-E\right)^2 + c^3\xi\left(3E^3 + 3z^2E + 2z^3\right) + c^2\xi^2\left(3E^3 + 4zE^2 + 6z^2E + z^3\right) + c\xi^3E\left(2z+E\right)^2 + \xi^4zE\left(z+E\right)\right)}{\left(c+\xi\right)^2}\\
&> 0,
\end{aligned}
\tag{95}
$$

where $\xi > 0$. It means that Equation (61) has no minimal period-four solution in this case. As we have already seen, the equation $\Phi(t,E,c+\xi,c) = 0$ has eventually positive roots only in the interval $t \in (c^2E/(c+\xi)^2, E)$, $\xi > 0$. Then,

$$
\begin{aligned}
\beta_4 &= c^3tE\left(\left(E-t\right)c^2 + \xi^2E + 2c\xi E\right) > 0,\\
\beta_3 &= c^5\left(E-t\right)\left(E^3 - t^3 + tE^2 + t^2E\right) + c^4\xi\left(4t^2E^2\right.\\
&\quad\left. + E^4 + t^3E + 2t^4\right) + c^3\xi^2t^2\left(t+E\right)\left(t+5E\right)\\
&\quad + 2c^2\xi^3t^2E\left(2t+E\right) + ct^3\xi^4E > 0,\\
\beta_2 &= c^5t\left(t-E\right)^2\left(t+E\right)^2 + c^4t\xi\left(3E^2\left(E^2 - t^2\right)\right.\\
&\quad\left. + 4tE^3 + 5t^3E + 3t^4\right) + c^3t\xi^2\left(2E^4 + 5tE^3 + 14t^3E\right.\\
&\quad\left. + 3t^4\right) + c^2t^2\xi^3\left(2E^3 + 2tE^2 + 14t^2E + t^3\right)\\
&\quad + ct^3\xi^4E\left(6t+E\right) + t^4\xi^5E > 0,\\
\beta_1 &= ctE^3\left(c+\xi\right)\left(c\xi\left(\left(c+\xi\right)t^2 + ct^2 + cE^2\right)\right.\\
&\quad\left. + \left(c+\xi\right)t\left(cE\xi + 2\left(\left(c+\xi\right)^2t - c^2E\right)\right)\right) > 0,\\
\beta_0 &= c^2tE^5\left(c+\xi\right)\left(\left(c+\xi\right)^2t - c^2E\right) > 0.
\end{aligned}
\tag{96}
$$

This implies $W(t,z) > 0$ for $c^2E/(c+\xi)^2 < t < E$ and $z > 0$, so system (73) has no solution in the case when the equation $\Phi(t,E,c+\xi,c) = 0$ has the positive roots in the interval $(c^2E/(c+\xi)^2, E)$, which further means that Equation (61) has no minimal period-four solution.

Also, the positive solution of the equation $\Lambda_2(t) = 0$ is

$$t_3 = \frac{E\left(-\xi + \sqrt{\xi(\xi+4c)}\right)}{2\xi}. \tag{97}$$

Note that $t_3 = z_2$. Now, we prove that (z_2, z_2) can not be solution of system (73). Indeed, suppose the opposite, i.e.,

$$\begin{aligned}
&U(z_2, z_2, c+\xi, c) = 0,\\
&W(z_2, z_2, c+\xi, c) = 0,\\
&\Updownarrow\\
&c^{10} + 2c^9\xi + 8c^8\xi^2 + 26c^7\xi^3 + 45c^6\xi^4 + 43c^5\xi^5\\
&\quad + 13c^4\xi^6 - 27c^3\xi^7 - 35c^2\xi^8 - 15c\xi^9 - 2\xi^{10} = 0,\\
&c^{10} - 2c^9\xi + 27c^8\xi^2 + 51c^7\xi^3 - 30c^6\xi^4 - 165c^5\xi^5\\
&\quad - 214c^4\xi^6 - 148c^3\xi^7 - 58c^2\xi^8 - 12c\xi^9 - \xi^{10} = 0,\\
&\Updownarrow\\
&(c = 0, \xi = 0),
\end{aligned} \tag{98}$$

which is a contradiction with the assumption that $c > 0$ and $\xi > 0$.

Consequently system (73) does not have positive solutions when $b > c$.

(b) Assume that $b = c$. Then, system (73)

$$\begin{aligned}
W(t,z,c,c) = 0,\\
U(t,z,c,c) = 0,
\end{aligned} \tag{99}$$

is of the form

$$\begin{aligned}
&(t-E)\left(t^4z^2 + t^3(z+E)z^2\right.\\
&\quad - t^2\left(z^3E + z^2E^2 - 2zE^3\right)\\
&\quad \left. - t\left(z^4E + z^3E^2 + z^2E^3 - E^5\right) - z^3E^3 = 0\right) = 0,\\
&(z-E)\left(t^4z^2 + t^3(z+E)z^2 - t^2\left(z^2E^2 - z^3E\right)\right.\\
&\quad - t\left(-z^4E - z^3E^2 + z^2E^3 + 2zE^4 + E^5\right) - z^3E^3\Big)\\
&\quad = 0,
\end{aligned} \tag{100}$$

and combining those equations, we have the following four cases:

(i)

$$\begin{aligned}
t - E = 0,\\
z - E = 0,
\end{aligned} \tag{101}$$

and the solution in this case is $t = z = E$,

(ii)

$$\begin{aligned}
&t - E = 0,\\
&t^4z^2 + t^3(z+E)z^2 - t^2\left(z^2E^2 - z^3E\right)\\
&\quad - t\left(-z^4E - z^3E^2 + z^2E^3 + 2zE^4 + E^5\right)\\
&\quad - z^3E^3 = 0,
\end{aligned} \tag{102}$$

and substituting t by E we obtain

$$E^2(z-E)(z+E)^3 = 0 \tag{103}$$

from which we get that the solution is $t = z = E$,

(iii)

$$\begin{aligned}
&t^4z^2 + t^3(z+E)z^2 - t^2\left(z^3E + z^2E^2 - 2zE^3\right)\\
&\quad - t\left(z^4E + z^3E^2 + z^2E^3 - E^5\right) - z^3E^3 = 0,\\
&z - E = 0,
\end{aligned} \tag{104}$$

i.e.,

$$E^2(t-E)(t+E)^3 = 0, \tag{105}$$

and the solution is $t = z = E$,

(iv)

$$\begin{aligned}
&t^4z^2 + t^3(z+E)z^2 - t^2\left(z^3E + z^2E^2 - 2zE^3\right)\\
&\quad - t\left(z^4E + z^3E^2 + z^2E^3 - E^5\right) - z^3E^3 = 0,\\
&t^4z^2 + t^3(z+E)z^2 - t^2\left(z^2E^2 - z^3E\right)\\
&\quad - t\left(-z^4E - z^3E^2 + z^2E^3 + 2zE^4 + E^5\right)\\
&\quad - z^3E^3 = 0.
\end{aligned} \tag{106}$$

By subtracting we get

$$-2tE(z-E)(z+E)\left(zE + E^2 + tz + z^2\right) = 0, \tag{107}$$

i.e.,

$$z = E. \tag{108}$$

Hence, the solution is $t = z = E$.

This means that (E, E) is a solution of system (73) and that Equation (61) does not possess a minimal period-four solution.

Thus, if $F = F_g < F_0$, then Equation (61) does not possess a minimal period-four solution. Consequently if $F = F_g = F_0$, then Equation (61) has the minimal period-four solutions of the form (62). □

Theorem 11. *Assume that $F = F_g = (B/b)^3c < F_0$. Then, the unique equilibrium point $\overline{x} = B/b$ of Equation (61) is globally asymptotically stable. Also, every solution of Equation*

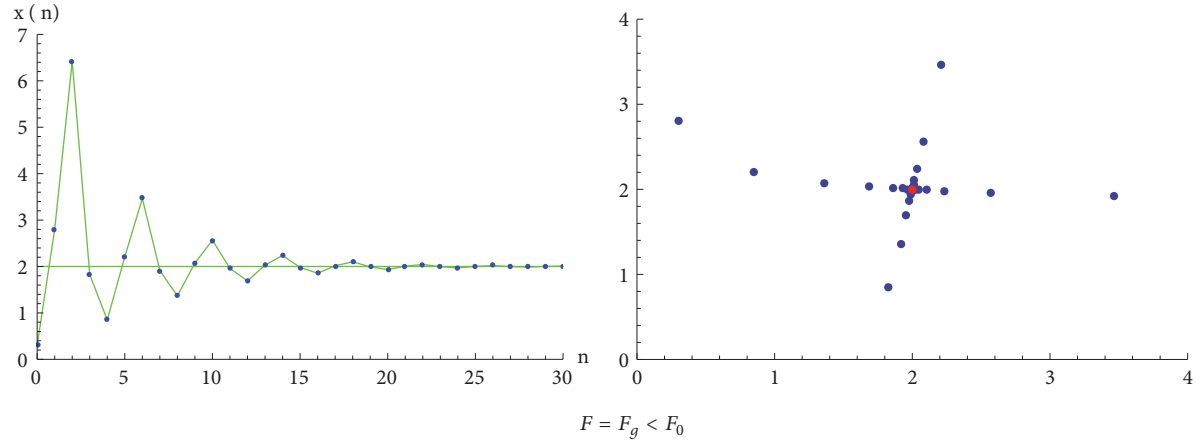

FIGURE 4: The orbit and the phase portrait for $b = 2$, $c = 1$, $B = 4$, $F = 8$, $F_g = 8$, $F_0 = 128$, and $(x_0, x_{-1}) = (0.3, 2.8)$ generated by Dynamica 4 [16].

(61) oscillates about the equilibrium point $\overline{x}$ with semicycles of length two.

Proof. Notice that

$$x_{n+1} - \frac{B}{b} = \frac{Bc\left(B + bx_{n-1}\right)}{b^2\left(bx_n + cx_{n-1}\right)x_{n-1}}\left(\frac{B}{b} - x_{n-1}\right), \tag{109}$$

i.e., x_{n+1} and x_{n-1} are from the different sides of the equilibrium point (see also Lemma 9, when $\sqrt{bF/Bc} = B/b$). Also, that means x_{n+1} and x_{n+5} are always from the same side of the equilibrium point $\overline{x} = B/b$. Since

$$\begin{aligned} x_{n+4} - x_n &= \frac{Bx_{n+3}x_{n+2} + \left(B^3/b^3\right)c}{bx_{n+3}x_{n+2} + c\left(x_{n+2}\right)^2} - x_n \\ &= \frac{H}{b^3\left(bx_{n+3}x_{n+2} + c\left(x_{n+2}\right)^2\right)}, \end{aligned} \tag{110}$$

where $H = B(b^3x_{n+3}x_{n+2} + B^2c) - b^3(bx_{n+3}x_{n+2} + c(x_{n+2})^2)x_n$ is a linear function in variable x_n, it can be seen that $H = 0 \Longleftrightarrow x_{n+4} = x_n = B/b$ because Equation (61) has no period-two solutions nor period-four solutions (and it holds that $x_n = B/b \Longrightarrow x_{n+2} = B/b \Longrightarrow x_{n+4} = B/b$, see Lemma 9). Also,

$$\begin{aligned} &x_n > \frac{B}{b} \Longrightarrow \\ &H < 0 \Longrightarrow \\ &x_n > x_{n+4} > \frac{B}{b}, \\ &\qquad n \in \mathbb{N}, \\ &x_n < \frac{B}{b} \Longrightarrow \\ &H > 0 \Longrightarrow \\ &x_n < x_{n+4} < \frac{B}{b}, \\ &\qquad n \in \mathbb{N}, \end{aligned} \tag{111}$$

which means that every sequence $\{x_{4k}\}_{k=1}^{\infty}$, $\{x_{4k+1}\}_{k=0}^{\infty}$, $\{x_{4k+2}\}_{k=0}^{\infty}$, $\{x_{4k+3}\}_{k=0}^{\infty}$ is monotone and bounded. That implies that each of the sequences is convergent. Since, by Lemmas 5 and 10, Equation (61) has neither minimal period-two nor period-four solutions, it holds

$$\begin{aligned} \lim_{k\to\infty} x_{4k} &= \lim_{k\to\infty} x_{4k+1} = \lim_{k\to\infty} x_{4k+2} = \lim_{k\to\infty} x_{4k+3} \\ &= \overline{x}, \end{aligned} \tag{112}$$

which implies that equilibrium $\overline{x}$ is an attractor and by using Theorem 4, which completes the proof of the theorem. □

For some numerical values of parameters we give a visual evidence for Theorem 11. See Figure 4.

Remark 12. One can see from Theorems 6, 8, and 11 that the equilibrium point $\overline{x}$ is globally asymptotically stable for all values of parameter F such that $0 < F \leq F_d$, where $F_g < F_0$, i.e., $c < b$ (see Figure 5(a)) and for all values of parameter F such that $0 < F < F_g = F_0 = F_d$, i.e., $c = b$ (see Figure 5(b)).

(d) $F = F_g = F_0$. Since $F_g = F_0$ implies $c = b$, Equation (61) is of the form

$$x_{n+1} = \frac{B}{b^3}\frac{b^2x_nx_{n-1} + B^2}{x_n\left(x_n + x_{n-1}\right)}. \tag{113}$$

In this case, by using Lemma 10, we see that Equation (61) has minimal period-four solutions of the form (62). Based on our many numerical simulations and the proof of Theorem 11, we believe that the following conjectures are true.

Conjecture 13. *If $F = F_g = F_0$ (that is $b = c$), then every solution of Equation (61) converges to some period-four solution of the form (62) or to the equilibrium point $\overline{x}$.*

For some numerical values of parameters we give a visual evidence for this case. See Figures 6 and 7.

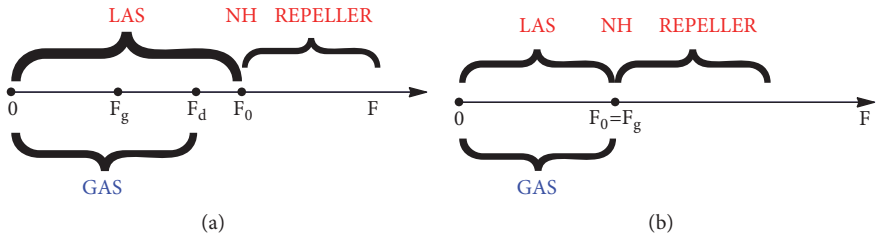

FIGURE 5: Visual representation of local and global asymptotic stability of Equation (1) when (a) $F_g < F_d < F_0$, i.e., $c < b$, and (b) $F_0 = F_g$, i.e., $c = b$.

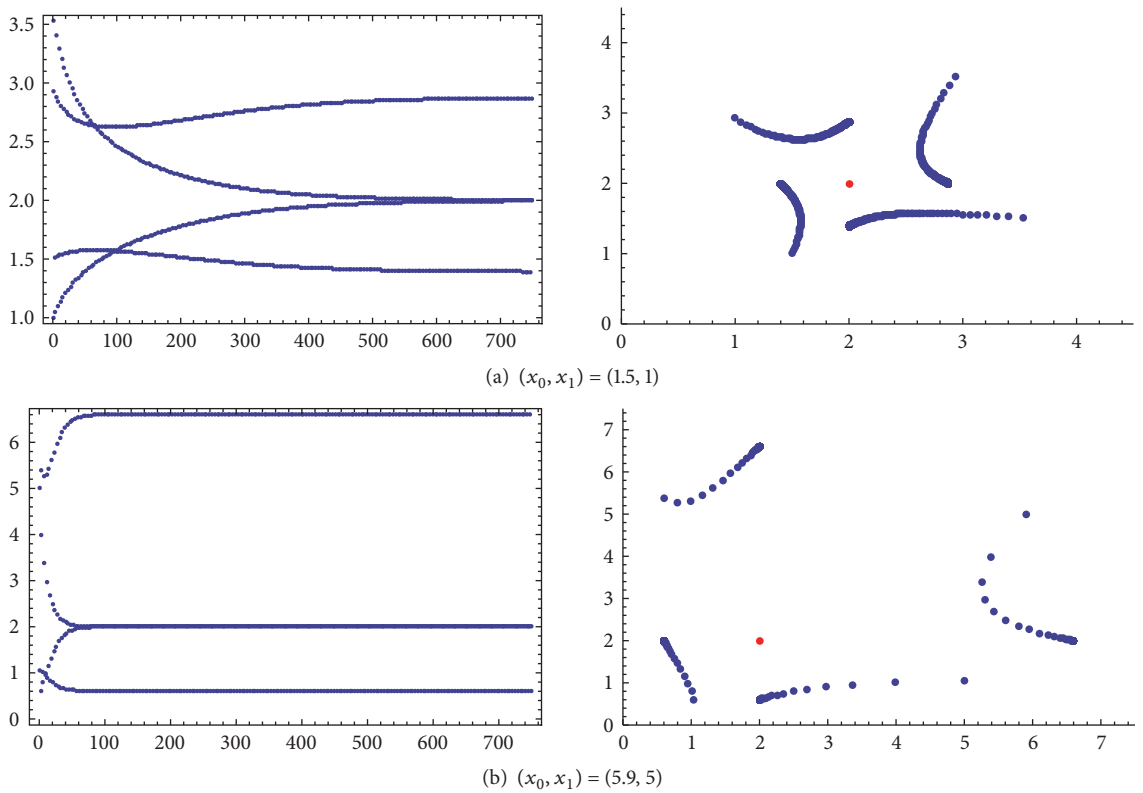

FIGURE 6: The orbit and phase portraits for $b = 1$, $c = 1$, $B = 2$, and $F = F_g = F_0 = 8$ generated by Dynamica 4 [16].

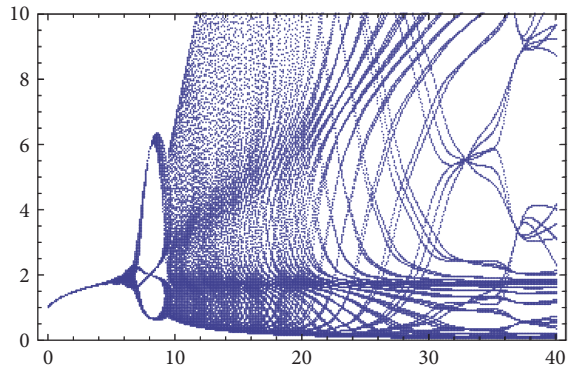

FIGURE 7: Bifurcation diagram in (F, x) plane for $b = 1$, $c = 1$, and $B = 2$, generated by Dynamica 4 [16].

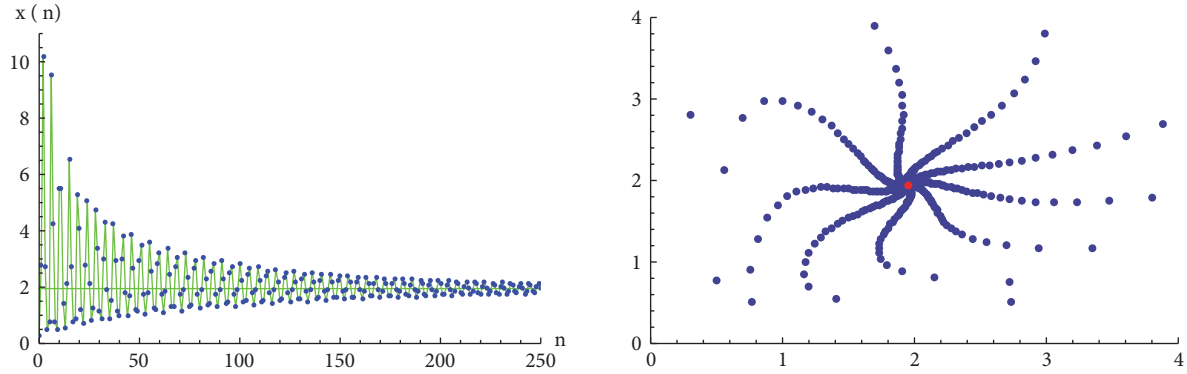

FIGURE 8: The orbit and phase portrait for $c = 2, b = 1, B = 4, F = 7, F_0 = 8, F_g = 128$, and $(x_0, x_{-1}) = (0.3, 2.8)$ generated by *Dynamica* 4 [16].

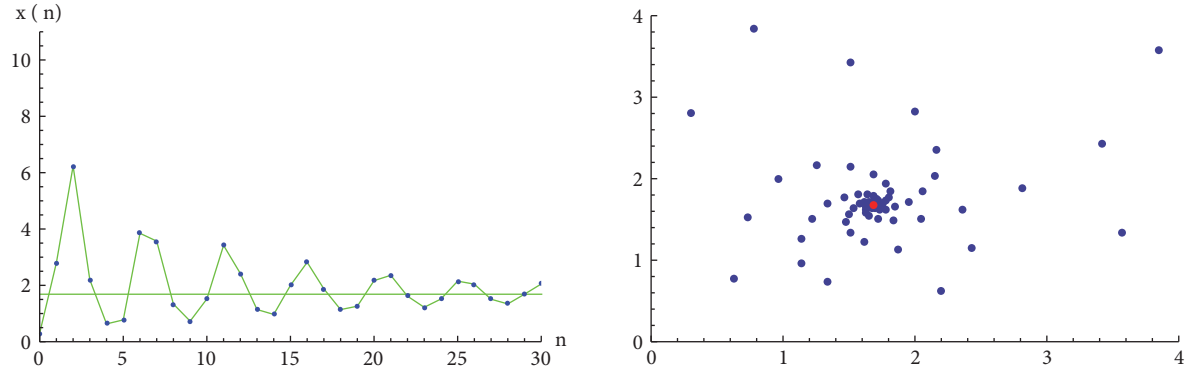

FIGURE 9: The orbit and phase portrait for $c = 2, b = 1, B = 4, F = 3, F_0 = 8, F_g = 128$, and $(x_0, x_{-1}) = (0.3, 2.8)$ generated by *Dynamica* 4 [16].

Case 2 ($F < F_0 < F_g$). We give a visual evidence for some numerical values of parameters which indicates very interesting behaviour and verifies our suspicion that the equilibrium point $\overline{x}$ is globally asymptotically stable in this case also. See Figures 8 and 9.

Conjecture 14. *If $F < F_0 < F_g$ (that is, $b < c$), then the equilibrium point $\overline{x}$ of Equation (1) is globally asymptotically stable.*

4. Naimark-Sacker Bifurcation for $b \neq c$

In this section, we consider bifurcation of a fixed point of map associated with Equation (1) in the case where the eigenvalues are complex conjugates and of unit module. We use the following standard version of the Naimark-Sacker result, see [28, 29]

Theorem 15 (Naimark-Sacker or Poincare-Andronov-Hopf Bifurcation for maps). *Let*

$$F : \mathbb{R} \times \mathbb{R}^2 \longrightarrow \mathbb{R}^2; \quad (\lambda, x) \longrightarrow F(\lambda, x) \tag{114}$$

be a C^4 map depending on real parameter λ satisfying the following conditions:

(i) $F(\lambda, 0) = 0$ *for λ near some fixed λ_0;*

(ii) $DF(\lambda, 0)$ *has two nonreal eigenvalues $\mu(\lambda)$ and $\overline{\mu(\lambda)}$ for λ near λ_0 with $|\mu(\lambda_0)| = 1$;*

(iii) $(d/d\lambda)|\mu(\lambda)| = d(\lambda_0) \neq 0$ *at $\lambda = \lambda_0$;*

(iv) $\mu^k(\lambda_0) \neq 1$ *for $k = 1, 2, 3, 4$.*

Then there is a smooth λ-dependent change of coordinate bringing F into the form

$$F(\lambda, x) = \mathscr{F}(\lambda, x) + O\left(\|x\|^5\right) \tag{115}$$

and there are smooth function $a(\lambda), b(\lambda)$, and $\omega(\lambda)$ so that in polar coordinates the function $\mathscr{F}(\lambda, x)$ is given by

$$\mathscr{F} : \begin{pmatrix} r \\ \theta \end{pmatrix} \longrightarrow \begin{pmatrix} |\mu(\lambda)| r - a(\lambda) r^3 \\ \theta + \omega(\lambda) + b(\lambda) r^2 \end{pmatrix}. \tag{116}$$

If $a(\lambda_0) > 0$, then there is a neighborhood U of the origin and a $\delta > 0$ such that for $|\lambda - \lambda_0| < \delta$ and $x_0 \in U$, then ω-limit set of x_0 is the origin if $\lambda < \lambda_0$ and belongs to a closed invariant C^1 curve $\Gamma(\lambda)$ encircling the origin if $\lambda > \lambda_0$. Furthermore, $\Gamma(\lambda_0) = 0$.

If $a(\lambda_0) < 0$, then there is a neighborhood U of the origin and a $\delta > 0$ such that for $|\lambda - \lambda_0| < \delta$ and $x_0 \in U$, then α-limit set of x_0 is the origin if $\lambda > \lambda_0$ and belongs to a closed invariant

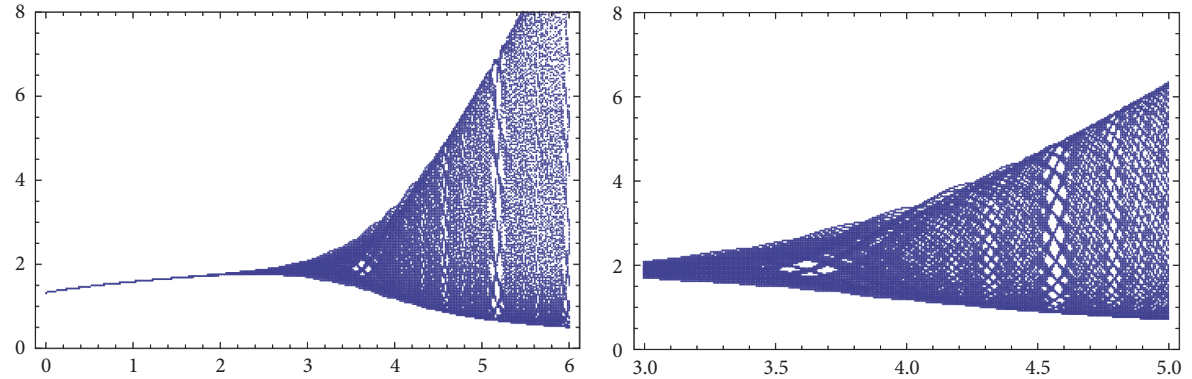

FIGURE 10: Bifurcation diagrams in (F, x) plane for $b = 0.5$, $c = 1$, and $B = 2$, generated by Dynamica 4 [16].

C^1 *curve* $\Gamma(\lambda)$ *encircling the origin if* $\lambda < \lambda_0$. *Furthermore,* $\Gamma(\lambda_0) = 0$.

Consider a general map $F(\lambda, x)$ that has a fixed point at the origin with complex eigenvalues $\mu(\lambda) = \alpha(\lambda) + i\beta(\lambda)$ and $\overline{\mu(\lambda)} = \alpha(\lambda) - i\beta(\lambda)$ satisfying $(\alpha(\lambda))^2 + (\beta(\lambda))^2 = 1$ and $\beta(\lambda) \neq 0$. By putting the linear part of such a map into Jordan Canonical form, we may assume F to have the following form near the origin:

$$F(\lambda, x) = \begin{pmatrix} \alpha(\lambda) & -\beta(\lambda) \\ \beta(\lambda) & \alpha(\lambda) \end{pmatrix} \begin{pmatrix} x_1 \\ x_2 \end{pmatrix} + \begin{pmatrix} g_1(\lambda, x_1, x_2) \\ g_2(\lambda, x_1, x_2) \end{pmatrix}. \tag{117}$$

Then the coefficient $a(\lambda_0)$ of the cubic term in Equation (116) in polar coordinate is equal to

$$a(\lambda_0) = \operatorname{Re}\left(\frac{(1 - 2\mu(\lambda_0))\overline{\mu(\lambda_0)}^2}{1 - \mu(\lambda_0)} \xi_{11}\xi_{20} \right) + \frac{1}{2}|\xi_{11}|^2 + |\xi_{02}|^2 - \operatorname{Re}\left(\overline{\mu(\lambda_0)}\xi_{21}\right), \tag{118}$$

where

$$\xi_{20} = \frac{1}{8}\left(\frac{\partial^2 g_1(0,0)}{\partial x_1^2} - \frac{\partial^2 g_1(0,0)}{\partial x_2^2} + 2\frac{\partial^2 g_2(0,0)}{\partial x_1 \partial x_2} + i\left(\frac{\partial^2 g_2(0,0)}{\partial x_1^2} - \frac{\partial^2 g_2(0,0)}{\partial x_2^2} - 2\frac{\partial^2 g_1(0,0)}{\partial x_1 \partial x_2} \right) \right), \tag{119}$$

$$\xi_{11} = \frac{1}{4}\left(\frac{\partial^2 g_1(0,0)}{\partial x_1^2} + \frac{\partial^2 g_1(0,0)}{\partial x_2^2} + i\left(\frac{\partial^2 g_2(0,0)}{\partial x_1^2} + \frac{\partial^2 g_2(0,0)}{\partial x_2^2} \right) \right), \tag{120}$$

$$\xi_{02} = \frac{1}{8}\left(\frac{\partial^2 g_1(0,0)}{\partial x_1^2} - \frac{\partial^2 g_1(0,0)}{\partial x_2^2} - 2\frac{\partial^2 g_2(0,0)}{\partial x_1 \partial x_2} + i\left(\frac{\partial^2 g_2(0,0)}{\partial x_1^2} - \frac{\partial^2 g_2(0,0)}{\partial x_2^2} + 2\frac{\partial^2 g_1(0,0)}{\partial x_1 \partial x_2} \right) \right), \tag{121}$$

and

$$\xi_{21} = \frac{1}{16}\left(\frac{\partial^3 g_1}{\partial x_1^3} + \frac{\partial^3 g_1}{\partial x_1 \partial x_2^2} + \frac{\partial^3 g_2}{\partial x_1^2 \partial x_2} + \frac{\partial^3 g_2}{\partial x_2^3} + i\left(\frac{\partial^3 g_2}{\partial x_1^3} + \frac{\partial^3 g_2}{\partial x_1 \partial x_2^2} - \frac{\partial^3 g_1}{\partial x_1^2 \partial x_2} - \frac{\partial^3 g_1}{\partial x_2^3} \right) \right). \tag{122}$$

Theorem 16. *Assume that* $b, c, B > 0$, $F_0 = (B/c)^3 b$, *and* $\overline{x} = B/c$.

(i) *If* $k_2 c < b < c$ *or* $c < b < k_3 c$, *where* k_2 *and* k_3 *are positive solutions of the equation* $3k^3 - 9k^2 - 3k + 1 = 0$, *then there is a neighborhood* U *of the equilibrium point* $\overline{x}$ *and* $\rho > 0$ *such that for* $|F - F_0| < \rho$ *and* $x_0, x_{-1} \in U$ *then* ω*-limit set of solution of Equation (1), with initial condition* x_0, x_{-1} *is the equilibrium point* $\overline{x}$ *if* $F < F_0$ *and belongs to a closed invariant* C^1 *curve* $\Gamma(F_0)$ *encircling the equilibrium point* $\overline{x}$ *if* $F > F_0$. *Furthermore,* $\Gamma(F_0) = 0$.

(ii) *If* $0 < b < k_2 c$ *or* $k_3 c < b < +\infty$, *then there is a neighborhood* U *of the equilibrium point* $\overline{x}$ *and a* $\rho > 0$ *such that for* $|F - F_0| < \rho$ *and* $x_0, x_{-1} \in U$ *then* α*-limit set of* x_0, x_{-1} *is the equilibrium point* $\overline{x}$ *if* $F > F_0$ *and belongs to a closed invariant* C^1 *curve* $\Gamma(F_0)$ *encircling the equilibrium point* $\overline{x}$ *if* $F < F_0$. *Furthermore,* $\Gamma(F_0) = 0$.

Proof. See Figures 10 and 11 for visual illustration. In order to apply Theorem 15 we make a change of variable

$$\begin{aligned} &y_n = x_n - \overline{x} \Longrightarrow \\ &x_n = y_n + \overline{x}, \\ &y_{n+1} = \frac{B(y_n + \overline{x})(y_{n-1} + \overline{x}) + F}{b(y_n + \overline{x})(y_{n-1} + \overline{x}) + c(y_{n-1} + \overline{x})^2} - \overline{x}. \end{aligned} \tag{123}$$

Set

$$\begin{aligned} u_n &= y_{n-1} \\ \text{and } v_n &= y_n \\ &\text{for } n = 0, 1, \ldots, \end{aligned} \tag{124}$$

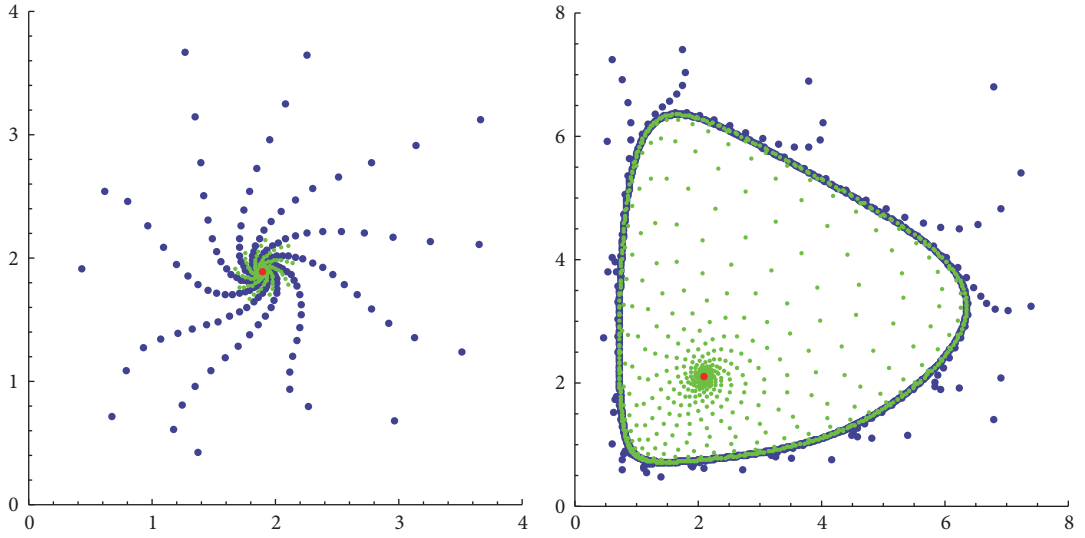

(a) $F = 3 < F_0$ (b) $F = 5 > F_0$

FIGURE 11: Phase portraits when $c = 1, b = 0.5, B = 2$, $x_{-1} = x_0 = 2.1$ (green), and $x_{-1} = x_0 = 6.8$ (blue), generated by *Dynamica* 4 [16].

then

$$u_{n+1} = v_n,$$
$$v_{n+1} = \frac{B\left(v_n + \overline{x}\right)\left(u_n + \overline{x}\right) + F}{b\left(v_n + \overline{x}\right)\left(u_n + \overline{x}\right) + c\left(u_n + \overline{x}\right)^2} - \overline{x}. \tag{125}$$

Let us define the function

$$K\begin{pmatrix} u \\ v \end{pmatrix} = \begin{pmatrix} v \\ \dfrac{B\left(v + \overline{x}\right)\left(u + \overline{x}\right) + F}{b\left(v + \overline{x}\right)\left(u + \overline{x}\right) + c\left(u + \overline{x}\right)^2} - \overline{x} \end{pmatrix}. \tag{126}$$

Then $K(u, v)$ has the unique fixed point $(0, 0)$. The Jacobian matrix of $K(u, v)$ is given by

$$J_K\begin{pmatrix} u \\ v \end{pmatrix} = \begin{pmatrix} 0 & 1 \\ -\dfrac{bF\left(v + \overline{x}\right) + c\left(u + \overline{x}\right)\left(2F + B\left(u + \overline{x}\right)\left(v + \overline{x}\right)\right)}{\left(u + \overline{x}\right)^2\left(c\left(u + \overline{x}\right) + b\left(v + \overline{x}\right)\right)^2} & \dfrac{-bF + Bc\left(u + \overline{x}\right)^2}{\left(u + \overline{x}\right)\left(c\left(u + \overline{x}\right) + b\left(v + \overline{x}\right)\right)^2} \end{pmatrix} \tag{127}$$

and its value at the zero equilibrium is

$$J_0 = J_K\begin{pmatrix} 0 \\ 0 \end{pmatrix} = \begin{pmatrix} 0 & 1 \\ -\dfrac{bF + 2cF + Bc\overline{x}^2}{\overline{x}^3\left(b + c\right)^2} & \dfrac{-bF + Bc\overline{x}^2}{\overline{x}^3\left(b + c\right)^2} \end{pmatrix}, \tag{128}$$

i.e.,

$$J_0 = J_K\begin{pmatrix} 0 \\ 0 \end{pmatrix} = \begin{pmatrix} 0 & 1 \\ -\dfrac{c}{b + c} - \dfrac{F}{\overline{x}^3\left(b + c\right)} & \dfrac{c}{b + c} - \dfrac{F}{\overline{x}^3\left(b + c\right)} \end{pmatrix}. \tag{129}$$

The eigenvalues $\mu(F)$, $\overline{\mu(F)}$, using (128), are

$$\mu\left(F\right) = \frac{-bF + Bc\overline{x}^2 \pm i\sqrt{4\left(b + c\right)^2\overline{x}^3\left(bF + 2cF + Bc\overline{x}^2\right) - \left(bF - Bc\overline{x}^2\right)^2}}{2\left(b + c\right)^2\overline{x}^3} \tag{130}$$

because

$$\begin{aligned}&\left(bF - Bc\overline{x}^2\right)^2 - 4(b+c)^2\overline{x}^3\left(bF + 2cF + Bc\overline{x}^2\right)\\&= \left(bF - Bc\overline{x}^2\right)^2 - 4(b+c)\left(B\overline{x}^2 + F\right)\left(bF + 2cF\right.\\&\left.+ Bc\overline{x}^2\right) = -\left(8F^2c + 3F^2b^2 + 3B^2c^2x^4 + 12F^2bc\right.\\&\left.+ 4BFb^2x^2 + 12BFc^2x^2 + 4B^2bcx^4 + 18BFbcx^2\right)^2\\&< 0.\end{aligned} \tag{131}$$

Then

$$\begin{aligned}&K\begin{pmatrix}u\\v\end{pmatrix}\\&= \begin{pmatrix}0 & 1\\ -\dfrac{c}{b+c} - \dfrac{F}{\overline{x}^3(b+c)} & \dfrac{c}{b+c} - \dfrac{F}{\overline{x}^3(b+c)}\end{pmatrix}\begin{pmatrix}u\\v\end{pmatrix}\\&+ \begin{pmatrix}f_1(F,u,v)\\f_2(F,u,v)\end{pmatrix},\end{aligned} \tag{132}$$

where

$$\begin{aligned}&f_1(F,u,v) = 0,\\&f_2(F,u,v) = \frac{B(v+\overline{x})(u+\overline{x}) + F}{b(v+\overline{x})(u+\overline{x}) + c(u+\overline{x})^2}\\&\qquad + \frac{c\overline{x}^3 + F}{\overline{x}^3(b+c)}u + \frac{F - c\overline{x}^3}{\overline{x}^3(b+c)}v - \overline{x}.\end{aligned} \tag{133}$$

Denote $F_0 = (B/c)^3 b$. For $F = F_0$ we have $\overline{x} = \sqrt[3]{F_0/b} = B/c$. The eigenvalues of J_0 are $\mu(F_0)$ and $\overline{\mu(F_0)}$ where

$$\begin{aligned}&\mu(F_0) = \frac{c - b + i\sqrt{(b+3c)(3b+c)}}{2(b+c)}\\&\text{and } \left|\mu(F_0)\right| = 1.\end{aligned} \tag{134}$$

The eigenvectors corresponding to $\mu(F_0)$ and $\overline{\mu(F_0)}$ are $v(F_0)$ and $\overline{v(F_0)}$ where

$$v(F_0) = \left(\frac{c - b + i\sqrt{(b+3c)(3b+c)}}{2(b+c)}, 1\right). \tag{135}$$

Further,

$$\begin{aligned}&\left|\mu(F_0)\right| = 1,\\&\mu^2(F_0)\\&\quad = -\frac{c^2 + 6bc + b^2}{2(b+c)^2} - i\frac{(c-b)\sqrt{(b+3c)(3b+c)}}{2(b+c)^2},\\&\mu^3(F_0)\\&\quad = \frac{(b-c)\left(b^2 + 4bc + c^2\right)}{(b+c)^3}\\&\qquad + i\frac{2bc\sqrt{(b+3c)(3b+c)}}{(b+c)^3},\\&\mu^4(F_0)\\&\quad = -\frac{b^4 - 4bc^3 - 4b^3c - 26b^2c^2 + c^4}{2(b+c)^4}\\&\qquad - i\frac{(b-c)\left(b^2 + 6bc + c^2\right)\sqrt{(b+3c)(3b+c)}}{2(b+c)^4},\end{aligned} \tag{136}$$

and $\mu^k(F_0) \neq 1$ for $k = 1, 2, 3, 4$ for $c > 0$, $b > 0$, and $b \neq c$. For $F = F_0$ and $\overline{x} = B/c$

$$K\begin{pmatrix}u\\v\end{pmatrix} = \begin{pmatrix}0 & 1\\ -1 & -\dfrac{b-c}{b+c}\end{pmatrix}\begin{pmatrix}u\\v\end{pmatrix} + \begin{pmatrix}h_1(u,v)\\h_2(u,v)\end{pmatrix}, \tag{137}$$

and

$$\begin{aligned}&h_1(u,v) = f_1(F_0,u,v) = 0,\\&h_2(u,v) = f_2(F_0,u,v)\\&\qquad = \frac{B\left(B^2b + B^2c + Bc^2u + Bc^2v + c^3uv\right)}{c(B+cu)\left(c^2u + Bb + Bc + bcv\right)} + u\\&\qquad + \frac{b-c}{b+c}v - \frac{B}{c}.\end{aligned} \tag{138}$$

Hence, for $F = F_0$ system (125) is equivalent to

$$\begin{pmatrix}u_{n+1}\\v_{n+1}\end{pmatrix} = \begin{pmatrix}0 & 1\\ -1 & -\dfrac{b-c}{b+c}\end{pmatrix}\begin{pmatrix}u_n\\v_n\end{pmatrix} + \begin{pmatrix}h_1(u_n,v_n)\\h_2(u_n,v_n)\end{pmatrix}. \tag{139}$$

Let $\begin{pmatrix}u_n\\v_n\end{pmatrix} = P\begin{pmatrix}\xi_n\\\eta_n\end{pmatrix}$, where

$$\begin{aligned}&P = \begin{pmatrix}\dfrac{c-b}{2(b+c)} & \dfrac{\sqrt{(b+3c)(3b+c)}}{2(b+c)}\\1 & 0\end{pmatrix},\\&P^{-1}\\&\quad = \begin{pmatrix}0 & 1\\ \dfrac{2(b+c)}{\sqrt{(b+3c)(3b+c)}} & -\dfrac{c-b}{\sqrt{(b+3c)(3b+c)}}\end{pmatrix}.\end{aligned} \tag{140}$$

Then system (125) is equivalent to its normal form

$$\begin{pmatrix}\xi_{n+1}\\ \eta_{n+1}\end{pmatrix} = \begin{pmatrix} \frac{c-b}{2(b+c)} & -\frac{\sqrt{(b+3c)(3b+c)}}{2(b+c)} \\ \frac{\sqrt{(b+3c)(3b+c)}}{2(b+c)} & \frac{c-b}{2(b+c)} \end{pmatrix}\begin{pmatrix}\xi_n\\ \eta_n\end{pmatrix} + P^{-1}H\left(P\begin{pmatrix}\xi_n\\ \eta_n\end{pmatrix}\right) \quad (141)$$

where

$$H\begin{pmatrix}u\\ v\end{pmatrix} := \begin{pmatrix}h_1(u,v)\\ h_2(u,v)\end{pmatrix}. \quad (142)$$

Let

$$G\begin{pmatrix}u\\ v\end{pmatrix} = \begin{pmatrix}g_1(u,v)\\ g_2(u,v)\end{pmatrix} = P^{-1}H\left(P\begin{pmatrix}u\\ v\end{pmatrix}\right). \quad (143)$$

By the straightforward calculation we obtain that

$$g_1(u,v) = -\frac{B}{c} + \frac{b-c}{b+c}u + \frac{(c-b)u + \sqrt{(b+3c)(3b+c)}v}{2(b+c)} + \Omega(u,v), \quad (144)$$

where

$$\begin{aligned}\Omega(u,v) &= \frac{2B(b+c)\kappa_1}{c\kappa_2\kappa_3},\\ \kappa_1 &= 2B^2b^2 + 2B^2c^2 + c^4u^2 + 4B^2bc + 3Bc^3u - bc^3u^2 + Bc^2v\sqrt{(b+3c)(3b+c)} + c^3uv\sqrt{(b+3c)(3b+c)} + Bbc^2u,\\ \kappa_2 &= c^2u + 2Bb + 2Bc + cv\sqrt{(b+3c)(3b+c)} - bcu,\\ \kappa_3 &= 2Bb^2 + 2Bc^2 + c^3u + c^2v\sqrt{(b+3c)(3b+c)} + bc^2u + 2b^2cu + 4Bbc,\end{aligned} \quad (145)$$

and

$$g_2(u,v) = \frac{b-c}{\sqrt{(b+3c)(3b+c)}}g_1(u,v). \quad (146)$$

Further,

$$\begin{aligned}\frac{\partial^2 g_1(0,0)}{\partial u^2} &= \frac{c(b-c)\left(3b^2+c^2\right)}{2B(b+c)^3},\\ \frac{\partial^2 g_1(0,0)}{\partial u\partial v} &= \frac{bc^2\sqrt{(b+3c)(3b+c)}}{B(b+c)^3},\\ \frac{\partial^2 g_1(0,0)}{\partial v^2} &= \frac{c(3b+c)(b+3c)}{2B(b+c)^2},\\ \frac{\partial^3 g_1(0,0)}{\partial u^3} &= -\frac{3c^2(b-c)\left(5b^4+4b^3c+6b^2c^2+c^4\right)}{4B^2(b+c)^5},\\ \frac{\partial^3 g_1(0,0)}{\partial u^2\partial v} &= \frac{c^2\left(-3b^4-8b^3c+2b^2c^2-8bc^3+c^4\right)\sqrt{(b+3c)(3b+c)}}{4B^2(b+c)^5},\\ \frac{\partial^3 g_1(0,0)}{\partial u\partial v^2} &= -\frac{c^2(3b+c)(b+3c)\left(-b^3+3b^2c+9bc^2+c^3\right)}{4B^2(b+c)^5},\\ \frac{\partial^3 g_1(0,0)}{\partial v^3} &= -\frac{3c^2(3b+c)(b+3c)\sqrt{(b+3c)(3b+c)}}{4B^2(b+c)^3}.\end{aligned} \quad (147)$$

Now, by using (118), (119), (120), (121), and (122) we obtain

$$\xi_{11} = \frac{c\left(7bc^2+5b^2c+3b^3+c^3\right)}{4B(b+c)^3}\left(1 + i\frac{b-c}{\sqrt{(b+3c)(3b+c)}}\right),$$

$$\xi_{20} = -\frac{c^2}{4B(b+c)^2}\left(3b+c+i\frac{7b^2+2bc-c^2}{\sqrt{(b+3c)(3b+c)}}\right),$$

$$\xi_{02} = \frac{c^2}{4B(b+c)^3}\left(-\left(5b^2+2bc+c^2\right) + i\frac{-b^3+11b^2c+5bc^2+c^3}{\sqrt{(b+3c)(3b+c)}}\right),$$

$$\xi_{21} = \frac{c^2}{8B^2(b+c)^4}\left(-\left(3b^4+2b^3c+8b^2c^2-c^4\right) + i\frac{3b^5+35b^4c+60b^3c^2+74b^2c^3+33bc^4+3c^5}{\sqrt{(b+3c)(3b+c)}}\right),$$

$$\frac{\left(1-2\mu\left(F_0\right)\right)\overline{\mu\left(F_0\right)}^2}{1-\mu\left(F_0\right)} = -\frac{8bc+b^2+3c^2}{2\left(b+c\right)^2} + i\sqrt{10bc+3b^2+3c^2}\,\frac{5b^2-c^2}{2\left(3b+c\right)\left(b+c\right)^2},$$

$$\xi_{11}\xi_{20} = -\frac{c^3\left(3b^3+5b^2c+7bc^2+c^3\right)}{16B^2\left(b+c\right)^5}\left(\frac{2\left(b^3+19b^2c+11bc^2+c^3\right)}{3b^2+10bc+3c^2} + i\frac{2\left(5b^2-c^2\right)}{\sqrt{3b^2+10bc+3c^2}}\right),$$

$$\operatorname{Re}\left(\frac{\left(1-2\mu\left(F_0\right)\right)\overline{\mu\left(F_0\right)}^2}{1-\mu\left(F_0\right)}\xi_{11}\xi_{20}\right) = \frac{c^3\left(13b^2+12bc+3c^2\right)\left(3b^3+5b^2c+7bc^2+c^3\right)}{8B^2\left(b+c\right)^4\left(3b+c\right)\left(b+3c\right)},$$

$$\frac{1}{2}\left|\xi_{11}\right|^2 = \frac{c^2\left(3b^3+5b^2c+7bc^2+c^3\right)^2}{8B^2\left(b+c\right)^4\left(3b+c\right)\left(b+3c\right)},$$

$$\left|\xi_{02}\right|^2 = \frac{19b^3c^4+15b^2c^5+5bc^6+c^7}{4B^2\left(3b+c\right)\left(b+3c\right)\left(b+c\right)^3},$$

$$\operatorname{Re}\left(\overline{\mu\left(F_0\right)}\xi_{21}\right) = \frac{c^2\left(3b^4+14b^3c+19b^2c^2+14bc^3+2c^4\right)}{8B^2\left(b+c\right)^4} \tag{148}$$

and finally,

$$a\left(F_0\right) = -\frac{bc^3\left(3b^3-9b^2c-3bc^2+c^3\right)}{8B^2\left(b+c\right)^4\left(3b+c\right)}. \tag{149}$$

If we substitute b with kc we obtain

$$\begin{aligned} &3b^3-9b^2c-3bc^2+c^3 \\ &\quad = 3\left(kc\right)^3-9\left(kc\right)^2c-3\left(kc\right)c^2+c^3 \\ &\quad = c^3\left(3k^3-9k^2-3k+1\right). \end{aligned} \tag{150}$$

So,

$$\begin{aligned} &a\left(F_0\right)=0 \Longleftrightarrow \\ &3k^3-9k^2-3k+1=0. \end{aligned} \tag{151}$$

Solutions, determined numerically, are $k_1 \approx -0.48445$, $k_2 \approx 0.21014$, and $k_3 \approx 3.2743$. Since $b > 0$ and $c > 0$ it must be $k > 0$. Now,

$$\begin{aligned} &a\left(F_0\right) > 0 \quad \text{for } b = kc,\ k \in \left(k_2, 1\right) \cup \left(1, k_3\right), \\ &a\left(F_0\right) < 0 \quad \text{for } b = kc,\ k \in \left(0, k_2\right) \cup \left(k_3, +\infty\right). \end{aligned} \tag{152}$$

Further,

$$\mu\left(F\right) = \frac{-bF+Bc\overline{x}^2 \pm i\sqrt{4\left(b+c\right)^2\overline{x}^3\left(bF+2cF+Bc\overline{x}^2\right)-\left(bF-Bc\overline{x}^2\right)^2}}{2\left(b+c\right)^2\overline{x}^3} \tag{153}$$

and $\mu(F)\overline{\mu(F)} = (bF + 2cF + Bcx^2)/(b + c)^2x^3$, i.e., $|\mu(F)| = \sqrt{(bF + 2cF + Bcx^2)/(b + c)^2x^3}$. By differentiating the equilibrium equation

$$\left(b+c\right)x^3 - Bx^2 - F = 0 \tag{154}$$

with respect to F and solving for $x'(F)$ we obtain $x'(F) = 1/(3(b + c)x^2 - 2Bx)$, i.e., $x(F_0) = \sqrt[3]{F_0/b} = B/c$.

$$x'\left(F_0\right) = \frac{1}{3\left(b+c\right)\left(B/c\right)^2-2B\left(B/c\right)} = \frac{c^2}{B^2\left(3b+c\right)}. \tag{155}$$

Now,

$$\begin{aligned} &\frac{d\left|\mu\left(F\right)\right|}{dF} \\ &\quad = \frac{1}{2\sqrt{\left(bF+2cF+Bcx^2\right)/\left(b+c\right)^2x^3}}\left(\frac{b+2c+2Bcxx'}{\left(b+c\right)^2x^3}\right. \\ &\quad \left. -\frac{3\left(bF+2cF+Bcx^2\right)x'}{\left(b+c\right)^2x^4}\right). \end{aligned} \tag{156}$$

By substituting $x'(F)$ in the above expression and considering the fact that $|\mu(F_0)| = 1$, we obtain

$$\frac{d\left|\mu\left(F\right)\right|}{dF}\left(F_0\right) = \frac{1}{2}\left(\frac{b+2c+2Bc\left(B/c\right)\left(c^2/\left(B^2\left(3b+c\right)\right)\right)}{\left(b+c\right)^2\left(B/c\right)^3} - \frac{3\left(c^2/\left(B^2\left(3b+c\right)\right)\right)}{B/c}\right), \tag{157}$$

i.e.,

$$\frac{d\left|\mu\left(F\right)\right|}{dF}\left(F_0\right) = \frac{c^4}{2B^3\left(b+c\right)\left(3b+c\right)} > 0 \tag{158}$$

and that completes the proof of the theorem. □

Data Availability

No data were used to support this study.

Conflicts of Interest

The authors declare that they have no conflicts of interest.

Authors' Contributions

The article is a joint work of all four authors who contributed equally to the final version of the paper. All authors read and approved the final manuscript.

Acknowledgments

This work is supported by the Fundamental Research Funds of Bosnia and Herzegovina $FMO01/2-3995-V/17$.

References

[1] M. Garić-Demirović, M. R. S. Kulenović, and M. Nurkanović, "Global dynamics of certain homogeneous second-order quadratic fractional difference equation," *The Scientific World Journal*, vol. 2013, Article ID 210846, 10 pages, 2013.

[2] M. Garić-Demirović, M. Nurkanović, and Z. Nurkanović, "Stability, periodicity and Neimark-Sacker bifurcation of certain homogeneous fractional difference equations," *International Journal of Difference Equations*, vol. 12, no. 1, pp. 27–53, 2017.

[3] S. Jašarević-Hrustic', Z. Nurkanović, M. R. S. Kulenović, and E. Pilav, "Birkhoff normal forms, KAM theory and symmetries for certain second order rational difference equation with quadratic term," *International Journal of Difference Equations*, vol. 10, no. 2, pp. 181–199, 2015.

[4] S. Jašarević Hrustić, M. R. Kulenović, and M. Nurkanović, "Local dynamics and global stability of certain second-order rational difference equation with quadratic terms," *Discrete Dynamics in Nature and Society*, vol. 2016, Article ID 3716042, 14 pages, 2016.

[5] S. Kalabušić, M. Nurkanović, and Z. Nurkanović, "Global Dynamics of Certain Mix Monotone Difference Equation," *Mathematics*, vol. 6, no. 1, p. 10, 2018.

[6] C. M. Kent and H. Sedaghat, "Global attractivity in a quadratic-linear rational difference equation with delay," *Journal of Difference Equations and Applications*, vol. 15, no. 10, pp. 913–925, 2009.

[7] C. M. Kent and H. Sedaghat, "Global attractivity in a rational delay difference equation with quadratic terms," *Journal of Difference Equations and Applications*, vol. 17, no. 4, pp. 457–466, 2011.

[8] M. R. Kulenović, S. Moranjkć, and Z. Nurkanović, "Naimark-Sacker bifurcation of second order rational difference equation with quadratic terms," *Journal of Nonlinear Sciences and Applications*, vol. 10, no. 7, pp. 3477–3489, 2017.

[9] M. R. S. Kulenović, S. Moranjkić, and Z. Nurkanović, "Global dynamics and bifurcation of perturbed Sigmoid Beverton_Holt difference equation," *Mathematical Methods in the Applied Sciences*, vol. 39, pp. 2696–2715, 2016.

[10] H. Sedaghat, "Global behaviours of rational difference equations of orders two and three with quadratic terms," *Journal of Difference Equations and Applications*, vol. 15, no. 3, pp. 215–224, 2009.

[11] H. Sedaghat, "Folding, cycles and chaos in planar systems," *Journal of Difference Equations and Applications*, vol. 21, no. 1, pp. 1–15, 2015.

[12] S. Moranjkić and Z. Nurkanović, "Local and global dynamics of certain second-order rational difference equations containing quadratic terms," *Advances in Dynamical Systems and Applications (ADSA)*, vol. 12, no. 2, pp. 123–157, 2017.

[13] G. G. Thomson, "A proposal for a treshold stock sizeand maximum fishing mortality rate," in *Risk Evaluation and Biological Reference Points for Fisheries Management. Canad. Spec. Publ. Fish.Aquat. Sci*, S. J. Smith, J. J. Hunt, and D. Rivard, Eds., vol. 120, pp. 303–320, NCR Research Press, Ottawa Canada, 1993.

[14] Y. Kostrov and Z. Kudlak, "On a second-order rational difference equation with a quadratic term," *International Journal of Difference Equations*, vol. 11, no. 2, pp. 179–202, 2016.

[15] V. L. Kocic and G. Ladas, "Global behavior of nonlinear difference equations of higher order with applications," in *Mathematics and Its Applications*, Kluwer Academic Publishers Group, Dordrecht, The Netherlands, 1993.

[16] M. R. Kulenović and O. Merino, *Discrete Dynamical Systems and Difference Equations with Mathematica*, Chapman and Hall/CRC Press, Boca Raton, Fla, USA, 2002.

[17] M. R. Kulenov and Z. Nurkanov, "Global behavior of a three-dimensional linear fractional system of difference equations," *Journal of Mathematical Analysis and Applications*, vol. 310, no. 2, pp. 673–689, 2005.

[18] G. Enciso, H. Smith, and E. Sontag, "Nonmonotone systems decomposable into monotone systems with negative feedback," *Journal of Differential Equations*, vol. 224, no. 1, pp. 205–227, 2006.

[19] M. R. S. Kulenović and G. Ladas, *Dynamics of Second Order Rational Difference Equations with Open Problems and Conjectures*, Chapman and Hall/CRC, Boca Raton, FL, USA, London, UK, 2001.

[20] M. R. S. Kulenović and O. Merino, "A global attractivity result for maps with invariant boxes," *Discrete and Continuous Dynamical Systems - Series B*, vol. 6, no. 1, pp. 97–110, 2006.

[21] A. M. Amleh, E. Camouzis, and G. Ladas, "On the dynamics of a rational difference equation, part I," *International Journal of Difference Equations*, vol. 3, no. 1, pp. 1–35, 2008.

[22] E. Camouzis and G. Ladas, "When does local asymptotic stability imply global attractivity in rational equations?" *Journal of Difference Equations and Applications*, vol. 12, no. 8, pp. 863–885, 2006.

[23] H. L. Smith, "Planar competitive and cooperative difference equations," *Journal of Difference Equations and Applications*, vol. 3, no. 5-6, pp. 335–357, 1998.

[24] M. Dehghan, C. M. Kent, R. Mazrooei-Sebdani, N. L. Ortiz, and H. Sedaghat, "Dynamics of rational difference equations containing quadratic terms," *Journal of Difference Equations and Applications*, vol. 14, no. 2, pp. 191–208, 2008.

[25] A. J. Harry, C. M. Kent, and V. L. Kocic, "Global behavior of solutions of a periodically forced Sigmoid Beverton-Holt model," *Journal of Biological Dynamics*, vol. 6, no. 2, pp. 212–234, 2012.

[26] N. Lazaryan and H. Sedaghat, "Periodic and chaotic orbits of a discrete rational system," *Discrete Dynamics in Nature and Society*, vol. 2015, Article ID 519598, 8 pages, 2015.

[27] J. M. Cushing, "Backward bifurcations and strong Allee effects in matrix models for the dynamics of structured populations," *Journal of Biological Dynamics*, vol. 8, no. 1, pp. 57–73, 2014.

[28] J. K. Hale and H. Kocek, "Dynamics and bifurcations," in *Texts in Applied Mathematics*, vol. 3, Springer-Verlag, New York, NY, USA, 1991.

[29] Y. A. Kuznetsov, *Elements of Applied Bifurcation Theory*, Springer, New York, NY, USA, 1998.

Hindawi
Discrete Dynamics in Nature and Society
Volume 2018, Article ID 3676083, 9 pages
https://doi.org/10.1155/2018/3676083

Research Article

Exponential Stability and Robust H_∞ Control for Discrete-Time Time-Delay Infinite Markov Jump Systems

Yueying Liu and Ting Hou

College of Mathematics and Systems Science, Shandong University of Science and Technology, Qingdao 266590, China

Correspondence should be addressed to Ting Hou; ht_math@sina.com

Received 4 August 2018; Revised 7 October 2018; Accepted 16 October 2018; Published 22 October 2018

Guest Editor: Abdul Qadeer Khan

In this paper, exponential stability and robust H_∞ control problem are investigated for a class of discrete-time time-delay stochastic systems with infinite Markov jump and multiplicative noises. The jumping parameters are modeled as an infinite-state Markov chain. By using a novel Lyapunov-Krasovskii functional, a new sufficient condition in terms of matrix inequalities is derived to guarantee the mean square exponential stability of the equilibrium point. Then some sufficient conditions for the existence of feedback controller are presented to guarantee that the resulting closed-loop system has mean square exponential stability for the zero exogenous disturbance and satisfies a prescribed H_∞ performance level. Numerical simulations are exploited to validate the applicability of developed theoretical results.

1. Introduction

During the past decades, Markov jump systems have been the subject of a great deal of research since they have been used extensively both in theory and in applications. Markov jump systems are hybrid dynamical systems composed of subsystems with the transitions determined by a Markov chain. A number of results that focused on Markov jump systems have been published ranging from filtering, stability, observability, and control to engineering application; see, for example, [1–15] and the references therein.

Note that most of the theoretical works related to Markov jump systems in the literatures concentrated on the case where the state space of the Markov chain is finite. However, it may be more appropriate to characterize abrupt changes in many real plants via an infinite-state Markov chain. As far as applications are concerned, infinite Markov jump systems are critical in some physics plants, such as solar thermal receiver, aircraft, and robotic manipulator systems. Theoretically, finite Markov jump systems are fundamentally different from those governed by infinite-state space. The work in [14] studied exponential almost sure stability of random jump systems. The work in [16] considered the definition and computation of an H_2-type norm for stochastic systems with infinite Markov jump and periodic coefficients. LQ-optimal control problem has been dealt with for discrete-time infinite Markov jump systems in [17]. The work in [18] demonstrated the inequivalence between stochastic stability and mean square exponential stability in discrete-time case. With this motivation, infinite Markov jump systems have stirred widespread research interests.

Time-delay is one of the inherent features of many practical systems and also is the big source of instability and poor performances in systems [19]. Moreover, stochastic modeling has had extensive applications. Hence, dynamical time-delay stochastic systems deserve our consideration. Stability analysis and controller design of time-delay Markov jump systems have been investigated by many authors [15, 20, 21]. Unfortunately, the literature about these issues for infinite Markov jump case is less developed. And, to the best of our knowledge, only a few results have been presented so far [18, 22, 23], let alone the problem involving time-delay. Actually, [18, 23] investigated the exponential stability and infinite horizon H_2/H_∞ control problem for discrete-time infinite Markov jump systems with multiplicative noises, respectively, but they neglected the effects of time-delay. Meanwhile, the authors in [22] considered time-delay, when discussing the stabilization problem for linear stochastic delay differential

equations with infinite Markovian switching, but it was hard for the obtained stability results to deal with control problem. As mentioned above, stability and control for time-delay stochastic systems with infinite Markov jump and multiplicative noises have not received enough attention despite their importance in practical applications, which motivates us for the present research.

We aim to address the exponential stability and H_∞ control problem for a class of discrete-time time-delay stochastic systems with infinite Markov jumps and multiplicative noises in this paper. The main contributions of this paper are as follows: First of all, we investigate exponential stability of the equilibrium point for the considered systems by employing a novel Lyapunov-Krasovskii functional. Further, a sufficient condition is established to ensure exponential stability with a given H_∞ performance index of the closed-loop system. And we introduce the slack matrix to decouple the Lyapunov matrices, which makes the H_∞ controller design feasible. Moreover, some numerical examples are provided to show the effectiveness of the proposed design approaches.

The remaining part of this paper is constructed as follows. In Section 2, we formulate the system model and recall some definitions and lemmas. In Section 3, we present our main results, where we derive some sufficient conditions for exponential stability with a given H_∞ performance index. Two numerical examples and their simulations are given to illustrate the effectiveness of the obtained results in Section 4. Conclusions are made in Section 5.

For convenience, we fix some notations that will be used throughout this paper. The n-dimensional real Euclidean space is denoted by $\mathscr{R}^n$. $\mathscr{R}^{m\times n}$ stands for the linear space of all m by n real matrices. Let $\|\cdot\|$ be the Euclidean norm of $\mathscr{R}^n$ or the operator norm of $\mathscr{R}^{m\times n}$. By S_n and $I(0)$ we denote the set of all $n\times n$ symmetric matrices and the identity (zero) matrix, respectively. A' denotes the transpose of a matrix (or vector) A. We say that A is positive (semipositive) definite if $A > 0 (\geq 0)$. $\lambda_{\max}(A)(\lambda_{\min}(A))$ represent the maximum (minimum) eigenvalue of A. $\delta_{(\cdot)}$ is called the Kronecker function. $\mathbf{Z}_+ := \{0, 1, \ldots\}$. $\mathscr{D} := \{1, 2, \ldots\}$. $l^2(\mathbf{Z}_+; \mathscr{R}^m) := \{\varsigma \in \mathscr{R}^m \mid \varsigma \text{ is } \mathscr{F}_t\text{-measurable, and } (\sum_{t=0}^{\infty} E\|y(t)\|^2)^{1/2} < \infty\}$.

2. Preliminaries

Consider the following discrete-time time-delay stochastic system with infinite Markov jump parameter and multiplicative noises:

$$\begin{aligned} x(t+1) &= C_0(s_t)x(t) + D_0(s_t)x(t-d) + R_0(s_t) \\ &\quad \cdot u(t) + H_0(s_t)v(t) + \sum_{k=1}^{r}\left[C_k(s_t)x(t)\right. \\ &\quad \left. + D_k(s_t)x(t-d) + R_k(s_t)u(t) + H_k(s_t)v(t)\right] \\ &\quad \cdot w_k(t), \\ 5pt\, y(t) &= L(s_t)x(t) + L_0(s_t)x(t-d) + N(s_t)u(t) \\ &\quad + E(s_t)v(t), \\ x(t_0) &= \phi(t_0), \\ t_0 &= -\tilde{d}, -\tilde{d}+1, \ldots, -1, 0,\ s(0) = s_0 \in \mathscr{D},\ t \in \mathbf{Z}_+, \end{aligned} \tag{1}$$

where $x(t) \in \mathscr{R}^n$ represents the system state, $u(t) \in \mathscr{R}^{n_u}$ is the control input, $v(t) \in \mathscr{R}^{n_v}$ denotes the disturbance, and $y(t) \in \mathscr{R}^{n_z}$ is the system output. $w(t) = \{w(t) \mid w(t) = (w_1(t), w_2(t), \ldots, w_r(t))',\ t \in \mathbf{Z}_+\}$ is a sequence of independent random vectors defined on a given complete probability space $(\Omega, \mathscr{F}, \mathscr{P})$, which satisfies $E(w(t)) = 0$ and $E(w(t)w(s)') = I_r\delta_{(t-s)}$. $\phi(t_0)$ is a vector-valued initial condition. d is the bounded constant delay with $0 \leq d \leq \tilde{d}$. Markov chain $\{s_t\}_{t\in Z_+}$ takes values in a countably infinite set $\mathscr{D}$ with transition probability matrix $\mathbf{P} = [p(i,j)]$, where $p(i,j) = P(s_{t+1} = j \mid s_t = i)$, and $\mathbf{P}$ is nondegenerate, $P(s_0 = i) > 0$ for all $i \in \mathscr{D}$. Assume $\{w_t\}_{t\in\mathbf{Z}_+}$ and $\{s_t\}_{t\in\mathbf{Z}_+}$ are mutually independent, and $\mathscr{F}_t = \{s_k, w_s \mid 0 \leq k \leq t,\ 0 \leq s \leq t-1\}$, $\mathscr{F}_0 = \sigma(s_0)$. Assume $v(t)$ belongs to $l^2(\mathbf{Z}_+; \mathscr{R}^{n_v})$.

We introduce the Banach spaces $\mathbb{A}_1^{m\times n} = \{A \mid A = (A(1), A(2), \ldots),\ A(i) \in \mathscr{R}^{m\times n},\ \|A\|_1 = \sum_{i=1}^{\infty}\|A(i)\| < \infty\}$ and $\mathbb{A}_\infty^{m\times n} = \{A \mid A = (A(1), A(2), \ldots),\ A(i) \in \mathscr{R}^{m\times n},\ \|A\|_\infty = \sup_{i\in\mathscr{D}}\|A(i)\| < \infty\}$. The notations $\mathbb{A}_1^{m\times n}(\mathbb{A}_\infty^{m\times n})$ will be written as $\mathbb{A}_1^n$ (resp., $\mathbb{A}_\infty^n$) and $\mathbb{A}_1^{n+}$ (resp., $\mathbb{A}_\infty^{n+}$) if and only if $m = n$ and $A(i) \in S_n$, $A(i) \geq 0$, $i \in \mathscr{D}$, respectively. When $Y, Z \in \mathbb{A}_1^{n+}$, $Y \leq Z$ means that $Y(i) \leq Z(i)$, $i \in \mathscr{D}$. Therefore, we have $\|Y\|_1 \leq \|Z\|_1$. For all coefficients of the considered systems, we suppose they have a finite norm $\|\cdot\|_\infty$.

Definition 1 (see [10, 18]). System (1) with $u(t) = 0$ and $v(t) = 0$ is called mean square exponential stability if there exist $\lambda \geq 1$ and $\tau \in (0, 1)$ such that

$$E\left\{\|x(t)\|^2\right\} \leq \lambda\tau^t \sup_{-\tilde{d}\leq l\leq 0} E\left\{\|\phi(l)\|^2\right\} \tag{2}$$

for all $t \in \mathbf{Z}_+$, $i \in \mathscr{D}$ and $x_0 \in \mathscr{R}^n$. Further, system (1) with $v(t) = 0$ is called exponential stabilizable if there exists a sequence $\{K(s_t)\}_{t\in\mathbf{Z}_+} \in \mathbb{A}_\infty^{n_u\times n}$ such that the closed-loop system

$$\begin{aligned} x(t+1) &= \left[C_0(s_t) + R_0(s_t)K(s_t)\right]x(t) + D_0(s_t)x(t \\ &\quad - d) + H_0(s_t)v(t) \\ &\quad + \sum_{k=1}^{r}\left\{\left[C_k(s_t) + R_k(s_t)K(s_t)\right]x(t)\right. \\ &\quad \left. + D_k(s_t)x(t-d) + H_k(s_t)v(t)\right\}w_k(t), \\ y(t) &= \left[L(s_t) + N(s_t)K(s_t)\right]x(t) + L_0(s_t)x(t-d) \\ &\quad + E(s_t)v(t), \\ x(t_0) &= \phi(t_0), \\ t_0 &= -\tilde{d}, -\tilde{d}+1, \ldots, -1, 0,\ s(0) = s_0 \in \mathscr{D},\ t \in \mathbf{Z}_+, \end{aligned} \tag{3}$$

with $v(t) = 0$ has mean square exponential stability, where $u(t) = K(s_t)x(t)$ is called exponentially stabilizing feedback.

Definition 2. Closed-loop system (3) is said to have an H_∞ noise disturbance attenuation level $\gamma > 0$, if under zero initial value the following condition is satisfied:

$$\sum_{t=0}^{\infty} E\left\{\|y(t)\|^2\right\} < \gamma^2 \sum_{t=0}^{\infty} \left\{E\|v(t)\|^2\right\} \tag{4}$$

for any $v(t) \in l^2(\mathbf{Z}_+; \mathscr{R}^{n_v})$.

Lemma 3 (see [22]). *We denote $\widetilde{\mathbb{A}}_\infty^{n+} = \{A \mid A \in \mathbb{A}_\infty^{n+}$, their exists $\varepsilon > 0$ not depengding upon i such that $A(i) \geq \varepsilon I_n$ for all $i \in \mathscr{D}\}$. Let*

$$B = \left\{\begin{bmatrix} B_{11}(i) & B_{12}(i) \\ B_{12}(i)' & B_{22}(i) \end{bmatrix}\right\}_{i\in\mathscr{D}}. \tag{5}$$

Assume that $B_{22}(i) \geq \varepsilon I_{n_2} > 0$ for all $i \in \mathscr{D}$ for some $\varepsilon > 0$. Then, $B \in \widetilde{\mathbb{A}}_\infty^{n+}$ if and only if $B \mid B_{22} \in \widetilde{\mathbb{A}}_\infty^{n_1+}$, where $n = n_1 + n_2$ and $B \mid B_{22} = \{B_{11}(i) - B_{12}(i)B_{22}(i)^{-1}B_{12}(i)'\}_{i\in\mathscr{D}}$ is called the Schur complement of B_{22} in B.

Remark 4. Lemma 3 is the infinite-dimensional version of Schur complements (see [24]).

3. Main Results

Firstly, stability will be analyzed, and a sufficient condition is obtained for system (1) with $u(t) = 0$ and $v(t) = 0$ to have mean square exponential stability.

Theorem 5. *System (1) with $u(t) = 0$ and $v(t) = 0$ is exponentially mean square stable, if we can find matrices $P \in \widetilde{\mathbb{A}}_\infty^{n+}$, $Q \in \widetilde{\mathbb{A}}_\infty^{n+}$ such that the following matrix inequality holds:*

$$\begin{bmatrix} -\mathscr{P} & C_x(i) & D_d(i) \\ * & -P(i) + \left(\tilde{d}+1\right)Q(i) & 0 \\ * & * & -Q(q) \end{bmatrix} < 0 \tag{6}$$

uniformly with respect to $(i, q) \in \mathscr{D} \times \mathscr{D}$, where

$$\begin{aligned} C_x(i) &= \left[C_0(i)', C_1(i)', \ldots, C_r(i)'\right]', \\ D_d(i) &= \left[D_0(i)', D_1(i)', \ldots, D_r(i)'\right]', \\ \mathscr{P} &= \operatorname{diag}\left\{\underbrace{\mathscr{E}_i(P)^{-1}, \ldots, \mathscr{E}_i(P)^{-1}}_{r+1}\right\}, \\ \mathscr{E}_i(P) &= \sum_{j=1}^{\infty} p(i,j) P(j). \end{aligned} \tag{7}$$

Proof. Construct the following Lyapunov-Krasovskii functional:

$$\begin{aligned} V(x(t), s_t) &= x(t)' P(s_t) x(t) \\ &\quad + \sum_{m=t-d}^{t-1} x(m)' Q(s_m) x(m) \\ &\quad + \sum_{\alpha=-\tilde{d}+1}^{0} \sum_{\beta=t-1+\alpha}^{t-1} x(\beta)' Q(s_\beta) x(\beta) \\ &= V_1(x(t), s_t) + V_2(x(t), s_t) \\ &\quad + V_3(x(t), s_t). \end{aligned} \tag{8}$$

By the assumption that $w(t)$ is independent of the Markov chain $\{s_t\}_{t\in\mathbf{Z}_+}$ and $E[w(t)] = 0$, besides $\mathscr{F}_{t-\tilde{d}} \subset \mathscr{F}_t$, we have

$$\begin{aligned} &E\left[V_1(x(t+1), s_{t+1}) - V_1(x(t), s_t) \mid \mathscr{F}_t, s_t = i\right] \\ &= \begin{bmatrix} x(t) \\ x(t-d) \end{bmatrix}' \begin{bmatrix} \sum_{k=0}^{r} C_k(i)' \mathscr{E}_i(P) C_k(i) - P(i) & \sum_{k=0}^{r} C_k(i)' \mathscr{E}_i(P) D_k(i) \\ \sum_{k=0}^{r} D_k(i)' \mathscr{E}_i(P) C_k(i) & \sum_{k=0}^{r} D_k(i)' \mathscr{E}_i(P) D_k(i) \end{bmatrix} \begin{bmatrix} x(t) \\ x(t-d) \end{bmatrix}, \end{aligned} \tag{9}$$

and

$$\begin{aligned} &E\left[V_2(x(t+1), s_{t+1}) - V_2(x(t), s_t) \mid \mathscr{F}_t, s_t = i\right] \\ &= x(t)' Q(i) x(t) - x(t-d)' Q(s_{t-d}) x(t-d) \\ &\quad + \sum_{\alpha=t-\tilde{d}}^{t-1} x(\alpha)' Q(s_\alpha) x(\alpha) \\ &\quad - \sum_{\alpha=t-\tilde{d}}^{t-1} x(\alpha)' Q(s_\alpha) x(\alpha) \\ &\leq x(t)' Q(i) x(t) - x(t-d)' Q(s_{t-d}) x(t-d) \\ &\quad + \sum_{\alpha=t-\tilde{d}}^{t-1} x(\alpha)' Q(s_\alpha) x(\alpha), \end{aligned} \tag{10}$$

and

$$\begin{aligned} &E\left[V_3(x(t+1), s_{t+1}) - V_3(x(t), s_t) \mid \mathscr{F}_t, s_t = i\right] \\ &= \tilde{d} x(t)' Q(i) x(t) - \sum_{\alpha=t-\tilde{d}}^{t-1} x(\alpha)' Q(s_\alpha) x(\alpha). \end{aligned} \tag{11}$$

Thus, combining (8) with (9)-(11), we get

$$E\left[V\left(x\left(t+1\right),s_{t+1}\right)-V\left(x\left(t\right),s_t\right)\mid\mathcal{F}_t,s_t=i\right]\leq a\left(t\right)'R_{iq}\left(P\right)a\left(t\right), \tag{12}$$

where

$$R_{iq}\left(P\right)=\begin{bmatrix}\sum_{k=0}^{r}C_k\left(i\right)'\mathscr{E}_i\left(P\right)C_k\left(i\right)-P\left(i\right)+\left(\widetilde{d}+1\right)Q\left(i\right) & \sum_{k=0}^{r}C_k\left(i\right)'\mathscr{E}_i\left(P\right)D_k\left(i\right)\\ \sum_{k=0}^{r}D_k\left(i\right)'\mathscr{E}_i\left(P\right)C_k\left(i\right) & \sum_{k=0}^{r}D_k\left(i\right)'\mathscr{E}_i\left(P\right)D_k\left(i\right)-Q\left(q\right)\end{bmatrix} \tag{13}$$

with $q=s_{t-d}$ and $a(t)$ is defined as $a(t)=\left[x(t)'\quad x(t-d)'\right]'$.

Applying Lemma 3 to (6) leads to

$$\operatorname{diag}\left\{-P\left(i\right)+\left(\widetilde{d}+1\right)Q\left(i\right),-Q\left(q\right)\right\}+\mathscr{M}\left(i\right)'\mathscr{P}^{-1}\mathscr{M}\left(i\right)<0, \tag{14}$$

where $\mathscr{M}(i)=\left[C_x(i)\quad D_d(i)\right]$. Further, we have $R_{iq}(P)<0$. It is clear from $R_{iq}(P)<0$ that there exists a sufficiently small scalar $\varepsilon>0$ such that $R_{iq}(P)<-\varepsilon I_n$. Therefore, it follows that

$$E\left[V\left(x\left(t+1\right),s_{t+1}\right)-V\left(x\left(t\right),s_t\right)\right]<-\varepsilon E\left[\left\|x\left(t\right)\right\|^2\right]. \tag{15}$$

On the other hand, by using (8), we deduce that

$$E\left[V\left(x\left(t\right),s_t\right)\right]\leq\theta_1E\left[\left\|x\left(t\right)\right\|^2\right]+\left(\widetilde{d}+1\right)\theta_2\sum_{\beta=t-\widetilde{d}}^{t-1}E\left[\left\|x\left(\beta\right)\right\|^2\right], \tag{16}$$

where

$$\theta_1=\max_{l\in\mathscr{D}}\lambda_{\max}\left(P\left(l\right)\right),\qquad\theta_2=\max_{p\in\mathscr{D}}\lambda_{\max}\left(Q\left(p\right)\right). \tag{17}$$

Noting (15) and (16), for any constant $\kappa>1$, we obtain that

$$\begin{aligned}&\kappa^{t+1}E\left[V\left(x\left(t+1\right),s_{t+1}\right)\right]-\kappa^tE\left[V\left(x\left(t\right),s_t\right)\right]\\&=\kappa^{t+1}E\left[V\left(x\left(t+1\right),s_{t+1}\right)-V\left(x\left(t\right),s_t\right)\right]+\kappa^t\left(\kappa-1\right)E\left[V\left(x\left(t\right),s_t\right)\right]\\&\leq\left[-\kappa\varepsilon+\left(\kappa-1\right)\theta_1\right]\kappa^tE\left[\left\|x\left(t\right)\right\|^2\right]+\left(\kappa-1\right)\theta_3\sum_{\beta=t-\widetilde{d}}^{t-1}\kappa^tE\left[\left\|x\left(\beta\right)\right\|^2\right],\end{aligned} \tag{18}$$

where $\theta_3=(\widetilde{d}+1)\theta_2$. By taking summation from 0 to $T-1$ on both sides of (18), for $T\geq\widetilde{d}+1$, it implies that

$$\begin{aligned}&\kappa^TE\left[V\left(x\left(T\right),s_T\right)\right]-E\left[V\left(x\left(0\right),s_0\right)\right]\leq\left[-\kappa\varepsilon+\left(\kappa-1\right)\theta_1\right]\sum_{t=0}^{T-1}\kappa^tE\left[\left\|x\left(t\right)\right\|^2\right]+\left(\kappa-1\right)\\&\cdot\theta_3\sum_{t=0}^{T-1}\sum_{\beta=t-\widetilde{d}}^{t-1}\kappa^tE\left[\left\|x\left(\beta\right)\right\|^2\right]\leq\left[-\kappa\varepsilon+\left(\kappa-1\right)\theta_1\right]\\&\cdot\sum_{t=0}^{T-1}\kappa^tE\left[\left\|x\left(t\right)\right\|^2\right]+\left(\kappa-1\right)\theta_3\\&\cdot\left\{\widetilde{d}\sum_{\beta=-\widetilde{d}}^{-1}\kappa^{\beta+\widetilde{d}}E\left[\left\|x\left(\beta\right)\right\|^2\right]+\widetilde{d}\sum_{\beta=0}^{T-1-\widetilde{d}}\kappa^{\beta+\widetilde{d}}E\left[\left\|x\left(\beta\right)\right\|^2\right]+\widetilde{d}\sum_{\beta=T-1-\widetilde{d}}^{T-1}\kappa^{\beta+\widetilde{d}}E\left[\left\|x\left(\beta\right)\right\|^2\right]\right\}\leq\left[-\kappa\varepsilon\right.\\&\left.+\left(\kappa-1\right)\theta_1\right]\sum_{t=0}^{T-1}\kappa^tE\left[\left\|x\left(t\right)\right\|^2\right]+\left(\kappa-1\right)\theta_3\\&\cdot\left\{\widetilde{d}\kappa^{\widetilde{d}}\max_{-\widetilde{d}\leq\beta\leq0}E\left[\left\|\phi\left(\beta\right)\right\|^2\right]+\widetilde{d}\kappa^{\widetilde{d}}\sum_{\beta=0}^{T-1}\kappa^\beta E\left[\left\|x\left(\beta\right)\right\|^2\right]\right\}=\left\{\left[-\kappa\varepsilon+\left(\kappa-1\right)\theta_1\right]\right.\\&\left.+\left(\kappa-1\right)\theta_3\widetilde{d}\kappa^{\widetilde{d}}\right\}\sum_{t=0}^{T-1}\kappa^tE\left[\left\|x\left(t\right)\right\|^2\right]+\left(\kappa-1\right)\\&\cdot\theta_3\widetilde{d}\kappa^{\widetilde{d}}\max_{-\widetilde{d}\leq\beta\leq0}E\left[\left\|\phi\left(\beta\right)\right\|^2\right].\end{aligned} \tag{19}$$

Recalling (8) and (16), denoting $\theta_0 = \min_{l\in\mathscr{D}}\lambda_{\min}(P(l))$ and $\theta = \max\{\theta_1, (\tilde{d}+1)\theta_2\}$, we have

$$E\left[V\left(x\left(T\right), s_T\right)\right] \geq \theta_0 E\left[\left\|x\left(T\right)\right\|^2\right], \tag{20}$$

and

$$E\left[V\left(x\left(0\right), s_0\right)\right] \leq \theta \max_{-\tilde{d}\leq\beta\leq 0} E\left[\left\|\phi\left(\beta\right)\right\|^2\right], \tag{21}$$

respectively. Furthermore, it suffices to show that there exists a constant $\kappa_0 > 1$ such that

$$\left[-\kappa_0\varepsilon + \left(\kappa_0 - 1\right)\theta_1\right] + \left(\kappa_0 - 1\right)\theta_3\tilde{d}\kappa_0^{\tilde{d}} = 0. \tag{22}$$

Actually, letting $f(\kappa) = [-\kappa\varepsilon + (\kappa-1)\theta_1] + (\kappa-1)\theta_3\tilde{d}\kappa^{\tilde{d}}$, then we have $f'(\kappa) > 0$ and $f(1) < 0$. Therefore, (22) has a unique solution $\kappa_0 > 1$. By substituting (20)-(22) into (19), we obtain

$$E\left[\left\|x\left(T\right)\right\|^2\right] \leq \lambda_0\left(\frac{1}{\kappa_0}\right)^T \max_{-\tilde{d}\leq\beta\leq 0} E\left[\left\|\phi\left(\beta\right)\right\|^2\right], \tag{23}$$

where $\lambda_0 = (\theta + (\kappa_0 - 1)\theta_3\tilde{d}\kappa_0^{\tilde{d}})/\theta_0$. This indicates that system (1) with $u(t) = 0$ and $v(t) = 0$ has mean square exponential stability. The proof is completed. □

Remark 6. Due to the consideration of an infinite-state Markov chain, the infinite dimension Banach spaces have been introduced. Furthermore, it should be pointed out that a novel Lyapunov-Krasovskii functional (8) has been constructed to analyze the mean square exponential stability for system (1) with $u(t) = 0$ and $v(t) = 0$.

Next, we prove that system (1) with $u(t) = 0$ verifies the H_∞ performance disturbance attenuation γ.

Theorem 7. *System (1) has mean square exponential stability for $u(t) = 0$ and $v(t) = 0$ with a prescribed H_∞ performance γ for $u(t) = 0$, if we can find matrices $P \in \widetilde{\mathbb{A}}_\infty^{n+}$, $Q \in \widetilde{\mathbb{A}}_\infty^{n+}$ such that the following matrix inequality holds:*

$$\begin{bmatrix} -\mathscr{P} & C_x(i) & D_d(i) & H_v(i) & 0 \\ * & -P(i) + \left(\tilde{d}+1\right)Q(i) & 0 & 0 & L(i)' \\ * & * & -Q(q) & 0 & L_0(i)' \\ * & * & * & -\gamma^2 I & E(i)' \\ * & * & * & * & -I \end{bmatrix} < 0, \tag{24}$$

uniformly with respect to $(i, q) \in \mathscr{D}\times\mathscr{D}$, where

$$H_v(i) = \left[H_0(i)', H_1(i)', \ldots, H_r(i)'\right]'. \tag{25}$$

Proof. It is well established that (24) implies (6). Applying Theorem 5 one obtains that system (1) has mean square exponential stability for $u(t) = 0$ and $v(t) = 0$.

Let us now show that system (1) with $u(t) = 0$ satisfies a prescribed H_∞ performance level. To this end, constructing the same Lyapunov-Krasovskii functional $V(x(t), s_t)$ as in Theorem 5 and under the zero initial condition, the following index is introduced:

$$\begin{aligned} J^T &= \sum_{t=0}^{T} E\left\{\left\|y(t)\right\|^2 - \gamma^2\left\|v(t)\right\|^2\right\} = \sum_{t=0}^{T} E\left\{\left\|y(t)\right\|^2\right. \\ &\left. - \gamma^2\left\|v(t)\right\|^2 + \left[V\left(x\left(t+1\right), s_{t+1}\right) - V\left(x\left(t\right), s_t\right)\right]\right\} \\ &- V\left(x\left(T+1\right), s_{T+1}\right) \leq \sum_{t=0}^{T} E\left\{\left\|y(t)\right\|^2 - \gamma^2\left\|v(t)\right\|^2\right. \\ &\left. + \left[V\left(x\left(t+1\right), s_{t+1}\right) - V\left(x\left(t\right), s_t\right)\right]\right\} \leq E\left\{b(t)'\right. \\ &\left. \cdot \left[\mathscr{A}\left(s_t, s_{t-d}\right) - \mathscr{B}\left(s_t\right)'\mathscr{C}\left(s_t\right)^{-1}\mathscr{B}\left(s_t\right)\right]b(t)\right\}, \end{aligned} \tag{26}$$

where

$$\begin{aligned} &\mathscr{A}\left(s_t, s_{t-d}\right) \\ &\quad = \operatorname{diag}\left\{-P\left(s_t\right) + \left(\tilde{d}+1\right)Q\left(s_t\right), -Q\left(s_{t-d}\right), -\gamma^2 I\right\}, \\ &\mathscr{B}(i) = \begin{bmatrix} C_x\left(s_t\right) & D_d\left(s_t\right) & H_v\left(s_t\right) \\ L\left(s_t\right) & L_0\left(s_t\right) & E\left(s_t\right) \end{bmatrix}, \\ &\mathscr{C}\left(s_t\right) = \operatorname{diag}\left\{-\mathscr{P}, -I\right\}, \end{aligned} \tag{27}$$

and $b(t)$ is defined as $b(t) = \left[x(t)' \;\; x(t-d)' \;\; v(t)'\right]'$. The last '$\leq$' in (26) holds as a result of the similar line with (12). Then, by using Lemma 3 in (24), we obtain that $\mathscr{A}(s_t, s_{t-d}) - \mathscr{B}(s_t)'\mathscr{C}(s_t)^{-1}\mathscr{B}(s_t) < 0$. Thus, $J^T < 0$. Taking the limit $T \longrightarrow \infty$ in (26), we have

$$\sum_{t=0}^{\infty} E\left[\left\|y(t)\right\|^2\right] < \gamma^2 \sum_{t=0}^{\infty} E\left[\left\|v(t)\right\|^2\right]. \tag{28}$$

This ends the proof. □

Combining Theorem 5 with Theorem 7, the following corollary can be easily derived for closed-loop system (3).

Corollary 8. *Let the feedback control gain $K(i)$, $i \in \mathscr{D}$, be given. Then closed-loop system (3) has mean square exponential stability for $v(t) = 0$ with a prescribed H_∞ performance γ if there exist two matrices $P \in \widetilde{\mathbb{A}}_\infty^{n+}$ and $Q \in \widetilde{\mathbb{A}}_\infty^{n+}$, such that*

$$\begin{bmatrix} -\mathscr{P} & \overline{C}_x(i) & D_d(i) & H_v(i) & 0 \\ * & -P(i) + \left(\tilde{d}+1\right)Q(i) & 0 & 0 & \overline{L}(i)' \\ * & * & -Q(q) & 0 & L_0(i)' \\ * & * & * & -\gamma^2 I & E(i)' \\ * & * & * & * & -I \end{bmatrix} < 0, \tag{29}$$

uniformly with respect to $(i,q) \in \mathscr{D} \times \mathscr{D}$, *where*

$$\begin{aligned}
&\overline{C}_x(i) = \Big[\left(C_0(i) + R_0(i)K(i)\right)', \\
&\quad \left(C_1(i) + R_1(i)K(i)\right)', \ldots, \left(C_r(i) + R_r(i)K(i)\right)'\Big]', \\
&\overline{L}(i) = L(i) + N(i)K(i).
\end{aligned} \tag{30}$$

Below, based on Corollary 8, we are ready to present the H_∞ controller design for system (1).

Theorem 9. *For system (1), a state feedback controller can be designed such that closed-loop system (3) has mean square exponential stability for* $v(t) = 0$ *and a given* H_∞ *performance* γ *can be ensured if there exist matrices* $\widehat{P} \in \widetilde{\mathbb{A}}_\infty^{n+}$, $\widehat{Q} \in \widetilde{\mathbb{A}}_\infty^{n+}$, $\widehat{K} \in \mathbb{A}_\infty^{n_u \times n}$, *and* $F \in \mathscr{R}^{n\times n}$ *such that*

$$\begin{bmatrix} \Phi(i) & \Gamma(i) & \Upsilon(i) \\ * & -I & 0 \\ * & * & -\widehat{\mathscr{P}} \end{bmatrix} < 0, \tag{31}$$

uniformly with respect to $(i,q) \in \mathscr{D} \times \mathscr{D}$, *where*

$$\begin{aligned}
&\Phi(i) \\
&= \begin{bmatrix} \widehat{P}(i) + \left(\widetilde{d}+1\right)\widehat{Q}(i) - F' - F & 0 & 0 \\ * & -\widehat{Q}(q) & 0 \\ * & * & -\gamma^2 I \end{bmatrix}, \\
&\Gamma(i) = \left[L(i)F + N(i)\widehat{K}(i), L_0(i)F, E(i)\right]', \\
&\Upsilon(i) = \left[C_x(i)F + R_u(i)\widehat{K}(i), D_d(i)F, H_v(i)\right]', \\
&R_u(i) = \left[R_0(i)', R_1(i)', \ldots, R_r(i)'\right]', \\
&\widehat{\mathscr{P}} = \operatorname{diag}\left\{\underbrace{\mathscr{E}_i\left(\widehat{P}\right)^{-1}, \ldots, \mathscr{E}_i\left(\widehat{P}\right)^{-1}}_{r+1}\right\}, \\
&\mathscr{E}_i\left(\widehat{P}\right) = \sum_{j=1}^{\infty} p(i,j)\widehat{P}(j)^{-1}.
\end{aligned} \tag{32}$$

Moreover, if matrix inequalities (31) are feasible, then an exponentially stabilizing feedback gain can be given by

$$K(i) = \widehat{K}(i)F^{-1}. \tag{33}$$

Proof. Via Lemma 3, we conclude that (29) is equivalent to the following matrix inequality:

$$\begin{bmatrix} -P(i) + \left(\widetilde{d}+1\right)Q(i) & 0 & 0 & \overline{L}(i)' & \overline{C}_x(i)' \\ * & -Q(q) & 0 & L_0(i)' & D_d(i)' \\ * & * & -\gamma^2 I & E(i)' & H_v(i)' \\ * & * & * & -I & 0 \\ * & * & * & * & -\mathscr{P} \end{bmatrix} < 0. \tag{34}$$

Premultiply $\operatorname{diag}\{F', F', I, I, I\}$ and postmultiply $\operatorname{diag}\{F, F, I, I, I\}$ with (34), and let

$$\begin{aligned}
\widehat{P}(i) &= P(i)^{-1}, \\
\widehat{Q}(i) &= F'Q(i)F, \\
\widehat{K}(i) &= K(i)F.
\end{aligned} \tag{35}$$

By a tedious calculation, one can rewrite (34) as

$$\begin{bmatrix} \widehat{\Phi}(i) & \Gamma(i) & \Upsilon(i) \\ * & -I & 0 \\ * & * & -\widehat{\mathscr{P}} \end{bmatrix} < 0, \tag{36}$$

where

$$\begin{aligned}
&\widehat{\Phi}(i) \\
&= \begin{bmatrix} -F'\widehat{P}(i)^{-1}F + \left(\widetilde{d}+1\right)\widehat{Q}(i) & 0 & 0 \\ * & -\widehat{Q}(q) & 0 \\ * & * & -\gamma^2 I \end{bmatrix}.
\end{aligned} \tag{37}$$

According to Corollary 8 and the fact that

$$\left(\widehat{P}(i) - F\right)'\widehat{P}(i)^{-1}\left(\widehat{P}(i) - F\right) \geq 0, \tag{38}$$

namely,

$$-F'\widehat{P}(i)^{-1}F \leq \widehat{P}(i) - F - F', \tag{39}$$

the desired result is derived. □

Remark 10. The work in [20] presented a necessary and sufficient condition for the existence of the mixed H_2/H_∞ control by four coupled matrix Riccati equations (CMREs). Note that CMREs are hardly solved in practice, and this motivates us to find a new sufficient condition in terms of matrix inequalities that can be easily solved to guarantee that the resulting closed-loop system has mean square exponential stability for the zero exogenous disturbance and satisfies a prescribed H_∞ performance level.

Remark 11. With the introduction of a slack matrix F, a sufficient condition is obtained in Theorem 9, in which the Lyapunov matrices are not involved in any product with system matrices. This makes the H_∞ controller design feasible and can be easily carried out by solving corresponding matrix inequalities.

Remark 12. It is worth noting that the obtained results can be extended to discrete-time time-delay infinite Markov jump stochastic systems with time-varying delays. Assume that the time-varying delay $d(t)$ satisfies $d_m \leq d(t) \leq d_M$; then by

similar procedures to the above and choosing the following Lyapunov-Krasovskii function

$$V(x(t), s_t) = x(t)' P(s_t) x(t) + \sum_{m=t-d(t)}^{t-1} x(m)' Q(s_m) x(m) + \sum_{\alpha=-d_M+2}^{-d_m+1} \sum_{\beta=t-1+\alpha}^{t-1} x(\beta)' Q(s_\beta) x(\beta), \tag{40}$$

the corresponding results can be derived.

4. Illustrative Example

In this section, some illustrative examples are presented to demonstrate the effectiveness of the developed method.

Example 1. Consider the following one-dimensional discrete-time time-delay stochastic system with infinite Markov jumps:

$$\begin{aligned} x(t+1) &= c_0(s_t) x(t) + d_0(s_t) x(t-d) \\ &\quad + \sum_{k=1}^{r} \left[c_k(s_t) x(t) + d_k(s_t) x(t-d) \right] w_k(t), \end{aligned} \tag{41}$$

where the transition probability is defined by $p(i,i) = 1/4$, $p(i,i+1) = 3/4$, $p(i,j) = 0$, $j \neq i, i+1$, $i, j \in \mathscr{D}$. Now take

$$\begin{aligned} c_0(i) &= \sqrt{\frac{i}{i+1}}, \\ c_1(i) &= \sqrt{\frac{1}{i+1}}, \\ c_k(i) &= 0, \quad k = 2, 3, \ldots, r, \ i \in \mathscr{D}, \\ d_0(i) &= \sqrt{\frac{i}{i+1}}, \\ d_1(i) &= \sqrt{\frac{1}{i+1}}, \\ d_k(i) &= 0, \quad k = 2, 3, \ldots, r, \ i \in \mathscr{D}. \end{aligned} \tag{42}$$

Let $P(i) = 4(i+1)/3i$, $Q(i) = 1/9i(i+1)$, and time-delay $d = 2$. By direct computation, (6) holds. According to Theorem 5, we deduce that system (41) has mean square exponential stability, and Figure 1 presents the state response of system (41) with initial conditions $\phi(t_0) = 0.5$ for $t_0 = -2, -1, 0$.

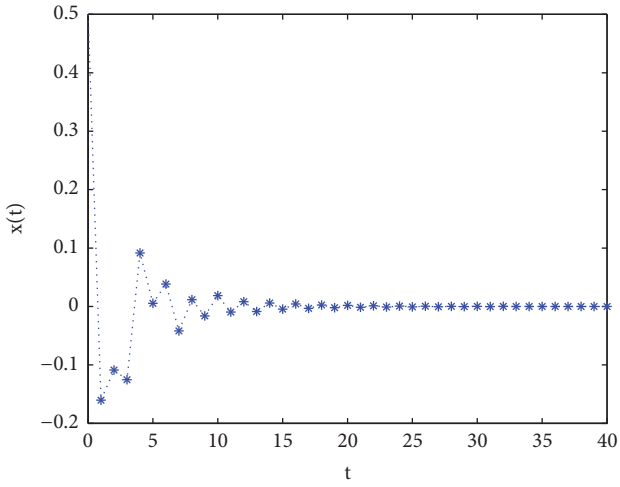

Figure 1: System state response in Example 1.

Example 2. Consider the following one-dimensional discrete-time time-delay stochastic system with infinite Markov jumps:

$$\begin{aligned} x(t+1) &= \left[c_0(s_t) + r_0(s_t) K(s_t) \right] x(t) + d_0(s_t) x(t - d) + h_0(s_t) v(t) \\ &\quad + \sum_{k=1}^{r} \left\{ \left[c_k(s_t) + r_k(s_t) K(s_t) \right] x(t) + d_k(s_t) x(t-d) + h_k(s_t) v(t) \right\} w_k(t), \\ y(t) &= \left[l(s_t) + n(s_t) K(s_t) \right] x(t) + l_0(s_t) x(t-d) + e(s_t) v(t), \\ x(t_0) &= \phi(t_0), \\ t_0 &= -\tilde{d}, -\tilde{d}+1, \ldots, -1, 0, \ s(0) = s_0 \in \mathscr{D}, \ t \in \mathbf{Z}_+, \end{aligned} \tag{43}$$

where the transition probability is defined by $p(i,i) = 1/2$, $p(i,i+1) = 1/2$, $p(i,j) = 0$, $j \neq i, i+1, i, j \in \mathscr{D}$. The coefficients of system (43) are reset to be

$$\begin{aligned} c_0(i) &= -\frac{i}{(i+1)^2}, \\ c_1(i) &= \frac{1}{i+1}, \\ c_k(i) &= 0, \quad k = 2, 3, \ldots, r, \ i \in \mathscr{D}, \\ d_0(i) &= -\frac{i}{2(i+1)}, \\ d_1(i) &= \frac{1}{i+1}, \\ d_k(i) &= 0, \quad k = 2, 3, \ldots, r, \ i \in \mathscr{D}, \end{aligned}$$

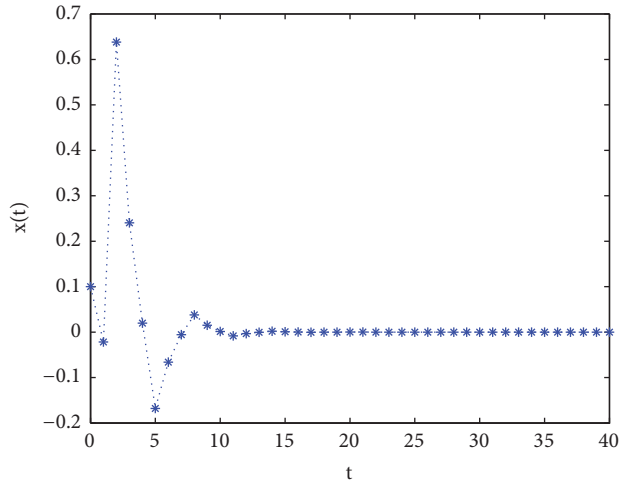

Figure 2: System state response in Example 2.

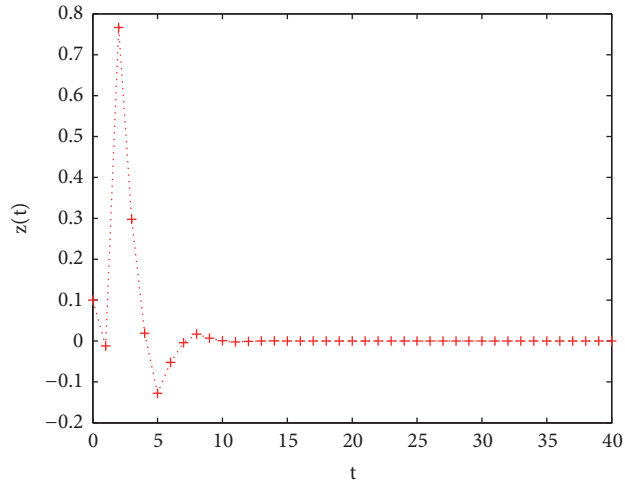

Figure 3: System output response in Example 2.

$$
\begin{aligned}
&r_0(i) = -\frac{i}{i+1},\\
&r_1(i) = 1,\\
&r_k(i) = 0,\\
&\qquad\qquad k = 2,3,\ldots,r,\ i \in \mathscr{D},\\
&h_0(i) = 1,\\
&h_1(i) = 1,\\
&h_k(i) = 0,\\
&\qquad\qquad k = 2,3,\ldots,r,\ i \in \mathscr{D},\\
&l(i) = \frac{1}{i+1},\\
&l_0(i) = 1,\\
&n(i) = 1,\\
&e(i) = 0.1.
\end{aligned}
\tag{44}
$$

The purpose here is to design an H_∞ controller such that the closed-loop system has mean square exponential stability and with a given H_∞ norm bound $\gamma = 0.5$. Applying Theorem 9, the H_∞ controller can be designed as

$$K(i) = -\frac{1}{i+1}. \tag{45}$$

With the initial conditions $\phi(t_0) = 0.1$ for $t_0 = -2, -1, 0$ and the exogenous disturbance $v(t) = 2e^{-t}\sin t$, Figures 2 and 3 show the state and output responses, respectively.

5. Conclusions

In this paper, the issue of exponential stability and robust H_∞ control for a class of discrete-time time-delay stochastic systems with infinite Markov jumps and multiplicative noises has been studied. Time-delay and infinite Markov jump are taken into consideration simultaneously. By using Lyapunov-Krasovskii functional and introducing slack matrix, an matrix inequality approach has been adopted to ensure the mean square exponential stability and satisfy a prescribed H_∞ performance level. Finally, some illustrative examples are given to demonstrate the usefulness of the proposed design methods. Further research directions would include the investigation on H_2/H_∞ control problem and asynchronous control problem for discrete-time time-delay stochastic systems with infinite Markov jumps.

Data Availability

The data used to support the findings of this study are included within the article.

Conflicts of Interest

The authors declare that they have no conflicts of interest.

Acknowledgments

This work is supported by National Natural Science Foundation of China under Grant 61673013, Natural Science Foundation of Shandong Province under Grant ZR2016JL022, and the SDUST Research Fund under Grant 2015TDJH105.

References

[1] Z. Lin, Y. Lin, and W. Zhang, "H_∞ filtering for nonlinear stochastic Markovian jump systems," *IET Control Theory & Applications*, vol. 4, no. 12, pp. 2743–2756, 2010.

[2] Y. Ni, W. Zhang, and H. Fang, "On the observability and detectability of linear stochastic systems with Markov jumps and multiplicative noise," *Journal of Systems Science & Complexity*, vol. 23, no. 1, pp. 102–115, 2010.

[3] Z. G. Wu, P. Shi, H. Su, and J. Chu, "Asynchronous $l_2 - l_\infty$ filtering for discrete-time stochastic Markov jump systems with randomly occurred sensor nonlinearities," *Automatica*, vol. 50, no. 1, pp. 180–186, 2014.

[4] C. Tan and W. H. Zhang, "On observability and detectability of continuous-time stochastic Markov jump systems," *Journal of Systems Science & Complexity*, vol. 28, no. 4, pp. 830–847, 2015.

[5] Z.-G. Wu, J. H. Park, H. Su, and J. Chu, "Stochastic stability analysis for discrete-time singular Markov jump systems with time-varying delay and piecewise-constant transition probabilities," *Journal of The Franklin Institute*, vol. 349, no. 9, pp. 2889–2902, 2012.

[6] L. Zhang, Y. Leng, and P. Colaneri, "Stability and stabilization of discrete-time semi-MARkov jump linear systems via semi-Markov kernel approach," *Institute of Electrical and Electronics Engineers Transactions on Automatic Control*, vol. 61, no. 2, pp. 503–508, 2016.

[7] S. Zhou, X. Liu, B. Chen, and H. Liu, "Stability analysis for a class of discrete-time nonhomogeneous markov jump systems with multiplicative noises," *Complexity*, vol. 2018, Article ID 1586846, 9 pages, 2018.

[8] Y. Zhao and W. Zhang, "Observer-based controller design for singular stochastic Markov jump systems with state dependent noise," *Journal of Systems Science & Complexity*, vol. 29, no. 4, pp. 946–958, 2016.

[9] Y. Wang, Z. Pan, Y. Li, and W. Zhang, "H_∞ control for nonlinear stochastic Markov systems with time-delay and multiplicative noise," *Journal of Systems Science & Complexity*, vol. 30, no. 6, pp. 1–23, 2017.

[10] V. Dragan, T. Morozan, and A. M. Stoica, *Mathematical Methods in Robust Control of Discrete-Time Linear Stochastic Systems*, Springer, New York, NY, USA, 2010.

[11] Z. J. Wu, J. Yang, and P. Shi, "Adaptive tracking for stochastic nonlinear systems with Markovian switching," *IEEE Transactions on Automatic Control*, vol. 55, no. 9, pp. 2135–2141, 2010.

[12] X. Luan, S. Zhao, and F. Liu, "H_∞ control for discrete-time Markov jump systems with uncertain transition probabilities," *IEEE Transactions on Automatic Control*, vol. 58, no. 6, pp. 1566–1572, 2013.

[13] L. Wu, X. Yao, and W. X. Zheng, "Generalized H_2 fault detection for two-dimensional Markovian jump systems," *Automatica*, vol. 48, no. 8, pp. 1741–1750, 2012.

[14] C. Li, M. Z. Chen, J. Lam, and X. Mao, "On exponential almost sure stability of random jump systems," *Institute of Electrical and Electronics Engineers Transactions on Automatic Control*, vol. 57, no. 12, pp. 3064–3077, 2012.

[15] L. Wu, X. Su, and P. Shi, "Sliding mode control with bounded $\mathscr{L}_2$ gain performance of Markovian jump singular time-delay systems," *Automatica*, vol. 48, no. 8, pp. 1929–1933, 2012.

[16] T. Morozan and V. Dragan, "An H_2 type norm of a discrete-time linear sotchastic systems with periodic coefficients simultaneously affected by an infinite Markov chain and multiplicative white noise perterbations," *Stochastic Analysis and Applications*, vol. 32, no. 5, pp. 776–801, 2014.

[17] O. L. V. Costa and M. D. Fragoso, "Discrete-time LQ-optimal control problems for infinite Markov jump parameter systems," *IEEE Transactions on Automatic Control*, vol. 40, no. 12, pp. 2076–2088, 1995.

[18] T. Hou and H. Ma, "Exponential stability for discrete-time infinite Markov jump systems," *IEEE Transactions on Automatic Control*, vol. 61, no. 12, pp. 4241–4246, 2016.

[19] M. Gao, L. Sheng, and W. Zhang, "Stochastic H_2/H_∞ control of nonlinear systems with time-delay and state-dependent noise," *Applied Mathematics and Computation*, vol. 266, pp. 429–440, 2015.

[20] Z. Wang, H. Qiao, and K. J. Burnham, "On stabilization of bilinear uncertain time-delay stochastic systems with Markovian jumping parameters," *Institute of Electrical and Electronics Engineers Transactions on Automatic Control*, vol. 47, no. 4, pp. 640–646, 2002.

[21] Z. Fei, H. Gao, and P. Shi, "New results on stabilization of Markovian jump systems with time delay," *Automatica*, vol. 45, no. 10, pp. 2300–2306, 2009.

[22] R. Song and Q. Zhu, "Stability of linear stochastic delay differential equations with infinite Markovian switchings," *International Journal of Robust and Nonlinear Control*, vol. 28, no. 3, pp. 825–837, 2018.

[23] Y. Liu, T. Hou, and X. Bai, "Infinite horizon H_2/H_∞ optimal control for discrete-time infinite Markov jump systems with (x, u, v)-dependent noise," in *Proceedings of the 36th Chinese Control Conference*, pp. 1955–1960, 2017.

[24] G. Corach, A. Maestripieri, and D. Stojanoff, "Generalized Schur complements and oblique projections," *Linear Algebra and Its Applications*, vol. 341, no. 1–3, pp. 259–272, 2002.

Hindawi
Discrete Dynamics in Nature and Society
Volume 2018, Article ID 6758302, 8 pages
https://doi.org/10.1155/2018/6758302

Research Article

An Improved Computationally Efficient Method for Finding the Drazin Inverse

Haifa Bin Jebreen [1] **and Yurilev Chalco-Cano** [2]

[1] *Mathematics Department, College of Science, King Saud University, Riyadh, Saudi Arabia*
[2] *Departamento de Matematica, Universidad de Tarapaca, Casilla 7D, Arica, Chile*

Correspondence should be addressed to Haifa Bin Jebreen; hjebreen@ksu.edu.sa

Received 2 July 2018; Revised 20 September 2018; Accepted 2 October 2018; Published 17 October 2018

Guest Editor: Tarek F. Ibrahim

Drazin inverse is one of the most significant inverses in the matrix theory, where its computation is an intensive and useful task. The objective of this work is to propose a computationally effective iterative scheme for finding the Drazin inverse. The convergence is investigated analytically by applying a suitable initial matrix. The theoretical discussions are upheld by several experiments showing the stability and convergence of the proposed method.

1. Introductory Notes

Methods for calculating the generalized inverses are a topic of current investigation in computational mathematics (see, e.g., [1, 2]). Enormous amount of work in the topic of generalized inverses has been done during the past 63 years. E.H. Moore (1920) was a pioneer in the area of a generalized algebraic matrix inverse. But intense activities started since 1955 [3, 4]. Note that R. Penrose (1955, 1956), C.R. Rao and S.K. Mitra (1971), and G.H. Golub and W. Kahan (1965) are just a couple of names who have contributed significantly in the area of generalized matrix inverse and its applications leaving very little scope for others to contribute in this area.

The terms "the minimum-norm least squares inverse," "the Moore-Penrose inverse," and "the pseudo-inverse" of a matrix are much more used than the term "Drazin inverse." This unique inverse is globally used for solving linear systems and linear optimization problems.

The fundamental partitioning method of Greville for calculating generalized inverses was discussed in [3]. This method demands many operations and clearly includes more round-off errors. A lot of computational schemes for computing the Drazin inverse lack numerical stability or slow convergence and accordingly it is requisite to study and propose new iterations for this aim.

It is known that cumulative rounding errors must be canceled completely, which is only doable via "symbolic computations." For such a case, variables are handled in the exact form, yielding no loss of precision in the process of computation. However, once the dimension of the input matrix is big, the calculation of its Drazin inverse via symbolic methods would be so time-consuming. This encouraged researchers to recommend computational stable and fast iterative methods for such a purpose; see, e.g., [5–7].

The author in [8] investigated that, in case of having the following square singular linear system

$$Ax = b, \tag{1}$$

the general solution can be represented as follows:

$$x = A^D b + \left(I - AA^D\right) z, \tag{2}$$

using the Drazin inverse, where $z \in \mathscr{R}(A^{k-1}) + \mathscr{N}(A)$.

Let $\mathbb{C}^{N\times N}$ and $\mathbb{C}_r^{N\times N}$ indicate the collection of $N \times N$ complex matrices and ones having rank r, respectively. Furthermore, with A^*, $\mathscr{R}(A)$, $rank(A)$, and $\mathscr{N}(A)$, we indicate the conjugate transpose, the range, the rank, and the null space of the matrix $A \in \mathbb{C}^{N\times N}$, respectively.

In the study of associative rings and semigroups, Drazin in the fundamental work [9] showed a different type of generalized inverse that does not possess the reflexivity feature

while commuting with the entry/element. The significance of this type of inverse and its calculation was then completely provided by Wilkinson in [10].

Before continuing, it is required to recall several useful definitions in what follows.

Definition 1. The smallest nonnegative integer k, so that

$$\operatorname{rank}\left(A^{k+1}\right) = \operatorname{rank}\left(A^{k}\right), \tag{3}$$

is named as the index of A and it is shown by $\operatorname{ind}(A)$.

Definition 2. Assume that A is an $n \times n$ complex matrix; then the Drazin inverse A^D of the matrix A is a unique matrix V that satisfies the following conditions

$$\begin{aligned} &\left(1^k\right)\ A^kVA = A^k,\\ &(2)\ VAV = V,\\ &(5)\ AV = VA, \end{aligned} \tag{4}$$

wherein $k = \operatorname{ind}(A)$ is the matrix index of A.

Recal that once $\operatorname{ind}(A) = 1$, then V is named as the group inverse of A. In addition, if A is nonsingular, thence it is straightforward to observe that $\operatorname{ind}(A) = 0$, and $A^D = A^{-1}$.

Note that the idempotent matrix AA^D is the projector on $\mathscr{R}(A^k)$ alongside $\mathscr{N}(A^k)$, whereas $\mathscr{R}(A^k)$ denotes the range of A^k and $\mathscr{N}(A^k)$ is the null space of A^k. Also, if A is nilpotent, then $A^D = 0$; see [11–14] for more.

Matrix iterations are sensitive upon the choice of the first approximation (V_0) to initiate the scheme and observe the convergence to A^D. Practically speaking, the iterative methods (like the Schulz-type iterations) are effective (particularly for sparse matrices having sparse inverses) but an issue lies in the initial value. However, this requirement was lifted by furnishing several suitable initial values in the literature. A vast discussion on choosing the initial choice V_0 is given in the work [15].

In this work, we concentrate on proposing and investigating a novel matrix iteration for calculating the Drazin inverse quickly and efficiently with a clear concentration on decreasing the elapsed CPU times in contrast to several well-known competitors in the literature. To do this, an analytical discussion will be furnished to manifest the behavior of the presented method. It is proven that the novel approach has a high convergence order using fewer number of matrix-matrix multiplications; i.e., it has a better computational efficiency index.

After a short introduction in Section 1 and a brief review on the most common iterative schemes for calculating the Drazin inverse in Section 2, we propose a novel iterative method for computing the Drazin inverse. Section 3 unfolds our contributed method as a novel high order efficient method. Section 4 furnishes a discussion regarding its convergence rate. Next in Section 5, we study the complexity of the iterative methods to analytically select the best iterative expression. In Section 6, we numerically investigate the application and usefulness of the novel scheme in the calculation of the Drazin inverse. A clear decrease of the elapsed CPU time will be seen therein. Ultimately in Section 7, summary and comments are brought forward.

2. The Literature

One of the fundamental techniques to calculate the inverse of a nonsingular complex matrix A is the Schulz method given in [16] as follows:

$$V_{n+1} = V_n\left(2I - AV_n\right), \quad n = 0, 1, 2, \ldots, \tag{5}$$

wherein I is the unit matrix of the same dimension as A.

In 2004, Li and Wei in [17] proved that the matrix method of Schulz (5) could be applied for calculating the Drazin inverse of square matrices having real or complex eigenvalues. They proposed the following initial matrix

$$V_0 = V_0 = \alpha A^l, \quad l \geq \operatorname{ind}(A) = k, \tag{6}$$

wherein the parameter α should be selected such that the following criterion holds

$$\left\|I - AV_0\right\| < 1. \tag{7}$$

Using the initial matrix of the form (6) along with (5) results in a quadratically convergent iterative scheme for calculating the well-known Drazin inverse.

Let us now briefly review some of the higher order iteration schemes for such a purpose. The notion of the need for efficient schemes is the fact that (5) is slow at its initial stage of iterates, and this would increase the computational burdensome of the scheme applied for matrix inversion.

Li et al. in [18] studied and discussed an iterative method in the following formulation

$$V_{n+1} = V_n\left(3I - AV_n\left(3I - AV_n\right)\right), \quad n = 0, 1, 2, \ldots, \tag{8}$$

with cubic convergence rate and also presented another scheme for calculating A^{-1} (and similarly for A^D using a suitable initial value) of the same order as it is provided in the coming formula:

$$V_{n+1} = V_n\left[I + \frac{1}{2}\left(I - AV_n\right)\left(I + \left(2I - AV_n\right)^2\right)\right], \quad n = 0, 1, 2, \ldots. \tag{9}$$

Recall that a general way for deriving similar iterations was furnished in [19, Chapter 5]. In fact, Krishnamurthy and Sen proposed the following quartically-convergent scheme:

$$V_{n+1} = V_n\left(I + R_n\left(I + R_n\left(I + R_n\right)\right)\right), \quad n = 0, 1, 2, \ldots, \tag{10}$$

in which $R_n = I - AV_n$. As another instance, a ninth-order matrix iteration can be written as follows:

$$\begin{aligned} V_{n+1} = V_n\big(&I + R_n\big(I + R_n\big(I\\ &+ R_n\left(I + R_n\left(I + R_n\left(I + R_n\left(I + R_n\right)\right)\right)\right)\right)\big)\big), \end{aligned} \tag{11}$$

$$n = 0, 1, 2, \ldots.$$

Generally speaking, applying Schröder's general iteration (often named as Schröder-Traub's sequence [20]) to the nonlinear matrix equation

$$AV = I, \tag{12}$$

one can obtain the following scheme [21]:

$$\begin{aligned} V_{n+1} &= V_n\left(I + R_n + R_n^2 + \cdots + R_n^{m-1}\right) \\ &= V_n\left(I + R_n\left(I + R_n\left(\cdots + R_n\right)\cdots\right)\right), \\ & \qquad n = 0, 1, 2, \ldots, \end{aligned} \tag{13}$$

of order m, needing m Horner's matrix products, whereas $R_n = I - AV_n$.

3. Proposing a New Method

Now, we propose a high order scheme which is computationally efficient in terms of the number of matrix-matrix multiplications. Let us first consider a tenth-order method using (13) as follows:

$$V_{n+1} = V_n\left(I + R_n + R_n^2 + \cdots + R_n^9\right). \tag{14}$$

To improve the performance of this scheme, we factorize (14) as much as possible so as to decrease the number of matrix-matrix products. First we can obtain

$$V_{n+1} = V_n\left(I + R_n\left(I + R_n + R_n^2\right)\left(I + R_n^3 + R_n^6\right)\right), \tag{15}$$

which includes seven matrix-matrix multiplications.

By further factorizations and simplifications, we can propose the following iterative method:

$$V_{n+1} = V_n\left(I + R_n\right)\left[\left(I + \alpha R_n^2 + R_n^4\right)\left(I + \beta R_n^2 + R_n^4\right)\right], \tag{16}$$

with only 6 matrix-matrix products per cycle where

$$\begin{aligned} \alpha &= \frac{1}{2}\left(1 - \sqrt{5}\right), \\ \beta &= \frac{1}{2}\left(1 + \sqrt{5}\right). \end{aligned} \tag{17}$$

Obtaining α and β so as to reduce the matrix matrix products is new and not easy. In fact, we should solve a system of equations in symbolic environment so as to do such a task.

The Schulz-type iterations such as (16) are numerically stable; i.e., they have the self-correcting characteristic and are exactly based upon matrix multiplication per cycle. Multiplication is efficiently parallelizable for special matrices. The method (16) could be mixed with sparse-saving techniques so as to decrease the burdensome of matrix-matrix products per cycle.

We can now apply (16) with tenth convergence rate for calculating the Drazin inverse when the first value is selected as follows:

$$V_0 = \frac{2}{\mathrm{Tr}\left(A^{k+1}\right)}A^k, \tag{18}$$

or

$$V_0 = \frac{1}{2\left\|A\right\|_2^{k+1}}A^k, \tag{19}$$

wherein $\mathrm{Tr}(\cdot)$ stands for the trace of an arbitrary square matrix with index k.

Before providing the main theorems regarding the convergence analysis and the rate of convergence of the proposed method, we recall the following lemmas.

Proposition 3 (see [22]). *Let $M \in \mathbb{C}^{n\times n}$ and $\varepsilon > 0$ be given. There is at least one matrix norm $\|\cdot\|$ so that*

$$\rho(M) \le \|M\| \le \rho(M) + \epsilon, \tag{20}$$

where $\rho(M)$ indicates the set of all eigenvalues of M (in the maximum of absolute value sense).

Proposition 4 (see [22]). *If $P_{L,M}$ indicates the projector on a space L along a space M, then*

(i) $P_{L,M}Q = Q$ *iff* $\mathscr{R}(Q) \subseteq L$;

(ii) $QP_{L,M} = Q$ *iff* $\mathscr{N}(Q) \supseteq M$.

4. Convergence Analysis

Theorem 5. *Assume that $A \in \mathbb{C}^{N\times N}$ is a singular square matrix. In addition, let the initial value V_0 be selected via (6) or (18). Thence, the matrices $\{V_n\}_{n=0}^{n=\infty}$ generated via (16) satisfy the following error estimate for calculating the Drazin inverse:*

$$\frac{\left\|A^D - V_n\right\|}{\left\|A^D\right\|} \le \left\|I - AV_0\right\|^{10^n}. \tag{21}$$

Also the convergence speed is ten.

Proof. Let us write

$$\begin{aligned} R_{n+1} &= I - AV_{n+1} = I - A\left(V_n\left(I + R_n\right)\right. \\ &\quad \left.\cdot\left[\left(I + \alpha R_n^2 + R_n^4\right)\left(I + \beta R_n^2 + R_n^4\right)\right]\right) = I \\ &\quad - A\left(V_n\left(I + R_n\left(I + R_n + R_n^2\right)\left(I + R_n^3 + R_n^6\right)\right)\right) \\ &= I \\ &\quad - A\left(V_n\left(I + R_n\left(I + R_n + R_n^2\right)\left(I + R_n^3 + R_n^6\right)\right)\right) \\ &= \left(I - AV_n\right)^{10} = R_n^{10}, \end{aligned} \tag{22}$$

wherein α and β are defined in (17). Applying an arbitrary matrix norm on relation (22), it is possible to write down

$$\left\|R_{n+1}\right\| \le \left\|R_n\right\|^{10}. \tag{23}$$

Since V_0 is chosen as in (6) or (18), it follows that

$$\mathscr{R}\left(V_0\right) \subseteq \mathscr{R}\left(A^k\right). \tag{24}$$

This could now state that

$$\mathscr{R}(V_n) \subseteq \mathscr{R}(V_{n-1}). \tag{25}$$

Thus, we can conclude that

$$\mathscr{R}(V_n) \subseteq \mathscr{R}\left(A^k\right), \quad n \geq 0. \tag{26}$$

Similarly if the novel scheme for the Drazin inverse is defined by left multiplying of V_n, we can state that

$$\mathscr{N}(V_n) \supseteq \mathscr{N}\left(A^k\right), \quad n \geq 0. \tag{27}$$

Now, an application of definition of the Drazin inverse yields

$$AA^D = A^D A = P_{\mathscr{R}(A^k),\mathscr{N}(A^k)}. \tag{28}$$

Proposition 4 along with (26), (27), and (28) could lead to

$$V_n AA^D = V_n = A^D AV_n, \quad n \geq 0. \tag{29}$$

To complete the proof, we proceed in what follows. The error matrix $\delta_n = A^D - V_n$ satisfies

$$\begin{aligned} \delta_n &= A^D - V_n = A^D - A^D AV_n = A^D(I - AV_n) \\ &= A^D R_n. \end{aligned} \tag{30}$$

Using (23), we obtain

$$\|\delta_n\| = \left\|A^D\right\| \|R_n\| \leq \left\|A^D\right\| \|R_0\|^{10^n}, \tag{31}$$

which is a confirmation of (21). As a direct result of (31) and Proposition 4, we can obtain

$$\begin{aligned} A\delta_{n+1} &= AA^D - AV_{n+1} = AA^D - I + I - AV_{n+1} \\ &= AA^D - I + R_{n+1}. \end{aligned} \tag{32}$$

Considering (22) and applying several simplifications, we obtain that

$$A\delta_{n+1} = AA^D - I + R_n^{10}. \tag{33}$$

Applying the idempotent property $(I - AA^D)^t = (I - AA^D)$, $t \geq 1$ being a positive integer from now on, and the following fact of (29):

$$\begin{aligned} \left(I - AA^D\right) A\delta_n &= \left(I - AA^D\right) A\left(A^D - V_n\right) \\ &= V_n - AA^D V_n = 0, \end{aligned} \tag{34}$$

we obtain for each $t \geq 1$ that (here we use (34) in simplifications)

$$\begin{aligned} \left(R_n\right)^t + AA^D - I &= \left(I - AV_n\right)^t + AA^D - I \\ &= \left(I - AA^D + AA^D - AV_n\right)^t \\ &\quad + AA^D - I \\ &= \left(\left(I - AA^D\right) + A\delta_n\right)^t + AA^D - I \\ &= I - AA^D + \left(A\delta_n\right)^t + AA^D - I \\ &= \left(A\delta_n\right)^t. \end{aligned} \tag{35}$$

From (35) and (33), we have

$$A\delta_{n+1} = \left(A\delta_n\right)^{10}. \tag{36}$$

Finally, we get that

$$\left\|A\delta_{n+1}\right\| \leq \left\|A\delta_n\right\|^{10}. \tag{37}$$

It is now straightforward to calculate the error inequality of the proposed iteration (16) considering (37) and the second criterion of (4), when computing the Drazin inverse, as comes next

$$\begin{aligned} \|\delta_{n+1}\| &= \left\|V_{n+1} - A^D\right\| = \left\|A^D AV_{n+1} - A^D AA^D\right\| \\ &= \left\|A^D\left(AV_{n+1} - AA^D\right)\right\| \leq \left\|A^D\right\| \left\|A\delta_{n+1}\right\| \\ &\leq \left\|A^D\right\| \|\delta_n\|^{10}. \end{aligned} \tag{38}$$

The inequalities in (38) lead to the fact that $V_n \longrightarrow A^D$ as $n \longrightarrow +\infty$ with the tenth convergence speed. The proof is ended now. □

Remark 6. An important issue is to find initial approximations V_0. In accordance with Proposition 3, V_0 must read as the following relation to guarantee the convergence in the Drazin inverse case:

$$\max_{1 \leq i \leq t} \left|1 - \lambda_i\left(AV_0\right)\right| < 1, \tag{39}$$

where

$$\operatorname{rank}\left(AV_0\right) = h, \tag{40}$$

and $\lambda_i(AV_0)$, $i = 1, 2, \ldots, h$, are eigenvalues of AV_0.

5. Efficiency Comparison

The computational complexity of the matrix inverse is O(mn-squared), where the order of the matrix is $m \times n$ (a rectangular matrix). Broadly speaking, if the complexity $O(n$-cubed) is brought down to $O(n^k)$, where $k < 3$, say 2.9 for a general matrix, then it is definitely an achievement. Reducing the complexity by a linear factor is not attractive since what we have currently in 2018 is exa-flops computing speed and desktop and laptop computers are available in 100s of millions worldwide unlike the period during mid-20th centuries.

Thus, we calculate and compare theoretically the computational efficiencies of various schemes (5), (8), (9), (10), (11), and (16), since they all could converge to A^D upon the choice of a suitable initial value (6).

By considering a unit cost for the arithmetic operations, typical of the floating point calculations, we can take into account the *inverse-finder informational efficiency index*. This index applies two values ρ and κ, which are for the convergence speed and the number of matrix-matrix products, respectively. Hence, this index is given by [20]

$$IIEI = \frac{\rho}{\kappa}. \tag{41}$$

Apart from this index, another useful one which is mainly in agreement with the CPU elapsed time of the iterative methods in numerical linear algebra is the *computational efficiency index* defined by [23]

$$CEI = \rho^{1/\kappa}. \tag{42}$$

Therefore, a fruitful scheme in analytical standpoint should achieve the speed ρ with fewer matrix products κ in contrast to the competitors (viz, $\kappa \leq \rho$).

In Table 1, we provide a comparison of the number of matrix products and the rate of convergence, accompanied by (41) and (42) for various schemes. The results indicate that the proposed scheme in Section 3 is more efficient than its competitors.

As a matter of fact, one may observe that the proposed iteration (16) decreases the calculation burdensome via applying fewer operations and yields a better balance between the higher order and the computational load. This fact will be numerically investigated later in Section 6.

6. Experiments

This section studies issues associated with the computational accuracy and times of finding the Drazin inverse. The new iteration (16) is free from matrix power in its implementation and this allows one to apply it for finding generalized inverses easily. For computational comparisons, we have used the methods (5), (8), (9), (10), (11), and (16), denoted by "SM2," "CM3," "LM3," "KMS4," "HM9," and "PM10," respectively.

A couple of remarks are in order:

(i) The simulations are done in Mathematica 11.0 [24].

(ii) The time needed to obtain the approximate inverses is reported in seconds.

(iii) Whenever the elapsed times are reported, the compared methods are programmed in the same environment.

Experiment 1. The aim of this experiment is to calculate the Drazin inverse while the input matrix is [17]

$$A = \begin{bmatrix} 2 & 0.4 & 0 & 0 & 0 & 0 & 0 & 0 & 0 & 0 & 0 & 0 \\ -2 & 0.4 & 0 & 0 & 0 & 0 & 0 & 0 & 0 & 0 & 0 & 0 \\ -1 & -1 & 1 & -1 & 0 & 0 & 0 & 0 & -1 & 0 & 0 & 0 \\ -1 & -1 & -1 & 1 & 0 & 0 & 0 & 0 & 0 & 0 & 0 & 0 \\ 0 & 0 & 0 & 0 & 1 & 1 & -1 & -1 & 0 & 0 & -1 & 0 \\ 0 & 0 & 0 & 0 & 1 & 1 & -1 & -1 & 0 & 0 & 0 & 0 \\ 0 & 0 & 0 & -1 & -2 & 0.4 & 0 & 0 & 0 & 0 & 0 & 0 \\ 0 & 0 & 0 & 0 & 2 & 0.4 & 0 & 0 & 0 & 0 & 0 & 0 \\ 0 & -1 & 0 & 0 & 0 & 0 & 0 & 0 & 1 & -1 & -1 & -1 \\ 0 & 0 & 0 & 0 & 0 & 0 & 0 & 0 & -1 & 1 & -1 & -1 \\ 0 & 0 & 0 & 0 & 0 & 0 & 0 & 0 & 0 & 0 & 0.4 & -2 \\ 0 & 0 & 0 & 0 & 0 & 0 & 0 & 0 & 0 & 0 & 0.4 & 2 \end{bmatrix}, \tag{43}$$

with $k = \text{ind}(A) = 3$. The exact Drazin inverse is given by

$$A^D = \begin{bmatrix} 0.25 & -0.25 & 0. & 0. & 0. & 0. & 0. & 0. & 0. & 0. & 0. & 0. \\ 1.25 & 1.25 & 0. & 0. & 0. & 0. & 0. & 0. & 0. & 0. & 0. & 0. \\ -1.66406 & -0.992187 & 0.25 & -0.25 & 0. & 0. & 0. & 0. & -0.0625 & -0.0625 & 0. & 0.15625 \\ -1.19531 & -0.679687 & -0.25 & 0.25 & 0. & 0. & 0. & 0. & -0.0625 & 0.1875 & 0.6875 & 1.34375 \\ -2.76367 & -1.04492 & -1.875 & -1.25 & -1.25 & 1.25 & 1.25 & 1.25 & 1.48438 & 2.57813 & 3.32031 & 6.64063 \\ -2.76367 & -1.04492 & -1.875 & -1.25 & -1.25 & 1.25 & 1.25 & 1.25 & 1.48438 & 2.57813 & 4.57031 & 8.51563 \\ 14.1094 & 6.30078 & 6.625 & 3.375 & 5. & -3. & -5. & -5. & -4.1875 & -8.5 & -10.5078 & -22.4609 \\ -19.3242 & -8.50781 & -9.75 & -5.25 & -7.5 & 4.5 & 7.5 & 7.5 & 6.375 & 12.5625 & 15.9766 & 33.7891 \\ -0.625 & -0.3125 & 0. & 0. & 0. & 0. & 0. & 0. & 0.25 & -0.25 & -0.875 & -1.625 \\ -1.25 & -0.9375 & 0. & 0. & 0. & 0. & 0. & 0. & -0.25 & 0.25 & -0.875 & -1.625 \\ 0. & 0. & 0. & 0. & 0. & 0. & 0. & 0. & 0. & 0. & 1.25 & 1.25 \\ 0. & 0. & 0. & 0. & 0. & 0. & 0. & 0. & 0. & 0. & -0.25 & 0.25 \end{bmatrix}. \tag{44}$$

The stopping termination is $\|V_{k+1} - V_k\|_\infty \leq \epsilon$ with $\epsilon = 10^{-8}$. Checking the conditions of Definition 2 for our proposed iterative method PM10 yields

$$\begin{aligned} \left\|A^{k+1}A^D - A^k\right\|_\infty &= 3.69638 \times 10^{-12}, \\ \left\|A^D A A^D - A^D\right\|_\infty &= 8.43992 \times 10^{-10}, \\ \left\|A A^D - A^D A\right\|_\infty &= 3.75205 \times 10^{-10}, \end{aligned} \tag{45}$$

which supports the theoretical discussions.

The practical application of the new scheme (16) lies in several problems; see, for example, [25, 26]. For instance, in the process of resolving second-kind integral equations via Wavelet-like technique, the whole discretized problem will be yielded to calculate the inverse of a large sparse matrix [27].

Additionally, we can apply/use (16), as an approach to provide good preconditioners for speeding-up modern Krylov methods, such as GMRES or BiCGSTAB, for solving large scale sparse linear systems; see, e.g., [28]. For such a task, we need to define a new initial matrix defined in Table 2 [29].

In modern numerical linear algebra, schemes like (16) should be coded in sparse form using some well-known commands such as `SparseArray[]` to reduce the computational burden and preserve the sparsity feature of the approximate inverse per computing step.

It is necessary to test the behavior of the new method in a fair environment with a clear comparison taking into account various competitors. On the other hand, since the generation of random square matrices having Drazin inverses is difficult, in what follows, we compare various competitors in terms of the elapsed computational time so as to attain regular approximate inverses for large sparse matrices.

Experiment 2. The aim of this experiment is to compare the elapsed CPU times of different methods for the following 25 large sparse random complex matrices:

```
SeedRandom[123]
n = 5000; number = 25;
Table[
    A[j] = SparseArray[{Band[{-100, 1100
    }] -> RandomReal[20],
        Band[{1, 1}] -> 2.,
        Band[{1000, -50}, {n - 20, n - 25
        }] -> {2.8, RandomReal[] + I},
        Band[{600, 150},
        {   n - 100, n - 400   }   ] ->   {
        -RandomReal[3], 3. + 3 I}}
    , {n, n}, 0.], {j, number}];
```

Here $I = \sqrt{-1}$. In this test, the stopping criterion is $\|V_{n+1} - V_n\|_1 \leq 10^{-6}$ and the maximum number of iterations allowed is set to 75. Moreover, the initial value is constructed via Form 3 of Table 2.

The results of comparisons for this test are presented in Figure 1. As is obvious that higher order methods require lower number of iterations to converge, thus we then put our focus on the computational time needed to satisfy the desired tolerance. As could be observed, our scheme (16) beats its competitors and also supports the analytical reports in Table 1.

Experiment 3. Here we rerun Experiment 2 with the stopping termination $\|V_{n+1} - V_n\|_\infty \leq 10^{-4}$ and initial value chosen by Form 2 of Table 2. The results are summarized in Figure 2. Furthermore, to check the usefulness of PM10, we rerun

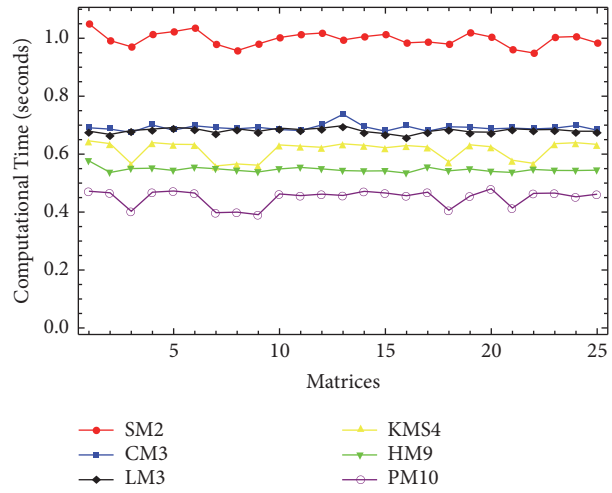

Figure 1: Comparison of the elapsed times for various methods in Experiment 2.

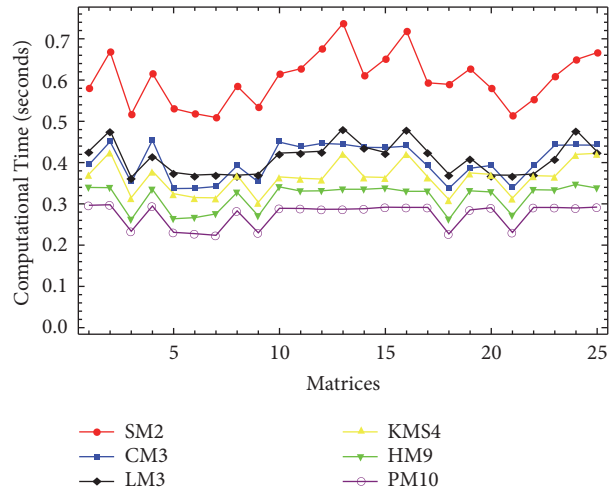

Figure 2: Comparison of the elapsed times for various methods in Experiment 3.

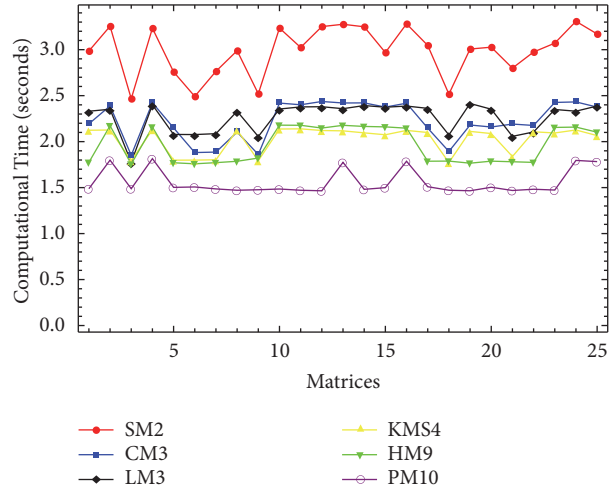

Figure 3: Comparison of the elapsed times for various methods in Experiment 3 for larger sizes $A_{10000\times10000}$ and a different initial value.

Table 1: A comparison on the calculational burdensome of various methods applying different indices.

Methods	(5)	(8)	(9)	(10)	(11)	(16)
ρ	2	3	3	4	9	6
κ	2	3	4	4	9	10
IIEI	$\frac{2}{2}=1$	$\frac{3}{3}=1$	$\frac{3}{4}=0.75$	$\frac{4}{4}=1$	$\frac{9}{9}=1$	$\frac{10}{6}\approx 1.666$
CEI	$2^{1/2}\simeq 1.414$	$3^{1/3}\simeq 1.442$	$3^{1/4}\simeq 1.316$	$4^{1/4}\simeq 1.414$	$9^{1/9}\simeq 1.276$	$10^{1/6}\simeq 1.467$

Table 2: Several choices for V_0 (for calculating A^{-1}).

Different ways	Form 1	Form 2	Form 3	Form 4	Form 5
Initial value	$\frac{A}{\|A\|_1^2}$	$\frac{A}{\|A\|_\infty^2}$	$\frac{A}{\|A\|_F^2}$	$\frac{A^T}{N\|A\|_1\|A\|_\infty}$	$\frac{A^*}{\|A\|_2^2}$

Experiment 2 with larger sizes matrices, i.e., when $n = 10000$, the stopping termination $\|V_{n+1} - V_n\|_\infty \leq 10^{-4}$ and initial value chosen by Form 1 of Table 2. The results of comparisons for this case are given in Figure 3.

The attained results have reverified the robustness of the proposed iterative method (16) by a clear reduction in the elapsed CPU times.

Note that the 10th-order method is better than a fourth-order method in CPU time. However, this is more tangible if a sharp initial approximation is chosen meaning that the 10th-order method arrives at the convergence phase quickly.

We also emphasise that the construction of any higher order method is meaningful only if we observe an improvement in CEI as discussed in Section 5. Accordingly, a member of the family (13) should be chosen such that we could arrive at the unknown parameters (e.g., like (17)) in order to improve CEI. An attempt to find an optimal iteration in this way is still a research topic in the field.

Remark 7. With the standard precision of 15 digits (most widely used globally, e.g., in Matlab or Mathematica), convergence of order 2 or 3 has been found to be computationally (amount of numerical computation) optimal [19].

7. Summary and Remarks

The Drazin inverse is investigated in the matrix theory (particularly in the topic of generalized inverses) and also in the ring theory; see, e.g., [30].

In this work, we have investigated a higher-order matrix scheme (16) for calculating the Drazin inverse. Convergence analysis of our scheme has been discussed and an investigation on the selection of the initial approximation so as to initiate the iterates and keep the convergence speed was furnished. We also discussed under what conditions the novel scheme can be taken into account for calculating the Drazin inverse of square matrices.

Furthermore, the total elapsed timings consuming of the proposed scheme (16) is low in contrast to the competitors of this type in the case of constructing approximate inverses.

Tackling on the generalization of the new scheme (16) for interval matrix inversion or the application of such matrix methods in option pricing in order to act as a preconditioner to reduce the ill-conditioning of the large sized matrices occuring in the process of pricing (see, e.g., [31]) could be taken into account as future investigations in this field of study.

Data Availability

The data used to support the findings of this study are included within the article.

Disclosure

The funding body had no role in the design of the study and collection, analysis, and interpretation of data and in writing the manuscript.

Conflicts of Interest

The authors declare that they have no conflicts of interest.

Acknowledgments

This research project was supported by a grant from the Research Center of the Female Scientific and Medical Colleges, Deanship of Scientific Research, King Saud University.

References

[1] M. Ghorbanzadeh, K. Mahdiani, F. Soleymani, and T. Lotfi, "A class of Kung-Traub-type iterative algorithms for matrix inversion," *International Journal of Applied and Computational Mathematics*, vol. 2, no. 4, pp. 641–648, 2016.

[2] X. Liu, G. Zhu, G. Zhou, and Y. Yu, "An analog of the adjugate matrix for the outer inverse AT,S (2)," *Mathematical Problems in Engineering*, Art. ID 591256, 14 pages, 2012.

[3] A. Ben-Israel and T. N. E. Greville, *Generalized Inverses: Theory and Applications*, Springer, New York, NY, USA, 2nd edition, 2003.

[4] A. Kumar, P. S. Stanimirović, F. Soleymani, M. Krstić, and K. Rajković, "Factorizations of hyperpower family of iterative methods via least squares approach," *Computational & Applied Mathematics*, vol. 37, no. 3, pp. 3226–3240, 2018.

[5] I. I. Kyrchei, "Cramer's Rule for Generalized Inverse Solutions," in *Advances in Linear Algebra Research*, I. Kyrchei, Ed., pp. 79–132, Nova Science Publishers, New York, NY,USA, 2015.

[6] V. Y. Pan, F. Soleymani, and L. Zhao, "An efficient computation of generalized inverse of a matrix," *Applied Mathematics and Computation*, vol. 316, pp. 89–101, 2018.

[7] F. Soleymani, "A Rapid Numerical Algorithm to Compute Matrix Inversion," *International Journal of Mathematics and Mathematical Sciences*, vol. 2012, Article ID 134653, 11 pages, 2012.

[8] Y. Wei, "Index splitting for the Drazin inverse and the singular linear system," *Applied Mathematics and Computation*, vol. 95, no. 2-3, pp. 115–124, 1998.

[9] M. P. Drazin, "Pseudo-inverses in associative rings and semigroups," *The American Mathematical Monthly*, vol. 65, pp. 506–514, 1958.

[10] J. H. Wilkinson, "Note on the practical significance of the Drazin inverse," in *Recent Applications of Generalized Inverses*, S. L. Campbell, Ed., vol. 66 of *Research Notes in Mathematics*, pp. 82–99, Pitman Advanced Publishing Program, Boston, 1982.

[11] I. Kyrchei, "Explicit formulas for determinantal representations of the Drazin inverse solutions of some matrix and differential matrix equations," *Applied Mathematics and Computation*, vol. 219, no. 14, pp. 7632–7644, 2013.

[12] F. Soleymani, P. S. Stanimirović, and F. Khaksar Haghani, "On hyperpower family of iterations for computing outer inverses possessing high efficiencies," *Linear Algebra and its Applications*, vol. 484, pp. 477–495, 2015.

[13] Y. Xia, T. Chen, and J. Shan, "A novel iterative method for computing generalized inverse," *Neural Computation*, vol. 26, no. 2, pp. 449–465, 2014.

[14] L. Zhao, "The Expression of the Drazin Inverse with Rank Constraints," *Journal of Applied Mathematics*, vol. 2012, Article ID 390592, 10 pages, 2012.

[15] V. Y. Pan, *Structured matrices and polynomials*, BirkhWauser Boston, Inc., Boston, MA; Springer-Verlag, New York, 2001.

[16] G. Schulz, "Iterative Berechung der reziproken Matrix," *ZAMM - Zeitschrift für Angewandte Mathematik und Mechanik*, vol. 13, no. 1, pp. 57–59, 1933.

[17] X. Li and Y. Wei, "Iterative methods for the Drazin inverse of a matrix with a complex spectrum," *Applied Mathematics and Computation*, vol. 147, no. 3, pp. 855–862, 2004.

[18] H.-B. Li, T.-Z. Huang, Y. Zhang, V.-P. Liu, and T.-V. Gu, "Chebyshev-type methods and preconditioning techniques," *Applied Mathematics and Computation*, vol. 218, no. 2, pp. 260–270, 2011.

[19] E. V. Krishnamurthy and S. K. Sen, *Numerical Algorithms: Computations in Science and Engineering*, Affiliated East-West Press, New Delhi, India, 2007.

[20] J. F. Traub, *Iterative Methods for the Solution of Equations*, Prentice-Hall, New York, NY. USA, 1964.

[21] S. K. Sen and S. S. Prabhu, "Optimal iterative schemes for computing the Moore-Penrose matrix inverse," *International Journal of Systems Science*, vol. 7, no. 8, pp. 847–852, 1976.

[22] F. Soleymani and P. S. Stanimirović, "A Higher Order Iterative Method for Computing the Drazin Inverse," *The Scientific World Journal*, vol. 2013, Article ID 708647, 11 pages, 2013.

[23] A. M. Ostrowski, "Sur quelques transformations de la serie de LiouvilleNewman," *Comptes rendus de l'Académie des Sciences, Paris*, vol. 206, pp. 1345–1347, 1938.

[24] M. Trott, *The Mathematica guidebook for numerics*, Springer, New York, NY, USA, 2006.

[25] S. L. Campbell, C. D. Meyer Jr., and N. J. Rose, "Applications of the Drazin inverse to linear systems of differential equations with singular constant coefficients," *SIAM Journal on Applied Mathematics*, vol. 31, no. 3, pp. 411–425, 1976.

[26] N. C. González, J. J. Koliha, and V. Rakocević, "Continuity and general perturbation of the Drazin inverse for closed linear operators," *Abstract and Applied Analysis*, vol. 7, pp. 335–347, 2002.

[27] B. Alpert, G. Beylkin, R. Coifman, and V. Rokhlin, "Wavelet-like bases for the fast solution of second-kind integral equations," *SIAM Journal on Scientific Computing*, vol. 14, no. 1, pp. 159–184, 1993.

[28] Y. Saad, *Iterative Methods for Sparse Linear Systems*, SIAM, 2nd edition, 2003.

[29] J. Rajagopalan, *An iterative algortihm for inversion of matrices, M.Sc. Thesis*, Concordia University, Canada, 1996.

[30] B. Cantó, C. Coll, and E. Sánchez, "Identifiability for a Class of Discretized Linear Partial Differential Algebraic Equations," *Mathematical Problems in Engineering*, vol. 2011, Article ID 510519, 12 pages, 2011.

[31] R. Company, V. N. Egorova, L. Jodar, and F. Soleymani, "A local radial basis function method for high-dimensional American option pricing problems," *Mathematical Modelling and Analysis*, vol. 23, no. 1, pp. 117–138, 2018.

Hindawi
Discrete Dynamics in Nature and Society
Volume 2018, Article ID 3151742, 13 pages
https://doi.org/10.1155/2018/3151742

Research Article

New Qualitative Results for Solutions of Functional Differential Equations of Second Order

Cemil Tunç and Sultan Erdur

Department of Mathematics, Faculty of Sciences, Van Yuzuncu Yil University, Campus, 65080, Van, Turkey

Correspondence should be addressed to Cemil Tunç; cemtunc@yahoo.com

Received 12 August 2018; Accepted 18 September 2018; Published 9 October 2018

Guest Editor: Abdul Qadeer Khan

In this paper, we are concerned with the existence of periodic solutions, stability of zero solution, asymptotic stability of zero solution, square integrability of the first derivative of solutions, and boundedness of solutions of nonlinear functional differential equations of second order by the second method of Lyapunov. We obtain sufficient conditions guaranteeing the existence of periodic solutions, stability of zero solution, asymptotic stability of zero solution, square integrability of the first derivative of solutions, and boundedness of solutions of the equations considered. We give an example for illustrations by MATLAB-Simulink, which shows the behaviors of the orbits. The findings of this paper extend and improve some results that can be found in the literature.

1. Introduction

Differential equations of second order with and without delay(s) can find a wide range of applications in atomic energy, biology, chemistry, control theory, economy, engineering technique fields, information theory, medicine, physics, population dynamics, and so forth (see Burton [1], El'sgol'ts [2], Hale [3], Krasovskii [4], Smith [5], and Yoshizawa [6]). During investigations, we would naturally be inclined to compute the solutions of differential equations of second order with and without delay(s) explicitly or numerically. However, as we know from practice, there are very few such equations, for example, linear equations with constant coefficients, but without delay(s), for which this can be effectively done. Further, it should be noted that finding analytical or explicit solutions of differential equations of second order with delay(s) is more difficult, even if, to the best of our knowledge, there is no general method in the literature to find the explicit solutions of those equations. In addition, most of the times, it is impossible to find analytical solutions for those equations. The problem therefore is to find convenient techniques that will be useful in obtaining some qualitative information such as stability, instability, convergence, global existence, integrability, boundedness of solutions, existence of periodic solutions, and so forth about the elusive solutions of ordinary or delay differential equations.

From the past till now, various methods have been constructed and are still discussed in order to investigate the various qualitative behaviors of solutions of ordinary or delay differential equations without solving those equations.

However, here, we would only like to summarize some works that can be found in the literature and methods used during the investigations of the existence of the periodic solutions, stability, asymptotic stability, square integrability, and boundedness of solutions of ordinary and functional differential equations of second order.

Yoshizawa [6] considered the following nonlinear differential equation of second order with constant delay:

$$x'' + \phi\left(t, x'\right) + f\left(x\left(t-\tau\right)\right) = p\left(t\right) \tag{1}$$

and he investigated the existence of $\omega-$periodic solutions of this equation by using the second method of Lyapunov.

Zhao at al. [7] obtained sufficient conditions for the existence of $\omega-$periodic solutions of the below nonlinear differential equation of second order with constant delay

$$x'' + ax' + g\left(x\left(t-\tau\right)\right) = p\left(t\right) \tag{2}$$

by the second method of Lyapunov.

Cong [8] considered a class of nonlinear differential equations of second order in the form

$$\frac{d}{dt}\left[p(t)\frac{dx}{dt}\right] + f(t,x) = 0. \tag{3}$$

Cong [8] proved that there exists a unique 2π−periodic solution of those differential equations under Landesman–Lazer type conditions by applying the Leray–Schauder principle.

Guo and Xu [9] studied the existence of periodic solutions of a differential equation of second order with a deviating argument by means of Mawhin's continuation theorem. In [9], a new result on the existence of periodic solutions is obtained.

Ji and Dong [10] discussed the existence and uniqueness of periodic solutions for a class of nonlinear differential equations of second order by using a comparison theorem and Leray-Schauder degree theory. The results obtained in [10] generalize and refine a recent work that can be found in the literature.

Tian and Zeng [11] studied the existence of periodic solutions to the second-order functional differential equation

$$\begin{aligned} &x''(t) + f(t, x(t), x(t-\tau(t)))\left(x'(t)\right)^n + a(t)x^2(t) \\ &\quad + b(t)x(t) = p(t), \quad n \geq 2, \end{aligned} \tag{4}$$

by applying Mawhin's continuation theorem of coincidence degree theory. In [11], some new results on the existence of at least two periodic solutions to this equation are obtained.

Li and Li [12] obtained existence results of positive ω−periodic solutions for the following functional differential equation of second order with multiple variable delays:

$$\begin{aligned} &u''(t) + a(t)u(t) \\ &\quad = f\left(t, u(t), u\left(t-\tau_1(t)\right), \ldots, u\left(t-\tau_n(t)\right)\right). \end{aligned} \tag{5}$$

In [12], the existence conditions concern the first eigenvalue of the associated linear periodic boundary problem and the discussion is based on the fixed-point index theory in cones.

Li and Zhang [13] established several criteria for the existence, multiplicity, and nonexistence of positive periodic solutions of the following system

$$x'' + A(t)x = f(t,x) \tag{6}$$

by combining some new properties of Green's function together with Krasnoselskii's fixed-point theorem on the compression and expression of cones.

Zu [14] studied periodic solutions for the following nonlinear second-order ordinary differential equation:

$$x'' = f\left(t, x, x'\right). \tag{7}$$

By constructing upper and lower boundaries and using Leray-Schauder degree theory, the author presented a result about the existence and uniqueness of a periodic solution for the above second-order ordinary differential equation with some assumptions.

Tunç and Yazgan [15] took into consideration the following nonlinear differential equation of second order with multiple fixed delays:

$$\begin{aligned} &x'' + \left[f\left(x, x'\right) + g\left(x, x'\right)x'\right]x' + h(x) \\ &\quad + \sum_{i=1}^{n} g_i\left(x\left(t-\tau_i\right)\right) = p(t) \end{aligned} \tag{8}$$

and they obtained the sufficient conditions for the existence of periodic solutions of this delay equation by the second method of Lyapunov.

Ma and Lu [16] showed the existence of positive T–periodic solutions of the below second-order functional differential equation:

$$u''(t) - p^2 u(t) + \lambda g(t) f\left(u\left(t-\tau(t)\right)\right) = 0. \tag{9}$$

The approach in [16] is based on global bifurcation theorem.

Jia and Shao [17] established sufficient conditions for the existence and uniqueness of periodic solutions of an ordinary differential equation of second order by applying Mawhin's continuation theorem of coincidence degree theory.

Ardjouni and Djoudi ([18, 19]) discussed the existence of periodic and positive periodic solutions for a class of nonlinear neutral differential equations of second order with variable delays by Burton-Krasnoselskii's hybrid fixed-point theorem.

Similarly, Lü et al. [20] and Tian [21] investigated the existence of multiple positive periodic solutions for certain ordinary differential equations of second order and a delay differential equation of second order, respectively. In addition, Zhang and Wang [22] studied the existence of periodic solutions for a class of second-order functional differential equations with deviating arguments by using the abstract continuation theorem of k−set contractive operator and some analysis techniques.

Zhou [23] considered the existence of periodic solutions for a class of semilinear second-order differential equations of the form

$$-x'' + f\left(t, x, x'\right)x' + e(t)g(x) = h(t). \tag{10}$$

By applying the viscosity solutions method and the classical upper-lower solutions method, as well as the Leray-Schauder fixed-point principle, the author established the existence of periodic solutions. The result of Zhou [23] improves and generalizes many results on the ropes mechanics equations in the existing literature.

Wei [24] proved the existence and uniqueness of periodic solutions for second-order ordinary differential equation

$$x'' = f\left(t, x, x'\right) \tag{11}$$

under some assumptions on the function f. The proofs in [24] are based on Schauder's fixed-point theorem.

Finally, more recently, Zhu and Li [25] discussed the existence of periodic solutions for the below differential equation of second order with multiple delays

$$\begin{aligned} &-u''(t) \\ &\quad = f\left(t, u(t), u\left(t-\tau_1\right), u\left(t-\tau_2\right), \ldots, u\left(t-\tau_n\right)\right) \end{aligned} \tag{12}$$

by using the monotone iterative method of upper and lower solutions.

Besides, for some other related papers, one can look at the book of Yoshizawa [26], the paper of Tunç and Çinar [27], and the references that can be found in the sources mentioned above.

In fact, through the papers or books presented above, it can be seen that the second method of Lyapunov has rarely been used to investigate the existence of periodic solutions of nonlinear differential equations of second order with and without delay(s) instead of the other mentioned methods. To the best of our knowledge, the basic reason for the lack of the papers by this method is to find suitable Lyapunov function(s) or functional(s), which give(s) meaningful results. In this paper, we study the existence of the periodic solutions by defining suitable new Lyapunov functionals. This is a contribution of this paper to the subject and literature.

On the other hand, the problems of the stability, asymptotic stability, convergence, integrability, and boundedness of solutions of linear and nonlinear differential equations of second order with and without delay(s) can appear in various physical, engineering, and many other scientific models. These kinds of differential equations are significant in describing fluid mechanical, nonlinear elastic mechanical phenomena, investigation of stability and instability of geodesic on Riemannian manifolds, dynamics process in electromechanical systems of physics and engineering, and so on. Many important theoretical and applied results related to these properties of solutions of differential equations of second order with and without delay(s) can be found in the literature (see Ahmad and Rama Mohana Rao [28], Burton [18], Burton and Hering [29], El'sgol'ts [2], Hale [3], Heidel [30], Kato [31, 32], Korkmaz and Tunç [33], Krasovskii [4], Liu and Huang [34, 35], Luk [36], Malyseva [37], Muresan [38], Mustafa and Tunç [39], Napoles Valdes [40], Amano [41], Sugie et al. [42], Tunç [43–52], Tunç and Dinç [53], Tunç and Tunç [54–57], Ye et al. [58], Yoshizawa [6], Yu and Xiao [59], Yu and Zhao [60], Zhang [61], Zhou and Xiang [62], and Zhou and Jiang [63] and their references).

In the sources mentioned, the second method of Lyapunov, perturbation theory, fixed-point method or theory, iterative techniques, the variation of constants formula, and some other tools are used to investigate the mentioned qualitative behaviors of solutions of linear and nonlinear differential equations of second order with and without delay(s). Here, for the sake of brevity, we would not like to give more details about these subjects. In addition, in view of the information given above, we would like to say that it is worthwhile to continue the investigation of the qualitative properties of the solutions of nonlinear differentials of second order with delay(s).

In this paper, we consider the following functional nonlinear differential equation of second order:

$$\left[a(t)x'\right]' + \phi\left(t, x'\right) + h\left(t, x'(t-\tau)\right) + g(x) + f(x(t-\tau)) = e\left(t, x, x'\right), \tag{13}$$

where $t \in \mathfrak{R}^+$, $\mathfrak{R}^+ = [0, \infty)$, $\tau \in \mathfrak{R}$, $\tau > 0$, if fixed constant delay, $x \in \mathfrak{R}$, $\mathfrak{R} = (-\infty, \infty)$, $a(t)$ is a continuous differentiable positive and $\omega-$periodic function with $\omega > 0$, $\omega \in \mathfrak{R}$, $a(t+\omega) = a(t)$; ϕ, h, and e are continuous functions according to their related arguments and $\omega-$periodic in t. That is, $\phi(t+\omega, x') = \phi(t, x')$, $h(t+\omega, x'(t-\tau)) = h(t, x'(t-\tau))$, and $e(t+\omega, x, x') = e(t, x, x')$. Finally, $f(x)$ and $g(x)$ are continuous differentiable functions with $f(0) = g(0) = 0$.

The following system can be written from (13):

$$\begin{aligned}
\dot{x} &= y,\\
\dot{y} &= -\frac{a'(t)}{a(t)}y - \frac{1}{a(t)}\phi(t, y) - \frac{1}{a(t)}h\left(t, y(t-\tau)\right)\\
&\quad - \frac{1}{a(t)}g(x) - \frac{1}{a(t)}f(x)\\
&\quad + \frac{1}{a(t)}\int_{-\tau}^{0} f'(x(t+\theta))\, y(t+\theta)\, d\theta\\
&\quad + \frac{1}{a(t)}e(t, x, y).
\end{aligned} \tag{14}$$

To the best of our knowledge from the literature, we did not find any paper on the existence of periodic solutions, stability, asymptotic stability, square integrability, and boundedness of solutions of a mathematical model like (13). The purpose of this paper is to give new sufficient hypotheses, five theorems, with an example by MATLAB-Simulink on existence of periodic solutions, stability of zero solution, asymptotic stability of zero solution, square integrability of the first derivative of solutions, and boundedness of solutions of (13) by the second method of Lyapunov. By the results of this paper, we extend and improve some results that can be found in the references of this paper (see [1–63]). These are the contributions of this paper to the mentioned topics and relevant literature.

2. Existence of Periodic Solutions

We now establish our some basic assumptions.

(A) Hypotheses. We suppose that the following hypotheses hold:

(A1) $a_0 \geq a(t) \geq 1$,

$a'(t) \geq 0$,

$a_0 \in \mathfrak{R}$, $t \in \mathfrak{R}^+$.

(A2) $\dfrac{\phi(t, y)}{y} > \alpha a(t) > 0$ for $|y| \geq A$, $(y \neq 0)$,

$\dfrac{h\left(t, y(t-\tau)\right)}{y} \geq b_0 > 0$

for $|y| \geq A$, $(y \neq 0)$, $t \in \mathfrak{R}^+$, $y \in \mathfrak{R}$,

$$
\begin{aligned}
&g(0) = 0,\\
&g(x)\operatorname{sgn} x \longrightarrow \infty\\
&\qquad \text{for } |x| \longrightarrow \infty,\ \left|g'(x)\right| \le L_0,\\
&f(0) = 0,\\
&f(x)\operatorname{sgn} x \longrightarrow \infty\\
&\qquad \text{for } |x| \longrightarrow \infty,\ \left|f'(x)\right| \le L,\ x \in \mathfrak{R},
\end{aligned}
\tag{15}
$$

where α, A, b_0, L_0, L, and $b_0 \in \mathfrak{R}$ are some positive real constants with $b_0 \ge 1$ and $\tau < \alpha/2L$.

$$
(A3)\quad \left|e(t,x,y)\right| \le \frac{\alpha a(t)\left|y\right|}{4},\quad t \in \mathfrak{R}^+,\ x, y \in \mathfrak{R}. \tag{16}
$$

Our first theorem for the existence of periodic solutions of system (14) can be given below.

Theorem 1. *If hypotheses* $(A1) - (A3)$ *hold, then system (14) has a* ω*-periodic solution.*

Proof. Let $V_0 = V_0(t, x_t, y_t)$ be a Lyapunov functional defined by

$$
\begin{aligned}
V_0 = {} & \frac{2}{a(t)}\int_0^x f(s)\,ds + \frac{2}{a(t)}\int_0^x g(s)\,ds + y^2\\
& + \frac{\alpha}{2\tau}\int_{-\tau}^{0}\left(\int_s^0 y^2(\theta)\,d\theta\right)ds\\
& + L\int_{-\tau}^{0}\left(\int_s^0 \left|y(\theta)\right|d\theta\right)ds.
\end{aligned}
\tag{17}
$$

It is obvious that the Lyapunov functional V_0 is positive definite.

By calculating the time derivative of the Lyapunov functional V_0 with respect to t along system (14) and by usage of hypotheses $(A1) - (A3)$ of Theorem 1, we have

$$
\begin{aligned}
\frac{d}{dt}V_0 \le {} & -\frac{2a'(t)}{a(t)}y^2 - \frac{2}{a(t)}\frac{\phi(t,y)}{y}y^2\\
& - \frac{2}{a(t)}\frac{h(t, y(t-\tau))}{y}y^2\\
& + \frac{2}{a(t)}y\int_{-\tau}^{0} f'(x(t+\theta))\,y(t+\theta)\,d\theta + \frac{\alpha}{2}y^2\\
& + L\tau\left|y\right| - L\int_{-\tau}^{0}\left|y(t+\theta)\right|d\theta\\
& + \frac{\alpha}{2\tau}\int_{-\tau}^{0} y^2(t)\,d\theta - \frac{\alpha}{2\tau}\int_{-\tau}^{0} y^2(t+\theta)\,d\theta.
\end{aligned}
\tag{18}
$$

It is clear that

$$
-\frac{2a'(t)}{a(t)} \le 0 \tag{19}
$$

by hypothesis $(A1)$ of Theorem 1. Then, from (18), we can write

$$
\begin{aligned}
\frac{dV_0}{dt} \le {} & -2\alpha y^2\\
& + \frac{2}{a(t)}\int_{-\tau}^{0}\left|f'(x(t+\theta))\right|\left|y(t)\right|\left|y(t+\theta)\right|d\theta\\
& + \frac{\alpha}{2}y^2 + L\tau\left|y\right| - L\int_{-\tau}^{0}\left|y(t+\theta)\right|d\theta\\
& + \frac{\alpha}{2\tau}\int_{-\tau}^{0} y^2(t)\,d\theta - \frac{\alpha}{2\tau}\int_{-\tau}^{0} y^2(t+\theta)\,d\theta\\
\le {} & -2\alpha y^2 + 2\int_{-\tau}^{0} L\left|y(t)\right|\left|y(t+\theta)\right|d\theta + \frac{\alpha}{2}y^2\\
& + L\tau\left|y\right| - L\int_{-\tau}^{0}\left|y(t+\theta)\right|d\theta\\
& + \frac{\alpha}{2\tau}\int_{-\tau}^{0} y^2(t)\,d\theta - \frac{\alpha}{2\tau}\int_{-\tau}^{0} y^2(t+\theta)\,d\theta
\end{aligned}
\tag{20}
$$

by hypotheses $(A1) - (A3)$ of Theorem 1.

Let $L < \alpha/2\tau$. Then, we have

$$
\begin{aligned}
\frac{dV_0}{dt} \le {} & -\int_{-\tau}^{0}\left[\frac{\alpha}{2\tau}y^2(t) - \frac{\alpha}{\tau}\left|y(t)\right|\left|y(t+\theta)\right|\right.\\
& \left. + \frac{\alpha}{2\tau}y^2(t+\theta)\right]d\theta - \frac{3}{2}\alpha y^2 + \frac{\alpha}{2}y^2 + L\tau\left|y\right|\\
& - L\int_{-\tau}^{0}\left|y(t+\theta)\right|d\theta + \frac{\alpha}{2\tau}\int_{-\tau}^{0} y^2(t)\,d\theta = -\frac{\alpha}{2\tau}\\
& \cdot\int_{-\tau}^{0}\left[\left|y(t)\right| - \left|y(t+\theta)\right|\right]^2 d\theta - \alpha y^2 + L\tau\left|y\right|\\
& - L\int_{-\tau}^{0}\left|y(t+\theta)\right|d\theta
\end{aligned}
\tag{21}
$$

by the last inequality. If $\tau < \alpha/2L$ and $|y(t)| \ge c = \max\{A, 2L\tau/\alpha + 1\}$, then we can obtain

$$
\frac{dV_0}{dt} \le -\frac{1}{2}\alpha y^2. \tag{22}
$$

Case I. We assume that $|y(t)| \le c$, $c \in \mathfrak{R}$, $c > 0$, and B_0 is a positive constant. Then, it is clear that

$$
\frac{2\left|y\right|\left|\phi(t,y)\right|}{a(t)} + \frac{\left|\phi(t,y)\right|}{a(t)} + \frac{\left|h(t, y(t-\tau))\right|}{a(t)} \le B_0. \tag{23}
$$

Suppose that $x(t) \ge d$, $d \in \mathfrak{R}$, $d > 0$ and define the Lyapunov functional

$$
V(t, x_t, y_t) = V_0(t, x_t, y_t) + y(t). \tag{24}
$$

Then, the time derivative of functional V along system (14) is given by

$$\begin{aligned}\frac{d}{dt}V &= \frac{d}{dt}V_0 + \frac{d}{dt}y(t)\\ &= \frac{d}{dt}V_0 - \frac{a'(t)}{a(t)}y - \frac{1}{a(t)}\phi(t,y)\\ &\quad - \frac{1}{a(t)}\left(h\left(t,y\left(t-\tau\right)\right)\right) - \frac{1}{a(t)}g(x)\\ &\quad - \frac{1}{a(t)}f(x)\\ &\quad + \frac{1}{a(t)}\int_{-\tau}^{0} f'\left(x\left(t+\theta\right)\right)y\left(t+\theta\right)d\theta\\ &\quad + \frac{e\left(t,x,y\right)}{a(t)}.\end{aligned} \tag{25}$$

In view of hypotheses $(A1)-(A3)$ of Theorem 1, we have

$$\begin{aligned}\frac{dV}{dt} &\le -\frac{2a'(t)}{a(t)}y^2 - \frac{2}{a(t)}\phi(t,y)\,y\\ &\quad - \frac{2}{a(t)}h\left(t,y\left(t-\tau\right)\right)y\\ &\quad + \frac{2}{a(t)}y\int_{-\tau}^{0} f'\left(x\left(t+\theta\right)\right)y\left(t+\theta\right)d\theta\\ &\quad + \frac{2}{a(t)}e\left(t,x,y\right)y + \frac{\alpha}{2\tau}\int_{-\tau}^{0} y^2(t)\,d\theta\\ &\quad - \frac{\alpha}{2\tau}\int_{-\tau}^{0} y^2\left(t+\theta\right)d\theta + L\tau\left|y\right|\\ &\quad - L\int_{-\tau}^{0}\left|y\left(t+\theta\right)\right|d\theta - \frac{a'(t)}{a(t)}y - \frac{1}{a(t)}\phi(t,y)\\ &\quad - \frac{1}{a(t)}\left(h\left(t,y\left(t-\tau\right)\right)\right) - \frac{1}{a(t)}g(x)\\ &\quad - \frac{1}{a(t)}f(x)\\ &\quad + \frac{1}{a(t)}\int_{-\tau}^{0} f'\left(x\left(t+\theta\right)\right)y\left(t+\theta\right)d\theta\\ &\quad + \frac{e\left(t,x,y\right)}{a(t)}.\end{aligned} \tag{26}$$

By hypotheses $(A1)-(A3)$ of Theorem 1, inequality (23), and the last estimate, we obtain

$$\begin{aligned}\frac{dV}{dt} &\le \left[\frac{2\left|y\right|\left|\phi\left(t,y\right)\right|}{a(t)} + \frac{1}{a(t)}\left|\phi\left(t,y\right)\right|\right.\\ &\quad \left. + \frac{1}{a(t)}\left|h\left(t,y\left(t-\tau\right)\right)\right|\right] + \frac{\alpha}{2}c^2\\ &\quad - \left[\frac{\alpha}{2\tau}\int_{-\tau}^{0} y^2(t)\,d\theta - 2L\int_{-\tau}^{0}\left|y(t)\right|\left|y\left(t+\theta\right)\right|d\theta\right.\\ &\quad \left. + \frac{\alpha}{2\tau}\int_{-\tau}^{0} y^2\left(t+\theta\right)d\theta\right] + \alpha c^2 + L\tau\left|y\right|\\ &\quad - L\int_{-\tau}^{0}\left|y\left(t+\theta\right)\right|d\theta - \frac{a'(t)}{a(t)}y - \frac{1}{a(t)}g(x)\\ &\quad - \frac{1}{a(t)}f(x) + L\int_{-\tau}^{0}\left|y\left(t+\theta\right)\right|d\theta + \frac{\left|e\left(t,x,y\right)\right|}{a(t)}\\ &\le B_0 + \frac{\alpha c^2}{2} - \frac{\alpha}{2\tau}\int_{-\tau}^{0}\left[\left|y(t)\right| - \left|y\left(t+\theta\right)\right|\right]^2 d\theta\\ &\quad + \alpha c^2 + L\tau c + a_0 c + \frac{\alpha c}{4} - \frac{1}{a(t)}g(x) - \frac{1}{a(t)}f(x).\end{aligned} \tag{27}$$

Since $a_0 \ge a(t) \ge 1$, it follows that

$$\frac{dV}{dt} \le B_0 + \frac{\alpha c^2}{2} + \alpha c^2 + a_0 c + \frac{3\alpha c}{4} - \left[g(x) + f(x)\right]. \tag{28}$$

In view of the hypotheses $f(x)\operatorname{sgn} x \longrightarrow \infty$ for $|x| \longrightarrow \infty$ and $g(x)\operatorname{sgn} x \longrightarrow \infty$ for $|x| \longrightarrow \infty$, it is obvious that

$$\frac{dV}{dt} \le -1 \tag{29}$$

when $|x| \longrightarrow \infty$.

Case II. We assume that

$$\begin{aligned}&\left|y(t)\right| \le c,\\ &x(t) \le -d,\\ &\qquad c,d \in \Re,\ c>0,\ d>0.\end{aligned} \tag{30}$$

It is known that the function $a(t)$ is bounded and $|y| \le c$. Then, inequality (23) holds.

We define a Lyapunov functional by

$$V\left(t,x_t,y_t\right) = V_0\left(t,x_t,y_t\right) - y(t). \tag{31}$$

The time derivative of the Lyapunov functional V along system (14) implies that

$$\begin{aligned}\frac{d}{dt}V &= \frac{d}{dt}V_0 - \frac{d}{dt}y(t)\\ &= \frac{dV_0}{dt} + \frac{a'(t)}{a(t)}y + \frac{1}{a(t)}\phi(t,y)\\ &\quad + \frac{1}{a(t)}h\left(t,y\left(t-\tau\right)\right) + \frac{1}{a(t)}g(x)\\ &\quad + \frac{1}{a(t)}f(x)\\ &\quad - \frac{1}{a(t)}\int_{-\tau}^{0} f'\left(x\left(t+\theta\right)\right)y\left(t+\theta\right)d\theta\\ &\quad - \frac{e\left(t,x,y\right)}{a(t)}.\end{aligned} \tag{32}$$

Hence, using inequality (18), we obtain

$$\begin{aligned}\frac{d}{dt}V \le & -\frac{2a'(t)}{a(t)}y^2 - \frac{2}{a(t)}\phi(t,y)\,y \\ & - \frac{2}{a(t)}h(t,y(t-\tau))\,y \\ & + \frac{2}{a(t)}y\int_{-\tau}^{0} f'(x(t+\theta))\,y(t+\theta)\,d\theta \\ & + \frac{2}{a(t)}e(t,x,y)\,y + \frac{\alpha}{2\tau}\int_{-\tau}^{0} y^2(t)\,d\theta \\ & - \frac{\alpha}{2\tau}\int_{-\tau}^{0} y^2(t+\theta)\,d\theta + L\tau|y| \\ & - L\int_{-\tau}^{0}|y(t+\theta)|\,d\theta + \frac{a'(t)}{a(t)}y + \frac{1}{a(t)}\phi(t,y) \\ & + \frac{1}{a(t)}\left(h(t,y(t-\tau))\right) + \frac{1}{a(t)}g(x) \\ & + \frac{1}{a(t)}f(x) \\ & - \frac{1}{a(t)}\int_{-\tau}^{0} f'(x(t+\theta))\,y(t+\theta)\,d\theta \\ & - \frac{e(t,x,y)}{a(t)}.\end{aligned} \tag{33}$$

After that, in view of hypotheses of Theorem 1, it follows that

$$\begin{aligned}\frac{d}{dt}V \le & -\frac{2}{a(t)}\phi(t,y)\,y + 2L\int_{-\tau}^{0}|y(t)|\,|y(t+\theta)|\,d\theta \\ & + \frac{\alpha}{2}c^2 + \frac{\alpha}{2\tau}\int_{-\tau}^{0} y^2(t)\,d\theta \\ & - \left[\frac{\alpha}{2\tau}\int_{-\tau}^{0} y^2(t)\,d\theta + \frac{\alpha}{2\tau}\int_{-\tau}^{0} y^2(t+\theta)\,d\theta\right] \\ & + \frac{\alpha}{2\tau}\int_{-\tau}^{0} y^2(t)\,d\theta + L\tau|y| \\ & - L\int_{-\tau}^{0}|y(t+\theta)|\,d\theta + \frac{a'(t)}{a(t)}y \\ & + \frac{1}{a(t)}|\phi(t,y)| + \frac{1}{a(t)}|h(t,y(t-\tau))| \\ & + \frac{1}{a(t)}g(x) + \frac{1}{a(t)}f(x) \\ & + \frac{1}{a(t)}\int_{-\tau}^{0}|f'(x(t+\theta))|\,|y(t+\theta)|\,d\theta + \frac{\alpha c}{4}.\end{aligned} \tag{34}$$

By taking into consideration the hypotheses of Theorem 1, it can be obtained that

$$\begin{aligned}\frac{d}{dt}V \le & B_0 + \frac{\alpha c^2}{2} - \frac{\alpha}{2\tau}\int_{-\tau}^{0}\left[|y(t)| - |y(t+\theta)|\right]^2 d\theta \\ & + \alpha c^2 + L\tau c + \beta c + \frac{\alpha c}{4} + \frac{1}{a(t)}g(x) \\ & + \frac{1}{a(t)}f(x) \\ \le & B_0 + \frac{\alpha c^2}{2} + \alpha c^2 + \beta c + \frac{3\alpha c}{4} + g(x) + f(x).\end{aligned} \tag{35}$$

Since $f(x)\operatorname{sgn} x \longrightarrow \infty$ for $|x| \longrightarrow \infty$ and $g(x)\operatorname{sgn} x \longrightarrow \infty$ for $|x| \longrightarrow \infty$, it can be easily concluded that

$$\frac{dV}{dt} \le -1. \tag{36}$$

Case III. Let

$$\begin{aligned}&|x(t)| \le d, \\ &y(t) \ge c, \\ &c, d \in \Re,\ c > 0,\ d > 0.\end{aligned} \tag{37}$$

We now define a Lyapunov functional by

$$V(t, x_t, y_t) = V_0(t, x_t, y_t) + \frac{c}{d}x(t). \tag{38}$$

Then, calculating the time derivative of the functional V with respect to t, using inequality (18) and hypotheses $(A1) - (A3)$ of Theorem 1, we have

$$\begin{aligned}\frac{d}{dt}V = & \frac{d}{dt}V_0 + \frac{c}{d}y(t) \\ \le & -\frac{2a'(t)}{a(t)}y^2 - \frac{2}{a(t)}\frac{\phi(t,y)}{y}y^2 \\ & - \frac{2}{a(t)}\frac{h(t,y(t-\tau))}{y}y^2 \\ & + \frac{2}{a(t)}y\int_{-\tau}^{0} f'(x(t+\theta))\,y(t+\theta)\,d\theta \\ & + \frac{2}{a(t)}e(t,x,y)\,y + \frac{\alpha}{2\tau}\int_{-\tau}^{0} y^2(t)\,d\theta \\ & - \frac{\alpha}{2\tau}\int_{-\tau}^{0} y^2(t+\theta)\,d\theta + L\tau|y| \\ & - L\int_{-\tau}^{0}|y(t+\theta)|\,d\theta + \frac{c}{d}y \\ \le & -2\alpha y^2 + 2L\int_{-\tau}^{0}|y(t)|\,|y(t+\theta)|\,d\theta + \frac{\alpha}{2}y^2 \\ & + \frac{\alpha}{2\tau}\int_{-\tau}^{0} y^2(t)\,d\theta + \frac{\alpha}{2\tau}\int_{-\tau}^{0} y^2(t)\,d\theta \\ & - \frac{\alpha}{2\tau}\int_{-\tau}^{0} y^2(t)\,d\theta - \frac{\alpha}{2\tau}\int_{-\tau}^{0} y^2(t+\theta)\,d\theta \\ & + \frac{\alpha}{2}|y| + \frac{c}{d}y\end{aligned}$$

$$\begin{aligned}
&\le -2\alpha y^2 + \frac{\alpha}{2}y^2 \\
&\quad - \frac{\alpha}{2\tau}\int_{-\tau}^{0}\left[|y(t)| - |y(t+\theta)|\right]^2 d\theta + \alpha y^2 \\
&\quad + \frac{\alpha}{2}|y| + \frac{c}{d}y \\
&\le -2\alpha y^2 + \frac{\alpha}{2}y^2 + \alpha y^2 + \frac{\alpha}{2}|y| + \frac{c}{d}y \\
&\le -\frac{1}{2}\alpha y^2 + \frac{c}{d}y \le -\frac{1}{4}\alpha y^2.
\end{aligned} \tag{39}$$

Case IV. Let

$$\begin{aligned}
&|x(t)| \le d, \\
&y(t) \le -c, \\
&\qquad c, d \in \Re,\ c > 0,\ d > 0.
\end{aligned} \tag{40}$$

We define a Lyapunov functional by

$$V(t, x_t, y_t) = V_0(t, x_t, y_t) - \frac{c}{d}x(t). \tag{41}$$

Like before, we can obtain

$$\begin{aligned}
\frac{d}{dt}V &= \frac{d}{dt}V_0 - \frac{c}{d}y(t) \\
&\le -\frac{2a'(t)}{a(t)}y^2 - \frac{2}{a(t)}\frac{\phi(t,y)}{y}y^2 \\
&\quad - \frac{2}{a(t)}\frac{h(t, y(t-\tau))}{y}y^2 \\
&\quad + \frac{2}{a(t)}y\int_{-\tau}^{0} f'(x(t+\theta))\, y(t+\theta)\, d\theta \\
&\quad + \frac{2}{a(t)}e(t,x,y)\, y + \frac{\alpha}{2\tau}\int_{-\tau}^{0} y^2(t)\, d\theta \\
&\quad - \frac{\alpha}{2\tau}\int_{-\tau}^{0} y^2(t+\theta)\, d\theta + L\tau|y| \\
&\quad - L\int_{-\tau}^{0}|y(t+\theta)|\, d\theta - \frac{c}{d}y \\
&\le -2\alpha y^2 + 2L\int_{-\tau}^{0}|y(t)|\,|y(t+\theta)|\, d\theta + \frac{\alpha}{2}y^2 \\
&\quad + \frac{\alpha}{2\tau}\int_{-\tau}^{0} y^2(t)\, d\theta + \frac{\alpha}{2\tau}\int_{-\tau}^{0} y^2(t)\, d\theta \\
&\quad - \frac{\alpha}{2\tau}\int_{-\tau}^{0} y^2(t)\, d\theta - \frac{\alpha}{2\tau}\int_{-\tau}^{0} y^2(t+\theta)\, d\theta \\
&\quad - \frac{c}{d}y \\
&\le -2\alpha y^2 + \frac{\alpha}{2}y^2 \\
&\quad - \frac{\alpha}{2\tau}\int_{-\tau}^{0}\left[|y(t)| - |y(t+\theta)|\right]^2 d\theta + \alpha y^2 \\
&\quad + \frac{\alpha}{2}|y| - \frac{c}{d}y \le -2\alpha y^2 + \frac{\alpha}{2}y^2 + \alpha y^2 - \frac{c}{d}y \\
&\le -\frac{1}{2}\alpha y^2 - \frac{c}{d}y \le -\frac{1}{4}\alpha y^2
\end{aligned} \tag{42}$$

by (18) and hypotheses $(A1) - (A3)$ of Theorem 1.

Case V. We suppose that $x(t) \ge d$ for $c, d \in \Re,\ c > 0,\ d > 0,\ y(t) \ge c$ or $x(t) \le -d,\ y(t) \le -c$.

We define a Lyapunov functional V by

$$V(t, x_t, y_t) = V_0(t, x_t, y_t) + c. \tag{43}$$

Case VI. Further, in the case of $x(t) \ge d,\ y(t) \le -c$, or $x(t) \le -d,\ y(t) \ge c$, we define Lyapunov functional by

$$V(t, x_t, y_t) = V_0(t, x_t, y_t) - c. \tag{44}$$

In view of the above two cases, that is, Cases V and VI, and the hypotheses of Theorem 1, since c is a positive constant, the time derivative of functional V along system (14) leads to the following:

$$\begin{aligned}
\frac{d}{dt}V &= \frac{d}{dt}V_0 \\
&\le -\frac{2a'(t)}{a(t)}y^2 - \frac{2}{a(t)}\frac{\phi(t,y)}{y}y^2 \\
&\quad - \frac{2}{a(t)}\frac{h(t, y(t-\tau))}{y}y^2 \\
&\quad + \frac{2}{a(t)}y\int_{-\tau}^{0} f'(x(t+\theta))\, y(t+\theta)\, d\theta \\
&\quad + \frac{2}{a(t)}e(t,x,y)\, y + \frac{\alpha}{2\tau}\int_{-\tau}^{0} y^2(t)\, d\theta \\
&\quad - \frac{\alpha}{2\tau}\int_{-\tau}^{0} y^2(t+\theta)\, d\theta + L\tau|y| \\
&\quad - L\int_{-\tau}^{0}|y(t+\theta)|\, d\theta
\end{aligned} \tag{45}$$

so that

$$\begin{aligned}
\frac{d}{dt}V &\le -2\alpha y^2 + 2L\int_{-\tau}^{0}|y(t)|\,|y(t+\theta)|\, d\theta + \frac{\alpha}{2}y^2 \\
&\quad + \frac{\alpha}{2\tau}\int_{-\tau}^{0} y^2(t)\, d\theta + \frac{\alpha}{2\tau}\int_{-\tau}^{0} y^2(t)\, d\theta \\
&\quad - \frac{\alpha}{2\tau}\int_{-\tau}^{0} y^2(t)\, d\theta - \frac{\alpha}{2\tau}\int_{-\tau}^{0} y^2(t+\theta)\, d\theta \\
&\le -2\alpha y^2 + \frac{\alpha}{2}y^2
\end{aligned}$$

$$
\begin{aligned}
&-\frac{\alpha}{2\tau}\int_{-\tau}^{0}\left[\left|y(t)\right|-\left|y(t+\theta)\right|\right]^2 d\theta+\alpha y^2\\
&+\frac{\alpha}{2}\left|y\right|\le -2\alpha y^2+\frac{\alpha}{2}y^2+\alpha y^2=-\frac{1}{2}\alpha y^2\\
&\le -\frac{1}{4}\alpha y^2.
\end{aligned}
\tag{46}
$$

Hence, it is obvious that the time derivative of functional V, that is, $(d/dt)V$, is negative semidefined for the above two cases. In addition, we can see that

$$
\begin{aligned}
&\frac{2}{a(t)}\int_0^x f(s)\,ds+\frac{2}{a(t)}\int_0^x g(s)\,ds+y^2-c\\
&\le 2\int_0^x f(s)\,ds+2\int_0^x g(s)\,ds+y^2-c\\
&\le V\left(t,x_t,y_t\right)\\
&\le 2\int_0^x f(s)\,\mathrm{d}s+2\int_0^x g(s)\,ds+c\\
&\quad+\frac{a}{2\tau}\int_{-\tau}^{0}\left(\int_{\tau}^{0}y^2(\theta)\,d\theta\right)ds\\
&\quad+L\int_{-\tau}^{0}\left(\int_{\tau}^{0}\left|y(\theta)\right|d\theta\right)ds.
\end{aligned}
\tag{47}
$$

Hence, "wedges" can be easily found (see Burton [1]), bounding the functional V_0 from bottom to top. Then, we can conclude that system (14) has a periodic solution of period ω (see Yoshizawa ([6, Theorem 37.2])). □

3. Stability of Solutions

Let $e(t,x,y)\equiv 0$.

(B) Hypothesis. It is assumed that the following hypothesis holds:

$$
\begin{aligned}
(A4)\quad &\phi(t,0)=0,\\
&\frac{\phi(t,y)}{y}>\alpha a(t)>0\\
&\qquad\text{for } y\in\Re,\ (y\neq 0),\\
&h(t,0)=0,\\
&\frac{h\left(t,y(t-\tau)\right)}{y}\ge b_0>0\\
&\qquad\text{for } t\in\Re^+,\ y\in\Re,\ (y\neq 0),\\
&g(0)=0,\\
&\frac{g(x)}{x}\ge g_0,\\
&\qquad x\in\Re,\ (x\neq 0),\\
&f(0)=0,\\
&\frac{f(x)}{x}\ge f_0,\\
&\qquad (x\neq 0),\ \left|f'(x)\right|\le M,\ x\in\Re,
\end{aligned}
\tag{48}
$$

where α, b_0, f_0, g_0, and $M\in\Re$ are some positive real constants with $b_0\ge 1$ and $\tau<\alpha/2M$.

Theorem 2. *If hypotheses* $(A1)$ *and* $(A4)$ *hold, then the zero solution of system (14) is stable.*

Proof. Consider the Lyapunov functional $V_1=V_1(t,x_t,y_t)$ defined by

$$
\begin{aligned}
V_1=&\frac{2}{a(t)}\int_0^x f(s)\,ds+\frac{2}{a(t)}\int_0^x g(s)\,ds+y^2\\
&+\frac{\alpha}{2\tau}\int_{-\tau}^{0}\left(\int_{s}^{0}y^2(\theta)\,d\theta\right)ds.
\end{aligned}
\tag{49}
$$

It is clear that

$$
V_1(t,0,0)=0 \tag{50}
$$

and

$$
\begin{aligned}
V_1=&\frac{2}{a(t)}\int_0^x\frac{f(s)}{s}s\,ds+\frac{2}{a(t)}\int_0^x\frac{g(s)}{s}s\,ds+y^2\\
&+\frac{\alpha}{2\tau}\int_{-\tau}^{0}\left(\int_{s}^{0}y^2(\theta)\,d\theta\right)ds\\
&\ge\left(\frac{f_0+g_0}{a_0}\right)x^2+y^2=\sigma\left(x^2+y^2\right),
\end{aligned}
\tag{51}
$$

where $\sigma=\min\{(f_0+g_0)a_0^{-1},1\}$, by hypotheses $(A1)$ and $(A4)$.

Differentiating the Lyapunov functional V_1 along system (14) and considering hypotheses $(A1)$ and $(A4)$, we obtain

$$
\begin{aligned}
\frac{d}{dt}V_1\le&-\frac{2}{a(t)}\frac{\phi(t,y)}{y}y^2-\frac{2}{a(t)}\frac{h\left(t,y(t-\tau)\right)}{y}y^2\\
&+\frac{2}{a(t)}y\int_{-\tau}^{0}f'\left(x(t+\theta)\right)y(t+\theta)\,d\theta\\
&+\frac{\alpha}{2\tau}\int_{-\tau}^{0}y^2(t)\,d\theta-\frac{\alpha}{2\tau}\int_{-\tau}^{0}y^2(t+\theta)\,d\theta.
\end{aligned}
\tag{52}
$$

Hence,

$$
\begin{aligned}
\frac{dV_1}{dt}\le&-\frac{3}{2}\alpha y^2-2\frac{b_0}{a_0}y^2\\
&+\frac{2}{a(t)}\int_{-\tau}^{0}\left|f'\left(x(t+\theta)\right)\right|\left|y(t)\right|\left|y(t+\theta)\right|d\theta\\
&-\frac{\alpha}{2\tau}\int_{-\tau}^{0}y^2(t+\theta)\,d\theta.\\
\le&-\frac{3}{2}\alpha y^2-2\frac{b_0}{a_0}y^2
\end{aligned}
$$

$$+\int_{-\tau}^{0} M\left[y^2(t)+y^2(t+\theta)\right]d\theta$$
$$-\frac{\alpha}{2\tau}\int_{-\tau}^{0} y^2(t+\theta)\,d\theta$$
$$\leq -\left[\frac{3}{2}\alpha+2\frac{b_0}{a_0}-M\tau\right]y^2$$
$$-\left[\frac{\alpha}{2\tau}-M\right]\int_{-\tau}^{0} y^2(t+\theta)\,d\theta \tag{53}$$

by hypotheses $(A1)$ and $(A4)$ of Theorem 2.

Let $\tau < \alpha/2M$. Then, it follows that

$$\frac{dV_1}{dt} \leq -\left(\alpha+2a_0b_0^{-1}\right)y^2. \tag{54}$$

This result completes that the zero solution of system (14) is stable. □

Corollary 3. *If hypotheses* $(A1)$ *and* $(A4)$ *hold, then the zero solution of system (14) is uniformly stable.*

Theorem 4. *If hypotheses* $(A1)$ *and* $(A4)$ *hold, then the zero solution of system (14) is asymptotically stable.*

Proof. In the proof of this theorem, we benefit from the Lyapunov functional V_1 given in the proof of Theorem 2.

In the light of the hypotheses of Theorem 4, we can conclude that

$$\frac{dV_1}{dt} \leq -\left(\alpha+2a_0b_0^{-1}\right)y^2. \tag{55}$$

Consider now the set defined by

$$S \equiv \left\{(t,x,y) : \dot{V}_1(t,x_t,y_t) = 0\right\}. \tag{56}$$

When we apply LaSalle's invariance principle, we observe that $(t,x,y) \in S$ implies that $y = 0$, and hence $x = \rho$ ($\rho \neq 0$ is a constant). The last estimate and system (14), together, necessarily imply that

$$\frac{1}{a(t)}g(x)+\frac{1}{a(t)}f(x) = 0. \tag{57}$$

When $x = \rho$, this equality can hold if and only if

$$g(\rho)+f(\rho) = 0. \tag{58}$$

Hence,

$$g(\rho)+f(\rho) = 0 \Longleftrightarrow \rho = 0, \tag{59}$$

which implies that $g(x)+f(x) = 0 \Longleftrightarrow x = 0$. Therefore, we have $x = y = 0$. In fact, this result shows that the largest invariant set contained in S is $(t,0,0) \in S$. Hence, we can conclude that the zero solution of system (14) is asymptotically stable. This completes the proof of Theorem 4. □

Theorem 5. *If hypotheses* $(A1)$ *and* $(A4)$ *hold, then the first derivatives of all solutions of (13) are square-integrable; that is,* $y(t) \in L^2[0,\infty)$*, where* $L^2[0,\infty)$ *is the space of all Lebesgue square-integrable functions on* $[0,\infty)$.

Proof. Here, we also use the functional V_1 used in both theorems given just above. Notice the hypotheses of Theorem 5; we have

$$\frac{d}{dt}V_1(t,x_t,y_t) \leq -ky^2 \leq 0, \quad k = \alpha+2a_0b_0^{-1} > 0. \tag{60}$$

Integrating the last inequality from t_0 to t, we have

$$V_1(t,x_t,y_t)-V_1\left(t_0,x_{t_0},y_{t_0}\right) \leq -k\int_{t_0}^{t}\left|y(s)\right|^2 ds. \tag{61}$$

From the above discussion, it can be seen that $V_1(t,x_t,y_t)$ is positive definite and a decreasing functional. Therefore, we can say that

$$V_1\left(t_0,x_{t_0},y_{t_0}\right) = \ell, \quad \ell > 0,\ \ell \in \Re, \tag{62}$$

and hence, it is clear that

$$k\int_{t_0}^{t}\left|y(s)\right|^2 ds \leq V_1\left(t_0,x_{t_0},y_{t_0}\right)-V_1(t,x_t,y_t)$$
$$\leq V_1\left(t_0,x_{t_0},y_{t_0}\right). \tag{63}$$

As the result of the above inequalities, we can conclude that

$$\int_{t_0}^{\infty}\left|y(s)\right|^2 ds \leq k^{-1}\ell. \tag{64}$$

This result is the end of the proof of Theorem 5. □

4. Boundedness of Solutions

Let $e(t,x,y) \neq 0$.

(C) Hypothesis. It is assumed that the following hypothesis holds:

$$(A5) \quad \left|e(t,x,y)\right| \leq \theta(t)\left|y\right|, \quad t \in \Re^+,\ x,y \in \Re, \tag{65}$$

where $\theta(t)$ is a nonnegative and continuous function for all $t \in \Re^+$ such that $\theta \in L^1[0,\infty)$, $L^1[0,\infty)$ is the space of all Lebesgue integrable functions on $[0,\infty)$.

Theorem 6. *If hypotheses* $(A1)$*,* $(A4)$*, and* $(A5)$ *hold, then all solutions of system (13) are bounded as* $t \longrightarrow \infty$.

Proof. Here, once again, we use the functional V_1 just given above. Notice the hypotheses of Theorem 6; we can have

$$\frac{d}{dt}V_1(t,x_t,y_t) \leq 2ye(t,x,y). \tag{66}$$

In view of hypothesis $(A5)$, we can get

$$\frac{d}{dt}V_1(t,x_t,y_t) \leq 2\theta(t)y^2 \leq 2\sigma^{-1}\theta(t)V_1(t,x_t,y_t). \tag{67}$$

Integrating the former inequality from t_0 to t, we have

$$V_1(t, x_t, y_t) - V_1(t_0, x_{t_0}, y_{t_0}) \leq 2\sigma^{-1} \int_{t_0}^{t} \theta(s) V_1(s, x_s, y_s)\, ds \tag{68}$$

so that

$$V_1(t, x_t, y_t) \leq \ell + 2\sigma^{-1} \int_{t_0}^{t} \theta(s) V_1(s, x_s, y_s)\, ds. \tag{69}$$

By the Gronwall inequality, it follows that

$$V_1(t, x_t, y_t) \leq \ell \exp\left(2\sigma^{-1} \int_{t_0}^{\infty} \theta(s)\, ds\right) < \infty. \tag{70}$$

Let

$$\ell \exp\left(2\sigma^{-1} \int_{t_0}^{\infty} \theta(s)\, ds\right) = k_1. \tag{71}$$

In addition, we also have

$$x^2 + y^2 \leq \sigma^{-1} V_1(t, x_t, y_t). \tag{72}$$

Hence, we can conclude that

$$x^2 + y^2 \leq \sigma^{-1} k_1. \tag{73}$$

This is the end of the proof of Theorem 6. □

Example 7. We consider the following second-order nonlinear differential equation with constant delay:

$$x'' + (3 + \sin t)\, x' + 3 + \sin t + x'^2(t-1), +2x + x(t-1) = \frac{1}{8} x' \sin t. \tag{74}$$

When we compare this equation with (13), it follows that

$$\begin{aligned} \phi(t, y) &= (3 + \sin t)\, y, \\ a(t) &= 1, \\ h(t, y(t-\tau)) &= 3 + \sin t + y^2(t-1), \\ f(x) &= x, \\ g(x) &= 2x \\ e(t, x, y) &= \frac{1}{8} y \sin t. \end{aligned} \tag{75}$$

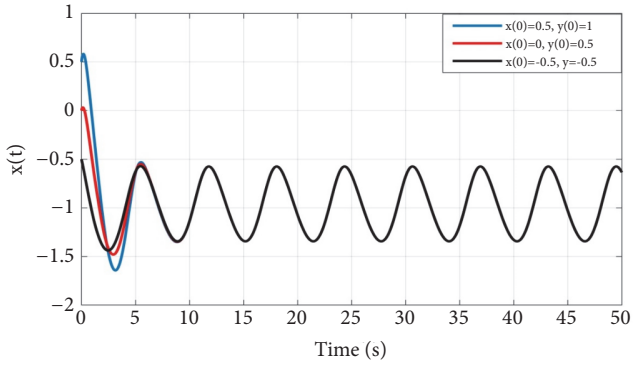

Figure 1: Trajectory of $x(t)$ for Example 7.

It is obvious that the hypotheses of Theorem 1 are satisfied:

$$\begin{aligned} \frac{\phi(t, y)}{y} &= 3 + \sin t > \alpha = 1, \\ h(t, y(t-\tau)) &= 3 + \sin^2 t + y^2(t-1) \geq 3 = b_0 > 0, \\ f(x) \operatorname{sgn} x &= x \operatorname{sgn} x \longrightarrow \infty \quad \text{for } |x| \longrightarrow \infty \\ |f'(x)| &= |x| = 1 \leq 2 = L, \\ |e(t, x, y)| &= \frac{1}{8}|y|\,|\sin t| \leq \frac{\alpha|y|}{4} = \frac{|y|}{4}, \quad \alpha = 1, \\ g(x) \operatorname{sgn} x &= 2x \operatorname{sgn} x \longrightarrow \infty \quad \text{for } |x| \longrightarrow \infty, \\ |g'(x)| &= |2| = 2 \leq L, \\ a(t) &= 1, \\ a'(t) &= 0. \end{aligned} \tag{76}$$

Therefore, the given differential equation satisfies all hypotheses of Theorem 1. Then, there exists a 2π−periodic solution of the above delay differential equation.

The orbits of the solutions of the considered delay differential equation are shown by Figures 1 and 2.

Remark 8. The differential equation with constant delay just given above by Example 7 can be modified and the related graphs of the orbits can be drawn by MATLAB-Simulink to verify the stability of zero solution, asymptotic stability of zero solution, square integrability of the first derivative of solutions, and boundedness of solutions. Here, we omit the details.

5. Conclusion

With the help of the second method of Lyapunov, the qualitative properties such as the existence of periodic solutions, stability of zero solution, asymptotic stability of zero solution, square integrability of the first derivative of solutions, and boundedness of solutions of a class of nonlinear differential equations of second order with constant delay are investigated. On the mentioned topics, five new theorems are

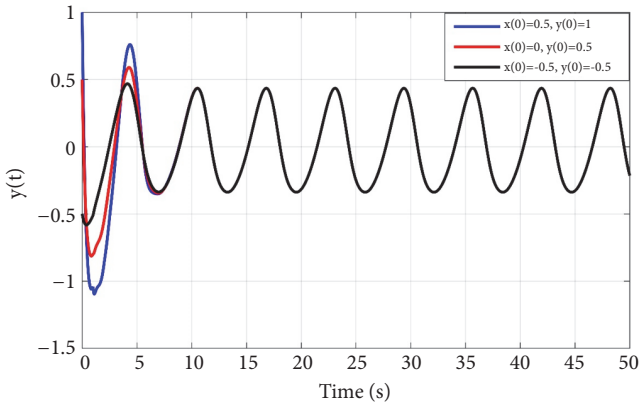

Figure 2: Trajectory of $y(t)$ for Example 7.

proven. The obtained results include and improve some results in the literature. We give an example to verify the applicability of the results by MATLAB-Simulink, which shows the behaviors of the orbits (see Figures 1 and 2).

Data Availability

The data used to support the findings of this study are included within the article.

Disclosure

The authors confirm that the paper has been read and approved by all named authors and that there are no other persons who satisfied the criteria for authorship but are not listed. The authors further confirm that the order of authors listed in the paper has been approved by all of them.

Conflicts of Interest

The authors declare that there are no conflicts of interest.

Acknowledgments

This research is supported by Van Yuzuncu Yil University, Van, Turkey (Grant No. FBA-2017-5868).

References

[1] T. A. Burton, *Stability and Periodic Solutions of Ordinary and Functional Differential Equations*, Academic Press, Orlando, Fla, USA, 1985.

[2] L. E. El'sgol'ts, *Introduction to The Theory of Differential Equations with Deviating Arguments*, Holden-Day, San Francisco, Calif, USA, 1966, Translated from the Russian by Robert J. McLaughlin.

[3] J. K. Hale, "Sufficient conditions for stability and instability of autonomous functional-differential equations," *Journal of Differential Equations*, vol. 1, pp. 452–482, 1965.

[4] N. N. Krasovskii, *Stability of Motion: Applications of Lyapunov's Second Method to Differential Systems and Equations with Delay*, Stanford University Press, Stanford, Calif, USA, 1963.

[5] H. Smith, *An Introduction to Delay Differential Equations with Applications to the Life Sciences*, Springer, New York, NY, USA, 2011.

[6] T. Yoshizawa, *Stability Theory by Lyapunov's Second Method*, The Mathematical Society of Japan, Tokyo, Japan, 1966.

[7] Z. Jie-min, H. Ke-lei, and L. Qi-shao, "The existence of periodic solutions for a class of functional differential equations and their application," *Applied Mathematics and Mechanics-English Edition*, vol. 15, no. 1, pp. 49–59, 1994.

[8] F. Cong, "Periodic solutions for second order differential equations," *Applied Mathematics Letters*, vol. 18, no. 8, pp. 957–961, 2005.

[9] C. Guo and Y. Xu, "Existence of periodic solutions for a class of second order differential equation with deviating argument," *Applied Mathematics and Computation*, vol. 28, no. 1-2, pp. 425–433, 2008.

[10] T. Ji and W. Dong, "Existence of periodic solutions for a class of differential equations of second order," in *Applied and Computational Mathematics*, pp. 255–257, WSEAS Press, Athens, Greece, 2008.

[11] D. S. Tian and X. W. Zeng, "Existence of several periodic solutions for a class of second-order functional differential equations," *Acta Mathematica Scientia. Series A*, vol. 30, no. 2, pp. 525–530, 2010.

[12] Q. Li and Y. Li, "On the existence of positive periodic solutions for second-order functional differential equations with multiple delays," *Abstract and Applied Analysis*, vol. 2012, Article ID 929870, 13 pages, 2012.

[13] X. Li and Z. Zhang, "On the existence of positive periodic solutions of systems of second order differential equations," *Mathematische Nachrichten*, vol. 284, no. 11-12, pp. 1472–1482, 2011.

[14] J. Zu, "Existence and uniqueness of periodic solution for nonlinear second-order ordinary differential equations," *Boundary Value Problems*, vol. 2011, Article ID 192156, 11 pages, 2011.

[15] Cemil Tunç and Ramazan Yazgan, "Existence of periodic solutions to multidelay functional differential equations of second order," *Abstract and Applied Analysis*, vol. 2013, Article ID 968541, 5 pages, 2013.

[16] R. Ma and Y. Lu, "Existence of positive periodic solutions for second-order functional differential equations," *Monatshefte für Mathematik*, vol. 173, no. 1, pp. 67–81, 2014.

[17] R. Jia and J. Shao, "Existence and uniqueness of periodic solutions of second-order nonlinear differential equations," *Journal of Inequalities and Applications*, vol. 2013, article 115, 10 pages, 2013.

[18] A. Ardjouni and A. Djoudi, "Existence of positive periodic solutions for a second-order nonlinear neutral differential equation with variable delay," *Advances in Nonlinear Analysis*, vol. 2, no. 2, pp. 151–161, 2013.

[19] A. Ardjouni and A. Djoudi, "Existence of periodic solutions for a second order nonlinear neutral differential equation with variable delay," *Palestine Journal of Mathematics*, vol. 3, no. 2, pp. 191–197, 2014.

[20] Y. Lü, P. Sun, H. Cai, and P.-s. Han, "Existence of multiple positive periodic solutions for second order differential equations," *Communications in Mathematical Research*, vol. 32, no. 3, pp. 272–280, 2016.

[21] D. S. Tian, "Existence of multiple periodic solutions for a second-order delayed differential equation," *Acta Mathematicae Applicatae Sinica*, vol. 39, no. 4, pp. 537–546, 2016.

[22] L. Zhang and Q. Y. Wang, "Existence of periodic solutions for a class of second-order functional differential equations with deviating arguments," *Acta Mathematica Scientia. Series A*, vol. 29, no. 2, pp. 253–261, 2009.

[23] T. F. Zhou, "Existence of periodic solutions for semi-linear second-order differential equations," *Chinese Journal of Engineering Mathematics*, vol. 32, no. 5, pp. 690–696, 2015.

[24] Y. Wei, "Existence and uniqueness of periodic solutions for second order differential equations," *Journal of Function Spaces*, vol. 2014, Article ID 246258, 5 pages, 2014.

[25] L. M. Zhu and Y. X. Li, "Existence of periodic solutions for second-order differential equations with multiple delays," *Journal of Jilin University*, vol. 55, no. 5, pp. 1077–1083, 2017.

[26] T. Yoshizawa, *Stability Theory and The Existence of Periodic Solutions and Almost Periodic Solutions*, Springer, 1975.

[27] C. Tunç and I. Çinar, "On the existence of periodic solutions to nonlinear differential equations of second order," *Differential Equations and Control Processes*, no. 3, pp. 20–25, 2008.

[28] S. Ahmad and M. R. M. Rao, *Theory of Differential Equations*, Affiliated East West Press Private, New Delhi, India, 1999.

[29] T. A. Burton and R. H. Hering, "Liapunov theory for functional-differential equations," *Rocky Mountain Journal of Mathematics*, vol. 24, no. 1, pp. 3–17, 1994.

[30] J. W. Heidel, "Global asymptotic stability of a generalized Liénard equation," *SIAM Journal on Applied Mathematics*, vol. 19, pp. 629–636, 1970.

[31] J. Kato, "On a boundedness condition for solutions of a generalized Liénard equation," *Journal of Differential Equations*, vol. 65, no. 2, pp. 269–286, 1986.

[32] J. Kato, "A simple boundedness theorem for a Liénard equation with damping," *Annales Polonici Mathematici*, vol. 51, pp. 183–188, 1990.

[33] E. Korkmaz and C. Tunç, "Convergence to non-autonomous differential equations of second order," *Journal of the Egyptian Mathematical Society*, vol. 23, no. 1, pp. 27–30, 2015.

[34] B. Liu and L. Huang, "Boundedness of solutions for a class of retarded Liénard equation," *Journal of Mathematical Analysis and Applications*, vol. 286, no. 2, pp. 422–434, 2003.

[35] B. Liu and L. Huang, "Boundedness of solutions for a class of Liénard equations with a deviating argument," *Applied Mathematics Letters*, vol. 21, no. 2, pp. 109–112, 2008.

[36] W. S. Luk, "Some results concerning the boundedness of solutions of Lienard equations with delay," *SIAM Journal on Applied Mathematics*, vol. 30, no. 4, pp. 768–774, 1976.

[37] I. A. Malyseva, "Boundedness of solutions of a Liénard differential equation," *Differentsial'nye Uravneniya*, vol. 15, no. 8, pp. 1420–1426, 1979.

[38] M. Mureşan, "Boundedness of solutions for Liénard type equations," *The Mathematica Journal*, vol. 40(63), no. 2, pp. 243–257, 1998.

[39] O. G. Mustafa and C. Tunç, "Asymptotically linear solutions of differential equations via Lyapunov functions," *Applied Mathematics and Computation*, vol. 215, no. 8, pp. 3076–3081, 2009.

[40] J. E. Nápoles Valdés, "Boundedness and global asymptotic stability of the forced Liénard equation," *Revista de la Unión Matemática Argentina*, vol. 41, no. 4, pp. 47–59, 2000.

[41] J. Sugie and Y. Amano, "Global asymptotic stability of nonautonomous systems of Liénard type," *Journal of Mathematical Analysis and Applications*, vol. 289, no. 2, pp. 673–690, 2004.

[42] J. Sugie, D.-L. Chen, and H. Matsunaga, "On global asymptotic stability of systems of Liénard type," *Journal of Mathematical Analysis and Applications*, vol. 219, no. 1, pp. 140–164, 1998.

[43] C. Tunc, "Some new stability and boundedness results on the solutions of the nonlinear vector differential equations of second order," *Iranian Journal of Science & Technology*, vol. 30, no. 2, pp. 213–221, 2006.

[44] C. Tunç, "A new boundedness theorem for a class of second order differential equations," *The Arabian Journal for Science and Engineering. Section A. Science*, vol. 33, no. 1, pp. 83–92, 2008.

[45] C. Tunç, "Some stability and boundedness results to nonlinear differential equations of Liénard type with finite delay," *Journal of Computational Analysis and Applications*, vol. 11, no. 4, pp. 711–727, 2009.

[46] C. Tunç, "Some new stability and boundedness results of solutions of Liénard type equations with a deviating argument," *Nonlinear Analysis: Hybrid Systems*, vol. 4, no. 1, pp. 85–91, 2010.

[47] C. Tunç, "A note on boundedness of solutions to a class of non-autonomous differential equations of second order," *Applicable Analysis and Discrete Mathematics*, vol. 4, no. 2, pp. 361–372, 2010.

[48] C. Tunç, "New stability and boundedness results of Liénard type equations with multiple deviating arguments," *Natsionalnaya Akademiya Nauk Armenii. Izvestiya. Matematika*, vol. 45, no. 4, pp. 47–56, 2010.

[49] C. Tunç, "Boundedness results for solutions of certain nonlinear differential equations of second order," *Journal of the Indonesian Mathematical Society*, vol. 16, no. 2, pp. 115–126, 2010.

[50] C. Tunç, "Stability and boundedness of solutions of non-autonomous differential equations of second order," *Journal of Computational Analysis and Applications*, vol. 13, no. 6, pp. 1067–1074, 2011.

[51] C. Tunç, "A note on the bounded solutions to $x'' + c(t, x, x') + q(t)b(x) = f(t)$," *Applied Mathematics & Information Sciences*, vol. 8, no. 1, pp. 393–399, 2014.

[52] C. Tunç, "On the qualitative behaviors of a functional differential equation of second order," *Applications and Applied Mathematics*, vol. 12, no. 2, pp. 813–842, 2017.

[53] C. Tunç and Y. Dinç, "Qualitative properties of certain nonlinear differential systems of second order," *Journal of Taibah University for Science*, vol. 11, no. 2, pp. 359–366, 2017.

[54] C. Tunc and E. Tunc, "On the asymptotic behavior of solutions of certain second-order differential equations," *Journal of The Franklin Institute*, vol. 344, no. 5, pp. 391–398, 2007.

[55] C. Tunc and O. Tunc, "A note on certain qualitative properties of a second order linear differential system," *Applied Mathematics & Information Sciences*, vol. 9, no. 2, pp. 953–956, 2015.

[56] C. Tunç and O. Tunç, "On the boundedness and integration of non-oscillatory solutions of certain linear differential equations of second order," *Journal of Advanced Research*, vol. 7, no. 1, pp. 165–168, 2016.

[57] C. Tunç and O. Tunç, "A note on the stability and boundedness of solutions to non-linear differential systems of second order," *Journal of the Association of Arab Universities for Basic and Applied Sciences*, vol. 24, pp. 169–175, 2017.

[58] G.-R. Ye, H.-S. Ding, and X.-L. Wu, "Uniform boundedness of solutions for a class of Liénard equations," *Electronic Journal of Differential Equations*, vol. 2009, no. 97, pp. 1–5, 2009.

[59] Y. Yu and B. Xiao, "Boundedness of solutions for a class of Liénard equation with multiple deviating arguments," *Vietnam Journal of Mathematics*, vol. 37, no. 1, pp. 35–41, 2009.

[60] Y. Yu and C. Zhao, "Boundedness of solutions for a Liénard equation with multiple deviating arguments," *Electronic Journal of Differential Equations*, vol. 2009, no. 14, pp. 1–5, 2009.

[61] B. Zhang, "Boundedness and stability of solutions of the retarded Liénard equation with negative damping," *Nonlinear Analysis. Theory, Methods & Applications*, vol. 20, no. 3, pp. 303–313, 1993.

[62] J. Zhou and L. Xiang, "On the stability and boundedness of solutions for the retarded Liénard-type equation," *Annals of Differential Equations*, vol. 15, no. 4, pp. 460–465, 1999.

[63] X.-f. Zhou and W. Jiang, "Stability and boundedness of retarded Liénard-type equation," *Chinese Quarterly Journal of Mathematics*, vol. 18, no. 1, pp. 7–12, 2003.

Hindawi
Discrete Dynamics in Nature and Society
Volume 2018, Article ID 8284121, 10 pages
https://doi.org/10.1155/2018/8284121

Research Article

Dynamics Analysis and Control of a Five-Term Fractional-Order System

Li-xin Yang [1] **and Xiao-jun Liu** [2]

[1] *School of Arts and Sciences, Shaanxi University of Science and Technology, Xi'an 710021, China*
[2] *School of Mathematics and Statistics, Tianshui Normal University, Tianshui 741001, China*

Correspondence should be addressed to Li-xin Yang; jiaodayanglixin@163.com

Received 31 May 2018; Revised 22 July 2018; Accepted 10 September 2018; Published 9 October 2018

Guest Editor: Abdul Qadeer Khan

This paper proposes a new fractional-order chaotic system with five terms. Firstly, basic dynamical properties of the fractional-order system are investigated in terms of the stability of equilibrium points, Jacobian matrices theoretically. Furthermore, rich dynamics with interesting characteristics are demonstrated by phase portraits, bifurcation diagrams numerically. Besides, the control problem of the new fractional-order system is discussed via numerical simulations. Our results demonstrate that the new fractional-order system has compound structure.

1. Introduction

Recently, the study of fractional calculus has attracted great attention due to its potential applications in various fields [1–3]. As a branch of mathematical analysis, fractional calculus can be considered as the generalization of the conventional calculus. Although the fractional-order derivative theory has a more than 300-year-old history, its application of the theory is just gaining attention [4–6]. In fact, most of the systems in interdisciplinary fields can be described via fractional calculus [7–9]. Moreover, fractional-order model can provide an explicit description and give a further insight into physical process. That is, fractional-order systems can serve as a valuable tool in the modeling of many phenomena. In view of the fact that fractional calculus provides another good way to describe, predict, and control physical systems accurately, it has been applied to control system, physics, and system modeling. Moreover, with the development of interdisciplinary applications, people found that various research fields can be elegantly described with the help of fractional derivatives, such as viscoelastic bodies, quantitative finance, dielectric polarization, electromagnetic waves, and polymer physics.

On the other hand, chaos and its applications have been intensively investigated and developed in many fields of science. In [9], the authors have presented analytical proofs of fold Hopf bifurcation in hyperchaotic Chen system and given sufficient conditions for stability and instability of the bifurcation periodic orbits. Researchers have investigated chaos synchronization of fractional-order systems via linear control [10–12]. Fractional-order systems possess long-range memory behavior and display complexity dynamics characteristic compared to its integral-order counterpart. On the other hand, there exist many significant differences between fractional-order system and the corresponding integer-order differential systems. Generally speaking, fractional-order nonlinear system can display more rich dynamical behaviors such as various bifurcations under certain conditions which are different from the corresponding integer-order system [13, 14]. Several studies have explored the complex dynamical properties in many fractional-order systems, such as fractional-order Chen system [15] and fractional-order Duffing system [16]. Until now, many researchers have investigated the dynamics of several fractional-order chaotic systems and obtained many excellent results [17–19]. In addition, searching for new chaotic systems with fewer terms in autonomous differential equations has been developed with much interest by scientists. In [20], the author has investigated the dynamics of a five-term chaotic attractor. However, this system with fractional order has not been actively and deeply explored, and it is very interesting in a number

of different fields. To the best of our knowledge, chaotic attractors with fewer than five terms in three fractional-order differential equations have never been investigated.

Motivated by the above, within this body of work, we focus on the dynamical behaviors of this fractional-order simplified system. This would be of mathematical and practical interests. Rich dynamical behaviors are studied via bifurcation diagrams with varying the system parameters and the fractional derivative orders. Moreover, the control problem of the new fractional system is also investigated.

The remainder of this paper is organized as follows. In Section 2, the definition for the fractional calculus is given. Section 3 is devoted to the investigation of the fractional-order new system. In Section 4, the control of the new fractional-order system is investigated. Conclusions of this paper will be drawn in Section 5.

2. Fractional Calculus

Fractional calculus can be considered as a generalization of integration and differentiation to a noninteger-order integrodifferential operator ${}_aD_t^q$ which is described as

$$ {}_aD_t^q = \begin{cases} \dfrac{d^q}{dt^q} & R(q) > 0 \\ 1 & R(q) = 0 \\ \displaystyle\int_a^t (d\tau)^{-q} & R(q) < 0, \end{cases} \tag{1} $$

where q denotes derivative order and $R(q)$ corresponds to the real part of q. The numbers a and t represent the limits of the operator. At present, there are several definitions of the fractional-order differential system. Riemann–Liouville and Caputo definitions are considered the most common and efficient fractional derivatives [21, 22].

Firstly, the Riemann–Liouville (RL) definition of fractional derivatives can be written as follows.

$$ {}_a^{RL}D_t^q f(t) = \frac{d^n}{dt^n} \frac{1}{\Gamma(n-q)} \int_a^t \frac{f(\tau)}{(t-\tau)^{q-n+1}} d\tau, \quad n-1 < q < n \tag{2} $$

The Caputo fractional derivative is given by the following.

$$ {}_a^{C}D_t^q f(t) = \frac{1}{\Gamma(n-q)} \int_a^t (t-\tau)^{n-q-1} f^{(n)}(\tau)\, d\tau, \quad n-1 < q < n \tag{3} $$

In the above formulations, $\Gamma(\cdot)$ represents the Gamma function.

$$ \Gamma(s) = \int_0^\infty t^{s-1} e^{-t} dt. \tag{4} $$

Note that the Caputo derivative guarantees a straightforward connection between the types of the initial condition and the fractional derivative. Hence, the Caputo derivative is adopted in this paper.

3. An Unusual Five-Term Fractional-Order System

At first, a simple chaotic integer-order system with five terms is described as follows [20]:

$$ \begin{aligned} \dot{x} &= a(y - x) \\ \dot{y} &= -xz \\ \dot{z} &= -b + xy, \end{aligned} \tag{5} $$

when the parameters are selected as $a = 5, b = 90$, system (5) consists of two quadratic nonlinearities and displays abundantly complex behaviors of chaotic dynamics.

In what follows, we suppose that the derivative orders are fractional; the equations of the fractional-order system are readily derived from the above integer-order counterpart

$$ \begin{aligned} D_*^{q_1} x &= a(x - y) \\ D_*^{q_2} y &= -xz \\ D_*^{q_3} z &= -b + xy, \end{aligned} \tag{6} $$

where q_i $(i = 1, 2, 3)$ are the fractional derivatives orders.

In the next step, the dynamical behaviors of this new fractional-order system are investigated.

3.1. Some Properties of the New Fractional-Order System. It should be noted that most of the theory for the integer-order dynamic system cannot be simply extended to the fractional-order system. Therefore, the sufficient conditions of the stability of the fractional-order systems are given [23].

Lemma 1. *An autonomous fractional-order system is asymptotically steady at the equilibrium, if all the eigenvalues of the Jacobian matrix of some equilibrium satisfy*

$$ \left|\arg(eig(J))\right| > \frac{q\pi}{2}, \quad q = \max(q_1, q_2, q_3), \tag{7} $$

where $eig(J)$ denotes the eigenvalues of matrix J.

Based on the above theorem, the equilibria of system (6) can be calculated by solving the following equations

$$ \begin{aligned} D_*^{q_1} x &= a(x - y) = 0 \\ D_*^{q_2} y &= -xz = 0 \\ D_*^{q_3} z &= -b + xy = 0. \end{aligned} \tag{8} $$

The system contains two equilibrium points, i.e.,

$$ \begin{aligned} P^+(x, y, z) &= \left(+\sqrt{b}, +\sqrt{b}, 0\right), \\ P^-(-x, -y, -z) &= \left(-\sqrt{b}, -\sqrt{b}, 0\right), \end{aligned} \tag{9} $$

and, for the equilibrium $P^+(x, y, z) = (+\sqrt{b}, +\sqrt{b}, 0)$, the Jacobian matrix of (6) at points P^+ is obtained as

$$ J^+ = \begin{bmatrix} -a & a & 0 \\ -z & 0 & -x \\ y & x & 0 \end{bmatrix} = \begin{bmatrix} -a & a & 0 \\ 0 & 0 & -\sqrt{b} \\ \sqrt{b} & \sqrt{b} & 0 \end{bmatrix}. \tag{10} $$

Then we can obtain the eigenvalues of the Jacobian matrix as follows.

$$\lambda_1 = -7.0943,$$
$$\lambda_2 = 1.4701 + 10.5444i \quad (11)$$
$$\lambda_3 = 1.4701 - 10.5444i$$

For the second equilibrium $P^-(x, y, z) = (-\sqrt{b}, -\sqrt{b}, 0)$, the Jacobian matrix of the fractional-order new system (6) is defined as

$$J^- = \begin{bmatrix} -a & a & 0 \\ -z & 0 & -x \\ y & x & 0 \end{bmatrix} = \begin{bmatrix} -a & a & 0 \\ 0 & 0 & \sqrt{b} \\ -\sqrt{b} & -\sqrt{b} & 0 \end{bmatrix}. \quad (12)$$

By computing $|\lambda E - J| = 0$, it is found that the eigenvalues of the Jacobian matrix J^- are the same as those of the Jacobian matrix J^+. That is, λ_1 is a negative real number and $|\arg(\lambda_{2,3})| = 1.4323$; then according to Lemma 1, the eigenvalues cannot satisfy (7) as $0.912 \le q \le 1.0$, and two equilibrium points of the nonlinear fractional-order system (6) are all unstable.

3.2. Chaos and Bifurcations with Fractional-Order Parameters. To investigate the existence of new attractors in the fractional-order system, this part is devoted to dynamics of system (6) by considering several values of the fractional derivatives orders.

First, system parameters are selected as $a = 5, b = 90$, and the order parameter q_i $(i = 1, 2, 3)$ is varied. Figure 1 shows several typical attractors for $q_1 = q_2 = q_3 = \theta$; in this case, the fractional-order system is a commensurate-order system. The initial states of the new fractional-order system are taken as $x(0) = 1$, $y(0) = 2$, $z(0) = 3$. From these figures, one can observe that the new fractional-order system exhibits rich dynamical behaviors.

When the derivative order $\theta = 0.84$ and $\theta = 0.86$, system (6) stabilizes to an equilibrium point, as shown in Figures 1(a) and 1(b). When θ further increases to 0.88, there exists a single attractor, as reflected in Figure 1(c). The system also shows a chaotic attractor for $\theta = 0.98$, but it is different from the case of $\theta = 0.88$, as shown in Figure 1(d).

In order to further study the complex dynamics of the fractional-order system, consequently, the bifurcation diagrams with fractional derivative orders are given. First of all, we focus on the case of commensurate-order system. The fractional derivative order q varies from 0.88 to 1. Figure 2 represents the bifurcation diagram of the fractional-order system. It is clearly shown that the new fractional-order system is chaotic over most of the scopes $q \in [0.89, 0.95]$ and $q \in [0.96, 1]$. There exist tangent bifurcations when parameter $q < 0.96$. And the fractional-order system enters into chaos again as $q > 0.96$.

Phase portraits are shown in Figures 3(a) and 3(b); from the two figures, it can be clearly seen that the system shows distinguishable dynamical behaviors for different values of q.

As we know, for the incommensurate-order system, dynamical behavior is more complex than the commensurate-order system. Therefore, here, several typical differential order values are selected. We focus our attention on bifurcations versus the different derivative orders.

Fix the fractional derivative orders $q_2 = q_3 = 0.98$; dynamical behavior of system (6) with fractional derivative order $q_1 \in [0.91, 0.99]$ is presented as Figure 4. With increasing of the order parameter q_1 from 0.91, the fractional-order system enters into chaos by a series of period-doubling bifurcations. It can be seen that the system is period-2 for $q = 0.92$, period-4 for $q = 0.93$. The route out of chaos for the system is tangent bifurcation. Also, it can be observed that saddle-node bifurcation occurs when $q_1 \in [0.975\ 0.983]$. In the next step, Figure 5 represents the bifurcation diagrams with q_2, q_3 varying by numerical simulation. It is observed that there exist tangent bifurcations for two parameters, but the values of q_2, q_3 are different. The route out of chaos for the system is through tangent bifurcation when $q_2 < 0.92$, but transient chaos is observed when $q_3 < 0.96$.

3.3. Chaos and Bifurcations with System Parameters. First, fix fractional derivative orders $q_1 = q_2 = q_3 = 0.98$, and let system parameter a vary. The parameter a varies from 5 to 8. The bifurcation diagram with parameter a is shown in Figure 6. System displays chaotic behavior when parameter $a < 5.2$, as shown in Figure 7(a). When bifurcation parameter a increases from 6 to 6.5, there exist a series of period-doubling bifurcations, such as period-1 and period-4 [see Figures 7(b) and 7(c)]. If a keeps increasing, bifurcation occurs and the system switches to a periodic motion, as Figure 7(d) shows.

To furthermore exhibit the bifurcation behavior of the system (6), the expanded periodic window $a \in [6.6\ 7.6]$ and $[5.8\ 6.2]$ are plotted in Figures 6(b) and 6(c). From these figures, it can be seen that period bifurcation and Hopf bifurcation happen under certain parameters. And different attractors are shown in Figures 7(a)–7(d).

In what follows, let the fractional derivative orders $q_1 = q_2 = q_3 = 0.91$, system parameter $a = 5$; the dynamical behaviors of the system (6) with the variation of parameter b are discussed. Numerically we calculate the values of the parameter b; the dynamical behaviors of (6) can be classified as follows:

(i) When $b \le 175$, system becomes period orbit, as shown in Figure 8(a).

(ii) When $175 < b < 193$, system displays a limit cycle, as shown in Figure 8(b).

(iii) When $b > 193$, system demonstrates a chaotic attractor, as shown in Figure 8(c).

It can be seen that the chaotic attractors structure changes qualitatively with the variation of the parameter b and the order q. When the parameter b increases from 175 to 200, the dynamics of system (6) becomes more and more rich.

4. Control of New Fractional-Order System

In this subsection, the control problem of commensurate-order fractional-order system is investigated. For simplicity, we assume the derivative order $q = 0.96$, a control parameter

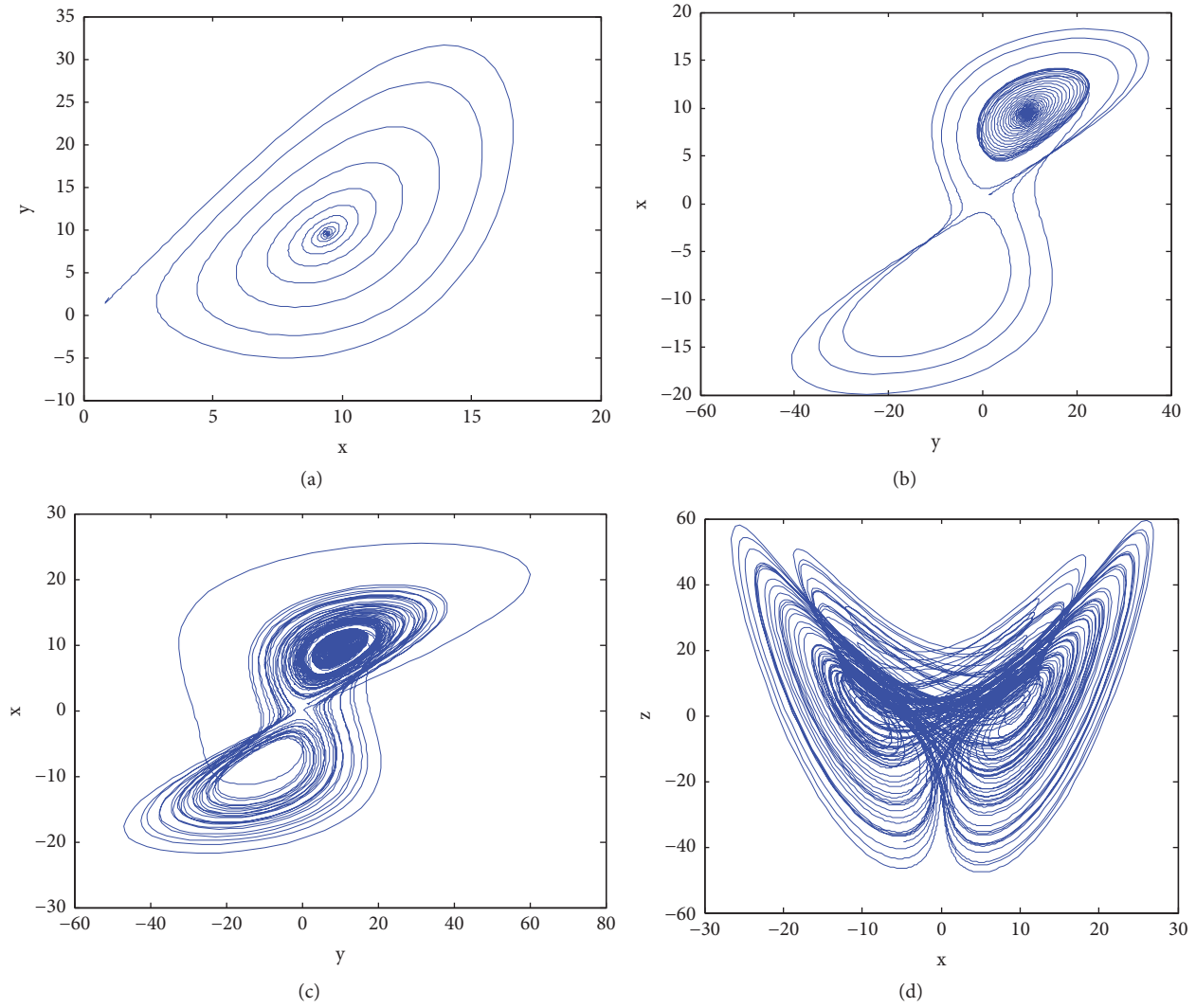

Figure 1: Attractors of system (6) for $q_1 = q_2 = q_3 = \theta$. (a) $\theta = 0.84$; (b) $\theta = 0.86$; (c) $\theta = 0.88$; (d) $\theta = 0.98$.

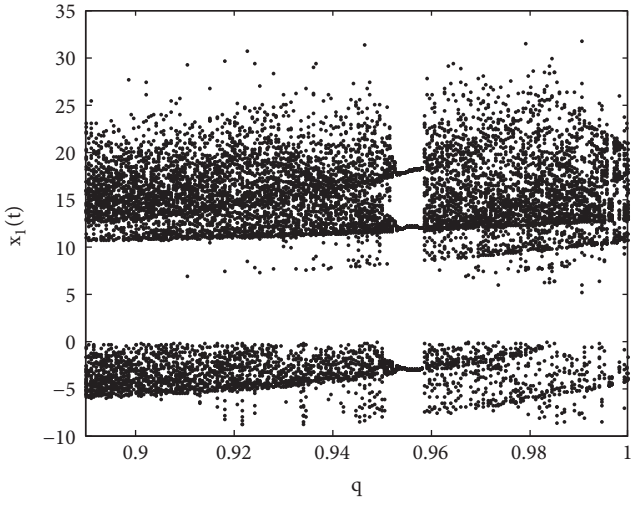

Figure 2: Bifurcation diagram of the fractional-order system (6) with $q \in (0.88, 1)$.

u is added to the second equation of system (6), and the controlled system can be written as

$$\begin{aligned} D_*^q x &= a(x - y) \\ D_*^q y &= -xz + u \\ D_*^q z &= -b + xy. \end{aligned} \tag{13}$$

Here, we use the predictor-corrector method to obtain the numerical solution of system (13). In our simulations, the time step and the running time are taken as $h = 0.001$ and $T = 100$ sec, respectively. The initial conditions of fractional-order system are selected as $x(0) = y(0) = z(0) = 1.0$. If the control parameter $u = -70$, one can obtain the left half-image of the original chaotic attractor (Figure 1(d)), as shown in Figure 9(a) for the x-z plane. However, when the control parameter $u = 70$, the right half-image of the original chaotic attractor can be isolated as shown in Figure 9(b). It implies that the new fractional-order system (6) consists of compound structures under certain conditions.

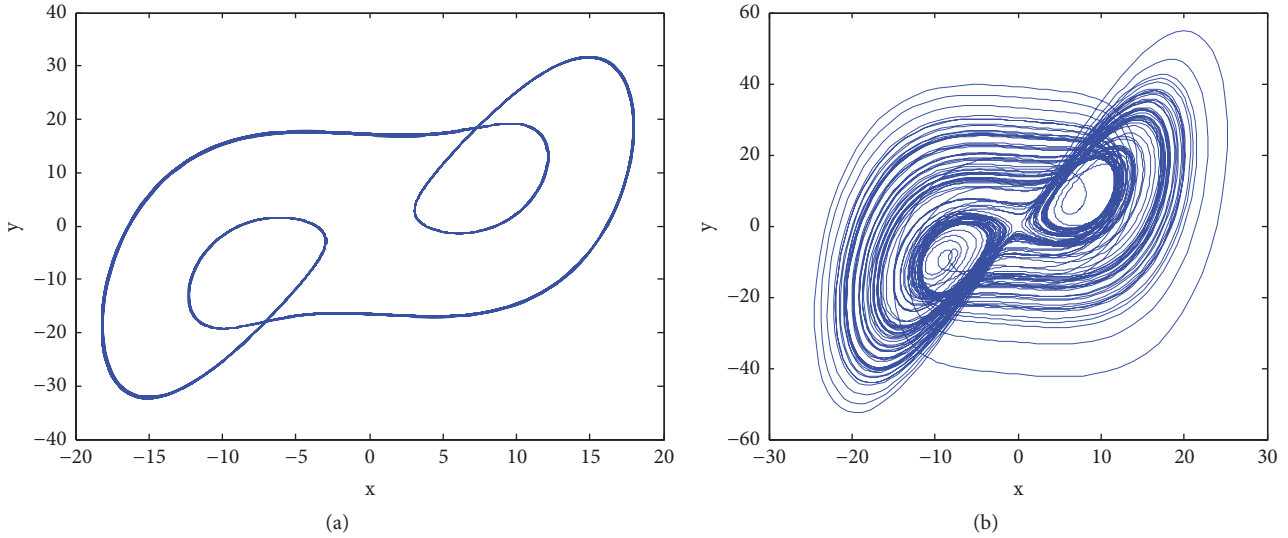

Figure 3: The phase portraits of the system for different values of q (a) $q = 0.95$; (b) $q = 0.98$.

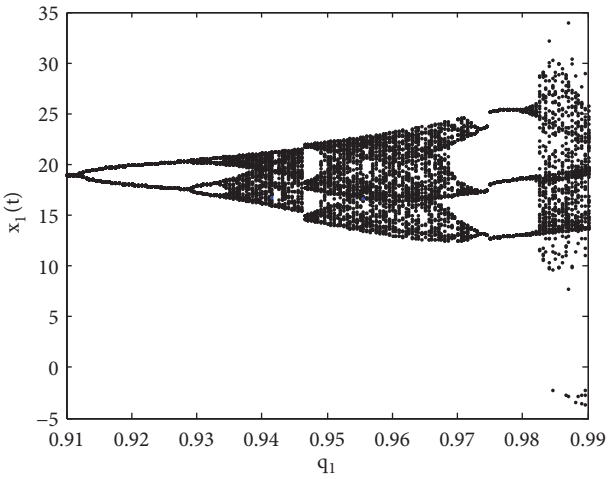

Figure 4: Bifurcation diagram of the fractional-order system (6) with $q_1 \in (0.91, 0.99)$.

In the following, fix system parameter $a = 5$, $b = 90$, and the fractional derivatives order $q = 0.98$; then we adjust the values of the control parameter u; complex dynamical behaviors of fractional-order system (13) can be summarized as follows:

(i) When $98 \le |u| \le 170$, system (13) displays limit cycles. For example, Figure 10(a) demonstrates a limit cycle at $u = 98$.

(ii) When $80 \le |u| \le 90$ and $71 \le |u| \le 80$, system (13) displays period-doubling bifurcations. Figures 10(b) and 10(c) give different period dynamics.

(iii) When $65 \le |u| \le 69$, system (13) exhibits partial attractors. Figure 10(d) shows a partially left, dominantly right attractor.

(iv) When $|u| = 70$, system (13) shows left and right half-image attractors, respectively, as shown in Figures 9(a) and 9(b).

Our results demonstrate that there are different formats of chaos with the variation of derivative order. One is a process of period-doubling bifurcations and the other is an interior crisis from single-scroll to double-scroll attractors. Certainly, the minimum effective dimension for fractional-order system to keep chaos is different between commensurate-order and incommensurate-order case. In order to know more about the dynamics of the system and to make further study in the future, the dynamics of system (6) with the variation of the different derivative order in the incommensurate-order case will be investigated in future work. In addition, future work on the topic should include the analysis of chaos control of the fractional-order system in detail.

5. Results and Discussion

In this paper, a novel fractional-order system is presented. Complex dynamics with interesting characteristics of the new fractional-order system are studied. Firstly, the basic properties of the new fractional-order system are analyzed via theoretical scheme. In addition, the phase diagrams for the different values of the parameters are obtained to show the rich dynamics of the system. Furthermore, the bifurcations and chaos dynamical phenomena in this system are numerically investigated by varying the fractional derivative orders and system parameters, respectively. The new fractional-order system displays several typical bifurcations, such as tangent bifurcations, period bifurcations, and various chaotic attractors. Meanwhile, the control problem of fractional-order system is investigated. Moreover, forming mechanisms of compound structures of the new fractional-order system is demonstrated via numerical simulations.

Appendix

A Brief Explanation regarding the Predictor-Corrector Algorithm

There are two approximation methods which can be used for numerical computation on chaos with fractional differential

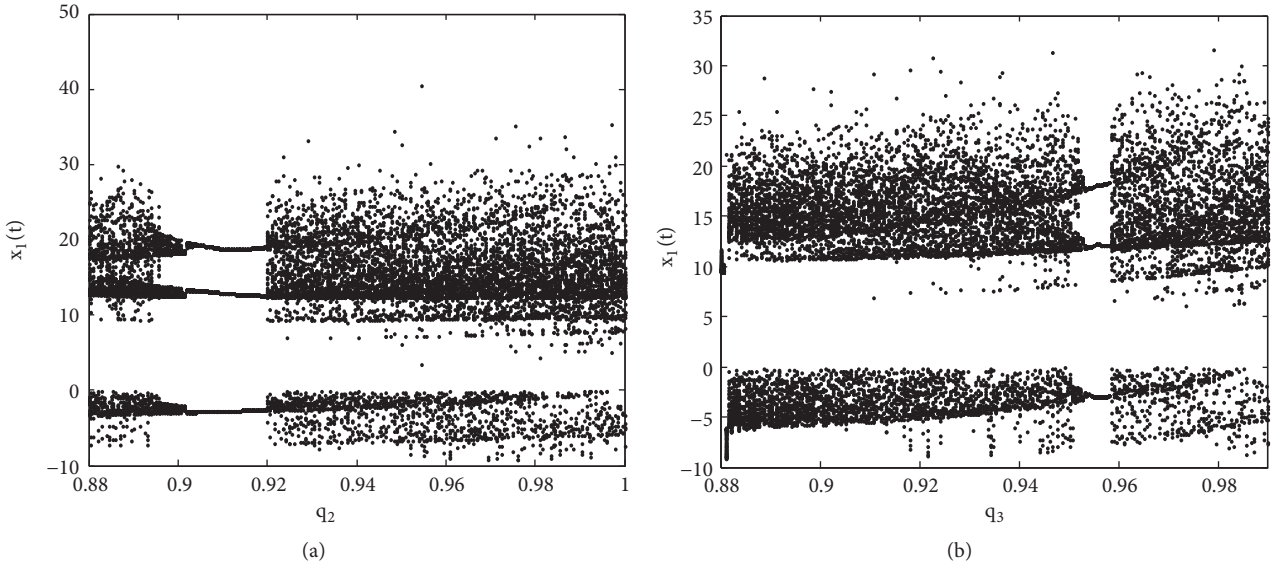

Figure 5: Bifurcation diagram of the fractional-order system (6) with (a) $q_2 \in (0.88, 1)$ (b) $q_3 \in (0.88, 0.99)$.

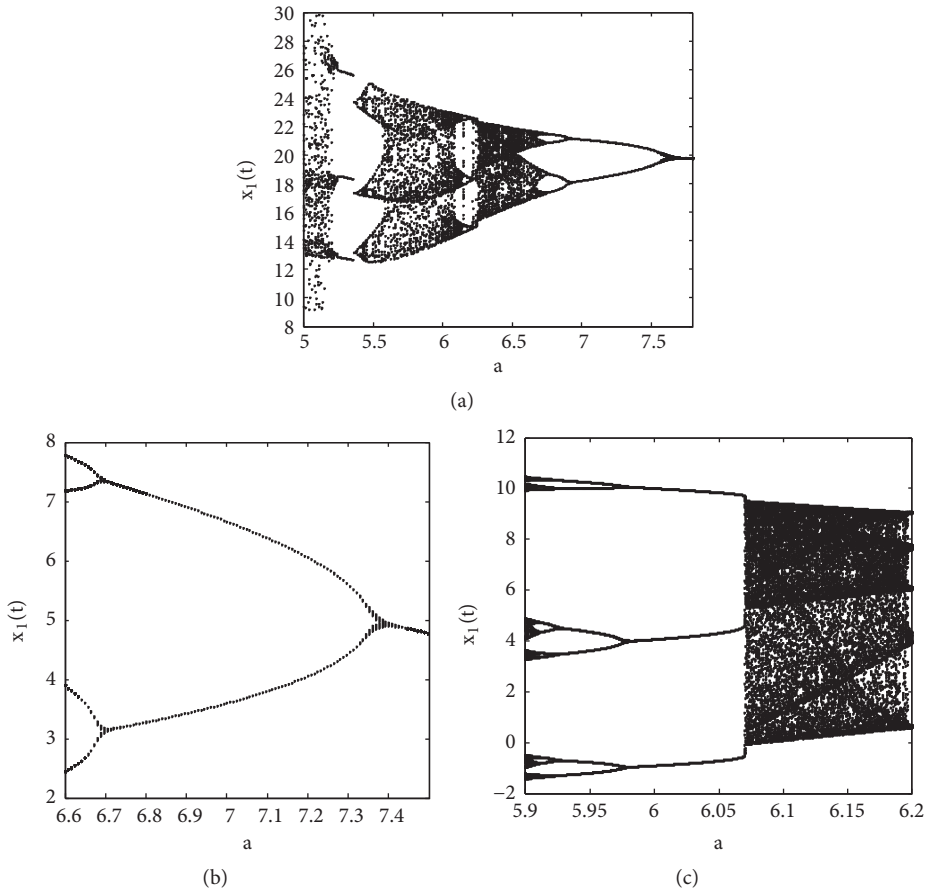

Figure 6: Bifurcation diagram of the fractional-order system (6) versus parameter a. (a) $a \in (5, 7.8)$; (b) $a \in (6.6, 7.5)$; (c) $a \in (5.8, 6.2)$.

equations. One is an improved version of Adams-Bashforth-Moulton algorithm based on the predictor-correctors scheme, which is a time-domain approach. The other is frequency domain approximation, based on numerical analysis of fractional-order systems in the frequency domain. In this paper, we employ the improved predictor-corrector algorithm for fractional-order differential equations. In what follows, the predictor-corrector algorithm is introduced.

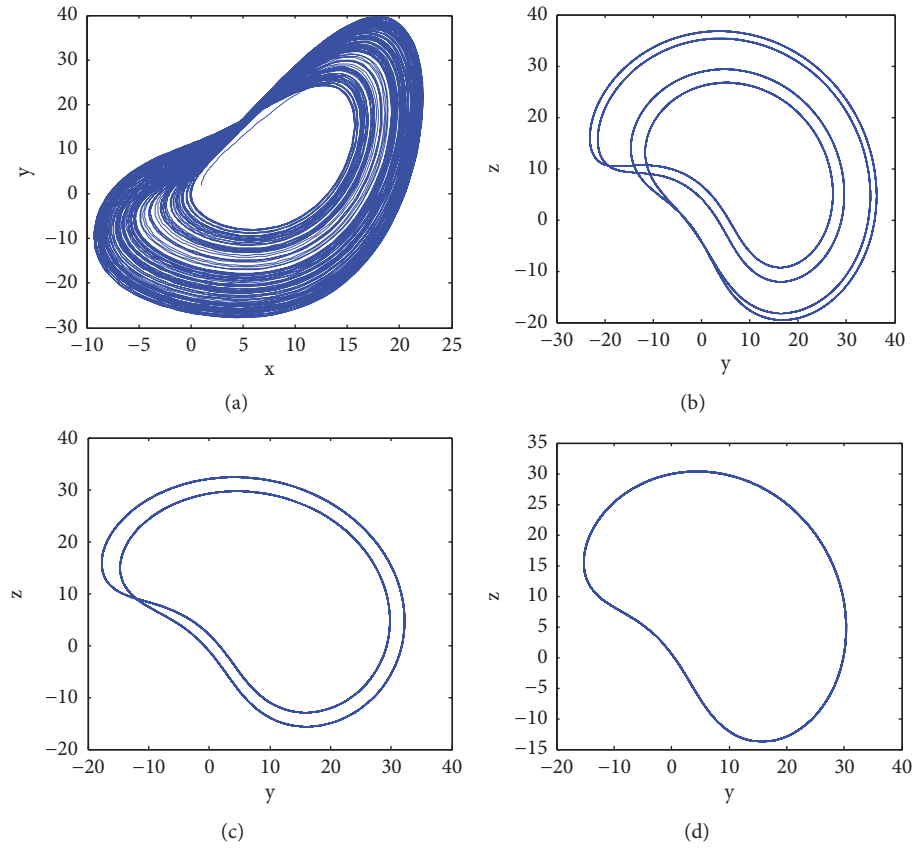

Figure 7: Phase portraits of the fractional-order system (6) for q_i $(i = 1, 2, 3) = 0.98$. (a) $a = 5.2$; (b) $a = 6.8$; (c) $a = 7.3$; (d) $a = 7.8$.

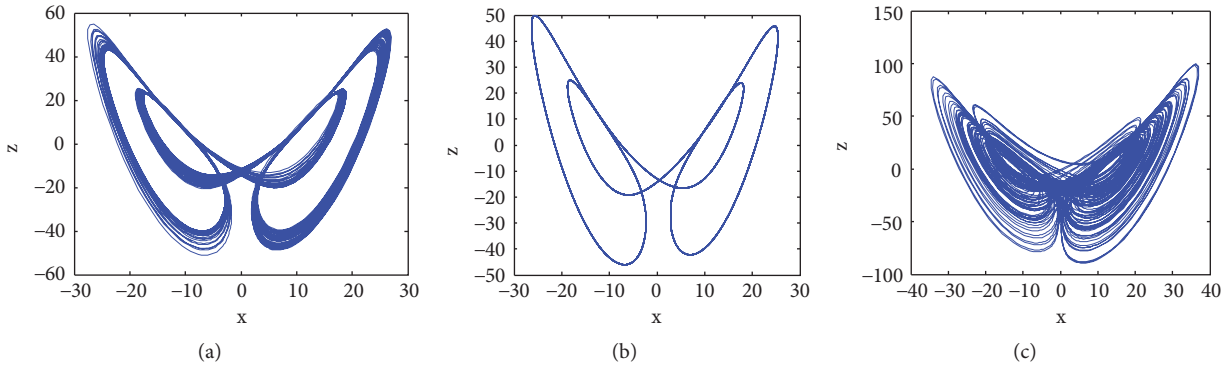

Figure 8: The phase portraits for system (6) at (a) $b = 175$; (b) $b = 180$; (c) $b = 200$.

To get the approximate solution of a fractional-order chaotic system by the predictor-corrector algorithm, the following equation is investigated

$$\frac{d^q x}{dt^q} = f(t, x) \quad 0 \le t \le T$$
$$x^k(0) = x_0^k \quad k = 0, 1, \ldots, [q] - 1, \tag{A.1}$$

which is equivalent to the Volterra integral equation.

$$x(t) = \sum_{k=0}^{[\alpha]-1} \frac{t^k}{k!} x_0^{(k)} + \frac{1}{\Gamma(\alpha)} \int_0^t (t-\tau)^{\alpha-1} f(\tau, x(\tau))\, d\tau \tag{A.2}$$

Set $h = T/N$, $t_j = jh$, $(j = 0, 1, \ldots, N)$. Then the corrector formula for (2) can be discretized as follows:

$$x_h(t_{n+1}) = \sum_{k=0}^{[\alpha]-1} \frac{t_{n+1}^k}{k!} x_0(k) + \frac{h^\alpha}{\Gamma(\alpha+2)} f\left(t_{n+1}, x_h^p(t_{n+1})\right)$$

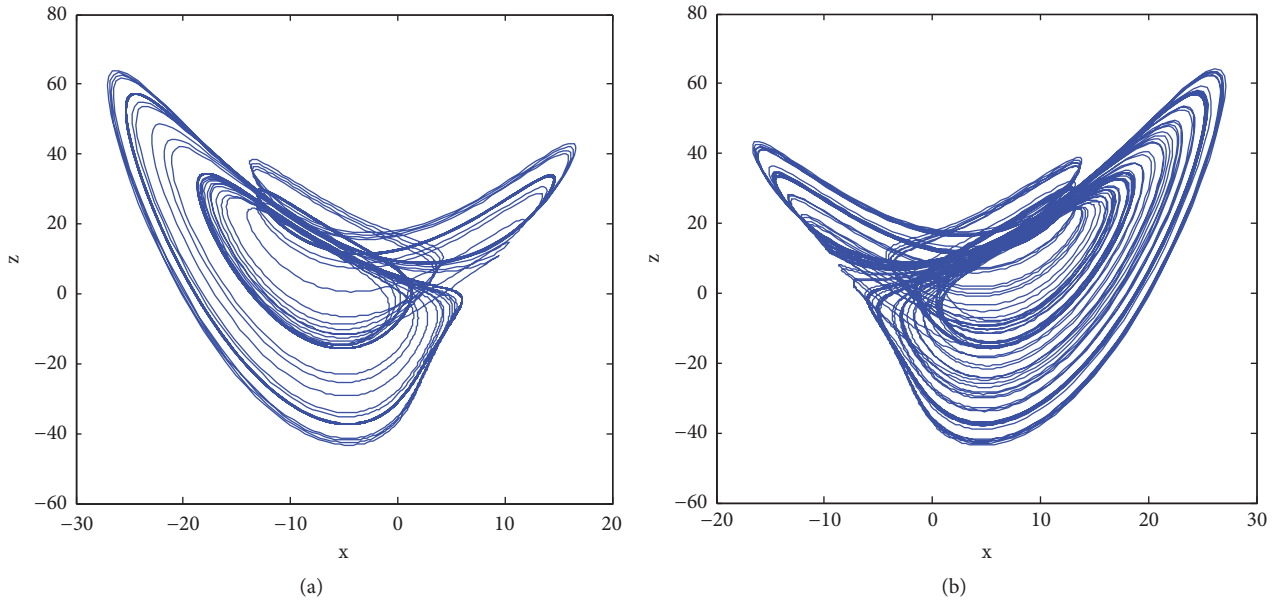

Figure 9: (a) Left half-image attractor for $u = -70$ (b) right half-image attractor for $u = 70$.

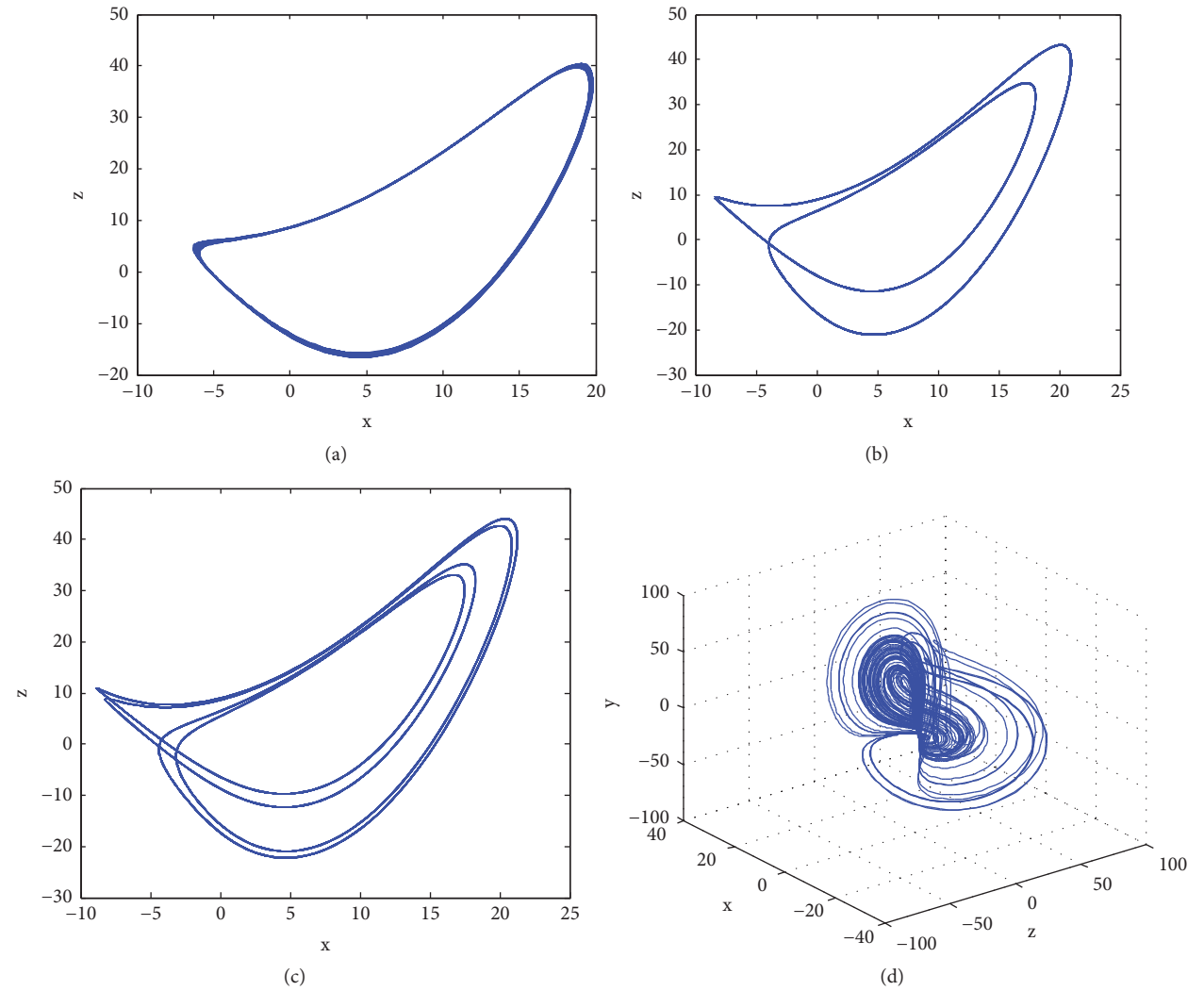

Figure 10: Attractors of system (13) at (a) $u = 98$; (b) $u = 90$; (c) $u = 88$; (d) $u = 68$.

$$+\frac{h^{\alpha}}{\Gamma(\alpha+2)}\sum a_{j,n+1}f\left(t_j,x_h\left(t_j\right)\right) \tag{A.3}$$

where predicted values $x_h(t_{n+1})$ are determined by the following formula.

$$x_h^p\left(t_{n+1}\right)=\sum_{k=0}^{[q]-1}x_0^{(k)}\frac{t_{n+1}^k}{k!}+\frac{1}{\Gamma(q)}\sum_{j=0}^{n}\beta_{j,n+1}f\left(t,x_h\left(t_j\right)\right), \tag{A.4}$$

Also

$$\alpha_{j,n+1}=\begin{cases}n^{q+1}-(n-q)(n+1)^q, & j=0\\ (n-j+2)^{q+1}+(n-j)^{q+1}-2(n-j+1)^{q+1}, & 1\le j\le n\\ 1, & j=n+1.\end{cases} \tag{A.5}$$

$$\beta_{j,n+1}=\frac{h^q}{q}\left((n-j+1)^q-(n-j)^q\right),\quad 1\le j\le n.$$

The error estimate of this approach can be presented: $\max_{j=0,1,\ldots,N}|x(t_j)-x_h(t_j)|=O(h^P)$, where $p=\min(2,1+q)$.

Data Availability

Data used to support the findings of this study are included within the paper.

Conflicts of Interest

The authors declare that they have no conflicts of interest.

Acknowledgments

This work is supported by the National Natural Science Foundation of China (NSFC) under grant No. 11702195 and No. 11702194 and Natural Science Preparatory Study Foundation of Shaanxi University of Science and Technology under grant No. 2017 BJ-49.

References

[1] C. P. Li, W. H. Deng, and D. Xu, "Chaos synchronization of the Chua system with a fractional order," *Physica A: Statistical Mechanics and its Applications*, vol. 360, no. 2, pp. 171–185, 2006.

[2] J. Huo and H. Zhao, "Dynamical analysis of a fractional SIR model with birth and death on heterogeneous complex networks," *Physica A: Statistical Mechanics and its Applications*, vol. 448, pp. 41–56, 2016.

[3] G. M. Mahmoud, T. Bountis, G. M. AbdEl-Latif, and E. E. Mahmoud, "Chaos synchronization of two different chaotic complex Chen and Lü systems," *Nonlinear Dynamics*, vol. 55, no. 1-2, pp. 43–53, 2009.

[4] S. Wang, Y. Yu, and G. Wen, "Hybrid projective synchronization of time-delayed fractional order chaotic systems," *Nonlinear Analysis: Hybrid Systems*, vol. 11, pp. 129–138, 2014.

[5] X. F. Li, Y. D. Chu, J. G. Zhang, and Y. X. Chang, "Nonlinear dynamics and circuit implementation for a new autonomous chaotic system," *Chaos Solitions and Fractals*, vol. 41, no. 5, pp. 2360–2370, 2009.

[6] S.-J. Ma, Q. Shen, and J. Hou, "Modified projective synchronization of stochastic fractional order chaotic systems with uncertain parameters," *Nonlinear Dynamics*, vol. 73, no. 1-2, pp. 93–100, 2013.

[7] Z. M. Odibat, "Adaptive feedback control and synchronization of non-identical chaotic fractional order systems," *Nonlinear Dynamics*, vol. 60, no. 4, pp. 479–487, 2010.

[8] H.-Y. Jia, Z.-Q. Chen, and W. Xue, "Analysis and circuit implementation for the fractional-order Lorenz system," *Acta Physica Sinica*, vol. 62, no. 14, Article ID 140503, 2013.

[9] X. Wang and H. Zhang, "Bivariate module-phase synchronization of a fractional-order lorenz system in different dimensions," *Journal of Computational and Nonlinear Dynamics*, vol. 8, no. 3, p. 031017, 2013.

[10] C. Li and G. Chen, "Chaos and hyperchaos in the fractional-order Rössler equations," *Physica A: Statistical Mechanics and its Applications*, vol. 341, no. 1–4, pp. 55–61, 2004.

[11] J.-L. Lavoie, T. J. Osler, and R. Tremblay, "Fractional derivatives and special functions," *SIAM Review*, vol. 18, no. 2, pp. 240–268, 1976.

[12] L. Kocarev and U. Parlitz, "General approach for chaotic synchronization with applications to communication," *Physical Review Letters*, vol. 74, no. 25, pp. 5028–5031, 1995.

[13] G. M. Mahmoud and T. Bountis, "The dynamics of systems of complex nonlinear oscillators: a review," *International Journal of Bifurcation and Chaos*, vol. 14, no. 11, pp. 3821–3846, 2004.

[14] B. Vinagre and V. Feliu, "Modeling and control of dynamic systems using fractional calculus: application to electrochemical processes and flexible structures," in *Proceedings of the 41st IEEE Conference on Decision and Control*, pp. 214–239, 2002.

[15] Z. M. Ge and C. Y. Ou, "Chaos in a fractional order modified Duffing system," in *Proceedings of the ECCTD*, pp. 1259–1262, 2005.

[16] J. G. Lu and G. R. Chen, "A note on the fractional-order Chen system," *Chaos Solitions and Fractals*, vol. 27, no. 3, pp. 685–688, 2006.

[17] X. Wu, H. Wang, and H. Lu, "Modified generalized projective synchronization of a new fractional-order hyperchaotic system and its application to secure communication," *Nonlinear Analysis: Real World Applications*, vol. 13, no. 3, pp. 1441–1450, 2012.

[18] Y. Kuang, *Delay Differential Equations with Applications in Population Dynamics*, Academic Press, New York, NY, USA, 1993.

[19] J.-G. Lu, "Chaotic dynamics of the fractional-order Ikeda delay system and its synchronization," *Chinese Physics*, vol. 15, no. 2, pp. 301–305, 2006.

[20] B. Munmuangsaen and B. Srisuchinwong, "A new five-term simple chaotic attractor," *Physics Letters A*, vol. 373, no. 44, pp. 4038–4043, 2009.

[21] S. Bhalekar, "Dynamical analysis of fractional order Uçar prototype delayed system," *Signal, Image and Video Processing*, vol. 6, no. 3, pp. 513–519, 2012.

[22] I. Podlubny, *Fractional Differential Equations*, vol. 198 of *Mathematics in Science and Engineering*, Academic Press, San Diego, Calif, USA, 1999.

[23] D. Matignon, "Stability results for fractional differential equations with applications to control processing," in *Proceedings of the IEEE-SMC Proceedings Computational engineering in systems and application multi-conference*, vol. 2, pp. 963–968, IMACS, Lille, France, 1996.

Hindawi
Discrete Dynamics in Nature and Society
Volume 2018, Article ID 6456107, 20 pages
https://doi.org/10.1155/2018/6456107

Research Article

Dynamics and Stability Analysis of a Brucellosis Model with Two Discrete Delays

Paride O. Lolika[1,2] and Steady Mushayabasa[1]

[1] *University of Zimbabwe, Department of Mathematics, P.O. Box MP 167, Harare, Zimbabwe*
[2] *University of Juba, Department of Mathematics, P.O. Box 82 Juba, Central Equatoria, South Sudan*

Correspondence should be addressed to Steady Mushayabasa; steadymushaya@gmail.com

Received 23 April 2018; Revised 29 June 2018; Accepted 17 July 2018; Published 8 August 2018

Academic Editor: Abdul Qadeer Khan

We present a mathematical model for brucellosis transmission that incorporates two discrete delays and culling of infected animals displaying signs of brucellosis infection. The first delay represents the incubation period while the second account for the time needed to detect and cull infectious animals. Feasibility and stability of the model steady states have been determined analytically and numerically. Further, the occurrence of Hopf bifurcation has been established. Overall the findings from the study, both analytical and numerical, suggest that the two delays can destabilize the system and periodic solutions can arise through Hopf bifurcation.

1. Introduction

Brucellosis is one of the neglected zoonotic diseases that remains a major public health problem world over, especially in Middle Eastern countries, southern Europe and North Africa, countries in South and Central Asia, sub-Saharan Africa, Mexico, the Caribbean, and countries in South and Central America [1], with an annual occurrence of more than 500 000 cases [2].

In animals, brucellosis is usually transmitted through direct contact between a susceptible and an infectious animal or indirectly, i.e., when a susceptible animal ingest contaminated forages or the excrement containing large quantities of bacteria, generally discharged by infected animals [3]. In humans, however, the majority of the infections result from direct or indirect exposure to infected animals or consumption of raw animal products such as unpasteurized milk or cheese [4]. Since human-to-human transmission of the disease is extremely rare [5], the ultimate management of human brucellosis can be achieved through effective control of brucellosis in livestock. Some researchers postulate that eradication of brucellosis in animals can be attained by combining vaccination with test-and-slaughter programs [1].

Mathematical models have proved to be essential guiding tools for epidemiologists, biologists, and policy makers. Models can provide solutions to phenomena which are difficult to measure practically. Recently, a number of mathematical models have been proposed to study the spread and control of brucellosis (see, for example, [3, 6–15] and references therein). A limitation of these previous studies, however, is the noninclusion of the time taken before an infectious animal is detected and culled, despite the fact that in many countries where the disease is endemic lack of financial and human resources often results in delay of detection and culling of infectious animals. The size of this delay may play an important role in minimizing the spread of the disease in the community.

It is therefore essential to gain a better and more comprehensive understanding of the effects of time delay on brucellosis transmission and control. Prior studies have shown that epidemic models with time delay often exhibit periodic solutions and as a consequence understanding the nature of these periodic outbreaks plays a crucial role in designing policies that can successfully control the disease. In fact, a recent analysis of brucellosis dataset in countries where the disease is endemic has shown that the disease

incidences exhibit a strong periodic behavior with mortality and morbidity of the disease concentrated in a few months each year [16, 17]. Understanding the impact of such seasonal variations is crucial in managing the spread of the disease in the community.

Our main goal in this study is to explore the dynamics and stability analysis of a brucellosis model with two discrete delays. Hence we formulated a mathematical model that incorporates two discrete delays. The first delay represents the incubation period while the second delay accounts for the time taken to detect and cull infectious animals. In addition, we subdivide the total animal population into classes of susceptible, vaccinated, infectious undetected, and infectious detected animals. In certain situations immediate slaughter of detected animals may not be feasible and more often these animals are isolated from the rest. However, due to lack of financial and human resources, in addition to lack of knowledge and attitude of farmers, isolation of detected animals has not been a successful practice in most developing nations where animal infections are rampant. Thus in our modelling process we assume that a proportion of detected animals that are not immediately culled are also responsible for disease transmission. Utilizing both analytical and numerical results we have demonstrated that the two delays can destabilize the system and lead to Hopf bifurcation.

The article is organised as follows. The model description is given in Section 2. Analytical and numerical results are given in Sections 3 and 4, respectively. We end with Section 5 of conclusions.

2. Mathematical Model

We subdivide the total animal population $N(t)$ into compartments of susceptible $S(t)$, vaccinated $V(t)$, undetected infectious animals $I_1(t)$, and infectious detected and unculled $I_2(t)$. Although brucellosis can be transmitted indirectly (environmental transmission), prior studies [6, 8] suggest that indirect transmission plays a relatively small role on the spread of brucellosis, and as such we have ignored this aspect in our study. Brucellosis dynamics in this study are governed by the following autonomous system:

$$\begin{aligned}
\frac{dS(t)}{dt} &= A - \beta\left[I_1(t) + (1-p)I_2(t)\right]S(t) - (\mu+\sigma)\\
&\quad \cdot S(t) + \kappa V(t),\\
\frac{dV(t)}{dt} &= \sigma S(t) - \gamma\beta\left[I_1(t) + (1-p)I_2(t)\right]V(t)\\
&\quad - (\mu+\kappa)V(t),\\
\frac{dI_1(t)}{dt} &= \beta\left[I_1(t-\tau_1) + (1-p)I_2(t-\tau_1)\right]\\
&\quad \cdot \left[S(t-\tau_1) + \gamma V(t-\tau_1)\right] - (\alpha+\mu+d)I_1(t),\\
\frac{dI_2(t)}{dt} &= \alpha I_1(t-\tau_2) - (\mu+c+d)I_2(t),
\end{aligned} \tag{1}$$

where A is the recruitment rate through birth, μ is the natural death rate, β is the disease direct transmission rate, p is fraction of detected animals that have been culled, σ is the vaccination rate, κ is the vaccination waning rate, τ_1 represents the latency delay, τ_2 is the delay in detection, γ is the modification factor, α is the rate at which animals are detected and quarantined, c is the culling rate of detected animals, and d is disease-induced death.

3. Analytical Results

3.1. Initial Conditions. The appropriate space for system (1) is $X = \mathscr{C}([-\tau, 0], \mathbb{R}^4_+)$ the Banach space of continuous functions mapping the interval $[-\tau, 0]$ into $\mathbb{R}^4_+$ equipped with subnorm where $\tau = \max\{\tau_1, \tau_2\}$. From the standard results of functional differential equations [18] it follows that, given any initial conditions $x_0 \in X$, there exists a unique solution $\phi(t, x_0) = (S(t, x_0), V(t, x_0), I_1(t, x_0), I_2(t, x_0))$ of system (1), which satisfies $\phi_0 = x_0$, the initial conditions are given by

$$\begin{aligned}
S(\theta) &= x_0^1(\theta),\\
V(\theta) &= x_0^2(\theta),\\
I_1(\theta) &= x_0^3(\theta),\\
I_2(\theta) &= x_0^4(\theta),\\
&\qquad \theta \in [-\tau, 0],
\end{aligned} \tag{2}$$

where $x_0 = (x_0^1, x_0^2, x_0^3, x_0^4) \in X$, with $x_0^i(\theta) \geq 0$, $(\theta \in [-\tau, 0],\ i = 1, 2 \ldots, 4)$ and $x_0^3(0), x_0^4(0) > 0$.

3.2. The Basic Reproduction Number. By direct calculation, we find that system (1) has a disease-free equilibrium $\mathscr{E}^0$, given by $\mathscr{E}^0 = (S^0, V^0, 0, 0)$, with

$$\begin{aligned}
S^0 &= \frac{A(\mu+\kappa)}{\mu(\mu+\sigma+\kappa)},\\
V^0 &= \frac{A\sigma}{\mu(\mu+\sigma+\kappa)},\\
S^0 + \gamma V^0 &= \frac{A(\mu+\kappa+\gamma\sigma)}{\mu(\mu+\sigma+\kappa)}.
\end{aligned} \tag{3}$$

By utilizing the next-generation matrix method [19], one can deduce that the basic reproduction number of model (1) is

$$\mathscr{R}_0 = \frac{\beta\left(S^0 + \gamma V^0\right)\left(\alpha(1-p) + k_2\right)}{k_1 k_2}, \tag{4}$$

with $k_1 = (\mu + \alpha + d)$, and $k_2 = (\mu + c + d)$.

3.3. Stability of the Disease-Free Equilibrium. In this section, we study the local and global stability of the disease-free equilibrium.

Theorem 1. *The disease-free equilibrium $\mathscr{E}^0$ of model (1) is locally asymptotically stable when $\mathscr{R}_0 < 1$ and unstable when $\mathscr{R}_0 > 1$.*

Proof. To study the local stability of the disease-free equilibrium $\mathscr{E}^0$, we linearized system (1) about this point and obtained the characteristic equation, given by the following determinant:

$$\begin{vmatrix} -(\mu+\sigma)-\lambda & \kappa & -\beta S^0 & -\beta(1-p)S^0 \\ \sigma & -(\mu+\kappa)-\lambda & -\gamma\beta V^0 & -\gamma\beta(1-p)V^0 \\ 0 & 0 & \left(S^0+\gamma V^0\right)\beta e^{-\lambda\tau_1}-k_1-\lambda & \beta\left(S^0+\gamma V^0\right)(1-p)e^{-\lambda\tau_1} \\ 0 & 0 & \alpha e^{-\lambda\tau_2} & -k_2-\lambda \end{vmatrix} = 0, \tag{5}$$

where λ is the eigenvalue.

From (5) the characteristic equation is

$$\begin{aligned} &\{\lambda+\mu\}\{\lambda+\sigma+\kappa+\mu\} \\ &\cdot\left\{[\lambda+k_2]\left[\lambda+k_1-\beta\left(S^0+\gamma V^0\right)e^{-\lambda\tau_1}\right]\right. \\ &\left.-(1-p)\alpha\beta\left(S^0+\gamma V^0\right)e^{-\lambda(\tau_1+\tau_2)}\right\}=0. \end{aligned} \tag{6}$$

Clearly, $-\mu$ and $-(\sigma+\kappa+\mu)$ are eigenvalues and the other two can be determined from the following equation:

$$\begin{aligned} &(\lambda+k_2)\left(\lambda+k_1-\beta\left(S^0+\gamma V^0\right)e^{-\lambda\tau_1}\right) \\ &-(1-p)\alpha\beta\left(S^0+\gamma V^0\right)e^{-\lambda(\tau_1+\tau_2)}=0. \end{aligned} \tag{7}$$

Let

$$\begin{aligned} g(\lambda,\tau_1,\tau_2) &= (\lambda+k_2)\left(\lambda+k_1-\beta\left(S^0+\gamma V^0\right)e^{-\lambda\tau_1}\right) \\ &-(1-p)\alpha\beta\left(S^0+\gamma V^0\right)e^{-\lambda(\tau_1+\tau_2)}. \end{aligned} \tag{8}$$

Through direct calculation one can easily verify that $g(\lambda,\tau_1,\tau_2)$ is an analytic function and it follows that

$$\begin{aligned} g(0,\tau_1,\tau_2) &= k_1k_2(1-\mathscr{R}_0), \\ g(\lambda,0,0) &= (\lambda+k_2)\left(\lambda+k_1-\beta\left(S^0+\gamma V^0\right)\right) \\ &-(1-p)\alpha\beta\left(S^0+\gamma V^0\right). \end{aligned} \tag{9}$$

Now we proceed to investigate the distribution of the solutions of (7) in the following cases:

(a) If $\mathscr{R}_0<1$, then $g(0,\tau_1,\tau_2)>0$. Since the derivative $g'_\lambda(\lambda,\tau_1,\tau_2)>0$ for $\lambda\geq 0$, $\tau_1>0$ and $\tau_2>0$, (7) has no zero root and positive real roots for all positive τ_1 and τ_2. Now we assume that the solution of (7) does not have any purely imaginary roots $\lambda=i\omega$, $(\omega>0)$ for some $\tau_1>0$, $\tau_2=0$. Then by computation, ω must be positive real root of

$$\begin{aligned} &\omega^4+\left\{k_1^2+k_2^2-\left[\beta\left(S^0+\gamma V^0\right)\right]^2\right\}\omega^2+(k_1k_2)^2 \\ &-\left[\beta\left(S^0+\gamma V^0\right)[k_2+\alpha(1-p)]\right]^2=0. \end{aligned} \tag{10}$$

If $\mathscr{R}_0<1$, (10) has no positive roots. Hence (7) does not have any purely imaginary roots. We can easily see that the roots of $g(\lambda,0,0)=0$ all have negative real parts when $\mathscr{R}_0<1$. By the implicit function theorem and the continuity of $g(\lambda,\tau_1,\tau_2)$, we know that all roots of (7) have negative real parts for positive τ_1 and $\tau_2=0$ which implies that $\mathscr{E}^0$ is stable.

(b) If $\mathscr{R}_0=1$ then $g(0,\tau_1,\tau_2)>0$. Since the derivative $g'(\lambda,\tau_1,\tau_2)>0$ for $\lambda\geq 0$, $\tau_1>0$ and $\tau_2>0$, (7) has a simple zero and no positive root for all positive τ_1 and τ_2. By the same argument in case (*a*), we can obtain that all roots of (7) have negative real parts for positive τ_1 and $\tau_2=0$ except a zero root. Thus $\mathscr{E}^0$ is a degenerate equilibrium of codimension and is stable except in one direction.

(c) If $\mathscr{R}_0>1$, then $g(0,\tau_1,\tau_2)<0$. Since we have $\lim_{\lambda\to\infty}g(\lambda,\tau_1,\tau_2)=\infty$ and $g'(\lambda,\tau_1,\tau_2)>0$ for $\lambda\geq 0$, $\tau_1>0$ and $\tau_2>0$, (7) has a unique positive real root for all positive τ_1 and $\tau_2=0$ and $\mathscr{E}^0$ is unstable.

□

Theorem 2. *The disease-free equilibrium of model (1) is globally asymptotically stable when $\mathscr{R}_0\leq 1$ and unstable when $\mathscr{R}_0>1$.*

Proof. We denote by x_t the translation of the solution of the system (1); that is, $x_t=(S(t+\theta),V(t+\theta),I_1(t+\theta),I_2(t+\theta))$, where $\theta\in[-\tau,0]$ and $\tau=\max\{\tau_1,\tau_2\}$. We consider the following Lyapunov functional:

$$\begin{aligned} \mathscr{U}(x_t) &= \frac{\beta[\alpha(1-p)+k_2]}{k_1k_2}I_1(t)+\frac{\beta(1-p)}{k_2}I_2(t) \\ &+\frac{\beta\alpha(1-p)}{k_2}\int_{t-\tau_2}^{t}[I_1(\theta)]\,d\theta+\frac{\beta^2[\alpha(1-p)+k_2]}{k_1k_2} \\ &\cdot\int_{t-\tau_1}^{t}\{[I_1(\theta)+(1-p)I_2(\theta)][S(\theta)+\gamma V(\theta)]\}\,d\theta. \end{aligned} \tag{11}$$

Taking the derivative of $\mathscr{U}$ along the solutions of (1) gives

$$\begin{aligned} \frac{d\mathscr{U}(x_t)}{dt} &= \frac{\beta[\alpha(1-p)+k_2]}{k_1k_2} \\ &\cdot\beta[I_1(t-\tau_1)+(1-p)I_2(t-\tau_1)] \end{aligned}$$

$$\cdot \left[S\left(t-\tau_1\right)+\gamma V\left(t-\tau_1\right)\right]-\frac{\beta\left[\alpha\left(1-p\right)+k_2\right]}{k_2}$$

$$\cdot I_1\left(t\right)+\frac{\beta\left(1-p\right)}{k_2}\alpha I_1\left(t-\tau_2\right)-\beta\left(1-p\right)I_2\left(t\right)$$

$$+\frac{\beta\left[\alpha\left(1-p\right)+k_2\right]}{k_1k_2}\beta\left[I_1\left(t\right)+\left(1-p\right)I_2\left(t\right)\right]$$

$$\cdot\left[S\left(t\right)+\gamma V\left(t\right)\right]-\frac{\beta\left[\alpha\left(1-p\right)+k_2\right]}{k_1k_2}$$

$$\cdot\beta\left[I_1\left(t-\tau_1\right)+\left(1-p\right)I_2\left(t-\tau_1\right)\right]$$

$$\cdot\left[S\left(t-\tau_1\right)+\gamma V\left(t-\tau_1\right)\right]+\frac{\beta\left(1-p\right)}{k_2}\alpha I_1\left(t\right)$$

$$-\frac{\beta\left(1-p\right)}{k_2}\alpha I_1\left(t-\tau_2\right)=\frac{\beta\left[\alpha\left(1-p\right)+k_2\right]}{k_1k_2}$$

$$\cdot\beta\left[S\left(t\right)+\gamma V\left(t\right)\right]\left[I_1\left(t\right)+\left(1-p\right)I_2\left(t\right)\right]$$

$$-\beta\left[I_1\left(t\right)+\left(1-p\right)I_2\left(t\right)\right]$$

$$\leq\beta\left[\frac{\beta\left[\alpha\left(1-p\right)+k_2\right]\left[S^0+\gamma V^0\right]}{k_1k_2}-1\right]$$

$$\cdot\left[I_1\left(t\right)+\left(1-p\right)I_2\left(t\right)\right]=\beta\left[\mathscr{R}_0-1\right]$$

$$\cdot\left[I_1\left(t\right)+\left(1-p\right)I_2\left(t\right)\right]. \tag{12}$$

Therefore, $\dot{\mathscr{U}}<0$ holds if $\mathscr{R}_0<1$. Furthermore, $\dot{\mathscr{U}}=0$ if $\mathscr{R}_0=1$. Therefore, the largest invariant set of $\dot{\mathscr{U}}$ is a singleton $\{\mathscr{E}^0\}$ such that $S(t)=S^0$, $V(t)=V^0$, $I_1(t)=I_2(t)=0$. It follows from LaSalle's invariance principle [20] that the disease-free equilibrium of system (1) denoted by $\mathscr{E}^0$ is globally asymptotically stable whenever $\mathscr{R}_0\leq 1$. This completes the proof of Theorem 2. □

3.4. Disease Persistence. System (1) is said to be uniformly persistent if there exists a constant $\eta_0>0$ such that any solution $(S(t),V(t),I_1(t),I_2(t))$ of (1) satisfies

$$\begin{aligned}
&\liminf_{t\longrightarrow\infty}S\left(t\right)\geq\eta_0,\\
&\liminf_{t\longrightarrow\infty}V\left(t\right)\geq\eta_0,\\
&\liminf_{t\longrightarrow\infty}I_1\left(t\right)\geq\eta_0,\\
&\liminf_{t\longrightarrow\infty}I_2\left(t\right)\geq\eta_0.
\end{aligned} \tag{13}$$

Now we give a result on the uniform persistence of system (1). To proceed we introduce the following notation and terminology. Denote by $P(t)$, $t\geq 0$ the family of solution operators corresponding to (1). ω-limit set $\omega(x)$ of x consists of $y\in X$ such that there exists a sequence $t_n\longrightarrow\infty$ as $n\longrightarrow\infty$ with $P(t_n)x\longrightarrow y$ as $n\longrightarrow\infty$.

Theorem 3. *System (1) is uniformly persistent, if it satisfies* $\mathscr{R}_0>1$.

Proof. Let $X^0=\{x_0\in X: x_0^3(0)>0, x_0^4(0)>0\}$, $\partial X=X\backslash X^0=\{x_0\in X: x_0^3(0)=0 \text{ or } x_0^4(0)=0\}$ which is relatively closed in X.

In what follows we demonstrate that X^0 is positively invariant for $P(t)$. From the third and fourth equations of (1) we have

$$\begin{aligned}
\frac{dI_1\left(t\right)}{dt}&\geq-\left(\alpha+\mu+d\right)I_1\left(t\right),\\
\frac{dI_2\left(t\right)}{dt}&\geq-\left(\mu+c+d\right)I_2\left(t\right).
\end{aligned} \tag{14}$$

Since $I_1(0,x_0)=x_0^3(0)>0$, we have $I_2(0,x_0)=x_0^4(0)>0$, and it follows from (14) that

$$\begin{aligned}
I_1\left(t,x_0\right)&\geq x_0^3\left(0\right).e^{-(\alpha+\mu+d)t},\\
I_2\left(t,x_0\right)&\geq x_0^4\left(0\right).e^{-(\mu+c+d)t},\\
&\forall t\geq 0.
\end{aligned} \tag{15}$$

Thus X^0 is positively invariant for $P(t)$.

We set

$$\begin{aligned}
M_\partial=\{&x_0\in X:\phi\left(t\right)x_0 \text{ satisfies (1) and } \phi\left(t\right)x_0\\
&\in\partial X,\ \forall t\geq 0\}.
\end{aligned} \tag{16}$$

We claim that

$$M_\partial=\{(S,V,0,0)\}. \tag{17}$$

Assuming $\phi(t)\in M_\partial$, $\forall t\geq 0$; it suffices to show that $I_1(t)=I_2(t)=0$, $\forall t\geq 0$. If it is not true, then there exists $t_0>0$ such that either (a) $I_1(t_0)>0$, $I_2(t_0)=0$; or (b) $I_1(t_0)=0$, $I_2(t_0)>0$. For case (a), from the fourth equation of (1), we have

$$\left[\frac{dI_2}{dt}\right]_{t=t_0}=\alpha I_1\left(t_0-\tau_2\right)>0. \tag{18}$$

Hence there is $\epsilon_0>0$ such that $I_2(t)>0$, $\forall t\in(t_0,t_0+\epsilon_0)$. On the other hand, from $I_1(t)>0$ there exists ϵ_1 $(0<\epsilon_1<\epsilon_0)$ such that $I_1(t)>0$, $\forall t\in(t_0,t_0+\epsilon_1)$. Thus we have $I_1(t)>0$, $I_2(t)>0$, $\forall t\in(t_0,t_0+\epsilon_1)$ which contradicts the assumption that $(S(t),V(t),I_1(t),I_2(t))\in M_\partial$, $\forall t\geq 0$. Similarly, we can obtain a contradiction for case (b). This proves the claim (17).

Let $\mathscr{F}=\bigcap_{x\in F_b}\omega(x)$, where F_b is the global attractor of $P(t)$ restricted to ∂X. We show that $\mathscr{F}=\{\mathscr{E}^0\}$. In fact, from $\mathscr{F}\subseteq M_\partial$ and the first and second equation of (1), we have $\lim_{t\longrightarrow\infty}S(t)=S^0$ and $\lim_{t\longrightarrow\infty}V(t)=V^0$. Thus, $\{\mathscr{E}^0\}$ is the isolated invariant set in X.

Next we show that $W^S(\mathscr{E}^0)\cap X_0=\emptyset$. If this is not true, then there exists a solution $(S^t,V^t,I_1^t,I_2^t)\in X^0$ such that

$$\begin{aligned}
\lim_{t\longrightarrow\infty}S\left(t\right)&=\frac{A\left(\mu+\kappa\right)}{\mu\left(\mu+\sigma+\kappa\right)},\\
\lim_{t\longrightarrow\infty}V\left(t\right)&=\frac{A\sigma}{\mu\left(\mu+\sigma+\kappa\right)},
\end{aligned}$$

$$\lim_{t\longrightarrow\infty} I_1(t) = 0,$$
$$\lim_{t\longrightarrow\infty} I_2(t) = 0, .$$
(19)

For any sufficiently small constant $\epsilon > 0$, there exists a positive constant $T_0 = T_0(\epsilon)$ such that $S(t) > S^0 - \epsilon > 0$, $V(t) > V^0 - \epsilon > 0$, $\forall t > T_0$. For the constant ϵ given above, it follows from the third and fourth equations of (1) that

$$\begin{aligned}\frac{dI_1(t)}{dt} &\geq \beta\left[I_1(t-\tau_1) + (1-p)I_2(t-\tau_1)\right]\\ &\quad\cdot\left[\left(S^0-\epsilon\right) + \gamma\left(V^0-\epsilon\right)\right] - (\alpha+\mu+d)I_1(t),\\ \frac{dI_2(t)}{dt} &= \alpha I_1(t-\tau_2) - (\mu+c+d)I_2(t),\\ &\qquad\qquad t \geq T_0 + \tau\end{aligned}$$
(20)

If $I_1(t), I_2(t) \longrightarrow \infty$, then, by a standard comparison argument and the nonnegativity, the solution $(\widetilde{I}_1(t), \widetilde{I}_2(t))$ of the following monotone system

$$\begin{aligned}\frac{d\widetilde{I}_1(t)}{dt} &= \beta\left[\widetilde{I}_1(t-\tau_1) + (1-p)\widetilde{I}_2(t-\tau_1)\right]\\ &\quad\cdot\left[\left(S^0-\epsilon\right) + \gamma\left(V^0-\epsilon\right)\right] - (\alpha+\mu+d)\widetilde{I}_1(t),\\ \frac{d\widetilde{I}_2(t)}{dt} &= \alpha\widetilde{I}_1(t-\tau_2) - (\mu+c+d)\widetilde{I}_2(t),\\ &\qquad\qquad t \geq T_0 + \tau\end{aligned}$$
(21)

with initial condition $\widetilde{I}_1(t) = I_1(t)$, $\widetilde{I}_2(t) = I_2(t)$, $\forall t \in [T_0, T_0+\tau]$ converges to $(0,0)$ as well. Thus $\lim_{t\longrightarrow\infty}\widehat{W}(t) = 0$, where $\widehat{W}(t) > 0$ is defined by

$$\begin{aligned}\widehat{W}(t) &= \frac{\beta\left[\alpha(1-p)+k_2\right]}{k_1k_2}\widetilde{I}_1(t) + \frac{\beta(1-p)}{k_2}\widetilde{I}_2(t)\\ &\quad+\frac{\beta\alpha(1-p)}{k_2}\int_{t-\tau_2}^{t}\left[\widetilde{I}_1(\zeta)\right]d\zeta\\ &\quad+\frac{\beta^2\left[\alpha(1-p)+k_2\right]\left[\left(S^0-\epsilon\right)+\gamma\left(V^0-\epsilon\right)\right]}{k_1k_2}\\ &\quad\cdot\int_{t-\tau_1}^{t}\left[\widetilde{I}_1(\zeta) + (1-p)\widetilde{I}_2(\zeta)\right]d\zeta.\end{aligned}$$
(22)

Differentiating $\widehat{W}(t)$ with respect to time t yields

$$\begin{aligned}&\left[\frac{d\widehat{W}(t)}{dt}\right]_{(12)}\\ &= \left[\frac{\beta^2\left[\alpha(1-p)+k_2\right]\left[\left(S^0-\epsilon\right)+\gamma\left(V^0-\epsilon\right)\right]}{k_1k_2}\right.\\ &\quad\left.-\beta\right]\left[\widetilde{I}_1(t) + (1-p)\widetilde{I}_2(t)\right].\end{aligned}$$
(23)

Since $\mathscr{R}_0 > 1$, we have $\beta^2[\alpha(1-p)+k_2][(S^0-\epsilon)+\gamma(V^0-\epsilon)]/k_1k_2 - \beta > 0$ for a sufficiently small ϵ. Therefore $\widehat{W}(t)$ goes to either infinity or a positive number as $t \longrightarrow \infty$, which leads to a contradiction with $\lim_{t\longrightarrow\infty}\widehat{W}(t) = 0$. Thus we have $W^S(\mathscr{E}^0) \cap X_0 = \emptyset$. Define $m : X \longrightarrow \mathbb{R}_+$ by $m(x_0) = \min\{x_0^3(0), x_0^4(0)\}$, $\forall x_0 \in X$. It is clear that $X^0 = m^{-1}(0,\infty)$ and $\partial X = m^{-1}(0)$. Thus by [21] theorem 3 we have $\liminf_{t\longrightarrow\infty}(I_1(t), I_2(t)) \geq (\eta_1, \eta_1)$ for some constant $\eta_1 > 0$. Let $\eta_0 = \min\{\eta_1, \epsilon\}$ where ϵ is the constant such that $\liminf_{t\longrightarrow\infty}S(t) \geq \epsilon > 0$, $\liminf_{t\longrightarrow\infty}V(t) \geq \epsilon > 0$. We showed that $\liminf_{t\longrightarrow\infty}S(t) \geq \eta_0$, $\liminf_{t\longrightarrow\infty}V(t) \geq \eta_0$, $\liminf_{t\longrightarrow\infty}I_1(t) \geq \eta_0$, $\liminf_{t\longrightarrow\infty}I_2(t) \geq \eta_0$. This completes the proof of Theorem 3. □

3.5. Existence of the Endemic Equilibrium

Theorem 4. *If $\mathscr{R}_0 > 1$, model (1) admits a unique endemic equilibrium.*

Proof. The endemic equilibrium $\mathscr{E}^* = (S^*, V^*, I_1^*, I_2^*)$ of model (1) is determined by the following:

$$\begin{aligned}&A - \beta\left[I_1(t) + (1-p)I_2(t)\right]S(t) - (\mu+\sigma)S(t)\\ &\quad+\kappa V(t) = 0,\\ &\sigma S(t) - \gamma\beta\left[I_1(t) + (1-p)I_2(t)\right]V(t)\\ &\quad-(\mu+\kappa)V(t) = 0,\\ &\beta\left[I_1(t) + (1-p)I_2(t)\right]\left[S(t) + \gamma V(t)\right]\\ &\quad-k_1I_1(t) = 0,\\ &\alpha I_1(t) - k_2I_2(t) = 0.\end{aligned}$$
(24)

From the last equation in (24) we have

$$I_2 = \frac{\alpha I_1}{k_2}.$$
(25)

The first two equations in (24) give

$$\begin{aligned}S &= \frac{A\left[\gamma\beta\left(1+\alpha(1-p)/k_2\right)I_1 + \mu + \kappa\right]}{\left[\beta\left(1+\alpha(1-p)/k_2\right)I_1 + \mu + \sigma\right]\left[\gamma\beta\left(1+\alpha(1-p)/k_2\right)I_1 + \mu + \kappa\right] - \kappa\sigma},\\ V &= \frac{A\sigma}{\left[\beta\left(1+\alpha(1-p)/k_2\right)I_1 + \mu + \sigma\right]\left[\gamma\beta\left(1+\alpha(1-p)/k_2\right)I_1 + \mu + \kappa\right] - \kappa\sigma}.\end{aligned}$$
(26)

For $I_1 \neq 0$, substituting (25) into the third equation in (24) gives

$$S + \gamma V = \frac{k_1 k_2}{\beta\left[\alpha\left(1-p\right)+k_2\right]}. \tag{27}$$

Substituting (26) into (27) yields

$$F\left(I_1\right) = \frac{A\left[\gamma\beta\left(1+\alpha\left(1-p\right)/k_2\right)I_1 + \mu + \kappa + \gamma\sigma\right]}{\left[\beta\left(1+\alpha\left(1-p\right)/k_2\right)I_1 + \mu + \sigma\right]\left[\gamma\beta\left(1+\alpha\left(1-p\right)/k_2\right)I_1 + \mu + \kappa\right] - \kappa\sigma} - \frac{k_1 k_2}{\beta\left[\alpha\left(1-p\right)+k_2\right]}. \tag{28}$$

Direct calculations show

$$F'\left(I_1\right) = -\frac{A\beta^2\left[1+\alpha\left(1-p\right)/k_2\right]^2\left[\gamma^2\beta I_1^2\left[1+\alpha\left(1-p\right)/k_2\right] + 2\gamma\left(\gamma\sigma+\mu+\kappa\right)I_1\right] + M}{\left[\left[\beta\left(1+\alpha\left(1-p\right)/k_2\right)I_1 + \mu + \sigma\right]\left[\gamma\beta\left(1+\alpha\left(1-p\right)/k_2\right)I_1 + \mu + \kappa\right] - \kappa\sigma\right]^2} < 0, \tag{29}$$

where

$$M = A\beta\left[1 + \frac{\alpha\left(1-p\right)}{k_2}\right] \cdot \left[\gamma\sigma\left(2\kappa+\mu\right) + \gamma^2\sigma\left(\mu+\sigma\right) + \left(\mu+\kappa\right)^2\right]. \tag{30}$$

then function $F(I_1)$ is monotonic decreasing for $I_1 > 0$, and then we can define the following function:

$$F\left(0\right) = \frac{k_1 k_2}{\beta\left[\alpha\left(1-p\right)+k_2\right]}\left[\mathscr{R}_0 - 1\right]. \tag{31}$$

Therefore, by monotonicity of a function $F(I_1)$ there exists a unique endemic equilibrium $\mathscr{E}^* = (S^*, V^*, I_1^*, I_2^*)$ □

3.6. Stability of the Endemic Equilibrium. In this section, we will investigate the local and global stability of the endemic equilibrium point.

Theorem 5. *The endemic equilibrium $\mathscr{E}^*$ of the system (1) is locally asymptotically stable if $\mathscr{R}_0 > 1$ and conditions (36) are satisfied.*

Proof. The characteristics equation of system (1) on the infected equilibrium $\mathscr{E}^*$ is given by the following determinant:

$$\begin{vmatrix} -\left(\mu+\sigma\right)-\lambda & \kappa & -\beta S^* & -\beta\left(1-p\right)S^* \\ \sigma & -\left(\mu+\kappa\right)-\lambda & -\gamma\beta V^* & -\gamma\beta\left(1-p\right)V^* \\ r_{31} & r_{32} & r_{33} & r_{34} \\ 0 & 0 & \alpha e^{-\lambda\tau_2} & -\left(\mu+c+d\right)-\lambda \end{vmatrix} = 0, \tag{32}$$

with

$$\begin{aligned} r_{31} &= \beta\left[I_1^* + \left(1-p\right)I_2^*\right]e^{-\lambda\tau_1}, \\ r_{32} &= \gamma\beta\left[I_1^* + \left(1-p\right)I_2^*\right]e^{-\lambda\tau_1}, \\ r_{33} &= \left(S^* + \gamma V^*\right)\beta e^{-\lambda\tau_1} - \left(\alpha+\mu+d\right) - \lambda, \\ r_{34} &= \beta\left(S^* + \gamma V^*\right)\left(1-p\right)e^{-\lambda\tau_1}. \end{aligned} \tag{33}$$

After some algebraic manipulations one can show that the characteristic equation has the following form:

$$\lambda^4 + a_1\lambda^3 + a_2\lambda^2 + a_3\lambda + a_4 = 0 \tag{34}$$

with

$$\begin{aligned} a_1 &= 4\mu + \kappa + \alpha + \sigma + 2d + c + \beta\left(\gamma+1\right)\left(I_1^* + \left(1-p\right)I_2^*\right) - \left(S^* + \gamma V^*\right)\beta e^{-\lambda\tau_1}, \\ a_2 &= \beta^2\left(S^* + \gamma^2 V^*\right)\left(I_1^* + \left(1-p\right)I_2^*\right)e^{-\lambda\tau_1} + \mu\left(\mu + \kappa + \sigma\right) + \gamma\beta^2\left(I_1^* + \left(1-p\right)I_2^*\right)^2 + \beta\left(\gamma\mu + \gamma\sigma + \kappa + \mu\right)\left(I_1^* + \left(1-p\right)I_2^*\right) - \alpha\beta\left(1-p\right)\left(S^* + \gamma V^*\right) \cdot e^{-\lambda\left(\tau_1+\tau_2\right)} + \left(\mu + \alpha + d - \left(S^* + \gamma V^*\right)\beta e^{-\lambda\tau_1}\right)\left(2\mu + \kappa + \sigma + \beta\left(\gamma+1\right)\left(I_1^* + \left(1-p\right)I_2^*\right)\right) + \left(\mu + c + d\right)\left(3\mu + \kappa + \sigma + \alpha + d + \beta\left(\gamma+1\right)\left(I_1^* + \left(1-p\right)I_2^*\right) - \beta\left(S^* + \gamma V^*\right)e^{-\lambda\tau_1}\right), \end{aligned}$$

$$
\begin{aligned}
a_3 = {} & \left[\beta\left(S^* + \gamma V^*\right)(\kappa + \gamma\sigma)\right. \\
& + \beta^2\gamma\left(S^* + \gamma V^*\right)\left(I_1^* + (1-p)I_2^*\right)\left.\right][I_1^* \\
& + (1-p)I_2^*]\,\beta e^{-\lambda\tau_1} + \left[\mu\left(S^* + \gamma^2 V^*\right)\right][I_1^* \\
& + (1-p)I_2^*]\,\beta^2 e^{-\lambda\tau_1} + \mu[\mu + \kappa + \sigma]\left[\mu + \alpha + d\right. \\
& \left. - \left(S^* + \gamma V^*\right)\beta e^{-\lambda\tau_1}\right] + \gamma\beta^2\left[I_1^* + (1-p)I_2^*\right]^2\left[\mu\right. \\
& \left. + \alpha + d - \left(S^* + \gamma V^*\right)\beta e^{-\lambda\tau_1}\right] + \mu[\mu + c + d][\mu \\
& + \kappa + \sigma] + \beta[\gamma\mu + \gamma\sigma + \mu + \kappa]\left[I_1^* + (1-p)I_2^*\right]\left[\mu\right. \\
& \left. + \alpha + d - \left(S^* + \gamma V^*\right)\beta e^{-\lambda\tau_1}\right] + \gamma\beta^2[\mu + c + d][I_1^* \\
& + (1-p)I_2^*]^2 + \beta^2[\mu + c + d]\left(S^* + \gamma^2 V^*\right)[I_1^* \\
& + (1-p)I_2^*]\,e^{-\lambda\tau_1} + \beta[\mu + c + d][\gamma\mu + \gamma\sigma + \kappa \\
& + \mu]\left[I_1^* + (1-p)I_2^*\right] + \alpha\beta^2(1-p)\left(S^* + \gamma^2 V^*\right) \\
& \cdot \left[I_1^* + (1-p)I_2^*\right]e^{-\lambda(\tau_1+\tau_2)} + [\mu + c + d][2\mu + \kappa \\
& + \sigma + \beta(\gamma+1)\left(I_1^* + (1-p)I_2^*\right)]\left[\mu + \alpha + d\right. \\
& \left. - \beta\left(S^* + \gamma V^*\right)e^{-\lambda\tau_1}\right] - \alpha\beta(1-p)\left(S^* + \gamma V^*\right)[2\mu \\
& + \kappa + \sigma + \beta(\gamma+1)\left(I_1^* + (1-p)I_2^*\right)]\,e^{-\lambda(\tau_1+\tau_2)}, \\
a_4 = {} & [\mu + c + d]\left[\beta\left(S^* + \gamma V^*\right)(\kappa + \gamma\sigma)\right. \\
& \left. + \gamma\beta^2\left(S^* + \gamma V^*\right)\left(I_1^* + (1-p)I_2^*\right)\right][I_1^* \\
& + (1-p)I_2^*]\,\beta e^{-\lambda\tau_1} + [\mu + c + d]\,\mu\left(S^* + \gamma^2 V^*\right) \\
& \cdot \left[I_1^* + (1-p)I_2^*\right]\beta^2 e^{-\lambda\tau_1} + \mu[\mu + c + d][\kappa + \mu \\
& + \sigma]\left[\mu + \alpha + d - \left(S^* + \gamma V^*\right)\beta e^{-\lambda\tau_1}\right] + \gamma\beta^2[\mu + \mathrm{c} \\
& + d]\left[I_1^* + (1-p)I_2^*\right]^2\left[\mu + \alpha + d\right. \\
& \left. - \left(S^* + \gamma V^*\right)\beta e^{-\lambda\tau_1}\right] + \beta[\mu + c + d][\gamma\mu + \gamma\sigma + \kappa \\
& + \mu]\left[I_1^* + (1-p)I_2^*\right]\left[\mu + \alpha + d\right. \\
& \left. - \left(S^* + \gamma V^*\right)\beta e^{-\lambda\tau_1}\right] + \alpha\gamma\beta^2(1-p)\left(S^*\sigma + \kappa V^*\right) \\
& \cdot \left[I_1^* + (1-p)I_2^*\right]e^{-\lambda(\tau_1+\tau_2)} + \alpha(\gamma\beta)^2(1-p)V^*[\mu \\
& + \sigma + \beta\left(I_1^* + (1-p)I_2^*\right)]\left[I_1^* + (1-p)I_2^*\right] \\
& \cdot e^{-\lambda(\tau_1+\tau_2)} + \alpha\beta^2(1-p)S^*[\mu + \kappa \\
& + \gamma\beta\left(I_1^* + (1-p)I_2^*\right)]\left[I_1^* + (1-p)I_2^*\right]e^{-\lambda(\tau_1+\tau_2)} \\
& - \alpha\beta(1-p)\left(S^* + \gamma V^*\right)[\mu(\kappa + \mu + \sigma) \\
& + \beta(\gamma\mu + \gamma\sigma + \kappa + \mu)\left(I_1^* + (1-p)I_2^*\right)]\,e^{-\lambda(\tau_1+\tau_2)} \\
& - \alpha\beta(1-p)\left(S^* + \gamma V^*\right)\left[\gamma\beta^2\left(I_1^* + (1-p)I_2^*\right)^2\right] \\
& \cdot e^{-\lambda(\tau_1+\tau_2)}.
\end{aligned}
\tag{35}
$$

By the Routh-Hurwitz criterion, all roots of the characteristics equation (34) have negative real parts and the endemic equilibrium $\mathscr{E}^*$ of system (1) is locally asymptotically stable if $\tau_1 = \tau_2 = 0$, if and only if $a_i > 0$ $(i = 1, 2, 3, 4)$, $M_1 = a_1 > 0$,

$$
\begin{aligned}
M_2 &= \begin{bmatrix} a_1 & a_3 \\ 1 & a_2 \end{bmatrix} > 0, \\
M_3 &= \begin{bmatrix} a_1 & a_3 & a_5 \\ 1 & a_2 & a_4 \\ 0 & a_1 & a_3 \end{bmatrix} > 0, \\
M_4 &= \begin{bmatrix} a_1 & a_3 & 0 & 0 \\ 1 & a_2 & a_4 & 0 \\ 0 & a_1 & a_3 & 0 \\ 0 & 1 & a_2 & a_4 \end{bmatrix} > 0.
\end{aligned}
\tag{36}
$$

Now, we wish to explore if there is a possibility of having complex roots with positive real part for (a) $\tau_1 > 0$, $\tau_2 = 0$ and (b) $\tau_1 = 0$, $\tau_2 > 0$. We now proceed to explore the above cases as follows.

(a) If $\tau_1 > 0$, $\tau_2 = 0$, then the characteristics equation (34) becomes

$$
\begin{aligned}
& \lambda^4 + a_{11}\lambda^3 + a_{21}\lambda^2 + a_{31}\lambda + a_{41} \\
& \quad = e^{-\lambda\tau_1}\left(m_{11}\lambda^3 + m_{21}\lambda^2 + m_{31}\lambda + m_{41}\right),
\end{aligned}
\tag{37}
$$

with

$$
\begin{aligned}
a_{11} = {} & 4\mu + \kappa + \alpha + \sigma + 2d + c + \beta(\gamma+1)\left(I_1^*\right. \\
& \left. + (1-p)I_2^*\right), \\
a_{21} = {} & \mu(\mu + \kappa + \sigma) + \gamma\beta^2\left(I_1^* + (1-p)I_2^*\right)^2 + \beta(\gamma\mu \\
& + \gamma\sigma + \kappa + \mu)\left(I_1^* + (1-p)I_2^*\right) + (\mu + \alpha + d)(2\mu \\
& + \kappa + \sigma + \beta(\gamma+1)\left(I_1^* + (1-p)I_2^*\right)) + (\mu + c \\
& + d)(3\mu + \kappa + \sigma + \alpha + d \\
& + \beta(\gamma+1)\left(I_1^* + (1-p)I_2^*\right)), \\
a_{31} = {} & \mu[\mu + \kappa + \sigma][\mu + \alpha + d] + \gamma\beta^2[I_1^* \\
& + (1-p)I_2^*]^2[\mu + \alpha + d] + \mu[\mu + c + d][\mu + \kappa \\
& + \sigma] + \beta[\gamma\mu + \gamma\sigma + \mu + \kappa]\left[I_1^* + (1-p)I_2^*\right][\mu + \alpha \\
& + d] + \gamma\beta^2[\mu + c + d]\left[I_1^* + (1-p)I_2^*\right]^2 + \beta[\mu
\end{aligned}
$$

$$
\begin{aligned}
&+ c + d]\,[\gamma\mu + \gamma\sigma + \kappa + \mu]\,[I_1^* + (1-p)\,I_2^*] + [\mu \\
&+ c + d]\,[2\mu + \kappa + \sigma + \beta(\gamma+1)(I_1^* + (1-p)\,I_2^*)] \\
&\cdot [\mu + \alpha + d],
\end{aligned}
$$

$$
\begin{aligned}
a_{41} &= \mu\,[\mu + c + d]\,[\kappa + \mu + \sigma]\,[\mu + \alpha + d] + \gamma\beta^2\,[\mu \\
&+ c + d]\,[I_1^* + (1-p)\,I_2^*]^2\,[\mu + \alpha + d] + \beta\,[\mu + c \\
&+ d]\,[\gamma\mu + \gamma\sigma + \kappa + \mu]\,[I_1^* + (1-p)\,I_2^*]\,[\mu + \alpha \\
&+ d],
\end{aligned}
$$

$$
m_{11} = (S^* + \gamma V^*)\,\beta,
$$

$$
\begin{aligned}
m_{21} &= -\beta^2\left(S^* + \gamma^2 V^*\right)(I_1^* + (1-p)\,I_2^*) + \alpha\beta\,(1 \\
&- p)\,(S^* + \gamma V^*) + (S^* + \gamma V^*)\,\beta\,(2\mu + \kappa + \sigma \\
&+ \beta(\gamma+1)(I_1^* + (1-p)\,I_2^*)) + (\mu + c + d)\,\beta\,(S^* \\
&+ \gamma V^*),
\end{aligned}
$$

$$
\begin{aligned}
m_{31} &= -\left[\beta(S^* + \gamma V^*)(\kappa + \gamma\sigma)\right. \\
&\left.+ \beta^2\gamma\,(S^* + \gamma V^*)(I_1^* + (1-p)\,I_2^*)\right][I_1^* \\
&+ (1-p)\,I_2^*]\,\beta - \left[\mu\left(S^* + \gamma^2 V^*\right)\right][I_1^* \\
&+ (1-p)\,I_2^*]\,\beta^2 + \mu\,[\mu + \kappa + \sigma]\,[(S^* + \gamma V^*)\,\beta] \\
&+ \gamma\beta^2\,[I_1^* + (1-p)\,I_2^*]^2\,[(S^* + \gamma V^*)] + \beta\,[\gamma\mu \\
&+ \gamma\sigma + \mu + \kappa]\,[I_1^* + (1-p)\,I_2^*]\,[(S^* + \gamma V^*)\,\beta] \\
&- \beta^2\,[\mu + c + d]\left(S^* + \gamma^2 V^*\right)[I_1^* + (1-p)\,I_2^*] \\
&- \alpha\beta^2\,(1-p)\left(S^* + \gamma^2 V^*\right)[I_1^* + (1-p)\,I_2^*] + [\mu \\
&+ c + d]\,[2\mu + \kappa + \sigma + \beta(\gamma+1)(I_1^* + (1-p)\,I_2^*)] \\
&\cdot [\beta(S^* + \gamma V^*)] + \alpha\beta\,(1-p)\,(S^* + \gamma V^*)\,[2\mu + \kappa \\
&+ \sigma + \beta(\gamma+1)(I_1^* + (1-p)\,I_2^*)],
\end{aligned}
$$

$$
\begin{aligned}
m_{41} &= -[\mu + c + c]\left[\beta(S^* + \gamma V^*)(\kappa + \gamma\sigma)\right. \\
&\left.+ \gamma\beta^2\,(S^* + \gamma V^*)(I_1^* + (1-p)\,I_2^*)\right][I_1^* \\
&+ (1-p)\,I_2^*]\,\beta - [\mu + c + d]\,\mu\left(S^* + \gamma^2 V^*\right)[I_1^* \\
&+ (1-p)\,I_2^*]\,\beta^2 + \mu\,[\mu + c + d]\,[\kappa + \mu + \sigma] \\
&\cdot [(S^* + \gamma V^*)\,\beta] + \gamma\beta^2\,[\mu + c + d]\,[I_1^* \\
&+ (1-p)\,I_2^*]^2\,[(S^* + \gamma V^*)\,\beta] + \beta\,[\mu + c + d]\,[\gamma\mu \\
&+ \gamma\sigma + \kappa + \mu]\,[I_1^* + (1-p)\,I_2^*]\,[(S^* + \gamma V^*)\,\beta] \\
&- \alpha\gamma\beta^2\,(1-p)\,(S^*\sigma + \kappa V^*)\,[I_1^* + (1-p)\,I_2^*] \\
&- \alpha\,(\gamma\beta)^2\,(1-p)\,V^*\,[\mu + \sigma + \beta\,(I_1^* + (1-p)\,I_2^*)] \\
&\cdot [I_1^* + (1-p)\,I_2^*] - \alpha\beta^2\,(1-p)\,S^*\,[\mu + \kappa \\
&+ \gamma\beta\,(I_1^* + (1-p)\,I_2^*)]\,[I_1^* + (1-p)\,I_2^*]
\end{aligned}
\tag{38}
$$

Now we need to show that all roots of (37) have negative real parts for all $\tau_1 \in (0, \tau^*)$. To do so, we show that (37) does not have any purely imaginary roots for all $\tau_1 \in (0, \tau^*)$. We assume that $\lambda = i\omega$ with $\omega > 0$ is a root of (37). Then ω must satisfy the following system:

$$
\begin{aligned}
\omega^4 - a_{21}\omega^2 + a_{41} &= \left(m_{41} - m_{21}\omega^2\right)\cos(\omega\tau_1) \\
&+ \left(m_{31}\omega - m_{11}\omega^3\right)\sin(\omega\tau_1), \\
a_{31}\omega - a_{11}\omega^3 &= \left(m_{31}\omega - m_{11}\omega^3\right)\cos(\omega\tau_1) \\
&- \left(m_{41} - m_{21}\omega^2\right)\sin(\omega\tau_1).
\end{aligned}
\tag{39}
$$

Now, we square both sides of each equation above and add the resulting equations; thus ω must be a positive root of

$$
\omega^8 + b_1\omega^6 + b_2\omega^4 + b_3\omega^2 + b_4 = 0, \tag{40}
$$

where

$$
\begin{aligned}
b_1 &= a_{11}^2 - 2a_{21} - m_{11}^2, \\
b_2 &= a_{21}^2 + 2\,(a_{41} - a_{11}a_{31} + m_{11}m_{31}) - m_{21}^2, \\
b_3 &= a_{31}^2 + 2\,(m_{21}m_{41} - a_{21}a_{41}) - m_{31}^2, \\
b_4 &= a_{41}^2 - m_{41}^2.
\end{aligned}
\tag{41}
$$

Let $z = \omega^2$; then (40) becomes

$$
F(z) = z^4 + b_1 z^3 + b_2 z^2 + b_3 z + b_4 = 0. \tag{42}
$$

One can observe that if $b_i \geq 0$, $(i = 1, 2, 3, 4)$, then (42) has no positive roots. Therefore (37) does not have any purely imaginary roots for all $\tau_1 \in (0, \tau^*)$ so that all roots of the characteristic equation (37) have negative real parts and the endemic equilibrium $\mathscr{E}^*$ of (1) is stable for all $\tau_1 \in (0, \tau^*)$.

(b) If $\tau_2 > 0$, $\tau_1 = 0$ then the characteristics equation (34) becomes

$$
\begin{aligned}
\lambda^4 + \alpha_{11}\lambda^3 + \alpha_{21}\lambda^2 + \alpha_{31}\lambda + \alpha_{41} &= e^{-\lambda\tau_2}\left(n_{11}\lambda^3\right. \\
&\left.+ n_{21}\lambda^2 + n_{31}\lambda + n_{41}\right) \\
\alpha_{11} &= 4\mu + \kappa + \alpha + \sigma + 2d + c + \beta(\gamma+1)\,(I_1^* \\
&+ (1-p)\,I_2^*) - (S^* + \gamma V^*)\,\beta, \\
\alpha_{21} &= \beta^2\left(S^* + \gamma^2 V^*\right)(I_1^* + (1-p)\,I_2^*) + \mu\,(\mu + \kappa \\
&+ \sigma) + \gamma\beta^2\,(I_1^* + (1-p)\,I_2^*)^2 + \beta\,(\gamma\mu + \gamma\sigma + \kappa \\
&+ \mu)\,(I_1^* + (1-p)\,I_2^*) + (\mu + \alpha + d
\end{aligned}
\tag{43}
$$

$$
\begin{aligned}
&- \left(S^* + \gamma V^*\right)\beta\left)\left(2\mu + \kappa + \sigma\right.\right.\\
&+ \beta\left(\gamma + 1\right)\left(I_1^* + \left(1 - p\right)I_2^*\right)\right) + \left(\mu + c + d\right)\left(3\mu\right.\\
&+ \kappa + \sigma + \alpha + d + \beta\left(\gamma + 1\right)\left(I_1^* + \left(1 - p\right)I_2^*\right)\\
&- \beta\left(S^* + \gamma V^*\right)\left.\right),\\
\alpha_{31} &= \left[\beta\left(S^* + \gamma V^*\right)\left(\kappa + \gamma\sigma\right)\right.\\
&+ \beta^2\gamma\left(S^* + \gamma V^*\right)\left(I_1^* + \left(1 - p\right)I_2\right)\left.\right]\left[I_1^*\right.\\
&+ \left(1 - p\right)I_2^*\left.\right]\beta + \left[\mu\left(S^* + \gamma^2 V^*\right)\right]\left[I_1^*\right.\\
&+ \left(1 - p\right)I_2^*\left.\right]\beta^2 + \mu\left[\mu + \kappa + \sigma\right]\left[\mu + \alpha + d\right.\\
&- \left(S^* + \gamma V^*\right)\beta\left.\right] + \gamma\beta^2\left[I_1^* + \left(1 - p\right)I_2^*\right]^2\left[\mu + \alpha\right.\\
&+ d - \left(S^* + \gamma V^*\right)\beta\left.\right] + \mu\left[\mu + c + d\right]\left[\mu + \kappa + \sigma\right]\\
&+ \beta\left[\gamma\mu + \gamma\sigma + \mu + \kappa\right]\left[I_1^* + \left(1 - p\right)I_2^*\right]\left[\mu + \alpha + d\right.\\
&- \left(S^* + \gamma V^*\right)\beta\left.\right] + \gamma\beta^2\left[\mu + c + d\right]\left[I_1^*\right.\\
&+ \left(1 - p\right)I_2^*\left.\right]^2 + \beta^2\left[\mu + c + d\right]\left(S^* + \gamma^2 V^*\right)\left[I_1^*\right.\\
&+ \left(1 - p\right)I_2^*\left.\right] + \beta\left[\mu + c + d\right]\left[\gamma\mu + \gamma\sigma + \kappa + \mu\right]\left[I_1^*\right.\\
&+ \left(1 - p\right)I_2^*\left.\right] + \left[\mu + c + d\right]\left[2\mu + \kappa + \sigma\right.\\
&+ \beta\left(\gamma + 1\right)\left(I_1^* + \left(1 - p\right)I_2^*\right)\left.\right]\left[\mu + \alpha + d\right.\\
&- \left.\beta\left(S^* + \gamma V^*\right)\right],\\
\alpha_{41} &= \left[\mu + c + c\right]\left[\beta\left(S^* + \gamma V^*\right)\left(\kappa + \gamma\sigma\right)\right.\\
&+ \left.\gamma\beta^2\left(S^* + \gamma V^*\right)\left(I_1^* + \left(1 - p\right)I_2^*\right)\right]\left[I_1^*\right.\\
&+ \left(1 - p\right)I_2^*\left.\right]\beta + \left[\mu + c + \mathrm{d}\right]\mu\left(S^* + \gamma^2 V^*\right)\left[I_1^*\right.\\
&+ \left(1 - p\right)I_2^*\left.\right]\beta^2 + \mu\left[\mu + c + d\right]\left[\kappa + \mu + \sigma\right]\left[\mu + \alpha\right.\\
&+ d - \left(S^* + \gamma V^*\right)\beta\left.\right] + \gamma\beta^2\left[\mu + c + d\right]\left[I_1^*\right.\\
&+ \left(1 - p\right)I_2^*\left.\right]^2\left[\mu + \alpha + d - \left(S^* + \gamma V^*\right)\beta\right] + \beta\left[\mu\right.\\
&+ c + d\left.\right]\left[\gamma\mu + \gamma\sigma + \kappa + \mu\right]\left[I_1^* + \left(1 - p\right)I_2^*\right]\left[\mu + \alpha\right.\\
&+ d - \left.\left(S^* + \gamma V^*\right)\beta\right],\\
n_{11} &= 0,\\
n_{21} &= \alpha\beta\left(1 - p\right)\left(S^* + \gamma V^*\right)\\
n_{31} &= -\alpha\beta^2\left(1 - p\right)\left(S^* + \gamma^2 V^*\right)\left[I_1^* + \left(1 - p\right)I_2^*\right]\\
&\cdot \alpha\beta\left(1 - p\right)\left(S^* + \gamma V^*\right)\left[2\mu + \kappa + \sigma\right.\\
&+ \left.\beta\left(\gamma + 1\right)\left(I_1^* + \left(1 - p\right)I_2^*\right)\right],\\
n_{41} &= -\alpha\gamma\beta^2\left(1 - p\right)\left(S^*\sigma + \kappa V^*\right)\left[I_1^* + \left(1 - p\right)I_2^*\right]\\
&- \alpha\left(\gamma\beta\right)^2\left(1 - p\right)V^*\left[\mu + \sigma + \beta\left(I_1^* + \left(1 - p\right)I_2^*\right)\right]\\
&\cdot \left[I_1^* + \left(1 - p\right)I_2^*\right] - \alpha\beta^2\left(1 - p\right)S^*\left[\mu + \kappa\right.\\
&+ \left.\gamma\beta\left(I_1^* + \left(1 - p\right)I_2^*\right)\right]\left[I_1^* + \left(1 - p\right)I_2^*\right] + \alpha\beta\left(1\right.\\
&- \left.p\right)\left(S^* + \gamma V^*\right)\left[\mu\left(\kappa + \mu + \sigma\right)\right.\\
&+ \left.\beta\left(\gamma\mu + \gamma\sigma + \kappa + \mu\right)\left(I_1^* + \left(1 - p\right)I_2^*\right)\right] + \alpha\beta\left(1\right.\\
&- \left.p\right)\left(S^* + \gamma V^*\right)\left[\gamma\beta^2\left(I_1^* + \left(1 - p\right)I_2^*\right)^2\right].
\end{aligned}
\tag{44}
$$

Using the same discussion as in the above case then (43) can be written as

$$h\left(z\right) = z^4 + c_1 z^3 + c_2 z^2 + c_3 z + c_4 = 0 \tag{45}$$

with

$$
\begin{aligned}
c_1 &= \alpha_{11}^2 - 2\alpha_{21},\\
c_2 &= \alpha_{21}^2 + 2\left(\alpha_{41} - \alpha_{11}\alpha_{31}\right) - n_{21}^2,\\
c_3 &= \alpha_{31}^2 + 2\left(n_{21}n_{41} - \alpha_{21}\alpha_{41}\right) - n_{31}^2,\\
c_4 &= \alpha_{41}^2 - n_{41}^2.
\end{aligned}
\tag{46}
$$

It follows that all roots of (43) have negative real parts for $\tau_2(0, \tau_2^*)$ when $c_j \geq 0$, $j = 1, 2, 3, 4$ and this implies that endemic equilibrium is locally asymptotically stable for $\tau_2 \in (0, \tau_2^*)$. This completes the proof. □

We now explore the global stability of the endemic equilibrium.

Theorem 6. *If $\mathscr{R}_0 > 1$, then $\mathscr{E}^*$ is globally asymptotically stable.*

Proof. Let us consider the Lyapunov function:

$$\mathscr{W}\left(t\right) = \mathscr{W}_1\left(t\right) + \mathscr{W}_2\left(t\right) + \mathscr{W}_3. \tag{47}$$

Here,

$$
\begin{aligned}
\mathscr{W}_1\left(t\right) &= \left\{S\left(t\right) - S^* - S^*\ln\left(\frac{S\left(t\right)}{S^*}\right)\right\} + \left\{V\left(t\right) - V^*\right.\\
&\left. - V^*\ln\left(\frac{V\left(t\right)}{V^*}\right)\right\} + \left\{I_1\left(t\right) - I_1^* - I_1^*\ln\left(\frac{I_1\left(t\right)}{I_1^*}\right)\right\}\\
&+ \frac{\beta\left(1 - p\right)\left(S^* + \gamma V^*\right)I_2^*}{\alpha I_1^*}\left\{I_2\left(t\right) - I_2^* - I_2^*\right.\\
&\left.\cdot\ln\left(\frac{I_2\left(t\right)}{I_2^*}\right)\right\},
\end{aligned}
$$

$$
\begin{aligned}
\mathscr{W}_2\left(t\right) &= \beta S^* I_1^*\int_0^{\tau_1}\left\{\frac{I_1\left(t - \omega\right)S\left(t - \omega\right)}{S^* I_1^*} - 1\right.\\
&\left. - \ln\left(\frac{I_1\left(t - \omega\right)S\left(t - \omega\right)}{S^* I_1^*}\right)\right\}d\omega
\end{aligned}
$$

$$+\beta\gamma V^* I_1^* \int_0^{\tau_1} \left\{ \frac{I_1(t-\omega)V(t-\omega)}{V^* I_1^*} - 1 - \ln\left(\frac{I_1(t-\omega)V(t-\omega)}{V^* I_1^*} \right) \right\} d\omega + \beta(1-p) \cdot S^* I_2^* \int_0^{\tau_1} \left\{ \frac{I_2(t-\omega)S(t-\omega)}{S^* I_2^*} - 1 - \ln\left(\frac{I_2(t-\omega)S(t-\omega)}{S^* I_2^*} \right) \right\} d\omega + \beta\gamma(1-p) V^* I_2^* \int_0^{\tau_1} \left\{ \frac{I_2(t-\omega)V(t-\omega)}{V^* I_2^*} - 1 - \ln\left(\frac{I_2(t-\omega)V(t-\omega)}{V^* I_2^*} \right) \right\} d\omega,$$

$$\mathscr{W}_3(t) = \beta(1-p)(S^* + \gamma V^*) I_2^* \int_0^{\tau_2} \left\{ \frac{I_1(t-\omega)}{I_1^*} - 1 - \ln\left(\frac{I_1(t-\omega)}{I_1^*} \right) \right\} d\omega. \tag{48}$$

The derivatives of $\mathscr{W}_1(t)$ are given by

$$\frac{d\mathscr{W}_1(t)}{dt} = \left(1 - \frac{S^*}{S(t)}\right)\frac{dS}{dt} + \left(1 - \frac{V^*}{V(t)}\right)\frac{dV}{dt} + \left(1 - \frac{I_1^*}{I_1(t)}\right)\frac{dI_1}{dt} + \frac{\beta(1-p)(S^* + \gamma V^*) I_2^*}{\alpha I_1^*}\left(1 - \frac{I_2^*}{I_2(t)}\right)\frac{dI_2}{dt}. \tag{49}$$

Substituting the appropriate differentials from (1) we have

$$\frac{d\mathscr{W}_1(t)}{dt} = \left\{1 - \frac{S^*}{S}\right\}\{A - \beta[I_1(t) + (1-p)I_2(t)] \cdot S(t) - (\mu+\sigma)S(t) + \kappa V(t)\} + \left\{1 - \frac{V^*}{V}\right\}\{\sigma S(t) - \gamma\beta[I_1(t) + (1-p)I_2(t)]V(t) - (\mu+\kappa)V(t)\} + \left\{1 - \frac{I_1^*}{I_1}\right\}\{\beta[I_1(t-\tau_1) + (1-p)I_2(t-\tau_1)] \cdot [S(t-\tau_1) + \gamma V(t-\tau_1)] - k_1 I_1(t)\} + \frac{\beta(1-p)(S^* + \gamma V^*) I_2^*}{\alpha I_1^*}\left\{1 - \frac{I_2^*}{I_2}\right\}\{\alpha I_1(t-\tau_2) - k_2 I_2(t)\}. \tag{50}$$

At endemic equilibrium, we have

$$\begin{aligned} A &= \beta[I_1^* + (1-p)I_2^*]S^* + (\mu+\sigma)S^* - \kappa V^*, \\ (\mu+\kappa)V^* &= \sigma S^* - \gamma\beta[I_1^* + (1-p)I_2^*]V^*, \\ k_1 I_1^* &= \beta[I_1^* + (1-p)I_2^*][S^* + \gamma V^*], \\ k_2 I_2^* &= \alpha I_1^*. \end{aligned} \tag{51}$$

Using the above constants, we have

$$\frac{d\mathscr{W}_1(t)}{dt} = \mu S^*\left(2 - \frac{S(t)}{S^*} - \frac{S^*}{S(t)}\right) + \kappa V^*\left(2 - \frac{S(t)}{S^*}\cdot\frac{V^*}{V(t)} - \frac{S^*}{S(t)}\cdot\frac{V(t)}{V^*}\right) + \mu V^*\left(3 - \frac{S^*}{S(t)} - \frac{V(t)}{V^*} - \frac{S(t)}{S^*}\cdot\frac{V^*}{V(t)}\right) + \beta I_1^* S^*\left(2 - \frac{S(t)}{S^*}\cdot\frac{I_1(t)}{I_1^*} - \frac{S^*}{S(t)}\right) + \beta(1-p)S^* I_2^*\left(2 - \frac{S(t)}{S^*}\cdot\frac{I_2(t)}{I_2^*} - \frac{S^*}{S(t)} - \frac{I_1(t)}{I_1^*}\right) + \beta\gamma V^* I_1^*\left(3 - \frac{S^*}{S(t)} - \frac{I_1(t)}{I_1^*}\cdot\frac{V(t)}{V^*} - \frac{S(t)}{S^*}\cdot\frac{V^*}{V(t)}\right) + \beta\gamma(1-p)V^* I_2^*\left(3 - \frac{S^*}{S(t)} - \frac{S(t)}{S^*}\cdot\frac{V^*}{V(t)} - \frac{I_2(t)}{I_2^*}\cdot\frac{V(t)}{V^*} - \frac{I_1(t)}{I_1^*}\right) + \beta I_1(t-\tau_1)S(t-\tau_1)\left(1 - \frac{I_1^*}{I_1(t)}\right) + \beta(1-p)I_2(t-\tau_1) \cdot S(t-\tau_1)\left(1 - \frac{I_1^*}{I_1(t)}\right) + \beta\gamma I_1(t-\tau_1)V(t-\tau_1) \cdot \left(1 - \frac{I_1^*}{I_1(t)}\right) + \beta\gamma(1-p)I_2(t-\tau_1)V(t-\tau_1)\left(1 - \frac{I_1^*}{I_1(t)}\right) + \beta(1-p)I_1(t-\tau_2)S^*\left(\frac{I_2^*}{I_1^*} - \frac{I_2^*}{I_2(t)}\cdot\frac{I_2^*}{I_1^*}\right) + \beta\gamma(1-p)I_1(t-\tau_2)V^*\left(\frac{I_2^*}{I_1^*} - \frac{I_2^*}{I_2(t)}\cdot\frac{I_2^*}{I_1^*}\right). \tag{52}$$

The derivatives of $\mathscr{W}_2$ are given by

$$\frac{d\mathscr{W}_2(t)}{dt} = \beta S^* I_1^* \frac{d}{dt}\int_0^{\tau_1}\left\{\frac{I_1(t-\omega)S(t-\omega)}{S^* I_1^*} - 1 - \ln\left(\frac{I_1(t-\omega)S(t-\omega)}{S^* I_1^*}\right)\right\} d\omega + \beta\gamma V^* I_1^* \frac{d}{dt}\int_0^{\tau_1}\left\{\frac{I_1(t-\omega)V(t-\omega)}{V^* I_1^*} - 1$$

$$
\begin{aligned}
&- \ln\left(\frac{I_1(t-\omega)V(t-\omega)}{V^*I_1^*}\right)\Bigg\} d\omega + \beta(1-p)\\
&\cdot S^*I_2^* \frac{d}{dt}\int_0^{\tau_1}\left\{\frac{I_2(t-\omega)S(t-\omega)}{S^*I_2^*} - 1\right.\\
&- \ln\left(\frac{I_2(t-\omega)S(t-\omega)}{S^*I_2^*}\right)\Bigg\} d\omega + \beta\gamma(1\\
&- p)V^*I_2^* \frac{d}{dt}\int_0^{\tau_1}\left\{\frac{I_2(t-\omega)V(t-\omega)}{V^*I_2^*} - 1\right.\\
&- \ln\left(\frac{I_2(t-\omega)V(t-\omega)}{V^*I_2^*}\right)\Bigg\} d\omega,\\
= {}& \beta S^*I_1^* \int_0^{\tau_1} \frac{d}{dt}\left\{\frac{I_1(t-\omega)S(t-\omega)}{S^*I_1^*} - 1\right.\\
&- \ln\left(\frac{I_1(t-\omega)S(t-\omega)}{S^*I_1^*}\right)\Bigg\} d\omega\\
&+ \beta\gamma V^*I_1^* \int_0^{\tau_1} \frac{d}{dt}\left\{\frac{I_1(t-\omega)V(t-\omega)}{V^*I_1^*} - 1\right.\\
&- \ln\left(\frac{I_1(t-\omega)V(t-\omega)}{V^*I_1^*}\right)\Bigg\} d\omega + \beta(1-p)\\
&\cdot S^*I_2^* \int_0^{\tau_1} \frac{d}{dt}\left\{\frac{I_2(t-\omega)S(t-\omega)}{S^*I_2^*} - 1\right.\\
&- \ln\left(\frac{I_2(t-\omega)S(t-\omega)}{S^*I_2^*}\right)\Bigg\} d\omega + \beta\gamma(1\\
&- p)V^*I_2^* \int_0^{\tau_1} \frac{d}{dt}\left\{\frac{I_2(t-\omega)V(t-\omega)}{V^*I_2^*} - 1\right.\\
&- \ln\left(\frac{I_2(t-\omega)V(t-\omega)}{V^*I_2^*}\right)\Bigg\} d\omega,\\
= {}& -\beta S^*I_1^* \int_0^{\tau_1} \frac{d}{d\omega}\left\{\frac{I_1(t-\omega)S(t-\omega)}{S^*I_1^*} - 1\right.\\
&- \ln\left(\frac{I_1(t-\omega)S(t-\omega)}{S^*I_1^*}\right)\Bigg\} d\omega\\
&- \beta\gamma V^*I_1^* \int_0^{\tau_1} \frac{d}{d\omega}\left\{\frac{I_1(t-\omega)V(t-\omega)}{V^*I_1^*} - 1\right.\\
&- \ln\left(\frac{I_1(t-\omega)V(t-\omega)}{V^*I_1^*}\right)\Bigg\} d\omega - \beta(1-p)\\
&\cdot S^*I_2^* \int_0^{\tau_1} \frac{d}{d\omega}\left\{\frac{I_2(t-\omega)S(t-\omega)}{S^*I_2^*} - 1\right.\\
&- \ln\left(\frac{I_2(t-\omega)S(t-\omega)}{S^*I_2^*}\right)\Bigg\} d\omega - \beta\gamma(1\\
&- p)V^*I_2^* \int_0^{\tau_1} \frac{d}{d\omega}\left\{\frac{I_2(t-\omega)V(t-\omega)}{V^*I_2^*} - 1\right.\\
&- \ln\left(\frac{I_2(t-\omega)V(t-\omega)}{V^*I_2^*}\right)\Bigg\} d\omega\\
= {}& \beta S^*I_1^*\left[\frac{I_1(t)S(t)}{S^*I_1^*} - \frac{I_1(t-\tau_1)S(t-\tau_1)}{S^*I_1^*}\right.\\
&\left.+ \ln\left(\frac{I_1(t-\tau_1)S(t-\tau_1)}{I_1(t)S(t)}\right)\right]\\
&+ \beta\gamma V^*I_1^*\left[\frac{I_1(t)V(t)}{V^*I_1^*} - \frac{I_1(t-\tau_1)V(t-\tau_1)}{V^*I_1^*}\right.\\
&\left.+ \ln\left(\frac{I_1(t-\tau_1)V(t-\tau_1)}{I_1(t)V(t)}\right)\right] + \beta(1-p)\\
&\cdot S^*I_2^*\left[\frac{I_2(t)S(t)}{S^*I_2^*} - \frac{I_2(t-\tau_1)S(t-\tau_1)}{S^*I_2^*}\right.\\
&\left.+ \ln\left(\frac{I_2(t-\tau_1)S(t-\tau_1)}{I_2(t)S(t)}\right)\right] + \beta\gamma(1-p)\\
&\cdot V^*I_2^*\left[\frac{I_2(t)V(t)}{S^*I_2^*} - \frac{I_2(t-\tau_1)V(t-\tau_1)}{V^*I_2^*}\right.\\
&\left.+ \ln\left(\frac{I_2(t-\tau_1)S(t-\tau_1)}{I_2(t)V(t)}\right)\right] = \beta I_1^*S^* \cdot \frac{S(t)}{S^*} \cdot \frac{I_1(t)}{I_1^*}\\
&+ \beta\gamma I_1^*V^* \cdot \frac{V(t)}{V^*} \cdot \frac{I_1(t)}{I_1^*} + \beta(1-p)I_2^*S^* \cdot \frac{S(t)}{S^*} \cdot\\
&\frac{I_2(t)}{I_2^*} + \beta\gamma(1-p)I_2^*V^* \cdot \frac{V(t)}{V^*} \cdot \frac{I_2(t)}{I_2^*} - \beta I_1(t-\tau_1)\\
&\cdot S(t-\tau_1) - \beta\gamma I_1(t-\tau_1)V(t-\tau_1) - \beta(1-p)\\
&\cdot I_2(t-\tau_1)S(t-\tau_1) - \beta\gamma(1-p)I_2(t-\tau_1)V(t\\
&- \tau_1) + \beta S^*I_1^* \ln\left(\frac{I_1(t-\tau_1)S(t-\tau_1)}{I_1(t)S(t)}\right)\\
&+ \beta\gamma V^*I_1^* \ln\left(\frac{I_1(t-\tau_1)V(t-\tau_1)}{I_1(t)V(t)}\right) + \beta(1-p)\\
&\cdot S^*I_2^* \ln\left(\frac{I_2(t-\tau_1)S(t-\tau_1)}{I_2(t)S(t)}\right) + \beta\gamma(1-p)\\
&\cdot V^*I_2^* \ln\left(\frac{I_2(t-\tau_1)V(t-\tau_1)}{I_2(t)V(t)}\right).
\end{aligned}
\tag{53}
$$

The derivatives of $\mathscr{W}_3(t)$ are given by

$$
\begin{aligned}
\frac{d\mathscr{W}_3(t)}{dt} = {}& \beta(1-p)(S^* + \gamma V^*)I_2^* \frac{d}{dt}\int_0^{\tau_2}\left\{\frac{I_1(t-\omega)}{I_1^*}\right.\\
&\left.- 1 - \ln\left(\frac{I_1(t-\omega)}{I_1^*}\right)\right\} d\omega = \beta(1-p)(S^*\\
&+ \gamma V^*)I_2^* \int_0^{\tau_2} \frac{d}{dt}\left\{\frac{I_1(t-\omega)}{I_1^*} - 1\right.\\
&\left.- \ln\left(\frac{I_1(t-\omega)}{I_1^*}\right)\right\} d\omega = -\beta(1-p)(S^*
\end{aligned}
$$

$$+\gamma V^*)\, I_2^* \int_0^{\tau_2} \frac{d}{d\omega}\left\{\frac{I_1(t-\omega)}{I_1^*} - 1 - \ln\left(\frac{I_1(t-\omega)}{I_1^*}\right)\right\} d\omega = \beta(1-p)(S^* + \gamma V^*)\, I_2^* \left\{\frac{I_1(t)}{I_1^*} - \frac{I_1(t-\tau_2)}{I_1^*} + \ln\left(\frac{I_1(t-\tau_2)}{I_1(t)}\right)\right\} = \beta(1-p)\, S^* I_2^* \cdot \frac{I_1(t)}{I_1^*} + \beta\gamma(1-p)\, V^* I_2^* \cdot \frac{I_1(t)}{I_1^*} - \beta(1-p)\, S^* I_2^* I_1(t-\tau_2) \cdot \frac{1}{I_1^*} - \beta\gamma(1-p)\, V^* I_2^* I_1(t-\tau_2) \cdot \frac{1}{I_1^*} + \beta(1-p)\, S^* I_2^* \ln\left(\frac{I_1(t-\tau_2)}{I_1(t)}\right) + \beta\gamma(1-p)\, V^* I_2^* \cdot \ln\left(\frac{I_1(t-\tau_2)}{I_1(t)}\right). \tag{54}$$

Combining the derivatives of $\mathscr{W}_j(t)$, for $j = 1, 2, 3$, we have

$$\begin{aligned}
\frac{d\mathscr{W}(t)}{dt} &= \mu S^* \left\{2 - \frac{S(t)}{S^*} - \frac{S^*}{S(t)}\right\} + \kappa V^* \left\{2 - \frac{S(t)\, V^*}{S^* V(t)} - \frac{S^* V(t)}{S(t)\, V^*}\right\} + \mu V^* \left\{3 - \frac{S^*}{S(t)} - \frac{V(t)}{V^*} - \frac{S(t)\, V^*}{S^* V(t)}\right\} + \beta I_1^* S^* \left\{2 - \frac{S^*}{S(t)} - \frac{S(t-\tau_1)\, I_1(t-\tau_1)}{S^* I_1(t)} + \ln\left(\frac{I_1(t-\tau_1)\, S(t-\tau_1)}{I_1(t)\, S(t)}\right)\right\} + \beta(1-p)\, S^* I_2^* \left\{2 - \frac{S^*}{S(t)} - \frac{S(t-\tau_1)\, I_2(t-\tau_1)\, I_1^*}{S^* I_2^* I_1(t)} - \frac{I_1(t-\tau_2)\, I_2^*}{I_1^* I_2(t)} + \ln\left(\frac{I_2(t-\tau_1)\, S(t-\tau_1)\, I_1(t-\tau_2)}{I_2(t)\, S(t)\, I_1(t)}\right)\right\} \\
&+ \beta\gamma V^* I_1^* \left\{3 - \frac{S^*}{S(t)} - \frac{S(t)\, V^*}{S^* \mathrm{V}} - \frac{V(t-\tau_1)\, I_1(t-\tau_1)}{V^* I_1(t)} + \ln\left(\frac{I_1(t-\tau_1)\, V(t-\tau_1)}{I_1(t)\, V(t)}\right)\right\} + \beta\gamma(1-p) \cdot V^* I_2^* \left\{3 - \frac{S^*}{S(t)} - \frac{S(t)\, V^*}{S^* V(t)} - \frac{V(t-\tau_1)\, I_1^* I_2(t-\tau_1)}{V^* I_1(t)\, I_2^*} - \frac{I_1(t-\tau_2)\, I_2^*}{I_1^* I_2(t)} + \ln\left(\frac{I_2(t-\tau_1)\, V(t-\tau_1)\, I_1(t-\tau_2)}{I_2(t)\, V(t)\, I_1(t)}\right)\right\}.
\end{aligned} \tag{55}$$

Note that

$$\begin{aligned}
2 &\le \frac{S(t)}{S^*} + \frac{S^*}{S(t)}, \\
2 &\le \frac{S(t)\, V^*}{S^* V(t)} + \frac{S^* V(t)}{S(t)\, V^*}, \\
3 &\le \frac{S^*}{S(t)} + \frac{V(t)}{V^*} + \frac{S(t)\, V^*}{S^* V(t)}
\end{aligned} \tag{56}$$

for all $S(t) > 0$ and $V(t) > 0$, because the arithmetic mean is greater than or equal to the geometric mean. Further, note that $G(t) = 1 - g(t) + \ln g(t)$ is always nonpositive for any function $g(t) > 0$, and $g(t) = 0$ if and only if $g(t) = 1$. Hence, it follows that $\dot{\mathscr{W}}(t) \le 0$ and, consequently, $\ddot{\mathscr{W}}(t) \le 0$. Moreover, the largest invariant set of $\ddot{\mathscr{W}}(t) = 0$ is a singleton, where $S(t) \equiv S^*$, $V(t) \equiv V^*$, $I_1(t) \equiv I_1^*$, and $I_2(t) \equiv I_2^*$. Using LaSalle's invariance principle [20], we conclude that the endemic equilibrium point $\mathscr{E}^*$ is globally asymptotically stable if $\mathscr{R}_0 > 1$. □

3.7. Hopf Bifurcation Analysis. In this section we determine criteria for Hopf bifurcation to occur using the time delay τ_1 and τ_2 as the bifurcation parameters to find the interval in which the infected equilibria is stable and unstable out of the same margins. Now to consider Hopf bifurcation we consider the cases (a) $\tau_1 = \tau_{10} > 0$, $\tau_2 = 0$ and (b) $\tau_2 = \tau_{20} > 0$ and $\tau_1 = 0$. Our analysis is as follows:

(a) When $\tau_1 = \tau_{10} > 0$ and $\tau_2 = 0$ we need to show that $d\mathrm{Re}\lambda(\tau_{10})/d\tau_1 > 0$ differentiating (37) with respect to τ_1 we get

$$\begin{aligned}
&\left(4\lambda^3 + 3a_{11}\lambda^2 + 2a_{21}\lambda + a_{31}\right)\frac{d\lambda}{d\tau_1} \\
&\quad = \left[-\tau_1 e^{-\lambda\tau_1}\left(m_{11}\lambda^3 + m_{21}\lambda^2 + m_{31}\lambda + m_{41}\right) + e^{-\lambda\tau_1}\left(3m_{11}\lambda^2 + 2m_{21}\lambda + m_{31}\right)\right]\frac{d\lambda}{d\tau_1} \\
&\quad - \lambda e^{\lambda\tau_1}\left(m_{11}\lambda^3 + m_{21}\lambda^2 + m_{31}\lambda + m_{41}\right).
\end{aligned} \tag{57}$$

This gives

$$\begin{aligned}
\left(\frac{d\lambda}{d\tau_1}\right)^{-1} &= \frac{4\lambda^3 + 3a_{11}\lambda^2 + 2a_{21}\lambda + a_{31}}{-\lambda e^{-\lambda\tau_1}\left(m_{11}\lambda^3 + m_{21}\lambda^2 + m_{31}\lambda + m_{41}\right)} + \frac{3m_{11}\lambda^2 + 2m_{21}\lambda + m_{31}}{\lambda\left(m_{11}\lambda^3 + m_{21}\lambda^2 + m_{31}\lambda + m_{41}\right)} - \frac{\tau_1}{\lambda} \\
&= \frac{3\lambda^4 + 2a_{11}\lambda^3 + a_{21}\lambda^2 - a_{41}}{-\lambda^2\left(\lambda^4 + a_{11}\lambda^3 + a_{21}\lambda^2 + a_{31}\lambda + a_{41}\right)} + \frac{2m_{11}\lambda^3 + m_{21}\lambda^2 - m_{41}}{\lambda^2\left(m_{11}\lambda^3 + m_{21}\lambda^2 + m_{31}\lambda + m_{41}\right)} - \frac{\tau_1}{\lambda}.
\end{aligned} \tag{58}$$

Thus,

$$\begin{aligned}
\operatorname{sign}\left[\frac{d(\operatorname{Re}\lambda)}{d\tau_1}\right]_{\lambda=i\omega_0} &= \operatorname{sign}\left[\operatorname{Re}\left(\frac{d\lambda}{d\tau_1}\right)^{-1}\right]_{\lambda=i\omega_0} = \operatorname{sign}\left[\operatorname{Re}\left[\frac{3\lambda^4+2a_{11}\lambda^3+a_{21}\lambda^2-a_{41}}{-\lambda^2\left(\lambda^4+a_{11}\lambda^3+a_{21}\lambda^2+a_{31}\lambda+a_{41}\right)}\right]_{\lambda=i\omega_0}\right] \\
&+ \operatorname{sign}\left[\operatorname{Re}\left[\frac{2m_{11}\lambda^3+m_{21}\lambda^2-m_{41}}{\lambda^2\left(m_{11}\lambda^3+m_{21}\lambda^2+m_{31}\lambda+m_{41}\right)}\right]_{\lambda=i\omega_0}\right] = \operatorname{sign}\left[\operatorname{Re}\left[\frac{3\omega_0^4-2a_{11}\omega_0^3 i-a_{21}\omega_0^2-a_{41}}{\omega_0^2\left(\omega_0^4-a_{11}\omega_0^3 i-a_{21}\omega_0^2+a_{31}\omega_0 i+a_{41}\right)}\right]\right] \\
&+ \operatorname{sign}\left[\operatorname{Re}\left[\frac{-2m_{11}\omega_0^3 i-m_{21}\omega_0^2-m_{41}}{-\omega_0^2\left(-m_{11}\omega_0^3 i-m_{21}\omega_0^2 i+m_{31}\omega_0 i+m_{41}\right)}\right]\right] \\
&= \operatorname{sign}\left[\frac{3\omega_0^8+2\left(a_{11}^2-2a_{21}\right)\omega_0^6+\left(a_{21}^2+2\left(a_{41}-a_{11}a_{31}\right)\right)\omega_0^4-a_{41}^2}{\omega_0^2\left[\left(\omega_0^4-a_{21}\omega_0^2+a_{41}\right)^2+\left(a_{31}\omega_0-a_{11}\omega_0^3\right)^2\right]}\right] \\
&+ \operatorname{sign}\left[\frac{m_{41}^2-2m_{11}^2\omega_0^6-\left(m_{21}^2-2m_{11}m_{11}\right)\omega_0^4}{\omega_0^2\left[\left(m_{41}-m_{21}\omega_0^2\right)^2+\left(m_{31}\omega_0-m_{11}\omega_0^3\right)^2\right]}\right] \\
&= \operatorname{sign}\left[\frac{3\omega_0^8+2\left(a_{11}^2-m_{11}^2-2a_{21}\right)\omega_0^6+\left(a_{21}^2-m_{21}^2+2\left(a_{41}+m_{11}m_{31}-a_{11}a_{31}\right)\right)\omega_0^4-a_{41}^2+m_{41}^2}{\omega_0^2\left[\left(\omega_0^4-a_{21}\omega_0^2+a_{41}\right)^2+\left(a_{31}\omega_0-a_{11}\omega_0^3\right)^2\right]}\right] \\
&= \operatorname{sign}\left[\frac{4\omega_0^6+3\left(a_{11}^2-m_{11}^2-2a_{21}\right)\omega_0^4+2\left(a_{21}^2-m_{21}^2+2\left(a_{41}+m_{11}m_{31}-a_{11}a_{31}\right)\right)\omega_0^2+k_0}{\left[\left(\omega_0^4-a_{21}\omega_0^2+a_{41}\right)^2+\left(a_{31}\omega_0-a_{11}\omega_0^3\right)^2\right]}\right].
\end{aligned} \tag{59}$$

with

$$k_0 = a_{31}^2 - m_{31}^2 + 2\left(m_{21}m_{41} - a_{21}a_{41}\right). \tag{60}$$

Lemma 7. *Suppose that x_i, $i = 1, 2, 3, 4$, are the roots of equation $g(x) = x^4 + \vartheta_1 x^3 + \vartheta_2 x^2 + \vartheta_3 x + \vartheta_4 = 0$ $(\vartheta_3 < 0)$ and x_4 is the largest positive root; then*

$$\left\{\frac{dg(x)}{dx}\right\}_{x=x_4} > 0. \tag{61}$$

In our case considering $F(z) = z^4 + b_1 z^3 + b_2 z^2 + b_3 z + b_4 = 0$ defined in (42), and assuming $b_3 < 0$ and ω_0^2 as the largest positive root, we have

$$\begin{aligned}
\frac{d\operatorname{Re}\lambda}{d\tau_1} &= \frac{dF(z)/dz}{\left[\left(\omega_0^4-a_{21}\omega_0^2+a_{41}\right)^2+\left(a_{31}\omega_0-a_{11}\omega_0^3\right)^2\right]} \\
&> 0.
\end{aligned} \tag{62}$$

The above analysis can be summarized into the following theorem.

Theorem 8. *Suppose that (a) $\mathscr{R}_0 > 1$. If either (b) $b_4 < 0$ or (c) $b_4 \geq 0$ and $b_3 < 0$ is satisfied, and ω_0 is the largest positive simple root of (42) then the infected equilibrium $\mathscr{E}^*$ of model (1) is locally asymptotically stable when $\tau_1 < \tau_{10}$ and unstable when $\tau_1 > \tau_{10}$ where*

$$\tau_{10} = \frac{1}{\omega_0}\arccos\left[\frac{\left(m_{41}-m_{21}\omega_0^2\right)\left(\omega_0^4-a_{21}\omega_0^2+a_{41}\right)+\left(m_{31}\omega_0-m_{11}\omega_0^3\right)\left(a_{31}\omega_0-a_{11}\omega_0^3\right)}{\left(m_{41}-m_{21}\omega_0^2\right)^2+\left(m_{31}\omega_0-m_{11}\omega_0^3\right)^2}\right], \tag{63}$$

when $\tau_1 = \tau_{10}$, a Hopf bifurcation occurs; that is, a family of periodic solutions bifurcates from $\mathscr{E}^*$ as τ_1 passes through the critical value τ_{10}.

(b) When $\tau_2 = \tau_{20} > 0$ and $\tau_1 = 0$ we also need to show that $d\operatorname{Re}\lambda(\tau_{20})/d\tau_2 > 0$ differentiating (43) with respect to τ_2 we get

$$\begin{aligned}
&\left(4\lambda^3+3\alpha_{11}\lambda^2+2\alpha_{21}\lambda+\alpha_{31}\right)\frac{d\lambda}{d\tau_2} \\
&= \left[-\tau_2 e^{-\lambda\tau_2}\left(n_{21}\lambda^2+n_{31}\lambda+n_{41}\right)\right. \\
&\left.+ e^{-\lambda\tau_2}\left(2n_{21}\lambda+n_{31}\right)\right]\frac{d\lambda}{d\tau_2} - \lambda e^{\lambda\tau_2}\left(n_{31}\lambda\right. \\
&\left.+ n_{41}\right).
\end{aligned} \tag{64}$$

This gives

$$\left(\frac{d\lambda}{d\tau_2}\right)^{-1} = \frac{4\lambda^3 + 3\alpha_{11}\lambda^2 + 2\alpha_{21}\lambda + \alpha_{31}}{-\lambda e^{-\lambda\tau_2}\left(n_{21}\lambda^2 + n_{31}\lambda + n_{41}\right)} + \frac{2n_{21}\lambda + n_{31}}{\lambda\left(n_{21}\lambda^2 + n_{31}\lambda + n_{41}\right)} - \frac{\tau_2}{\lambda}$$

$$= \frac{3\lambda^4 + 2\alpha_{11}\lambda^3 + \alpha_{21}\lambda^2 - \alpha_{41}}{-\lambda^2\left(\lambda^4 + \alpha_{11}\lambda^3 + \alpha_{21}\lambda^2 + \alpha_{31}\lambda + \alpha_{41}\right)} + \frac{n_{21}\lambda^2 - n_{41}}{\lambda^2\left(n_{21}\lambda^2 + n_{31}\lambda + n_{41}\right)} - \frac{\tau_2}{\lambda}. \tag{65}$$

Thus,

$$\begin{aligned}
\operatorname{sign}\left[\frac{d\left(\operatorname{Re}\lambda\right)}{d\tau_2}\right]_{\lambda=i\omega_0} &= \operatorname{sign}\left[\operatorname{Re}\left(\frac{d\lambda}{d\tau_2}\right)^{-1}\right]_{\lambda=i\omega_0} = \operatorname{sign}\left[\operatorname{Re}\left[\frac{3\lambda^4 + 2\alpha_{11}\lambda^3 + \alpha_{21}\lambda^2 - \alpha_{41}}{-\lambda^2\left(\lambda^4 + \alpha_{11}\lambda^3 + \alpha_{21}\lambda^2 + \alpha_{31}\lambda + \alpha_{41}\right)}\right]_{\lambda=i\omega_0}\right] \\
&+ \operatorname{sign}\left[\operatorname{Re}\left[\frac{n_{21}\lambda^2 - n_{41}}{\lambda^2\left(n_{21}\lambda^2 + n_{31}\lambda + n_{41}\right)}\right]_{\lambda=i\omega_0}\right] = \operatorname{sign}\left[\operatorname{Re}\left[\frac{3\omega_0^4 - 2\alpha_{11}\omega_0^3 i - \alpha_{21}\omega_0^2 - \alpha_{41}}{\omega_0^2\left(\omega_0^4 - \alpha_{11}\omega_0^3 i - \alpha_{21}\omega_0^2 + \alpha_{31}\omega_0 i + \alpha_{41}\right)}\right]\right] \\
&+ \operatorname{sign}\left[\operatorname{Re}\left[\frac{-n_{21}\omega_0^2 - n_{41}}{-\omega_0^2\left(-n_{21}\omega_0^2 i + n_{31}\omega_0 i + n_{41}\right)}\right]\right] = \operatorname{sign}\left[\frac{3\omega_0^8 + 2\left(\alpha_{11}^2 - 2\alpha_{21}\right)\omega_0^6 + \left(\alpha_{21}^2 + 2\left(\alpha_{41} - \alpha_{11}\alpha_{31}\right)\right)\omega_0^4 - \alpha_{41}^2}{\omega_0^2\left[\left(\omega_0^4 - \alpha_{21}\omega_0^2 + \alpha_{41}\right)^2 + \left(\alpha_{31}\omega_0 - \alpha_{11}\omega_0^3\right)^2\right]}\right] \\
&+ \operatorname{sign}\left[\frac{n_{41}^2 - n_{21}^2\omega_0^4}{\omega_0^2\left[\left(n_{41} - n_{21}\omega_0^2\right)^2 + n_{31}^2\omega_0^2\right]}\right] \\
&= \operatorname{sign}\left[\frac{3\omega_0^8 + 2\left(\alpha_{11}^2 - 2\alpha_{21}\right)\omega_0^6 + \left(\alpha_{21}^2 - n_{21}^2 + 2\left(\alpha_{41} - \alpha_{11}\alpha_{31}\right)\right)\omega_0^4 - \alpha_{41}^2 + n_{41}^2}{\omega_0^2\left[\left(\omega_0^4 - \alpha_{21}\omega_0^2 + \alpha_{41}\right)^2 + \left(\alpha_{31}\omega_0 - \alpha_{11}\omega_0^3\right)^2\right]}\right] \\
&= \operatorname{sign}\left[\frac{4\omega_0^6 + 3\left(\alpha_{11}^2 - 2\alpha_{21}\right)\omega_0^4 + 2\left(\alpha_{21}^2 - n_{21}^2 + 2\left(\alpha_{41} - \alpha_{11}\alpha_{31}\right)\right)\omega_0^2 + \alpha_{31}^2 - n_{31}^2 + 2\left(n_{21}n_{41} - \alpha_{21}\alpha_{41}\right)}{\left[\left(\omega_0^4 - \alpha_{21}\omega_0^2 + \alpha_{41}\right)^2 + \left(\alpha_{31}\omega_0 - \alpha_{11}\omega_0^3\right)^2\right]}\right].
\end{aligned} \tag{66}$$

Lemma 9. *Suppose that x_i, $i = 1, 2, 3, 4$, are the roots of equation $g(x) = x^4 + \varphi_1 x^3 + \varphi_2 x^2 + \varphi_3 x + \varphi_4 = 0$ ($\varphi_3 < 0$) and x_4 is the largest positive root; then*

$$\left\{\frac{dg(x)}{dx}\right\}_{x=x_4} > 0. \tag{67}$$

In our case considering $h(z) = z^4 + c_1 z^3 + c_2 z^2 + c_3 z + c_4 = 0$ defined in (45), and assuming $c_3 < 0$ and ω_0^2 as the largest positive root, we have

$$\frac{d\operatorname{Re}\lambda}{d\tau_2} = \frac{dh(z)/dz}{\left[\left(\omega_0^4 - \alpha_{21}\omega_0^2 + \alpha_{41}\right)^2 + \left(\alpha_{31}\omega_0 - \alpha_{11}\omega_0^3\right)^2\right]} > 0. \tag{68}$$

The above analysis can be summarized into the following theorem.

Theorem 10. *Suppose that (a) $\mathscr{R}_0 > 1$. If either (b) $c_4 < 0$ or (c) $c_4 \geq 0$ and $c_3 < 0$ is satisfied, and ω_0 is the largest positive simple root of (45) then the infected equilibrium $\mathscr{E}^*$ of model (1) is locally asymptotically stable when $\tau_2 < \tau_{20}$ and unstable when $\tau_2 > \tau_{20}$ where*

$$\tau_{20} = \frac{1}{\omega_0}\arccos\left[\frac{\left(n_{41} - n_{21}\omega_0^2\right)\left(\omega_0^4 - \alpha_{21}\omega_0^2 + \alpha_{41}\right) + n_{31}\omega_0\left(\alpha_{31}\omega_0 - \alpha_{11}\omega_0^3\right)}{\left(n_{41} - n_{21}\omega_0^2\right)^2 + n_{31}^2\omega_0^2}\right], \tag{69}$$

when $\tau_2 = \tau_{20}$, a Hopf bifurcation occurs; that is, a family of periodic solutions bifurcates from $\mathscr{E}^*$ as τ_2 passes through the critical value τ_{20}.

From the analysis above, we can deduce that Hopf bifurcations may arise if conditions in Theorems 8 and 10 are satisfied. Thus, the introduction of time delay in system (1) can destabilize the system.

4. Numerical Results

In order to explore the behavior of system (1) and illustrate the stability of the equilibria solutions, we numerically solve system (1) using MATLAB and parameter values adopted from Table 1.

In Figure 1 we illustrate the effects of varying the delay ($\tau_1 = \tau_2$) on the dynamics of system (1). Figures 1(a) and 1(b)

Table 1: Model parameters and variables and their baseline values.

Symbol	Definition	Value	Unit	Source
d	Elimination rate due to brucellosis	0.15	year^{-1}	[8]
p	Fraction of infectious animals culled upon detection	0.5	-	[22]
β	Direct transmission rate	3.844×10^{-6}	$\text{animal}^{-1}\text{year}^{-1}$	[6]
κ	Vaccination waning rate	0.4	year^{-1}	[8]
μ	Natural elimination rate	0.25	year^{-1}	[6]
γ	Modification factor	0.18	-	[8]
A	Recruitment rate	76434	animals year^{-1}	[6]
σ	Vaccination rate	0.316	year^{-1}	[8]
α	Detection rate	Varied	year^{-1}	-
c	Culling rate	0.15	year^{-1}	[8]

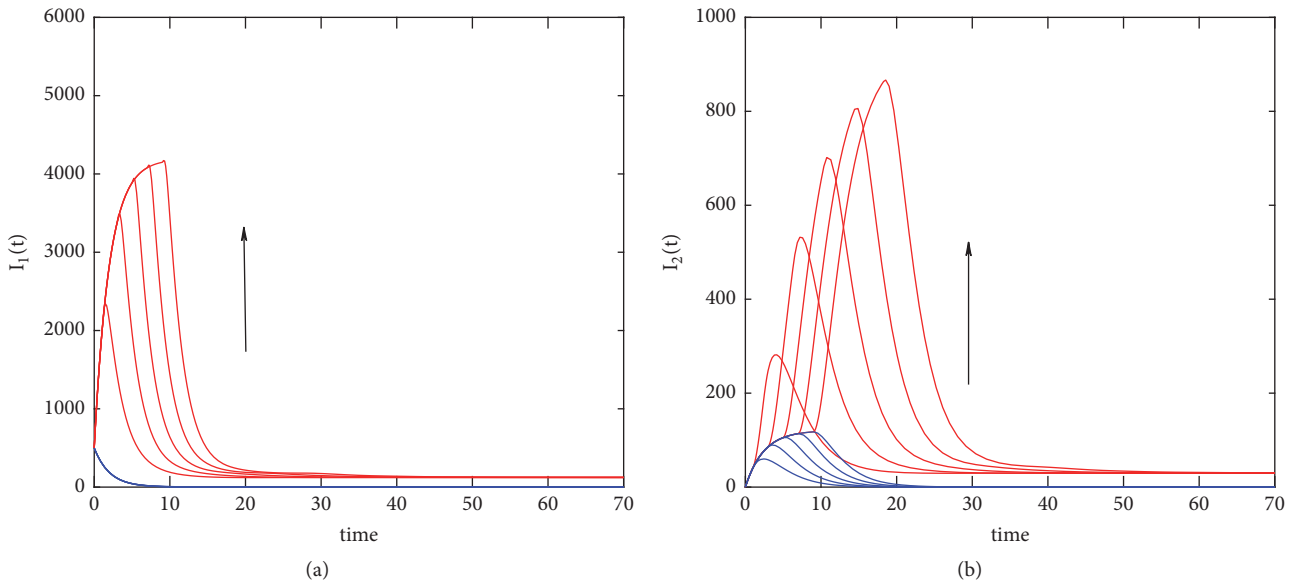

Figure 1: Stability of the infected and free-infected equilibrium of model system (1) showing plots of $I_1(t)$ and $I_2(t)$ with varying delay ($\tau_1 = \tau_2$). The direction of the arrow depicts an increase in delay with a step size of 2.0 starting from 2.0 to 10. The blue patterns in both (a) and (b) highlight brucellosis dynamics when $\mathcal{R}_0 < 1$ while the red pattern is for $\mathcal{R}_0 > 1$. Initial population levels were assumed as follows: $S(0) = 1000$ animals, $V(0) = 500$ animals, $I_1(0) = 500$ animals, and $I_2(0) = 0$ animals.

demonstrate that the system approaches the stable disease-free or endemic equilibrium for $\mathcal{R}_0 < 1$ and $\mathcal{R}_0 > 1$, respectively. One should note that, according to Theorems 2 and 6, the stability of the model steady states does not depend on the value of the time delays, but rather on the basic reproduction number $\mathcal{R}_0$, only. In addition, we observe that the range of values for the two time delays does not lead to periodic solutions but an increase in both delays translate to an increase in the infectious population, both detected and undetected.

Figure 2 depicts the numbers of infectious undetected and infectious detected animals over time with varying delays. The results clearly show that the incubation related delay (τ_1) has more influence on shaping the dynamics of brucellosis compared to the culling related delay (τ_2). More precisely, the incubation period delay significantly increases the infectious population (both detected and undetected) for $0 < t < 20$ and thereafter its impact will be the same as that of detection (τ_2).

In Figure 3 we illustrate the stability of the disease-free equilibrium $\mathcal{E}^0$ with $\tau_1 = 30$ and $\tau_2 = 5$ (note that $\mathcal{R}_0 = 0.686281$). As we can observe, for certain parameter values and initial population levels, system (1) exhibits some periodic oscillation. Precisely, we note that the infected population ($I_1(t)$ and $I_2(t)$) oscillates with a reduced amplitude from the start till when t is approximately 400; thereafter the oscillations dies off the solutions converges to the disease-free equilibrium. These simulation results demonstrate the occurrence of periodic solutions through Hopf bifurcation for delay values $\tau_1 = 30$ and $\tau_2 = 5$. In contrast, we can observe that there are no periodic oscillations for the uninfected populations $S(t)$ and $V(t)$.

In Figure 4, we demonstrate the dynamic for model system (1) with respect to the stability of infection-free

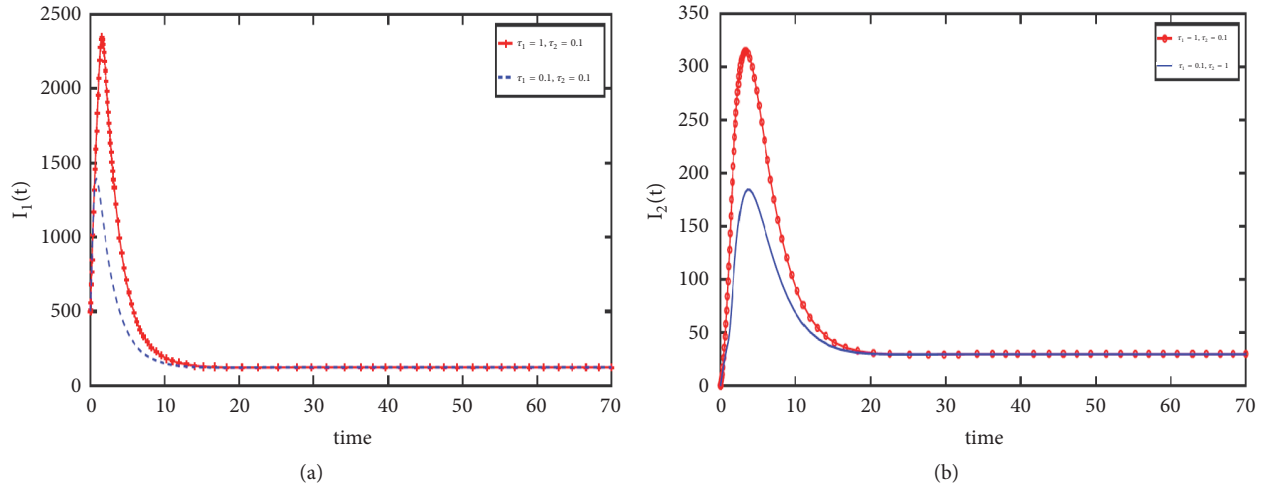

FIGURE 2: Numerical solutions of model system (1) illustrating the effects of different time delay on brucellosis infection level in the community. Initial population levels were assumed as follows: $S(0) = 1000$ animals, $V(0) = 500$ animals, $I_1(0) = 500$ animals, and $I_2(0) = 0$ animals.

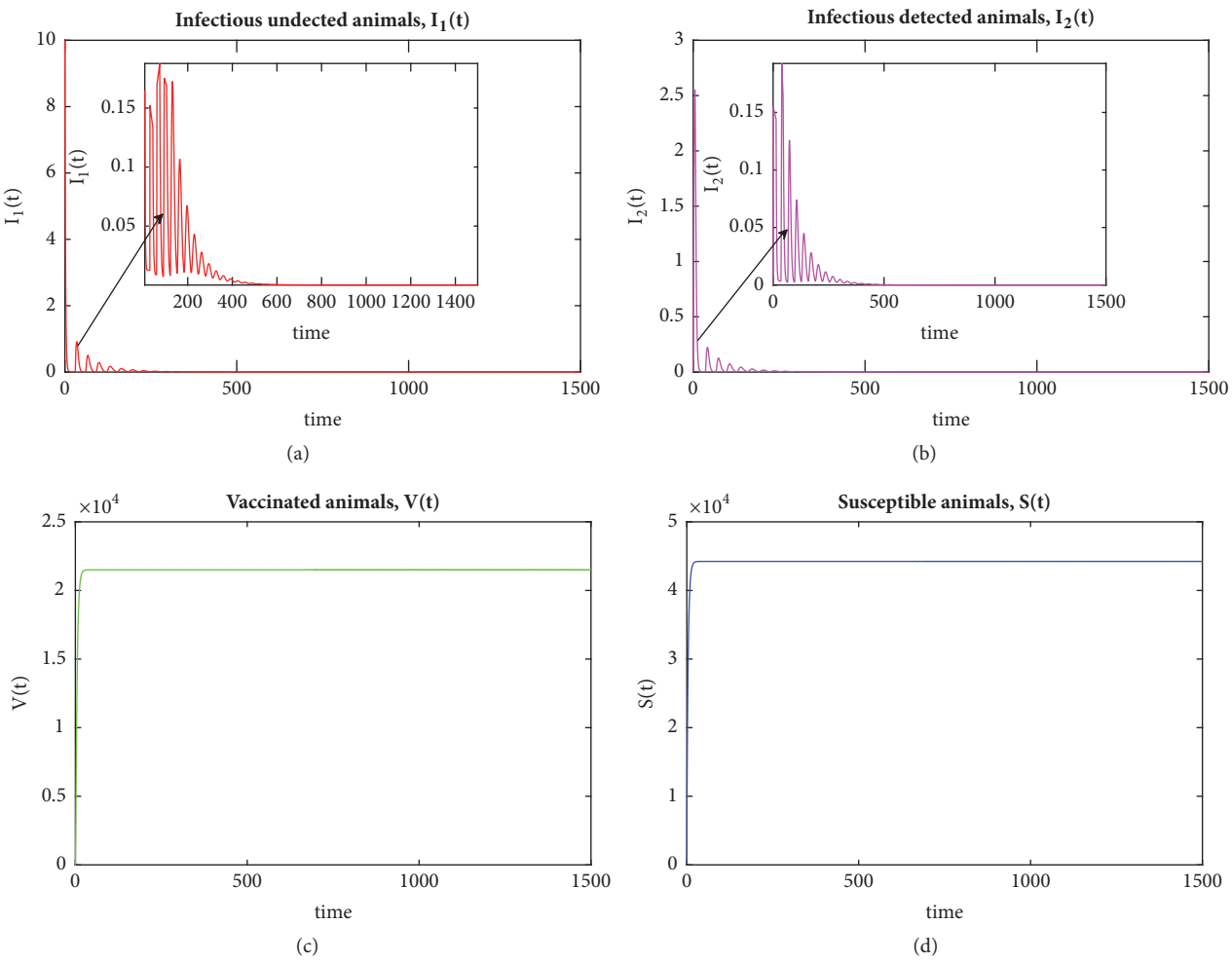

FIGURE 3: Numerical solutions demonstrating the stability of $\mathscr{E}^0$ equilibrium of model system (1) with $\mathscr{R}_0 = 0.686281$. We set $\tau_1 = 30$, $\tau_2 = 5$, $\beta = 6.844 \times 10^{-6}$ animal^{-1} year^{-1}, $\gamma = 0.2$, $\alpha = 0.15$ year^{-1}, $A = 16434$ animals year^{-1}, and the remainder retained the baseline values in Table 1. Further, we set the initial conditions as follows: $S(0) = 100$ animals, $V(0) = 0$ animals, $I_1(0) = 10$ animals, and $I_2(0) = 0$ animals.

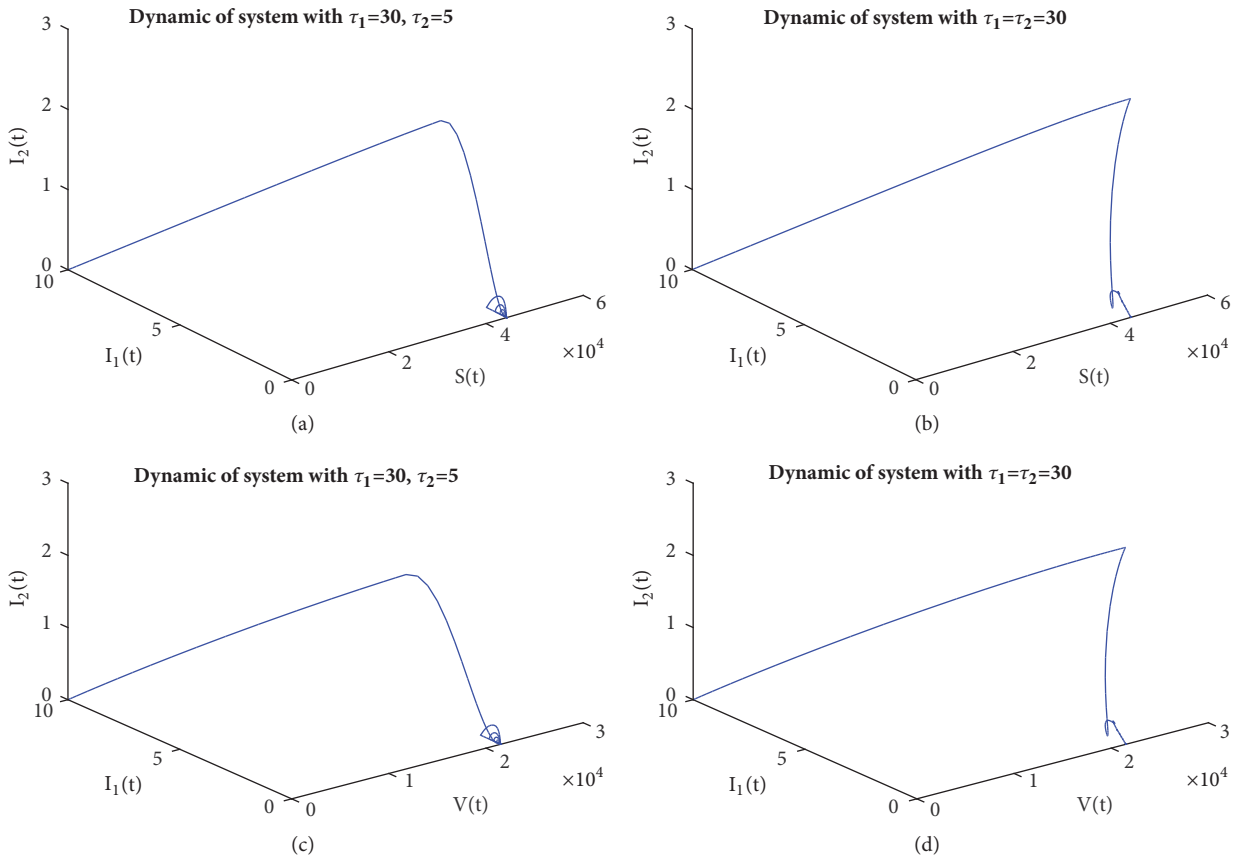

FIGURE 4: Dynamics of model system (1) for different values of (τ_1, τ_2), which illustrate the stability of infection-free equilibrium $\mathscr{E}^0$ at $\mathscr{R}_0 = 0.686281$. We set $\beta = 6.844 \times 10^{-6}$ animal^{-1} year^{-1}, $\gamma = 0.2$, $\alpha = 0.15$ year^{-1}, $A = 16434$ animals year^{-1}, and the remainder retained the baseline values in Table 1. Further, we set the initial conditions as follows: $S(0) = 100$ animals, $V(0) = 0$ animals, $I_1(0) = 10$ animals, and $I_2(0) = 0$ animals.

equilibrium for different pair of delay values (τ_1, τ_2) and from the simulation results we can conclude that both delays do not have a huge influence on the stability of disease-free equilibrium.

In Figure 5 we observe that, for certain parameter values and initial population levels, system (1) may admit periodic oscillations when $\mathscr{R}_0 > 1$. As we can observe, when $\mathscr{R}_0 = 3.77333$ both the solutions of the infected and uninfected populations exhibit periodic oscillation for a certain period, before stability at endemic point is attained.

In Figure 6, we illustrate the dynamics for model system (1) with respect to the stability of endemic equilibrium for several pair of delay values (τ_1, τ_2). The results confirm that the incubation related delay τ_1 has more influence on shaping the dynamic of brucellosis compared to the culling related delay τ_2.

To explore influence of model parameters on the reproduction number $\mathscr{R}_0$, we perform a local sensitivity analysis of the basic reproduction number following the approach in [23]. The local sensitivity analysis will be useful on identifying parameters with greatest influence to change $\mathscr{R}_0$. To this end, denoting by Φ the generic parameter of system (1), we evaluate the *normalised sensitivity index*:

$$S_\Phi = \frac{\Phi}{\mathscr{R}_0} \frac{\partial \mathscr{R}_0}{\partial \Phi}, \tag{70}$$

which indicates how sensitive $\mathscr{R}_0$ is to a change of parameter Φ. Model parameters with positive index increase the value of $\mathscr{R}_0$ whenever they are increased while those with a negative index decrease the value of $\mathscr{R}_0$ whenever they are increased. We consider the parameter values in Table 1, and we set $\alpha = 0.015$ in order to evaluate the normalized sensitivity index and the results are depicted in Figure 7. Here, we observe that parameters A, β, κ, γ have a positive correlation with $\mathscr{R}_0$, such that increasing these parameters will increase $\mathscr{R}_0$. However, it is the increase of A and β that has the greatest influence to change $\mathscr{R}_0$. Precisely, increasing either A or β by 50% will increase $\mathscr{R}_0$ by 50%. We also note that increasing parameters, c, μ, σ, d, p, and α, will lower the reproduction number.

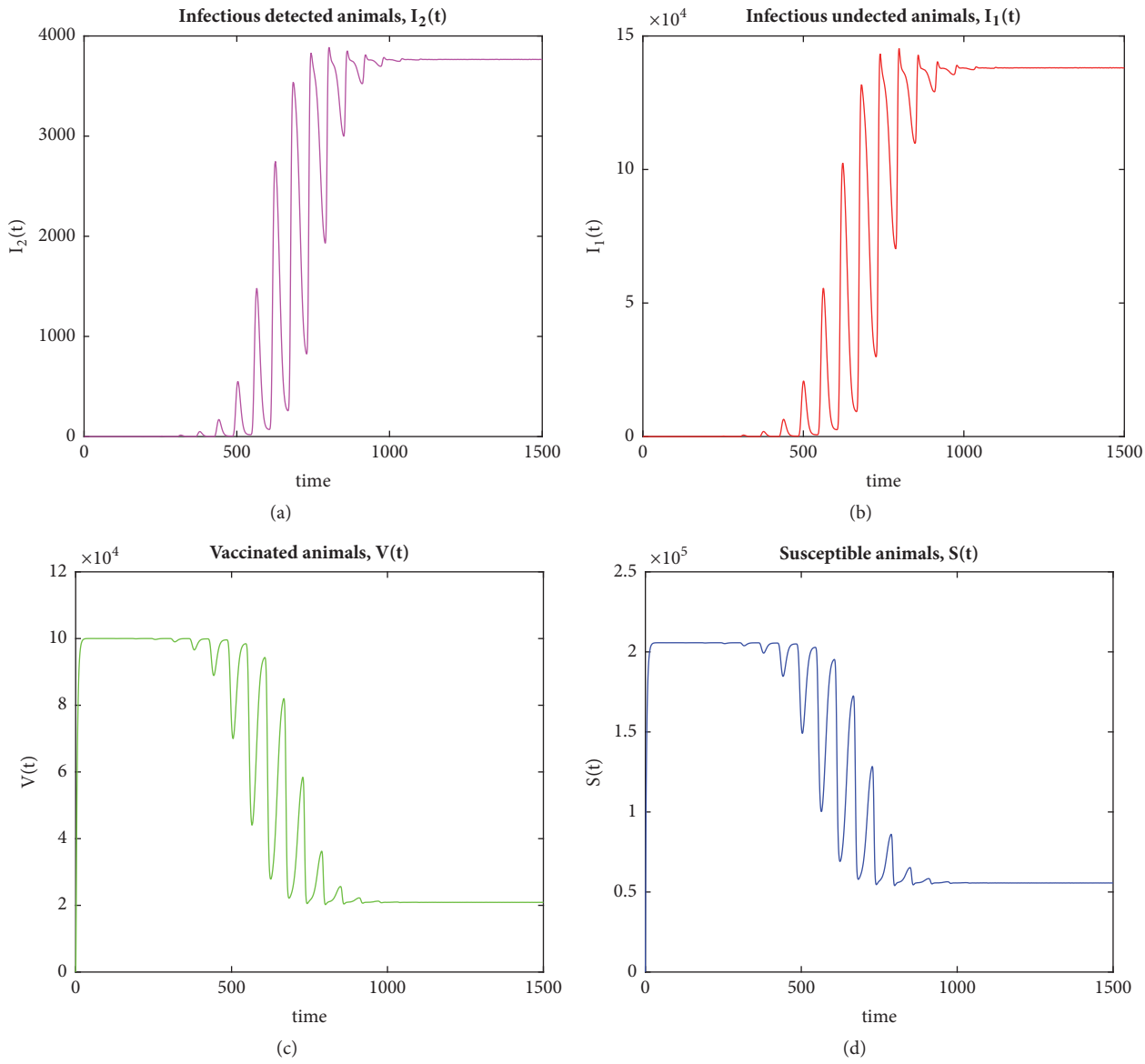

FIGURE 5: Stability of $\mathscr{E}^*$ equilibrium of model system (1) with $\mathscr{R}_0 = 3.77333$. The time delay τ_1 was fixed to be 60 and τ_2 was fixed to be 1. We set the model parameters and variables as follows: $\beta = 6.844 \times 10^{-6}$ animal^{-1}year^{-1}, $\gamma = 0.2$, $\alpha = 0.015$ year^{-1}, $S(0) = 100$ animals, $V(0) = 0$ animals, $I_1(0) = 10$ animals, and $I_2(0) = 0$ animals while the other parameter values are as in Table 1.

5. Conclusion

Zoonotic brucellosis remains a major public health problem in many developing nations. This is mainly attributed to several challenges associated with effective disease control in these nations. The challenges for effective control of brucellosis in developing nations range from inadequate veterinary personnel and vaccines as well as the failure by farmers to adhere to some of the aforementioned brucellosis control and eradication program activities. Furthermore, these challenges often lead to delay in detection and culling of infectious animals. In this study, we developed and analysed a mathematical model for brucellosis infection that incorporates two discrete delays. The first delay accounts for the latent period and the second delay represents the time taken to detect infectious animals. We computed the basic reproduction number and demonstrated that it is an important threshold quantity for stability of equilibria. By constructing suitable Lyapunov functionals, it has been shown that the model has a globally asymptotically stable infection-free equilibrium whenever the reproduction is less than unity. Further, it has been demonstrated that whenever the model reproduction number is greater than unity then the model has a unique endemic equilibrium point which is globally asymptotically stable. Numerical simulations are carried out to illustrate the main results.

Although culling of symptomatic animals is a relatively easy strategy to implement, it is worth noting that some

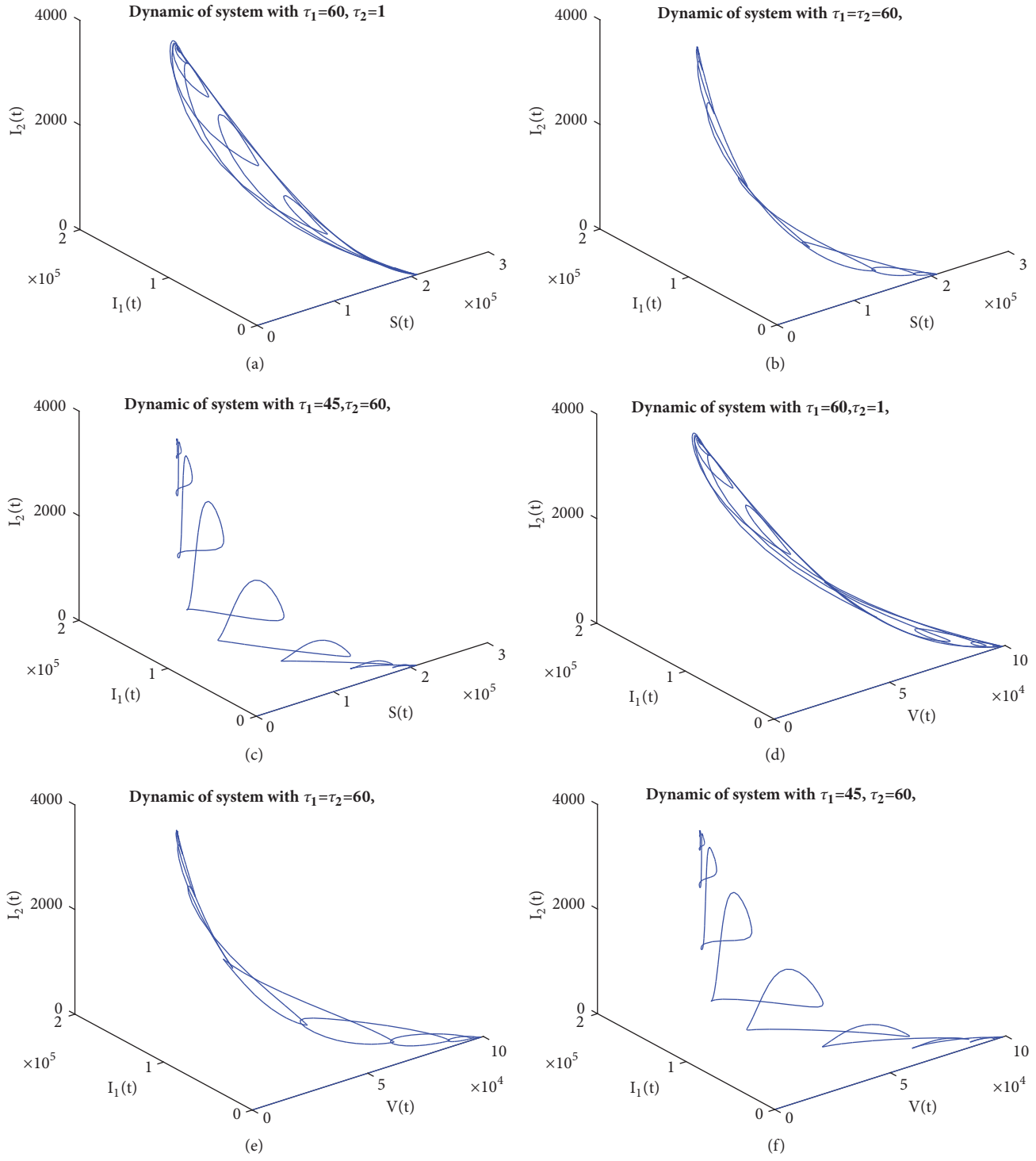

FIGURE 6: Numerical results of model system (1) for different values of (τ_1, τ_2), which demonstrate the stability of infected equilibrium $\mathscr{E}^*$ at $\mathscr{R}_0 = 3.77333$. We set the model parameters and variables as follows: $\beta = 6.844 \times 10^{-6}$ animal^{-1}year^{-1}, $\gamma = 0.2$, $\alpha = 0.015$ year^{-1}, $S(0) = 100$ animals, $V(0) = 0$ animals, $I_1(0) = 10$ animals, and $I_2(0) = 0$ animals while the other parameter values are as in Table 1.

studies suggest that culling of both infected and susceptible animal may be more effective [24, 25]. The rationale is that by decreasing the host density, then the number of contacts per unit time between animals is low, thereby reducing disease transmission. In [25] it was demonstrated that culling of both susceptible and symptomatic animals only can be effective whenever the number of infected host is above a certain critical level [25]. We expect to improve this study in our future work by developing brucellosis model(s) with time delay that will enable us to compare aforementioned aspects.

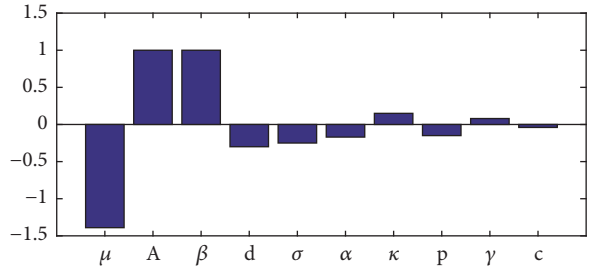

Figure 7: Sensitivity index for $\mathscr{R}_0$ with respect to model parameters that define it.

Data Availability

The data used to support the findings of this study are included within the article.

Conflicts of Interest

The authors declare that they have no conflicts of interest.

References

[1] E. M. Potter, "Brucellosis," in *Foodborne Infectionsand Intoxication*, J. G. Morris and E. M. Potter, Eds., Elsevier Inc., 4th, 2013.

[2] E. Shevtsova, A. Shevtsov, K. Mukanov et al., "Epidemiology of brucellosis and genetic diversity of Brucella abortus in Kazakhstan," *PLoS ONE*, vol. 11, no. 12, Article ID e0167496, 2016.

[3] J. Zhang, G.-Q. Sun, X.-D. Sun et al., "Prediction and control of brucellosis transmission of dairy cattle in Zhejiang Province, China," *PLoS ONE*, vol. 9, no. 11, Article ID e108592, 2014.

[4] J. A. Al-Tawfiq and A. AbuKhamsin, "A 24-year study of the epidemiology of human brucellosis in a health-care system in Eastern Saudi Arabia," *Journal of Infection and Public Health*, vol. 2, no. 2, pp. 81–85, 2009.

[5] J. Godfroid, "Brucellosis in wildlife," *Revue Scientifique et Technique de l'OIE*, vol. 21, no. 2, pp. 277–286, 2002.

[6] Q. Hou and X.-D. Sun, "Modeling sheep brucellosis transmission with a multi-stage model in Changling COUnty of Jilin Province, China," *Applied Mathematics and Computation*, vol. 51, no. 1-2, pp. 227–244, 2016.

[7] P. O. Lolika, S. Mushayabasa, C. P. Bhunu, C. Modnak, and J. Wang, "Modeling and analyzing the effects of seasonality on brucellosis infection," *Chaos, Solitons & Fractals*, vol. 104, pp. 338–349, 2017.

[8] Q. Hou, X. D. Sun, J. Zhang, Y. J. Liu, Y. M. Wang, and Z. Jin, "Modeling the transmission dynamics of sheep brucellosis in Inner Mongolia Autonomous Region, China," *Mathematical Biosciences*, vol. 242, no. 1, pp. 51–58, 2013.

[9] P. Lou, L. Wang, X. Zhang, J. Xu, and K. Wang, "Modelling Seasonal Brucellosis Epidemics in Bayingolin Mongol Autonomous Prefecture of Xinjiang, China, 2010–2014," *BioMed Research International*, vol. 2016, Article ID 5103718, 17 pages, 2016.

[10] C. Yang, P. O. Lolika, S. Mushayabasa, and J. Wang, "Modeling the spatiotemporal variations in brucellosis transmission," *Nonlinear Analysis: Real World Applications*, vol. 38, pp. 49–67, 2017.

[11] V. Racloz, E. Schelling, N. Chitnis, F. Roth, and J. Zinsstag, "Persistence of brucellosis in pastoral systems," *Revue Scientifique et Technique de l'OIE*, vol. 32, no. 1, pp. 61–70, 2013.

[12] J. Tumwiine and G. Robert, "A mathematical model for treatment of bovine brucellosis in cattle population," *Journal of Mathematical Modelling*, vol. 5, no. 2, pp. 137–152, 2017.

[13] J. Zhang, Z. Jin, L. Li, and X.-D. Sun, "Cost assessment of control measure for brucellosis in Jilin province, China," *Chaos, Solitons & Fractals*, vol. 104, pp. 798–805, 2018.

[14] M.-T. Li, Z. Jin, G.-Q. Sun, and J. Zhang, "Modeling direct and indirect disease transmission using multi-group model," *Journal of Mathematical Analysis and Applications*, vol. 446, no. 2, pp. 1292–1309, 2017.

[15] M.-T. Li, G.-Q. Sun, Y.-F. Wu, J. Zhang, and Z. Jin, "Transmission dynamics of a multi-group brucellosis model with mixed cross infection in public farm," *Applied Mathematics and Computation*, vol. 237, no. 11, pp. 582–594, 2014.

[16] K. Aune, J. C. Rhyan, R. Russell, T. J. Roffe, and B. Corso, "Environmental persistence of Brucella abortus in the Greater Yellowstone Area," *The Journal of Wildlife Management*, vol. 76, no. 2, pp. 253–261, 2012.

[17] W. Beauvais, I. Musallam, and J. Guitian, "Vaccination control programs for multiple livestock host species: An age-stratified, seasonal transmission model for brucellosis control in endemic settings the LCNTDR Collection: Advances in scientific research for NTD control," *Parasites & Vectors*, vol. 9, no. 1, p. 55, 2016.

[18] J. K. Hale and S. M. Verduyn Lunel, *Introduction to Functional-Differential Equations*, Springer, Berlin, Germany, 1993.

[19] P. van den Driessche and J. Watmough, "Reproduction numbers and sub-threshold endemic equilibria for compartmental models of disease transmission," *Mathematical Biosciences*, vol. 180, pp. 29–48, 2002.

[20] J. P. LaSalle, *The Stability of Dynamical Systems*, SIAM, Philadelphia, Pa, USA, 1976.

[21] H. Smith and X. Zhao, "Robust persistence for semi-dynamical systems," *Nonlinear Analysis: Theory, Methods & Applications*, vol. 46, pp. 6169–6179, 2001.

[22] L. Zhou, M. Fan, Q. Hou, Z. Jin, and X. Sun, "Transmission dynamics and optimal control of brucellosis in Inner Mongolia of China," *Mathematical Biosciences and Engineering*, vol. 15, no. 2, pp. 543–567, 2018.

[23] L. Arriola, "Sensitivity analysis for quantifying uncertainty in mathematical models," in *Mathematical and Statistical Estimation Approaches in Epidemiology*, G. Chowell, J. M. Hyman, L. M. A. Bettencourt, and C. Castillo-Chavez, Eds., pp. 195–248, Springer, New York, NY, USA, 2009.

[24] L. Bolzoni, V. Tessoni, M. Groppi, and G. A. De Leo, "React or wait: which optimal culling strategy to control infectious diseases in wildlife," *Journal of Mathematical Biology*, vol. 69, no. 4, pp. 1–5, 2013.

[25] W. Zhou, Y. Xiao, and R. A. Cheke, "A threshold policy to interrupt transmission of West Nile Virus to birds," *Applied Mathematical Modelling*, vol. 40, no. 19-20, pp. 8794–8809, 2016.